A split enzyme for biosensors

Janice Robottom BSc. (Hons)

Submitted in accordance with the requirements for the degree of Doctor of Philosophy

The University of Leeds School of Molecular and Cellular Biology

January 2018

The candidate confirms that the work submitted is her own and that appropriate credit has been given where reference has been made to the work of others.

Acknowledgements

To describe this as a journey is an understatement. It has been hard work, ridiculously difficult at times, but extremely rewarding, and I am surprised and amazed to have made it to this point. I have a number of people to thank for their support in getting this far on my doctoral journey. I would like to express my sincere appreciation to my Supervisors, Prof. Mike McPherson and Prof. Christoph Wälti for the constant guidance and encouragement, without it this work would not have been possible. I am also grateful to all the members of the McPherson and Tomlinson Lab for their support and I gratefully acknowledge BBSRC for financial support

A huge thank you to some very special colleagues: Amanda McDonald, Bob Schiffren, Birthe Lang and Modupe Ajayi, who I have been lucky enough to have had travelling this same journey alongside me, and whose constant support, practical advice and optimism has helped to keep me going, and dragged me to the finish line. Also to Dr. Thembi Gaule and Tom Taylor who helped me develop my scientific skills and for their friendship.

On a more personal note I would like to mention Melanie one of my closest friends, thank you for encouraging me, supporting me and making me realize that I should never let being dyslexic (or anything else) hold me back from what I want to do.

Most of all a massive thank you to my husband, friend and confidant, Gavin, and my lovely children, Joshua, and Helena for all their love and support, for putting up with my moods and grumpiness at times. You have been so supportive in whatever I do in my life and allowed me time away from family stuff to get this PhD completed, and to you three this thesis is dedicated. I am also forever indebted to my mum, because without her support, especially with childcare, I could not have gone to university in the first place.

With all my heart I would like to thank the LORD my God who has walked with me threw out the whole journey, and by extension all the people at Life church; thank you for your encouraging words.

Abstract

Split enzymes have been used in Protein Complementation Assays (PCA) for several years to study protein-protein interactions. Recently Affimers, non-antibody binding proteins, have been created as new tools for studying molecular interactions. Combining these technologies offers substantial benefits for development of highly sensitive and specific diagnostic devices. For proof-of-principle, two fragments of β-lactamase have been generated with two His tags. The binding of the His tag on each fragment to nickel ions facilitates the association of β-lactamase fragments to generate a functional enzyme capable of substrate turnover. Substrates, such as the cephalosporin nitrocefin giving rise to a colour change (yellow to red) detectable at 492 nm.

Following this proof of principle, the project focuses upon a novel split alkaline phosphatase to underpin an amperometric detection system developed with colleagues in the School of Electronic Engineering, University of Leeds. Alkaline phosphatase is a homodimer and the monomeric form of this protein does not turnover substrate. Current work in this study is focused on engineering the dimer interface to generate novel monomers that do not spontaneously associate. This is followed by exploring whether the mutated monomers can become associated and brought together, and catalyse substrate turnover.

This study also focuses on preparing Affimers that can bind a target molecule, mGFP, at two separate epitopes. Followed by generating a cross linked protein between the Affimers and alkaline phosphatase. The binding of Affimer to target will be amplified by enzyme activity allowing detection. The system should allow single step detection of a target present at very low concentrations in a complex sample

Table of Contents

List of Figures

List of Tables

Abbreviations

4ANP	4-amino-1-naphthyl phosphate
AP	Alkaline phosphatase
APS	ammonium persulfate
AUC	analytical ultracentrifugation
BCA	Bicinchoninic acid
BiFC	Bimolecular fluorescent complementation
CBG	click beetle Green
CBR	click beetle red
CD	Circular dichroism
CFP	Cyan fluorescent protein
CRP	C-reactive protein
CV	column volume
DHFR	dihydrofolate reductase
DNA	Deoxyribose nucleic acid
ECAP	*E. coli* alkaline phosphatase
EDTA	ethylenediaminetetraacetic acid
EIA	Enzyme Immunoassay
ELISA	Enzyme-Linked Immunosorbent Assay
FAD	flavin adenine dinucleotide
GDH	glucose dehydrogenase
GFP	green fluorescent protein
GOx	glucose oxidases
HCMV	human cytomegalovirus
HIV	Human Immunodeficiency Virus
HRP	horseradish peroxidase
IgG	immunoglobulin G
IL8	Interleukin 8
NEB	New England Biolabs
PAGE	polyacrylamide gel electrophoresis
PBS	Phosphate Buffered Saline
PBST	Phosphate buffered saline with Tween
PCA	Protein Complementation Assay
PCR	Polymerase Chain Reaction
PDB	protein data bank
pNPP	para-nitrophenyl phosphate
PPI	protein-protein interactions
PQQ	pyrroloquinoline quinone
SAM	self-assembled monolayer

SEC	size exclusion chromatography
SELEX	Systematic Evolution of Ligand Exponential Enrichment
SOD	Superoxide dismutase
TAE	Tris-acetate-EDTA
TBE	Tris-borate-EDTA
TBST	Tris buffered saline with Tween
TCEP	Tris [2-carboxyethyl] phosphine hydrochloride
TEMED	N,N,N’,N’,-tetramethylethylenediamine
TMB	3,3',5,5'-Tetramethylbenzidine
TUGGE	transverse urea gradient gel electrophoresis
wt	wild type
YFP	Yellow fluorescent protein

Chapter 1

Background and Literature Review

1.1 Diagnostics in healthcare

Healthcare and improved health are two of the long term social and economic factors affecting the stability of many countries, including the UK (Regidor 2006). There are hundreds of diagnostic tests and medical procedures used in healthcare to help physicians treat patients (Siontis *et al*. 2014). It follows then that if the diagnosis can be improved and made more informative and cost effective then so can healthcare in general. Early diagnosis can reduce the morbidity and mortality of disease outcomes. Human Immunodeficiency Virus (HIV) diagnosis is a good example of how diagnostic assays have improved over time (Cornett and Kirn 2013). The HIV virus is undetectable in blood plasma until 10 days after infection, and there are different types of infection by HIV-1 and HIV-2. The first generation of enzyme immunoassay (EIA) that detected HIV-1 antibodies was introduced in 1985 but was unable to detect infection until 6-8 weeks after infection. A similar second-generation assay was introduced which allowed diagnosis up to one week earlier. The antigen used in this assay was produced using recombinant technology. A major improvement came in 2007 with the third-generation diagnostic. This assay was able to detect antibodies against both types of virus just three weeks after infection. A fourth-generation assay can detect infection just two weeks after infection, and detects both the antibody response and a protein called p24 antigen which is produced by the virus. If a blood sample is sent to a laboratory for an EIA it typically takes a few days but can be available on the same day and requires a 4 ml blood sample. HIV rapid tests give a result in just 30 minutes based on a lateral flow device which detects the same antibodies as EIA (Cornett and Kirn 2013).

1.1.1 Biomarkers

A medical biomarker is a molecule that indicates the presence, or absence, of a disease state (Strimbu and Tavel 2010). There are **pre-disposition biomarkers** that distinguish patients at a high risk of developing a particular disease. Screening biomarkers help with early detection of a specific disease. **Diagnostic biomarkers** identify a patient with an actual disease, and **prognostic biomarkers** help ascertain a particular prognosis (Henry and

Hayes 2012). Cancer biomarkers, for example, can be a germline mutation such as the BRCA1 mutation that indicates a higher estimated risk for development of breast and ovarian cancer (Easton, *et al*. 1995). An example of a screening biomarker would be prostate specific antigen, which is used for screening for prostate cancers. It is usually elevated above 4 ng/ml of blood in men with prostate cancer (Lin, *et al*. 2008). An example of a diagnostic biomarker is the antibodies the human body produces in response to an infection, such as the antibody against HIV (Cornett and Kirn 2013). Mutations in the KRAS protein can help predict a patient's response to therapy in colorectal cancers (Allegra, *et al*. 2009). To investigate recurrence of germ cell tumors α-fetoprotein can be monitored in serum (Gilligan, *et al*. 2010). The use of these types of biomarkers can help improve healthcare, through monitoring people with predisposition to certain illness or disease. This will lead to earlier diagnosis, as would the use of diagnostic biomarkers, which can lead to earlier treatment. Prognostic biomarkers improve healthcare by helping the practitioner decide on a course of treatment.

1.1.2 Environmental Analytes

Analytes in environmental samples can indicate contaminants, or toxins, which could be identified then removed and disposed of in an appropriate safe manner. Bisphenol A is known to migrate from packaging to food and could be used as a food safety marker (Baluka and Rumbeiha 2016). Oil companies have an obligation to avoid harmful effects to the environment, including marine life (Sanni, *et al*. 2017). To monitor the contaminants in the aquatic environment, the level of alkylated phenols, polycyclic aromatic hydrocarbons, and carbazoles, which are found in crude oil, need to be tested. These all have a detrimental effect on the environment and levels should be kept as low as possible (Harman, *et al*. 2008). A biosensor can detect these biomarkers allowing safe and effective removal.

1.2 Biosensors

A biosensor comprises a recognition element, a transducer, and an output device as depicted in Figure 1.1. (Bohunicky and Mousa 2010). Biosensors

have the potential to offer a portable, inexpensive and rapid substitute to traditional lab-based analytical processes, by determining the presence of a biomarker or analyte. Some biosensors can give further information, such as the concentration of the analyte. Multiplex devices simultaneously provide information on a range of different biomarkers or analytes thus streamlining testing and diagnosis.

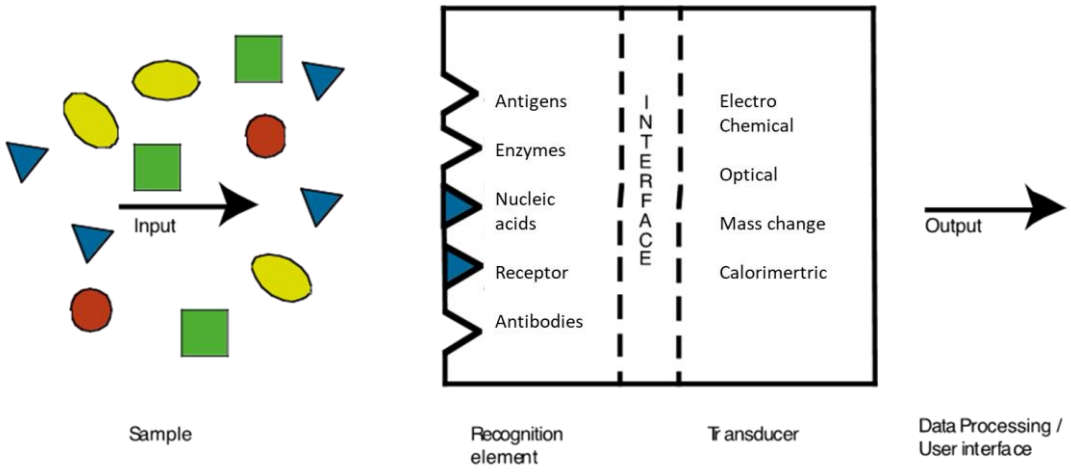

Figure 1.1 Illustration of the process by which biosensors function.

The input from a sample analyte interacts with the recognition element. The transducer converts the recognition event into a measurable signal. The output signal can then be measured by electronic instrumentation and an output can be read on a computer or other electronic device.

1.2.1 Elements of a biosensor

Figure 1.1 illustrates the elements of a biosensor. The input from a sample is taken up by the recognition element, usually a binding event for example when a biomarker binds an antibody. A transducer converts that binding event into a measurable signal: the output.

1.2.1.1 Recognition element

The recognition element of a biosensor is the part of the sensor that interacts with the biomarker or analyte. The typical molecular receptors include; antigens, enzymes, nucleic acids, receptors, and antibodies. The different types of molecule have different advantages and disadvantages in areas such as selectivity, ease of production, expense and stability, as discussed below.

1.2.1.1.1 Antigens.

Antigens are molecules that elicit an immune response and produce antibodies in the host immune system. If an antigen is used to detect a particular antibody then it would need to be the same structure as the disease causing agent or a section of it. An example of using an antigen in a biosensor is the HIV-1 peptide gp41 and gp120. These correspond to envelope regions of HIV-1 (Delaney, *et al*. 2011). The peptide(s) interacts with antibodies in whole blood in the sample that contains HIV-1. These systems are usually very specific, but the antigens can be difficult to produce in sufficient quantities.

1.2.1.1.2 Enzymes

An enzyme can be used as a recognition element where the active site recognises the biomarker or analyte, and can, therefore, interact with it. The glucose biosensor uses glucose oxidase and is the most widely studied enzyme for uses as a recognition element. The medical importance of diabetes, particularly type I, drove the need for a glucose biosensor as there is a need for glucose monitoring (Heller and Feldman 2008, Lan, *et al*. 2016). Glucose oxidase binds to glucose in the blood, and turns it over to give a signal. A detailed description can be found in Section 1.2.4.

Lysozyme is an enzyme which binds to a peptidoglycan molecule that is present in the cell wall of bacteria. It has been utilised as a recognition element in an experiment where lysozyme was labeled with fluorescein. The lysozyme was able to bind different bacteria including *Staphylococcus aureus, Bacillus cereus, Micrococcus luteus, Edwardsiella tarda, Vibrio alginolyticus,* and *Escherichia coli.* Detection by fluorescence was seen in all cases, but there was a much greater response for *S. aureus, B. cereus,* and *M. luteus* as these

are Gram-positive bacteria. There are more peptidoglycan molecules in Gram-positive bacteria, thus the lysozyme can bind more readily (Zheng, *et al*. 2016).

Urease is an enzyme that binds urea, which is indicator of renal function. High levels of urea are a sign of kidney failure. A study by Barhoumi *et al* (2006) used urease in a biosensor which could monitor the level of urea from 100 µM to 100 mM. Table 1-1 lists these and more examples of enzymes that have been used as recognition elements.

Table 1-1 Enzymes used as recognition elements in biosensors.

Enzyme	Brief Description
Glucose oxidase	Binds directly to glucose in blood samples (Heller and Feldman 2008, Lan, *et al*. 2016).(Saglam, *et al*. 2016)
Lysozyme	Lysozyme binds to peptidoglycan molecules that are present in the cell wall of bacteria. Lysozyme was labeled with fluorescein (Zheng, *et al*. 2016).
Urease	Urease binds urea for monitoring for both medical and environmental applications (Barhoumi, *et al*. 2006).
Alcohol dehydrogenase	A study by (Gomez-Anquela, *et al.* 2015) uses alcohol dehydrogenase on gold nanoparticles to monitor ethanol oxidation
Glucose dehydrogenase	PQQ glucose dehydrogenase was used to measure calcium ion concentrations in biological fluid (Guo, *et al*. 2016)
Lactate dehydrogenase	A study by (Azzouzi, *et al.* 2015) uses lactate dehydrogenase on gold nanoparticles to monitor lactate which is a tumour biomarker.
Alcohol oxidase	An electrochemical sensor for detecting the alcohol level using sweat, utilised alcohol oxidase as the recognition element (Gamella, *et al*. 2014).
Ascorbate oxidase	Vitamin C sensors have been established using ascorbate oxidase as recognition elements (Liu, *et al*. 2011, Wen, *et al*. 2012).
cholesterol esterase, oxidase, and peroxidase	The amount of cholesterol in blood has been measured using cholesterol esterase, oxidase, and peroxidase (Lata, *et al.* 2016)

1.2.1.1.3 Nucleic acids

Libraries of nucleic acids; either DNA or RNA, called aptamers, can be produced using the systematic evolution of ligand exponential enrichment (SELEX) (Tuerk and Gold 1990). These oligonucleotides can bind a wide range of targets including small molecules, proteins and whole cells (Chambers, *et al.* 2008). A DNA aptamer for α-synuclein, which is a biomarker for the diagnosis of Parkinson's disease, has been used recently. When the aptamer was adsorbed onto gold nanoparticles in high salt concentration they remained monomeic in solution with a red colour. When the aptamer was bound to the α-synuclein, the nanoparticles were able to aggregate, triggered by the high salt concentration, and turned from red to blue (Sun, *et al*. 2017).

1.2.1.1.4 Receptors

Similar to an enzyme, a receptor protein or domain can be used as a recognition element. For example, the oestrogen receptor protein can be used as a recognition element to detect a number of pollutants. The oestrogen receptor naturally binds a wide range of endocrine disrupting chemicals, which are toxic but are increasingly found in water products. The ligand binding domain of the oestrogen receptor is sufficiently small and stable to be produced in *E. coli*, and can be used in an Enzyme-Linked Immunosorbent Assay (ELISA) type assay instead of an antibody, which is normally specific to just one endocrine disrupting chemical (Pedotti, *et al*. 2015).

1.2.1.1.5 Antibodies

Antibodies are typically 'Y' shaped molecules and consist of constant and variable regions, and are secreted by B-cells as part of a humoral immune response. Antibodies generally consist of two heavy chains made up of at least four domains, and two light chains that generally have two domains (Figure 1.2). Each of the domains comprises approximately 110 amino acids and have similar secondary and tertiary structures, known as the immunoglobulin fold and which is a very stable, β-strand structure. The variable region is at the N-terminal end of each of the peptide chains (Janeway, *et al*. 2008). The recognition site that binds an antigen consists of six

hypervariable loops, three each from the variable regions of the heavy chain and the light chains (Skerra 2003).

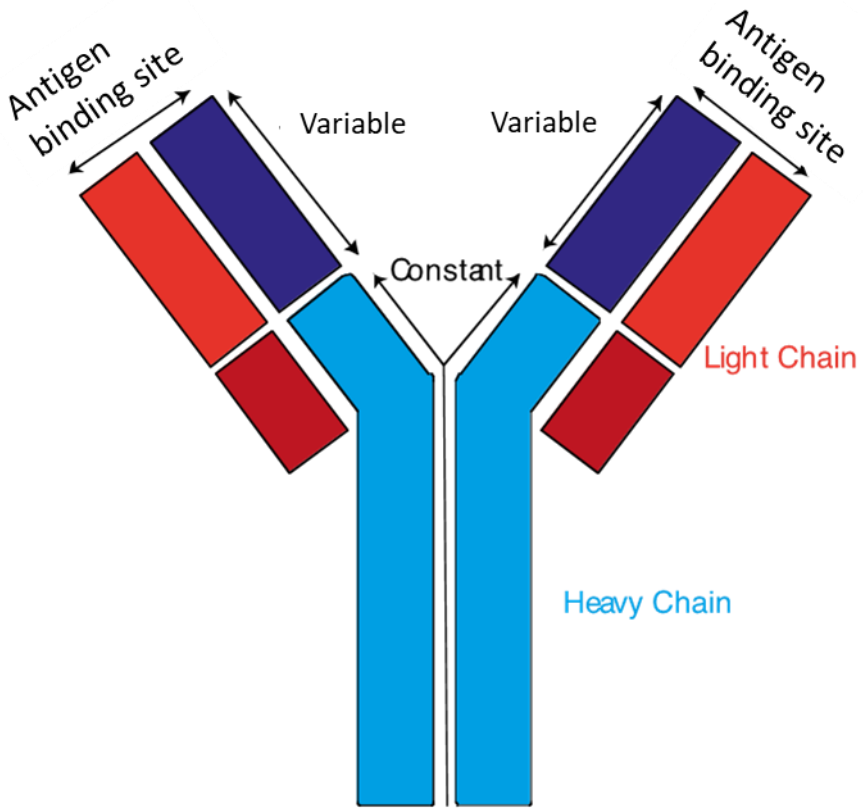

Figure 1.2 Structure of an antibody molecule.

This schematic shows the heavy chain in blue and the light chain in red. The constant and variable regions are also shown. The variable regions of both the light and heavy chain make up the antigen binding site.

Given that antibodies in nature are required to bind to foreign antigens entering the immune system, they are an ideal molecule for a recognition element. Anti C-reactive protein (CRP) antibodies were used to detect CRP in blood and saliva samples (Justino, *et al*. 2013, Justino, *et al*. 2014, Justino, *et al*. 2016). Anti HER3 antibodies have been used to detect HER3, which is a biomarker for cancer. An impedimetric biosensor was functionalised with anti-HER3 and was able to detect a range from 0.4 pg/ml to 2.4 pg/ml.(Sonuc and Sezginturk 2014).

In a recent study by Vasques *et al*. (2017) two antibodies that bind to two different epitopes of *Streptococcus agalactiae* were used to fashion a biosensor. *S. agalactiae* is a Gram-positive bacterium which can be responsible for sepsis and meningitis. The antibodies were able to bind to the bacteria; one antibody was biotinylated, and the other was conjugated to horseradish peroxidase (HRP). After incubation with the *S. agalactiae* cells, the biotinylated antibody was fixed to a neutravidin coated electrode and the second antibody was incubated with the antibody *S. agalactiae* mixture. The activity of the HRP was measured to identify whether or not the *S. agalactiae* was present (Vasquez, *et al*. 2017).

1.2.2 Scaffold Proteins.

A scaffold is a robust protein that has a region which is permissible to mutations, insertions, and deletions. Scaffolds are generally much smaller than antibodies, (Hey, *et al*. 2005) with some being based on antibody molecules or fragments of antibody molecules, others are engineered from non-immunological domains (Wurch, *et al.* 2008, Wurch, *et al.* 2012). Antibody-derived domains are based on the immunoglobulin fold. However, it is just the isolated variable chain, without any constant domains. Antibody fragments that have been evolved to be monomeric and soluble have been used as binding molecules. Some antibodies, for example antigen receptors in sharks (IgNAR) or camelids, are only made up of the heavy chain and no light chain (Skerra 2007). Non-antibody binding proteins are not based on antibodies and include proteins, such as the anticalins, whose scaffold is based on lipocalins, the AdNectin scaffold, which is based on fibronectin DARPin, which in turn are based on ankyrin repeats, Avimers, which are based on a domain of the LDL receptor (Wurch, *et al*. 2012) and Affimers developed in Leeds.

1.2.2.1 Affimer™

An Affimer (Tiede, *et al.* 2014), shown in Figure 1.3, is a scaffold protein and was developed by the BioScreening Technology Group (BSTG) at the University of Leeds using a scaffold constructed from phytocystatins. These are plant cystatins that inhibit cysteine proteases (Abe, *et al.* 1991). Fifty-

seven coding sequences of phytocystatins were used to generate a consensus sequence. In theory, this should produce a very stable protein as the most conserved residues are included in the sequence and the non-conserved areas tolerate changes, such as inserts and mutations. The two loops shown in Figure 1.3 are VVAG and PWE and are consensus sequences that interact with proteins that are degraded by cysteine proteases. Since the scaffold was developed from cysteine proteases inhibitor the end result turned out to be, as expected, a very good cysteine protease inhibitor. These highly conserved loop regions, which already represent protein interactions loops, were replaced to remove the inherent protease inhibitory activity and to provide the sites for generation of library of proteins containing the variable regions. The Affimer library was constructed by splice overlap extension of two PCR products. The two nine amino acid variable regions were introduced by the second PCR product, which has degenerate regions corresponding to the loop regions. Trimers representing a single codon for each of the 19 amino acids (excluding cysteine) were introduced by degenerate (NNN) primers. The library of Affimers expressed from phagemid vectors are displayed as N-terminal fusions to a truncated D2-D3 pIII protein of M13 phage, in a process known as phage display (Tiede, *et al.* 2014).

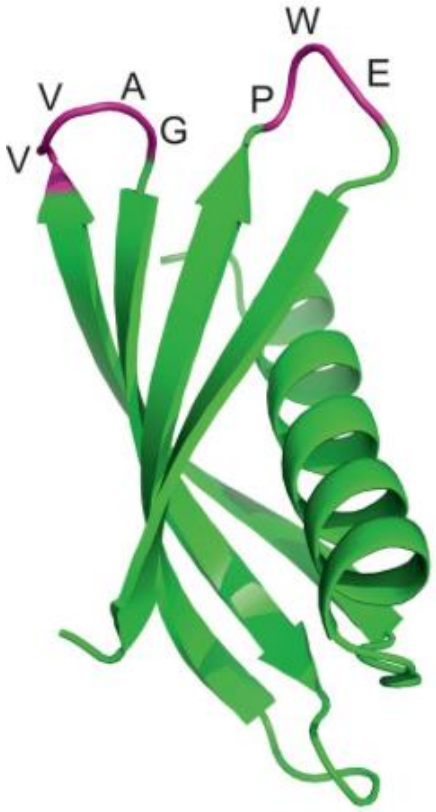

Figure 1.3 Structure of an Affimer.

The binding loops on the top of this picture are the original loop from the consensus sequence. There are four β-strands making up a β-sheet and a α-helix. From PBD ID 4N6U, adapted from Tiede *et al* (2017)

A screening process, wherein the library is panned against an immobilised target of interest, is used to narrow the search for a suitable binding protein. The unbound phage are then washed away leaving an enriched library of Affimers. These are eluted and amplified to use in a second round of panning. A phage ELISA against the target is performed after panning and 'hits', Affimer-expressing phage that bind the target, are confirmed as described in Figure 1.4. The 'hits' are then recovered as phagemid DNA containing the coding region for the Affimer and are available to be sub-cloned as necessary.

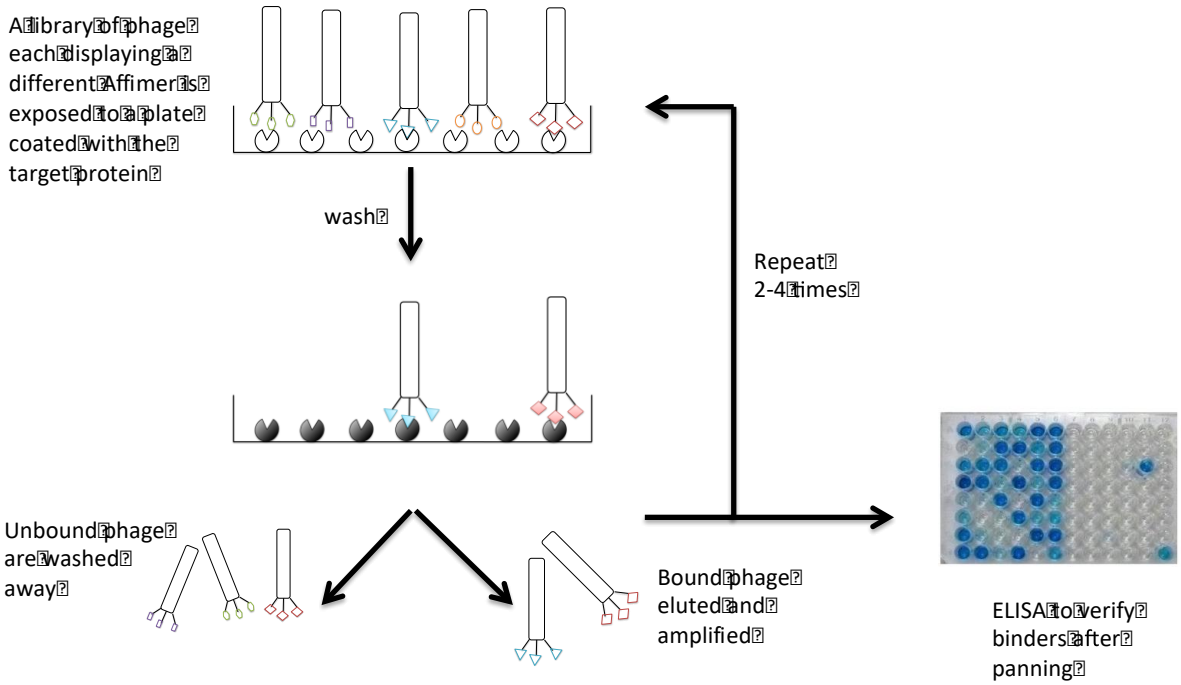

Figure 1.4 Phage display of Affimers.

A library of phage each displaying a different Affimer are exposed to a target, the unbound phage are washed off, enriching the bound phage. These are eluted and amplified for the next round. To verify 'hits' Affimer that have bound the target a phage ELISA is done after panning.

Affimers have a wide range of uses (Bedford, *et al*. 2017, Tiede, *et al*. 2017, Xie, Tiede *et al*. 2017), the first published use of an Affimer was as a recognition element for the myc protein (Raina, *et al.* 2015). This was on an impedance based biosensor and could detect concentrations between 6.7 pM and 6.7 nM (Raina, Sharma *et al.* 2015). An IL8 Affimer was used as a recognition element to create an impedance biosensor for interleukin 8 (IL8) (Sharma, *et al*. 2016). IL8 is an inflammation biomarker and is involved in the recruitment of neutrophils during injury or infection. The Affimer, described in the paper as a small non-antibody binding protein, has a K_D of 35 ± 10 nM. Using an impedance based biosensor, concentrations as low as 90 fg/ml were detected. Given that clinically relevant levels are 5-10 pg/ml the biosensor could therefore easily pick up the target molecule at clinically relevant levels (Sharma, *et al*. 2016).

1.2.3 Transducers

A transducer converts the interactions of the recognition element into a signal that can be measured. These can be made up of a simple physical component such as an electrode, but more often have a chemical component linking the recognition element to the working electrode. Electrodes have three parts: the working electrode, where you place a sample, the counter electrode and a reference electrode. The reference electrode has a stable, established electrode potential. A schematic of a screen-printed electrode is shown in Figure 1.5 (Hernández, *et al*. 2016).

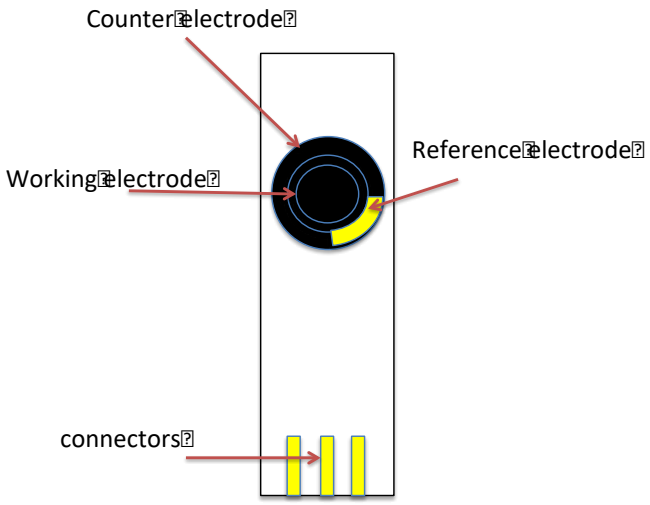

Figure 1.5 A schematic of a screen printed electrode.

The working, counter and a reference electrode are shown, as well as the connections for each of the electrodes.

1.2.3.1 Electrochemical Biosensors

Electrochemical sensors offer the advantage of being small and easy to use. The glucose meter, described in section 1.2.4 is an example of an electrochemical biosensor. Electrochemical biosensors include amperometric, conductometric and potentiometric sensors.

1.2.3.1.1 Amperometric

An amperometric biosensor measures electrical current and is often based on oxidase enzymes that generate hydrogen peroxide and consume oxygen (Wu, *et al*. 2017). The movement of electrons is detected when a potential is applied between two electrodes. Superoxide dismutase (SOD) was used to create an amperometric biosensor to measure the total antioxidant capacity of several berry samples. The SOD biosensor was compared with established laboratory methods: a spectrophotometric method and a spectrofluorimetric method. The SOD was immobilised in Kappa carrageenan gel and sandwiched in between two membranes and fixed to an electrode. The total antioxidant capacity was measured as a concentration of superoxide radicals. SOD converts superoxide radicals and hydrogen ions to hydrogen peroxide and molecular oxygen. The release of hydrogen peroxide was oxidised at the anode giving an amperometric signal proportional to the concentration of superoxide radicals present. The magnitude of the measurement was different for the three methods, but the trend of total antioxidant capacity of the different samples was the same (Tomassetti, *et al*. 2015).

1.2.3.1.2 Conductometric

An impedance biosensor measures the electrical impedance of an interface. The impedance of an electrode solution interface changes when a target is captured (Daniels and Pourmand 2007). As an example, a gold electrode was functionalised with a monothiol-alkane-PEG acid self-assembled monolayer (SAM). The carboxylic acid group was activated with 1-ethyl-3-(3-dimethylaminopropyl)carbodiimide hydrochloride (EDC) and N-hydroxysulfosuccinimide (NHS) and an IL8 binding protein was then immobilised via a covalent bond on to the SAM. This electrode was then used to detect IL8 by the electrochemical impedance (Sharma, *et al*. 2016).

1.2.3.1.3 Potentiometric

A potentiometric biosensor measures a change in the distribution of charge using ion-selective electrodes, for example, a pH meter. A potentiometric biosensor was developed to detect the presence of urea in milk. The biosensor used an NH_4^+ electrode with urease immobilised on to the membrane of the

electrode. The biosensor had a detection limit of 25 μM, with a response time of 20 to 30 seconds (Trivedi, *et al*. 2009).

1.2.3.2 Biosensor Output

The output of a biosensor is made up of three parts: amplifier, processor, and display. The electrodes translate the bio recognition event into an electrical signal in an electrochemical biosensor. This signal can then be measured by electronic instrumentation and an output can be read on a computer or other electronic device (Li, *et al*. 2016). Photometric biosensors can detect either fluorescent or luminescent photons with photomultiplier tubes or a photo diode system. Piezoelectric devices detect the specific angle at which electron waves are emitted. Colourimetric biosensor devices have an output that can be seen, for example the pregnancy test when a coloured line is displayed. In other systems the colour might not be able to be seen by eye, but a UV-VIS spectrometer can detect absorbance within the visual spectrum.

1.2.4 Glucose Biosensor

One of the most widely used biosensors on the market is a glucose sensor. People with diabetes require a glucose meter to measure the level of glucose in their blood. The biosensor recognises glucose, which is a biomarker in blood, and gives an electrochemical signal as an output, that is then converted into a concentration. The resulting number assists the diabetic person to calculate the amount of insulin needed, or how to modify their diet to change that level (Lan, *et al.* 2016). The development of this particular biosensor has changed dramatically since the 1970's when a semi-quantitative device was used that required multiple steps and took over 2 minutes and required about 25 μl of blood. The latest device is an electrochemical quantitative device that takes approximately 5 seconds and requires as little of 0.3 μl of blood (Heller and Feldman 2008, Lan, *et al.* 2016).

Modern glucose meters use a disposable test strip, which contains a capillary that draws up a specific amount of blood. The glucose in the blood reacts with the recognition element, an enzyme electrode. A mediator reagent oxidizes the enzyme, and an electric current is generated by the mediator once reoxidized at the electrode (Peng, *et al*. 2013). There are two main families of

enzymes that are used in blood glucose meters; glucose oxidases (GOx) and glucose dehydrogenases (GDH). These enzymes have been engineered to improve their production, improve the purification process and specific activity, and enhance the stability and the selectivity for glucose (Heller and Feldman 2008).

Glucose oxidase requires a cofactor; the mediator, flavin adenine dinucleotide (FAD). Together the enzyme and the cofactor turn the glucose and oxygen substrates into hydrogen peroxide and gluconolactone. FAD is an electron acceptor from glucose, which is oxidised to gluconolactone, and FAD is reduced to FADH, which is normally oxidised by oxygen, and oxygen is reduced to hydrogen peroxide (Wohlfahrt, *et al.* 1999, Newman and Turner 2005). Glucose oxidase based biosensors use an electrode instead of oxygen to take up the electrons. In many cases the electron acceptor, FAD or ubiquitin, is replaced by ferrocene or its derivatives as a mediator reagent (Newman and Turner 2005).

Glucose dehydrogenase (GDH) enzymes use a mechanism that is independent of oxygen. Glucose is oxidised to gluconolactone like glucose oxidase, but a cofactor such as NAD^+ is used and NADH is produced. The NAD^+ cofactor is unstable, but other GDHs use pyrroloquinoline quinone (PQQ) as a cofactor, PQQ-GDH is an efficient enzyme as the electron transfer rate is high, but it is expensive compared with the other GDHs (Newman and Turner 2005).

1.3 Optimisation of Enzymes for Biosensors

Enzymes in nature are evolved for their biological function in the environment in which they are required to operate. In a biosensor, this function is being exploited for a different purpose for which it is not optimised. Mutagenesis is often used as a means to optimise an enzyme, by changing the genetic code in order to create variant forms of the enzyme. Furthermore, orientation and proximity of the enzyme to, its cofactor, or substrates, or products, and in some case all of these are essential for the enzymatic reaction and release of

product. In the case of biosensors, the orientation and proximity of the enzyme to the electrode is fundamental to optimal function.

PQQ GDH is one such enzyme that has been modified for use in biosensor technology. PQQ-GDH was engineered to enable direct electron transfer to the electrode instead of using an electron mediator (Okuda and Sode 2004). The cytochrome c domain of quinohemoprotein ethanol dehydrogenase was fused to the C-terminal of PQQ-GDH. The fusion protein showed intra-molecular electron transfer, between PQQ and heme, and electron transfer from heme to the electrode (Okuda and Sode 2004). Initially, Guo *et al.* (2016) engineered PQQ-GDH, for use as a Ca^{2+} biosensor. This was done by inserting calmodulin into a loop within PQQ-GDH (Guo, *et al*. 2016). This was then adapted to be used as a universal biosensor platform, by splitting the protein into two fragments at the previous insertion site, but held together using two interacting proteins. The two interacting proteins were replaced with receptors or protein domains for immunosuppressant drugs, α-amylase protein and proteases. The newly engineered PGG-GDH was used for the detection of immunosuppressant drugs, α-amylase protein, and for detecting protease activity of thrombin and Factor Xa (Guo, *et al.* 2016, Guo, *et al.* 2016).

1.3.1 Optimisation of Electron Transfer pathways

The proximity and orientation of an enzyme and an electrode have a fundamental effect on electron transfer. Historically, most amperometric biosensors use a mediator between the electron active centre of the enzyme and an electrode (Degani and Heller 1987). Direct electron transfer from the enzyme to the electrode is better because it reduces interference from side reactions and it better mimics the redox potential of the enzyme. Furthermore, it is a simpler process as there is only one step in the reaction (Gorton, *et al*. 1999). In either case; with or without a mediator, the distance between the electrode and the electron centre is of paramount importance for a functioning biosensor. Figure 1.6 demonstrates how the orientation of an attached enzyme can affect the distance an electron has to travel. Electrons from the active site in (A) would probably not transfer to the electrode, whereas when the enzyme is orientated as in (B), the distance is much shorter and electrons can reach the electrode (Freire, *et al.* 2003).

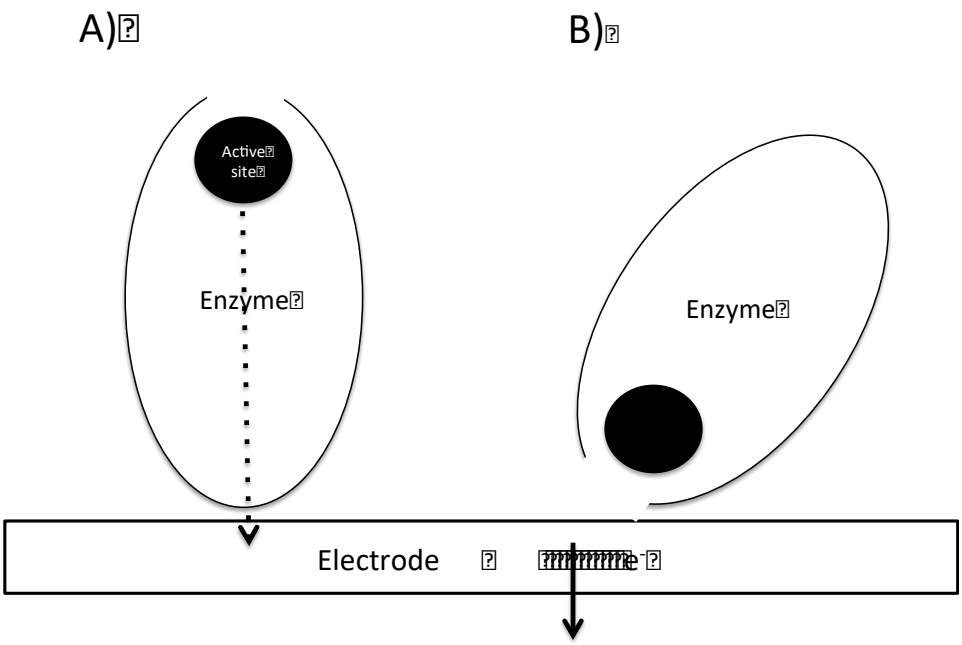

Figure 1.6 Enzyme orientation and proximity of the active site to an electrode.

Electrons in the active site of the enzyme (A) would likely not reach the electrode whereas those from (B) would reach the electrode and create an electrical signal. Figure adapted from (Freire, *et al*. 2003)

1.3.1.1 Immobilisation

There are different ways to immobilise an enzyme to an electrode surface. Physical adsorption, as depicted in Figure 1.7A, is where the enzyme interacts with the electrode with a combination of different interactions including electrostatic attraction, hydrophobic/hydrophilic interaction, hydrogen bonding, and Van der Waals interactions (Moulton, *et al.* 2003, Walcarius, *et al*. 2013). Crosslinking or inclusion in a conducting polymer is depicted in Figure 1.7B. The enzyme is either mixed with or crosslinked with the polymer at some point in the polymerisation process (Walcarius, *et al*. 2013). Finally, oriented attachment to self-assembled monolayers is depicted in Figure 1.7C. This orientation would assist in the transfer of electrons.

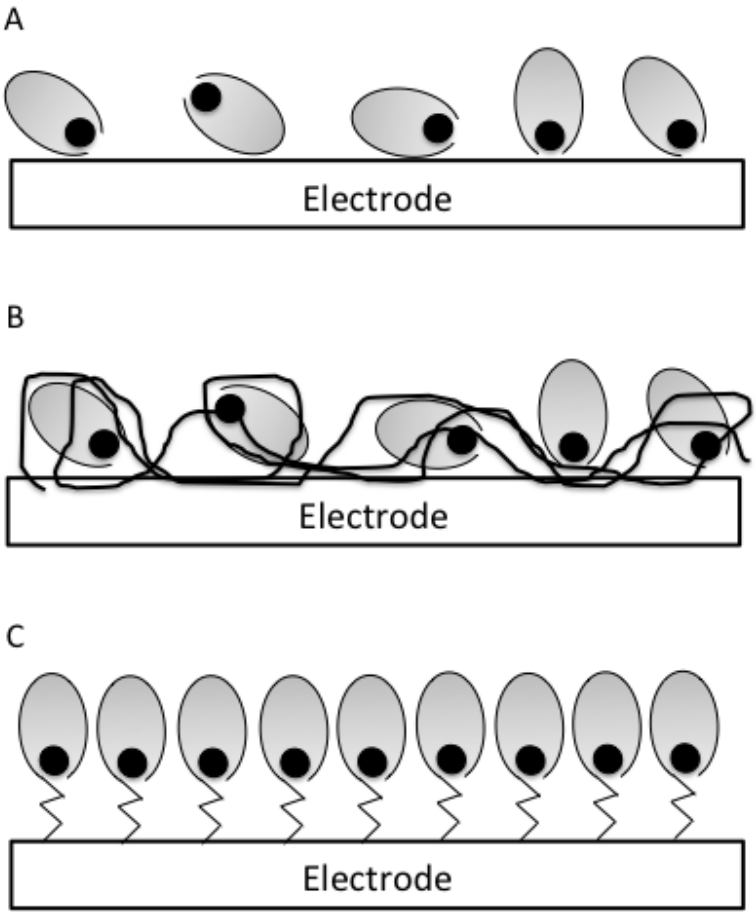

Figure 1.7 Immobilisation of enzyme to an electrode.

A) physical adsorption. B) crosslinking or inclusion in conducting polymer C) orientated attachment to self-assembly monolayers. Figure adapted from (Freire, *et al*. 2003)

To aid correct orientation, a variant enzyme can be generated by inserting or changing a residue in a specific position to a chemically active residue. Examples of chemically active residues include a cysteine, which has a thiol group, a lysine, which has an amino group, or a glutamate or aspartate, which have a carboxyl group. The most commonly used for directed orientation is the introduction of a cysteine.

1.4 Split proteins

The use of split proteins for diagnostics in biosensors is a relatively new concept, but they have been used in protein complementation assays (PCA) for some time (Kerppola 2006, Remy, *et al*. 2007). Protein complementation or split enzyme assays have been used to map protein-protein interactions (PPI) for several years. The assays have used small proteins such as ubiquitin (Johnsson and Varshavsky 1994); enzymes, for example β-lactamase (Galarneau, *et al*. 2002), luciferase (Villalobos, *et al.* 2008) and dihydrofolate reductase (DHFR) (Pelletier, *et al*. 1998); and fluorescent proteins such as green fluorescent protein (GFP) and derivatives (Figure 1.9) (Kerppola 2006). These proteins have been split into N- and C-terminal fragments, Figure 1.8 depicts different fragments; highlighted in different colours (blue and red); of GFP, firefly luciferase and β-lactamase. Each of the fragments are fused to one of a pair of potential interacting target proteins. If the target proteins interact with each other, this interaction brings the two protein fragments together and a signal is produced (Michnick 2003, Barnard 2007). The individual protein fragments should not exhibit any activity on their own. When the two fragments are mixed in solution they should have a very low affinity for each other, but when brought together by the PPI, the restored activity of the two fragments should create a sustained measurable signal (Shekhawat and Ghosh 2011). When splitting a protein, it is not always obvious at which site to generate the fragments and they are often insoluble or do not re-associate due to incorrect folding or assembly (Paschon, *et al*. 2005).

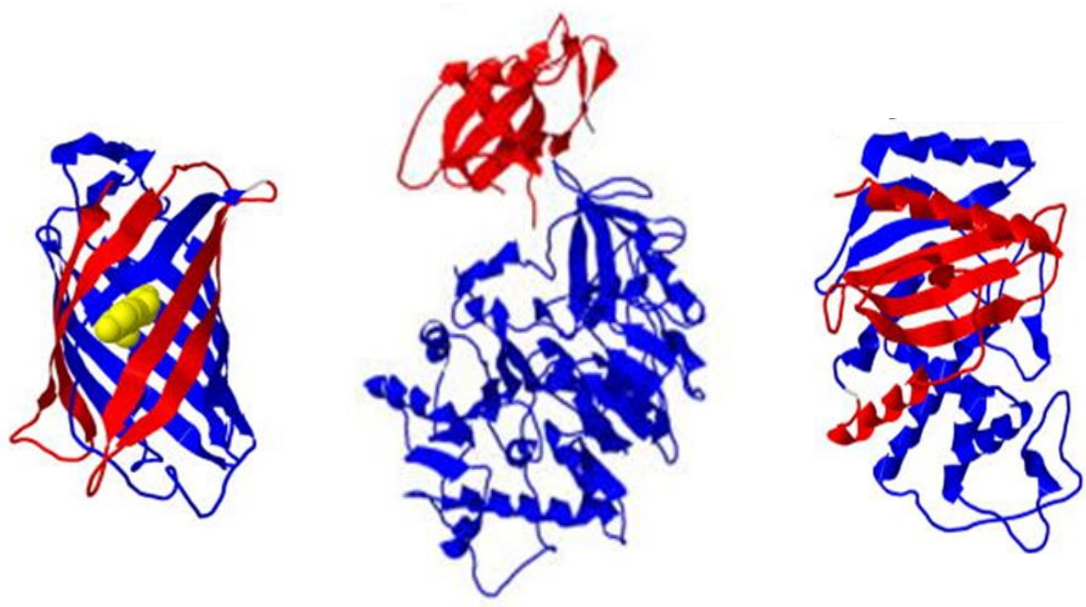

Figure 1.8 Examples of protein fragments that can be used to study protein interactions.

The fragments are shown in red and blue using models based on the X-ray crystal structures of the intact proteins. Figure adapted from (Kerppola 2006)

1.4.1 Fluorescent Proteins

Bimolecular fluorescent complementation (BiFC) is a sub-type of protein complementation assay. In BiFC a fluorescent protein is split and the signal change observed on the association of fragments is the fluorescence created by the fluorophore (Kerppola 2006). GFP has 238 amino acids, three of which (Ser-65, Tyr-66 and Gly-76) are used to form the fluorophore (Tsien 1998). These residues initially cyclise followed by a dehydration reaction and an oxidation reaction to form the p-hydroxybenzylideneimidazolinone fluorophore (Tsien 1998). Fluorescent proteins do not require a substrate or a small molecule, and are non-toxic to most cells, which make them a convenient reporter molecule in complementation assays. GFP and its derivatives have been split into two fragments, each fragment being fused to a specific protein; when an interaction is observed, a green fluorescence is detected (Michnick 2003, Remy and Michnick 2003, Kerppola 2006, Morell, *et al.* 2009, Shekhawat and Ghosh 2011).

An advantage of BiFC compared with other protein fragment assays is the intrinsic fluorescence of the complex. Once the fusion proteins are produced, no other reagents are required; just the association of the component parts. Furthermore, several interactions can be seen at the same time in the same cell by using different fluorescent proteins. Figure 1.9 shows the principle of the approach for two proteins, A and B, which can both interact with protein Z. If A interacts with Z then a yellow fluorescence is detected, but if B interacts with Z then a cyan fluorescence is detected. Cell images show, by coloured fluorescence, where proteins A and B are localised (Kerppola 2008).

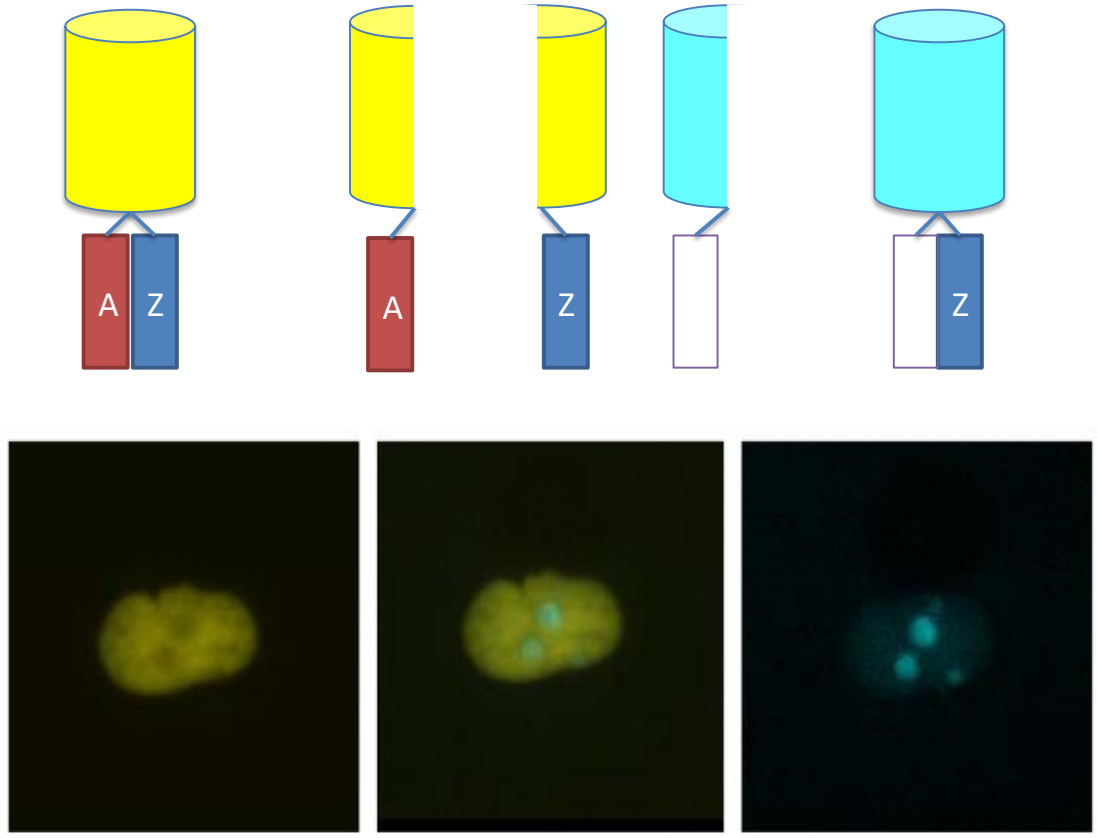

Figure 1.9 Multicolour Fluorescence complementation.

Protein Z interacts with both protein A and protein B. When protein Z and A interact, the fluorescent protein recombines to make yellow fluorescent protein. When protein Z and B interact, the fluorescent protein recombines to make cyan fluorescent protein. The cell images show where the different protein localise within a cell. Adapted from (Kerppola 2008).

If the position of the interacting proteins is unknown, then 8 pairs of different interacting fusion proteins may need to be tested. This is made up of 8 fusion proteins in total. Each interacting partner needs to be fused to the N and C terminus of each of the protein fragments as demonstrated in Figure 1.10 In this theoretical example, only a subset will create a fluorescent signal.

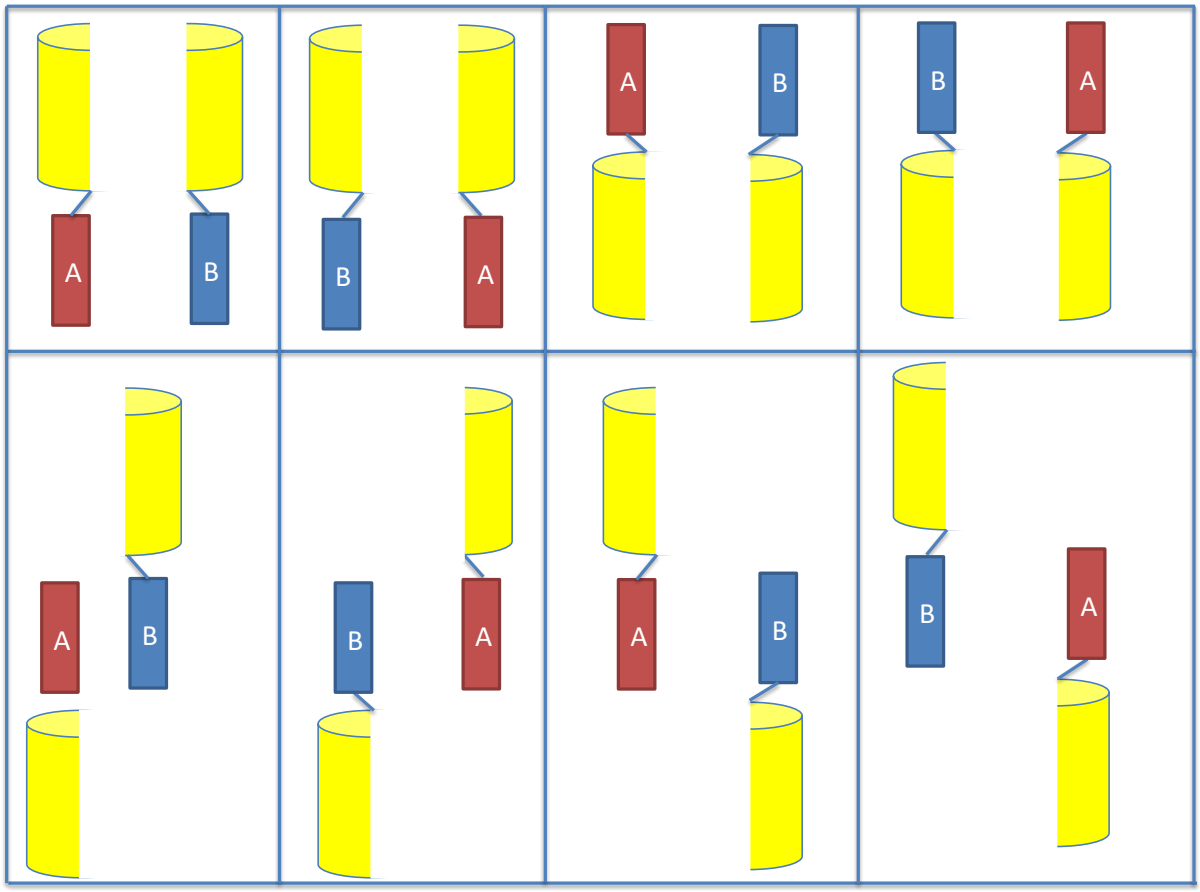

Figure 1.10 Multiple combinations of Fluorescent protein fragments and interacting partners.

Where the interactions are not known and a rational design cannot be implemented, then 8 different combinations of fusion protein should be tested. Both interacting proteins: A & B, on the C and N terminal of both fragments. Only the combinations that bring the fragments of fluorescent protein together will give a signal. Image adapted from (Kerppola 2008).

There are advantages and disadvantages of different combinations of fluorescent protein fragments in BiFC analysis. Yellow fluorescent protein (YFP) has a low spontaneous association, and would, therefore, give a low background, but the fluorescence intensity is weak. YFP can be combined with CFP so multi-colour analysis is possible. Venus, a derivative of YFP, has a higher fluorescence intensity, but also a higher occurrence of spontaneous association, it too can be combined with CFP fragments. The addition of the mutation M153T to Venus lowers the spontaneous association (Kerppola 2008).

The rates of the multiple steps in fluorophore formation vary for different fluorescent proteins (Robida and Kerppola 2009). Thus, in selecting the BiFC method, consideration must be given to the time taken for the fluorophore of the fluorescent protein to form. Furthermore, once the fluorescent protein has been formed it cannot dissociate, therefore dynamic reactions cannot be observed. However, this method is excellent for determining if protein 'X' interacts with protein 'Y' (Morell, *et al.* 2009). In several recent studies by Robida and Kerppola (Kerppola 2006 A, Kerppola 2006 B, Kerppola 2006 C, Robida and Kerppola 2009), BiFC was used to visualize PPI in living cells, and showed that conditional BiFC complex formation depends upon the folding environment in the cell and the folding efficiencies of each of the fluorescent proteins. In these studies, the interaction between the FK506-binding protein (FKBP) and FKBP rapamycin binding domain (FRB) was used as a model interaction. Figure 1.11 shows this model interaction, which has been well documented and is inducible by rapamycin. FKBP and FRB fused to complementary fragments of YFP were expressed. Inhibition of the interaction between FKBP and FRB stopped the further formation of the fluorescent protein but did not disrupt existing fluorescence. More than one split fluorescent protein can be used at the same time. If more than one colour of fluorescence is used, this gives the chance to see multiple PPIs simultaneously. Care must be given to which fluorescent proteins are chosen, as their emission spectra must be distinguishable, and the time taken for fluorophore formation must be similar (Robida and Kerppola 2009).

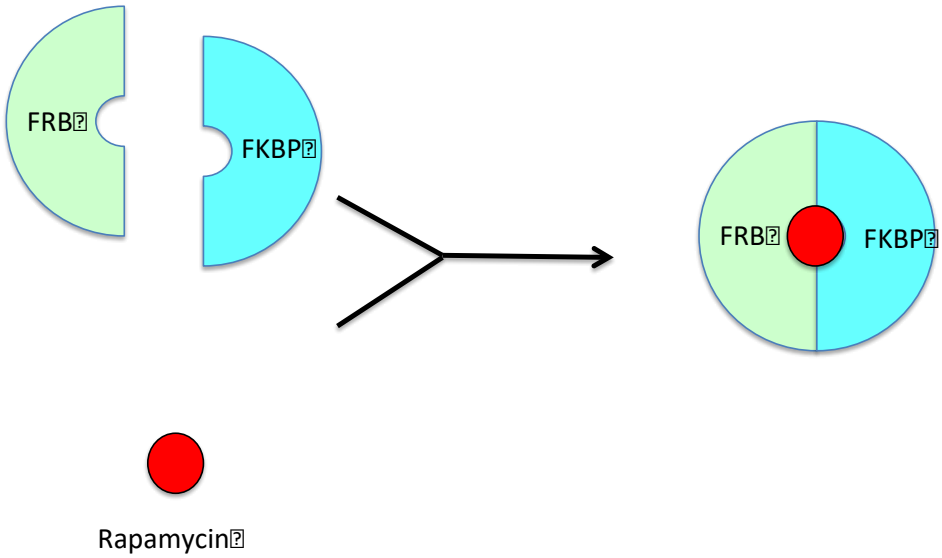

Figure 1.11 Rapamycin inducible interaction between FKBP (the FK506-binding protein) and FRB.

This interaction is inducible by rapamycin, and is often used as a model interaction that can be turned on and off.

1.4.2 Luciferases

Several different luciferases have been split into two fragments, and these have been used to show many different PPIs in different cell types. The luciferases are enzymes that produce bioluminescence through oxidation. Firefly (Paulmurugan and Gambhir 2003, Luker, *et al.* 2004, Paulmurugan, *et al.* 2006), Renilla (Paulmurugan and Gambhir 2003) and Guassia (Remy and Michnick 2006) luciferases have been split for use in PCAs. More recently, click beetle luciferase has been split for use in dual colour PCAs (Villalobos, *et al.* 2010). Intramolecular systems have also been designed where the target of interest is expressed in the middle of the two split luciferase fragments, and correct folding of the luciferase is induced on a ligand binding to the target protein (Binkowski, *et al.* 2009, Ataei, *et al*. 2013). An advantage of the use of luciferases compared to fluorescent proteins is that the interaction is reversible and can provide information about transient interactions (Morell, *et al.* 2009).

Firefly luciferase was originally fragmented between amino acid 437 and 438. Paulmurugan *et al* (2005) fused fragments of firefly luciferase to MyoD and Id, which are two proteins that are known to interact. Firefly luciferase oxidised D-luciferin when both fusion fragments were present, and bioluminescence was observed. Studies showed similar results in both live mice and HEK 293T cells (Paulmurugan, *et al.* 2005, Paulmurugan, *et al.* 2006, Paulmurugan and Gambhir 2005). There was, however, a high background due to residual activity in the N-terminal fragment. Analysing many different fragments improved the signal to noise ratio. The optimal protein fragments have an 18 amino acid overlap, which would not have been predicted by rational design (Paulmurugan and Gambhir 2005).

Firefly luciferase can be used in conjunction with Renilla luciferase. Renilla luciferase oxidises a different substrate, coelenterazine. The resulting emission spectrum of Renilla is different to that of Firefly luciferase, and therefore both systems can be used simultaneously to observe more than one interaction (Michnick, *et al*. 2010). Split Renilla luciferase has also been used individually, for example to detect viral PPIs in influenza. Influenza B polymerase acidic protein and basic protein were known to interact, which is consistent with literature (Deng, *et al.* 2011).

Guassia luciferase is much smaller than Firefly and Renilla luciferase and its luminescence is 100-fold more intense (Tannous, *et al.* 2005). Remy and Micknick developed an assay by fusing the split Guassia luciferase to each part of a leucine zipper (Remy and Michnick 2006). They demonstrated that the system could work with a reversible PPI using the rapamycin inducible FKBP/FRB interaction (Figure 1.11). Levels of bioluminescence observed correlated well with rapamycin concentrations (Remy and Michnick 2006).

Despite only 48% sequence identity, the two click beetle luciferases have very similar predicted secondary structures to Firefly luciferase. The click beetle luciferases were dissected into fragments based on those that had been engineered for firefly luciferase. The fragments comprised amino acids 2-413, and amino acids 395-542. The emission spectra of click beetle red (CBR) and click beetle green (CBG) have a λ_{max} of 615 nm and 540 nm respectively.

While CBR and CBG both turn over the same substrate, their emission maxima are far enough apart to be resolved. These fragment pairs were successfully tested with the rapamycin inducing interaction between FKBP and FRB (Figure 1.11). Both pairs of click beetle luciferase were used to show signalling in the ubiquitin - proteasome pathway. The N-terminal fragment of CBR (red) was fused to IκBα and the N-terminal fragment of CBG (green) was fused to β-catenin (β-cat), while the C-terminal fragment of CBG was fused to β-TrCP, which is a common partner of both β-cat and IκBα (Figure 1.12). All three constructs were co-transfected into cells and luminescence was monitored and successfully showed the different interactions of the target proteins at different times (Villalobos, Naik *et al.* 2010).

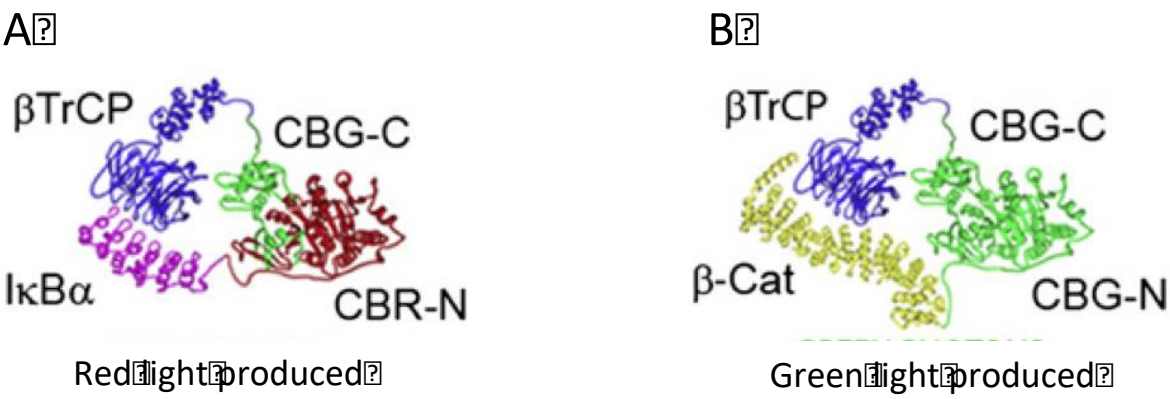

Figure 1.12 Fusion proteins for click beetle green (CBG) and click beetle red (CBR) luciferase.

A) The N-terminal of CBR was fused to IκBα, and the N-terminal of CBG was fused to β-cat. B) The C-terminal of CBG was fused to βTrCP. Image adapted from Villalobos, *et al*. (2010).

Recently, purified firefly luciferase fragments have been used in a completely *in vitro* system, in the first demonstration that this type of assay with a luciferase is ideal for diagnostics. The split firefly luciferase was fused to FKBP and FRB and the interaction was induced with rapamycin (Figure 1.11). There was a high signal to background ratio and the detection of luminescence was very quick. The stability was investigated by incubating the interacting proteins for 1 h at 37ºC and then, on completing the assay, the luminescence reduced to just 1.5%. The stability would have to be improved for further use in

diagnostics, but these results show potential (Ohmuro-Matsuyama, *et a*l. 2013).

1.4.3 Split TEM-1 β-lactamase

The ampicillin resistance gene (amp) encodes the 29 kDa, monomeric TEM-1 β-lactamase that inactivates β-lactam antibiotics. Wehrman, *et al* (2002) and Galarneau, *et al* (2002) split β-lactamase for use in PCAs. In both cases, the enzyme was split at almost the same position (Galarneau, *et al*. 2002, Wehrman, *et al*. 2002), residues 26-196 (BLF[1]) & 198-290 (BLF[2]) and residues 25-197 (α-fragment) & 198-288 (ω-fragment) respectively. Flexible Gly_4Ser linkers of different lengths were introduced between the target protein and the β-lactamase fragments in both studies (Galarneau, *et al.* 2002, Wehrman, *et al.* 2002). The β-lactamase signal was optimised in the Galarneau *et al* (2002) study by introducing the M182T mutation that stabilises wt β-lactamase (Sideraki, *et al.* 2001) within the BLF[1] fragment (Galarneau, *et al*. 2002). The mutant version of BLF[1] displayed superior results compared with the original BLF[1] fragment (Galarneau, *et al*. 2002).

In the Wehrman *et al* (2002) study, the fragments of β -lactamase were fused to the Jun and Fos helices of the transcription factor AP1, that are known to interact (Wehrman, *et al.* 2002). The interaction between the helices mimics the interaction of two target proteins in a PCA. Using the interaction between Jun and Fos a library was made to screen for improvement in the split β-lactamase system. The library comprised tri-peptide inserts that were introduced between the C-terminus of the α-fragment and the linker, and the N-terminus of the ω-fragment and the linker. The peptides were produced from a reduced alphabet that enriched charged peptides by using the degenerate codon VRK, where ‘V’ is any base except thymine, ‘R’ is either of the 2 purines, and ‘K” is a Ketone. Therefore, this degenerate codon set only produces the amino acids His, Gln, Arg, Asn, Lys, Ser, Asp, Glu, and Gly. The purpose of enriching charged peptides relied on the premise that a charge-charge interaction would have the greatest effect on stabilising the two fragments once they were brought together by the Fos and Jun helices. After

selecting for clones using increasing ampicillin concentrations, 12 clones exhibiting enhanced activity were chosen and analysed. The tripeptide inserts always occurred in the α-fragment, so the ω-fragment remained unchanged. The α-fragment with the insert Asn-Gly-Arg (NGR) exhibited the greatest effect and was further analysed. The NGR mutant reduced the signal to noise ratio 1000-fold for interaction with just the Jun and Fos helix. A further interaction between the extracellular domain of the human immune cell antigen CD40, and a 12-mer peptide (BW10-1), which had previously been shown to interact, was also tested. Here, the NRG mutant showed a 12-fold increase over the original α-fragment. In the same study the rapamycin induced interaction between FKBP and FRB (Figure 1.11) was also used as a model interaction to successfully test this split protein assay in mammalian cells (Wehrman and Kleavelan. 2002).

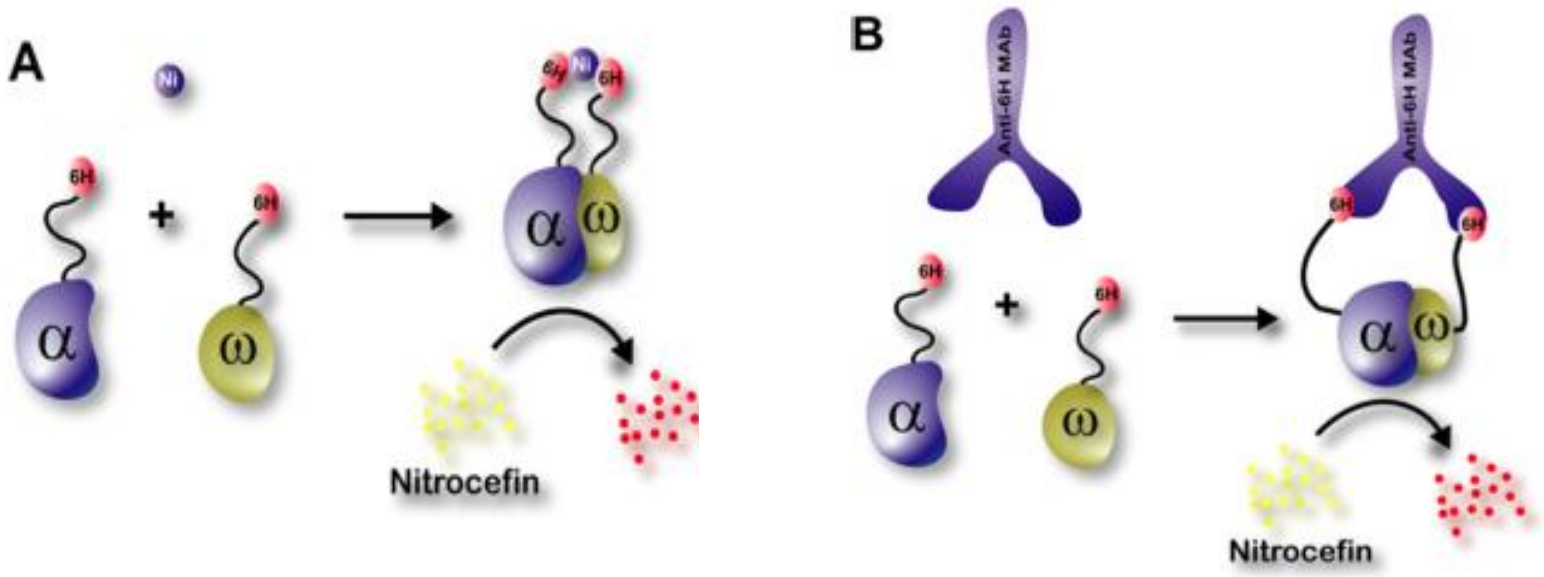

Figure 1.13 *In vitro* nitrocefin assay with fragments of β-lactamase

This schematic displays the interaction of the two β-lactamase fragments. (A) Demonstrates the interaction being brought together with a small molecule, the divalent metal nickel, in this case. (B) Demonstrates the two fragments being brought together by a large molecule, in this case, an anti His antibody. Figure adapted from de las Heras, *et al*. (2008).

Split proteins generally perform much better *in vivo* than *in vitro*. The act of splitting a protein will compromise the integrity and stability of the protein. The reason split proteins are better in cells is most likely due to the presence of chaperone proteins (Wehr and Rossner 2016). There have, however, been some *in vitro* studies involving β-lactamase fragments (de las Heras, *et al*. 2008, Fry, *et al*. 2008, Schnee, *et al.* 2012).

In vitro studies have been conducted utilising purified fragments of split β-lactamase. These were expressed with a His6 tag separated from the fragment by a linker. As demonstrated in Figure 1.13 association of the fragments was initially mediated by using nickel ions and then using an anti-His-tag antibody. The interaction of the two β-lactamase fragments was detected using nitrocefin, showing functional complementation (de las Heras, *et al*. 2008). The same purified split β-lactamase system was used to detect anti-herpes simplex virus (HSV) type 1 and type 2 immunoglobulin G (IgG) (Fry, *et al*. 2008). One of the enzyme fragments was linked to a peptide, which is specific for HSV IgG, and the second enzyme fragment was linked to protein G, which binds all IgGs. Upon peptide and protein G binding to HSV IgG the enzyme fragments were brought together.

Split β-lactamase was used in another cell free assay to investigate the interactions of the human cytomegalovirus (HCMV) nuclear egress complex (Schnee, *et al*. 2012). The two non-functioning fragments of β-lactamase (Galarneau, *et al.* 2002) were fused to the two proteins of interest from HCMV nuclear egress complex and then purified. When brought together in a cell-free PCA, a nitrocefin assay confirmed that the HCMV proteins interacted (Schnee, *et al*. 2012).

1.4.4 Other split enzymes of interest

In one particular study, the redox enzyme horseradish peroxidase HRP has been split and used in a PCA assay (Martell, *et al*. 2016). This is of particular interest, in the context of this thesis, because HRP is a redox enzyme and could be used in conjunction with an electrode to create an amperometric biosensor. Martell *et al* determined by rational design, 17 different split sites chosen on solvent exposed loops, shown on Figure 1.14. When tested, 7 of

the 17 fragment pairs that were created, regained some activity (Martell, Yamagata *et al.* 2016).

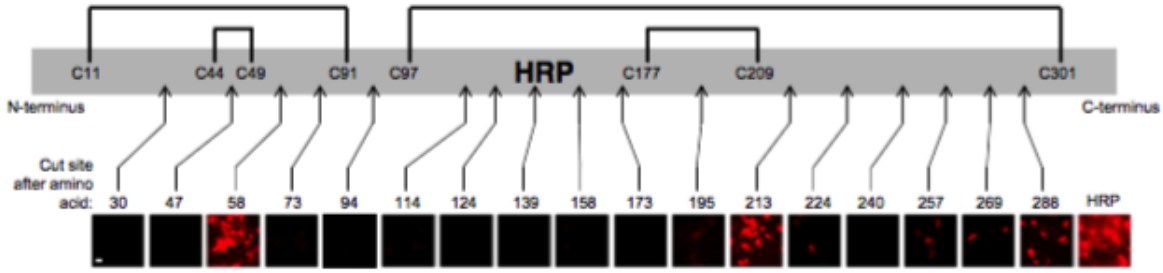

Figure 1.14 HRP gene with arrows indicating the 17 cut sites.

Fluorescent images show that cut sites at 58, 195, 213, 224, 257, 269, and 288 have some fluorescence. Disulphide bonds are shown. Figure adapted from (Martell, Yamagata *et al.* 2016)

The most active fragment pair, sHRPa' and sHRPb', still gave a lower fluorescence intensity than full-length HRP when tested with Amplex UltraRed in live cells. The brightness was improved by directed evolution of the sHRPa' and sHRPb' fragments in turn, using yeast display. The clones of interest were then tested in mammalian cells and two were shown to yield a signal as intense as full-length HRP (Martell, *et al*. 2016). This has only been shown in vivo and there are serious challenges to expression of full length HRP in bacterial systems and so it is unlikely that this will be a useful system for in vitro PCAs. However, alternative simpler redox enzymes that can be produced and purified from bacteria may be developed, such as ascorbate peroxidase.

1.4.5 Split enzymes in biosensor technology

A split-protein protease sensor has been designed where intramolecular coiled coils were connected via a linker to the C-terminal domain of firefly luciferase. As depicted in Figure 1.15, upon cleavage of the intramolecular coiled-coil, a second coil attached to the N-terminal fragment of firefly luciferase interacted with the first coil, thus bringing the two fragments of luciferase back together. Figure 1.15 demonstrates how the cleavage leading to an 'on' state and light was produced (Shekhawat, Porter *et al*. 2009).

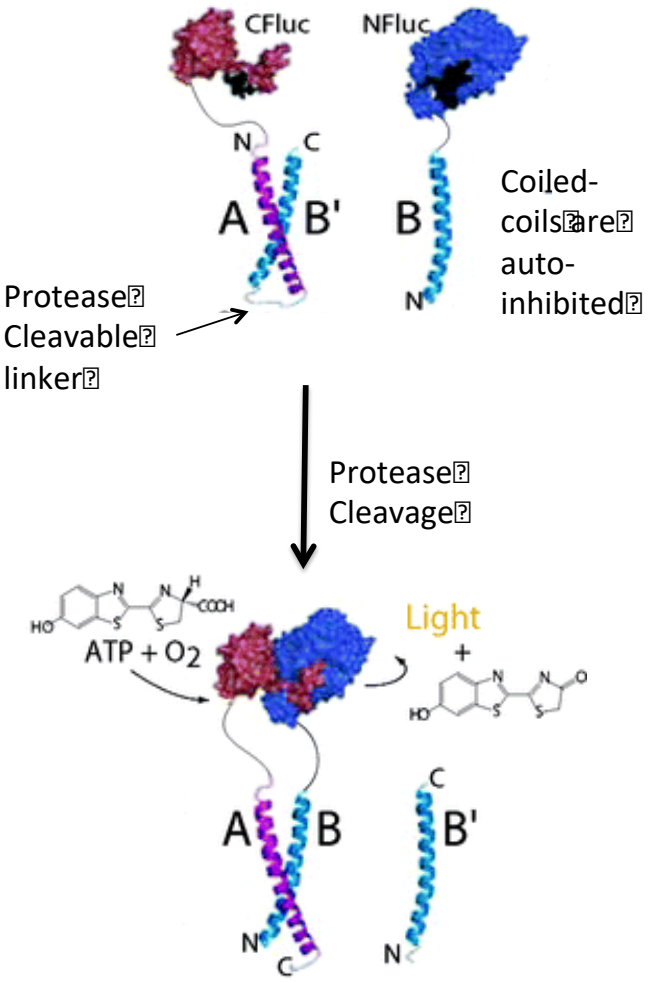

Figure 1.15 Split firefly luciferase used in a protease sensor.

Auto inhibited coiled coils attached to fragments of firefly luciferase. Upon cleavage of the coiled coils the fragments can come together and light is produced. Figure adapted from Shekhawat, *et al*. (2009).

Shekhawat *et al* (2009) went on to use the same auto-inhibited coiled coil system with split β-lactamase with success. These experiments were performed in rabbit reticulocyte lysates like many other PCA assays (Shekhawat, *et al*. 2009).

1.5 Alkaline phosphatase

In nature there are many alkaline phosphatases (APs; EC 3.1.3.1) that occur in numerous organisms from all three domains of life: archaea (Wende, *et al*. 2010, Sharma, *et al*. 2014) bacteria (Kim and Wyckoff 1991) and eukarya (Sharma *et al.*, 2014). Generally, alkaline phosphatases are homodimeric enzymes and each catalytic site contains two zinc ions and one magnesium ion. Mammalian alkaline phosphatases are less thermostable, have a higher pH optimum, and have higher *K*m values compared with bacterial APs. These properties, however, differ noticeably between the different mammalian AP isozymes (Millan 2006). *E. coli* has three isozymes of alkaline phosphatase, identified by different migration patterns on a starch gel and from different patterns after tryptic digest. (Schlesinger and Andersen 1968). The three isoforms are a product of 2 slightly different monomers, which differ only in an N-terminal arginine. Isozyme 1 contains identical monomers with the arginine. Isozyme 3 contains identical monomers without the arginine, and isozyme 2 is a mixture of the two different monomers (Piggot, *et al.* 1972).

The structure and mechanism of *E. coli* alkaline phosphatase (ECAP) is well studied and many wild type and mutant crystal structures are available. It is a homodimer with 449 residues in each monomer without the N-terminal arginine (Garen and Levinthal 1960). There are 43 structures in the Protein Data Bank (PDB) to date, for ECAP. These entries include wild type alkaline phosphatase (Kim and Wyckoff 1991, Stec, *et al*. 2000, Bobyr, *et al*. 2012), and ECAP in complex with tungsten, vanadate, cobalt phosphonic acid, mercaptomethyl phosphate and aluminium fluoride, (Holtz, *et al.* 1999, Holtz, *et al*. 2000, Wang, *et al.* 2005, Peck, *et al*. 2016) to help study intermediate catalytic states. Other structures include mutations in the active site (Stec, *et al*. 1998, Wang and Kantrowitz 2006, Andrews, *et al.* 2013), mutation of residues that coordinate with metal ions (Tibbitts, *et al*. 1994, Ma, *et al*. 1995, Murphy, *et al.* 1995, Ma and Kantrowitz 1996, Tibbitts, *et al*. 1996, Murphy, *et al.* 1997, Zalatan, *et al*. 2008) and mutations that change the kinetic parameters (Dealwis, *et al.* 1995, Dealwis, *et al.* 1995, Le Du, *et al.* 2002, Sunden, *et al*. 2015). The residues responsible for catalysis have been investigated and are well understood (Garen and Garen 1963), and therefore the mechanism for catalysis can be

deduced.

1.5.1 Alkaline phosphatase mechanism

Alkaline phosphatase catalyses the hydrolysis of phosphate monoesters, but a transphosphorylation reaction occurs when there is a large concentration of a phosphate acceptor, as depicted in the kinetic scheme for alkaline phosphatase, Figure 1.16 (Coleman 1992).

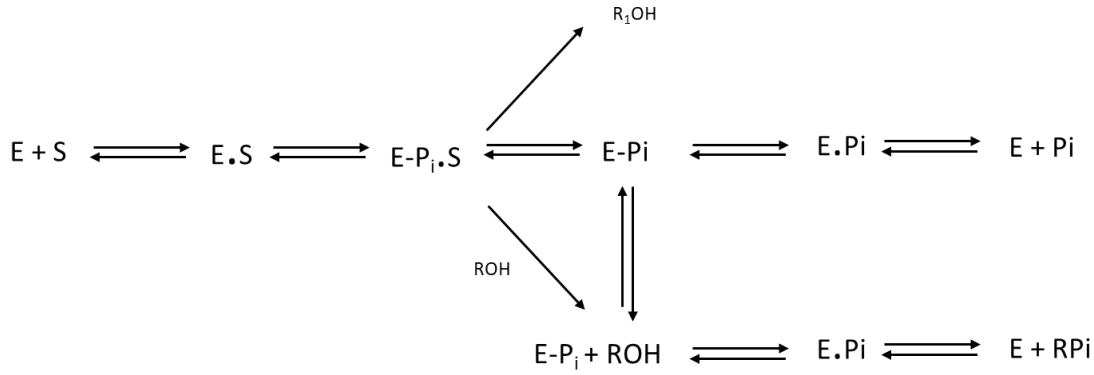

Figure 1.16 Kinetic scheme for alkaline phosphatase.

This description takes into account both hydrolysis and transphosphorylation. E is the enzyme, E-Pi is the phosphoenzyme complex, S is the substrate, R_1OH is the alcohol product, ROH is the phosphate acceptor, and P_i is the inorganic phosphate

The crystal structures of wild type ECAP, with and without phosphate in the active site, along with the crystal structure of the Cd (II) substituted enzyme, give enough information to suggest a mechanism. Alkaline phosphatase without phosphate is clearly the native state, whereas when phosphate is bound, it is predominantly in the $E{\cdot}P_i$ form. The Cd (II) substituted enzyme is mainly in the $E\text{-}P_i$ form (Kim and Wyckoff 1991). As shown in Figure 1.16 alkaline phosphatase has two different types of activity; hydrolysis and transphosphorylation. It is understood that the serine at position 102 creates the phospho-serine intermediate and both reactions go through a phospho-serine intermediate ($E\text{-}P_i$). The structures of many mutant enzymes, with mutations all around the active site, are available (Murphy, *et al*. 1995, Tibbitts, *et al*. 1996, Holtz, *et al*. 2000, Wang, *et al.* 2005, Wang and Kantrowitz 2006,

O'Brien, *et al.* 2008, Zalatan, *et al*. 2008). Other amino acids around the active site and the metal ion hold the substrate in place ready for catalysis, as shown in Figure 1.17. The rate limiting step is the release of phosphate (Murphy, *et al.* 1995, Tibbitts, *et al.* 1996, Holtz, *et al*. 2000, Wang, *et al.* 2005, Wang and Kantrowitz 2006, O'Brien, *et al.* 2008, Zalatan, *et al*. 2008).

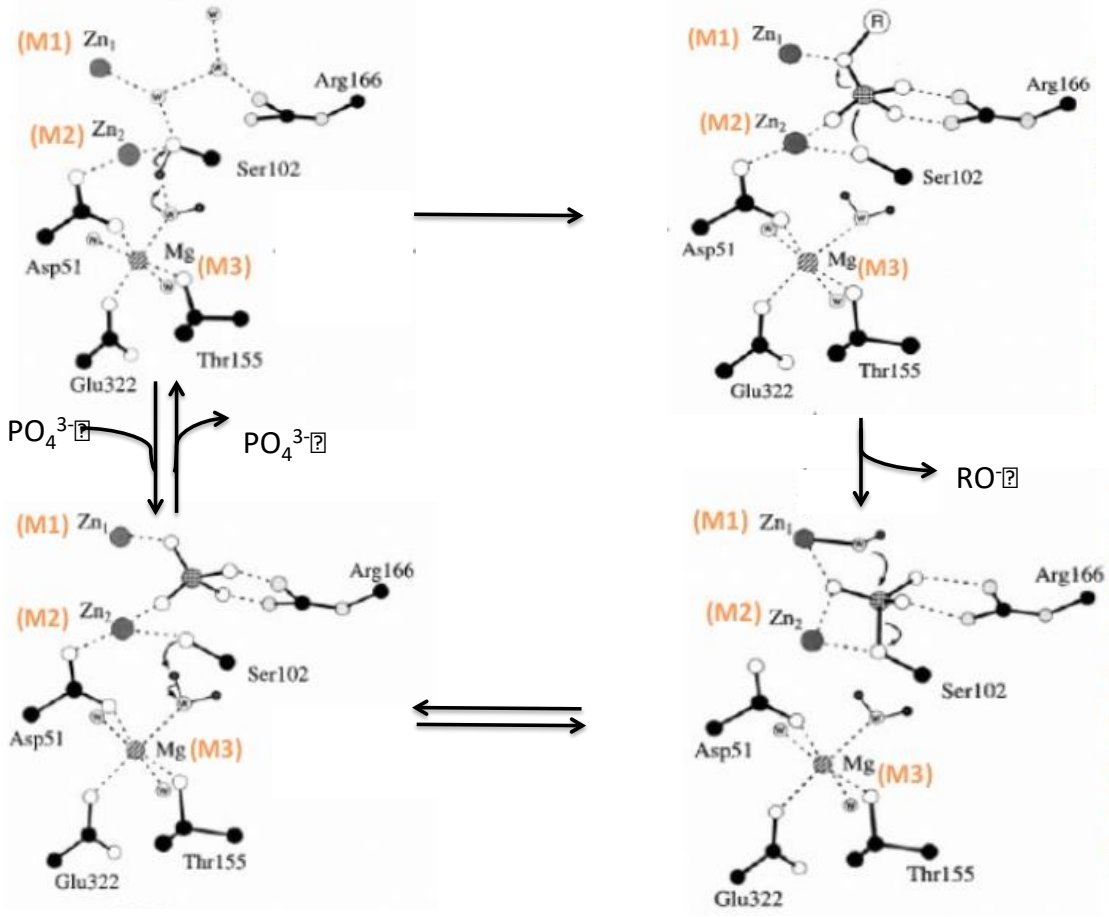

Figure 1.17 Chemical mechanism for alkaline phosphatase.

Serine 103 is activated by the M2 zinc, which initiates a nucleophilic attack on the phosphate group of the phosphate. The M1 zinc activate a water molecule which attacks the intermediate and releases the product. Adapted from (Stec, *et al.* 2000)

As shown in Figure 1.17 the zinc atom (M2) activates Ser 102, which in turn does a nucleophilic attack on the phosphate group of the substrate, creating the phospho-serine intermediate. The M1 zinc is positioned to activate a water molecule which attacks the phospho-serine intermediate, releasing the phosphate product (Stec, *et al.* 2000).

1.5.2 Mutational studies on the active site of alkaline phosphatase

Before the amino acid composition was known it was identified that there was a catalytically important arginine residue (Daemen and Riordan 1974). This was discovered by chemical modification using butanedione and 3 different glyoxals, which rapidly inactivated the enzyme (Daemen and Riordan 1974). The nucleotide sequence of the alkaline phosphatase gene of *E. coli* was determined by Chang *et al* (Chang, *et al.* 1986). The function of the arginine at position 166 has been investigated by site directed mutagenesis showing that this residue is involved in the catalytic mechanism of alkaline phosphatase (Chaidaroglou, *et al.* 1988). However, in this study the arginine was not determined to be essential. The mutant versions of alkaline phosphatase; R166S and R166A had very similar kinetic properties, particularly the $k_{cat,}$ to wild type. The reason given for the inactivation with butanedione is that it is bulky and may have sterically hindered catalysis. However, in conditions where transphosphorylation occurs, the K_m did differ (Chaidaroglou, *et al*. 1988).

When Ser102 is replaced by Cys, the enzyme turnover can still proceed, which is consistent with a phospho-enzyme intermediate using the thiol group instead of the hydroxyl group (Butler-Ransohoff, *et al*. 1988). When Ser102 is replaced with a glycine or an alanine a reduction in excess of 2000-fold in k_{cat} was observed (Wang and Kantrowitz 2006). When Ser102 is replaced with a threonine (S102T) it shows a reduction in excess of 4000-fold in k_{cat} and effectively traps the enzyme in a covalent intermediate state (Wang and Kantrowitz 2006). Some S102T crystals were soaked with inorganic phosphate (Pi), and the structures were determined both with and without Pi. The threonine was covalently attached to the phosphate a shift of the phosphate by 1.3 Å compared to wild type was observed. The stereochemistry of the phosphorus was inverted compared to the wild type enzyme, which is probably why this mutation allows the covalent intermediate structure to be trapped (Wang and Kantrowitz 2006).

1.5.2.1 The effects of zinc in *E. coli* alkaline phosphatase

Zinc is essential for alkaline phosphatase activity (Schlesinger 1966). The two zinc ions are referred to as Zn1 and Zn2. Zn1 is penta-coordinate: The imidazole nitrogens of His331 and His412, both carboxyl oxygens of Asp327, and one of the phosphate oxygens. Zn2 is tetra-coordinated by the imidazole nitrogen of His 370; the carboxyl oxygens of Asp51 and Asp369, and one of the phosphate oxygens (Figure 1.15) (Kim and Wyckoff 1991).

1.5.2.2 Increasing catalytic efficiency

Chaidaroglou and Kantrowitz (1998) mutated aspartate 101 to alanine (D101A) and showed that it had enhanced the catalytic activity in the presence of a phosphate acceptor. In the absence of a phosphate acceptor the turnover rate is 37 s^{-1} compared to 70 s^{-1} for wild type. The K_m for para-nitrophenyl phosphate (pNPP) decreases to 3.7 μM for D101A from 7.4 μM for wild type. Therefore, there is little difference in k_{cat}/K_m (Chaidaroglou and Kantrowitz 1989).

Mandecki *et al.* (1991) investigated 9 different amino acids which were within 10 Å of the catalytically important residue Ser 102. These were residues Val 99, Thr 100, Thr 101, Ala 103, Ala 104, Ser 105, Ala 106 and Thr 107 along with Lys 328. Approximately 170 mutants were screened and 8 showed an increase in specific activity. These were V99A, T100V, T100I, D101S, A103S, A103C, T107V and K328R. D101S had more than a 4-fold increase in specific active over wild type at pH 8.0, and an increase of over 35-fold at pH 10. This represented the highest increase in activity of the 8 mutants (Mandecki, *et al*. 1991). Chen *et al.* successfully crystallised the D101S mutant and determined a 3D structure. This structural information and subsequent experiments, where both wild type and D101S crystals were soaked with phosphatase, suggested that the D101S mutant does not retain the product phosphate to the same extent as wild type (Chen, *et al.* 1992). It is well documented that alkaline phosphatase is inhibited by phosphate (Applebury and Coleman 1969, Applebury, *et al.* 1970) and the release of phosphate is the rate limiting step (Hull, *et al.* 1976) this, explains why the D101S variant is catalytically enhanced (Chen, *et al.* 1992).

Alkaline phosphatase does not turn over substrate when monomeric, but only when it is in a dimer. This indicates there is some form of cooperativity between the subunits. (Schlesinger 1965, Schlesinger and Barrett 1965). Subunit cooperativity could be either conformational selection or induced fit. This is poorly understood, and therefore in order to create a stable monomer, and to understand the mechanism of control and regulation of AP due to subunit interactions, several mutants of the enzyme were constructed (Martin, *et al.* 1999, Boulanger and Kantrowitz 2003, Orhanovic, *et al.* 2006).

1.5.3 Mutational studies on the alkaline phosphatase dimeric interface.

The kinetic properties of wild type ECAP and several mutants: R10A, R10K, R24A, R24A, R24K, R10A-R24A and T59A were assessed in a study by Martin *et al.* (1999). The intramolecular interactions on the dimeric interface of R10, R24 and T59 are shown in Figure 1.18. The studies were performed in 1.0 M Tris, which is a phosphate acceptor, thus the activity being observed is both transphosphorylation and hydrolysis. There is less than a 26% decrease from 69.5 s^{-1} in k_{cat} in all cases and less than a 30 % decrease in K_m from 20.6 μM. The kinetic parameters for all of the variants were similar to wild type at pH 8.0, 25^o C and 1.0 M Tris using pNPP as a substrate (Martin, *et al.* 1999).

The key difference between variants and the wild type was in their stability. They were tested at a range of pH values (3.0 – 7.4) to investigate the pH at which the dimers would separate into monomers. A sucrose density profile showed the wild type enzyme was monomeric at pH 3, a mixture of species at pH 3.5 and a dimer at pH 4 and above. The same conditions were tested on a size exclusion column, and the data agreed with those of the sucrose gradient. A sucrose gradient at pH 4 indicated that all of the mutant proteins are monomeric but, as expected, the wild type remained dimeric. At pH 4.5 R10A, R24A and R24K are monomeric, R10A-R24A, R10K and T59A show a mixed population. Finally, at pH 5.0, R24K, R24A and R10A-R24A show a mixed population whereas T59A and R10A both show dimeric peaks (Martin, *et al*. 1999).

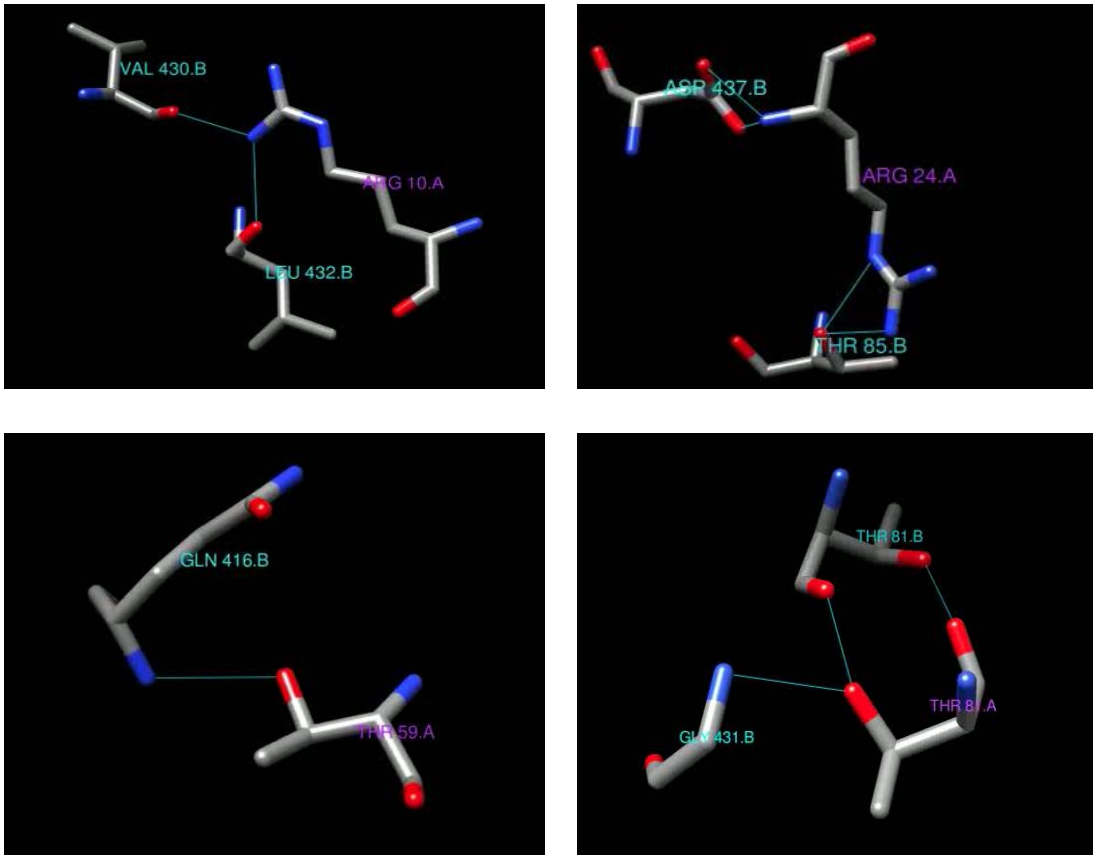

Figure 1.18 Interactions of R10, R24, T59, and T81 of one subunit (A; purple) that are all located at the dimeric interface.

Hydrogen bonds are shown as blue lines to residues on the other subunit (B; cyan). (a) R10 interacts with backbone carbonyl oxygens of V430 and L432. (b) R24 interacts with side chains of T85 and D437. (c) T59 interacts with the main chain of Q416. (d) T81 interacts with T81 and G431.

The study (Martin *et al.,* 1999) went on to show transverse urea gradient gel electrophoresis (TUGGE). Folded compact proteins travel with high mobility in the absence of urea. Unfolded chains in high urea will be retarded in the gel. Wild type AP has a distinct pattern with fast moving protein below 2.7 M urea and slow moving protein at a higher concentration of urea. All of the six mutants had the same unfolding pattern as each other but different from the wild type enzyme. The mutants unfolded at a lower concentration of urea. This demonstrates that each variant forms a less stable dimer than the wild type enzyme (Martin, *et al.* 1999).

As shown in Figure 1.18 the side chain of R10 forms hydrogen bonds to the backbone oxygens of L432 and V430. In this study Martin *et al.* (1999) changed R10 to both an alanine and a lysine. Substituting to an alanine negates both of the hydrogen bonds whereas a lysine only negates the hydrogen bond to V430. The side chain of R24 interacts through a hydrogen bond with the side chain of T85 and D437, and the backbone of T433. Mutating to an alanine negates all three interactions. Finally, the R group of T59 forms a hydrogen bond with the backbone of Glu416 (Martin, *et al.* 1999). The mutations most prone to dissociation were identified as R24A and R24K, suggesting that of the three residues studied, R24 is the most important for dimer stability. Further to the quaternary stability, the TUGGE demonstrated these mutations also have an effect upon the tertiary structure (Martin, Pastra-Landis *et al.* 1999).

The T81A mutation is also at the subunit interface as shown in Figure 1.18. It has a limited effect on substrate turnover, but as a consequence of the mutation the stability was reduced (Orhanovic, *et al*. 2006). In this study, the T81A mutation was chosen because it interacts with T81 in the opposite monomer via a hydrogen bond in the centre of the dimeric interface, and it was postulated that it might have some role in dimeric stability. If there was a small conformational change it would not be obvious in a crystal structure, but the β-sheet stretching underneath the active site to the dimeric interface seems to communicate, via a hydrogen bond, between two threonines at position 81 and Gln83 (Orhanovic, *et al*. 2006) .

The kinetic properties of T81A were compared with the wild type enzyme. The K_m for wild type and T81A were 7.8 μM and 7.3 μM respectively. The assay conditions were the same as in the study by Martin *et al*. (1999). The k_{cat} was reduced for T81A to 37.0 s^{-1} from 61.8 s^{-1} for wild type AP. The metal ions from wild type and T81A were removed by chelation with EDTA and then were re-introduced, and wild type activity was restored but T81A activity was not. (Orhanovic, *et al*. 2006) .

A mutation that successfully produced a stable monomer was T59R (Boulanger and Kantrowitz 2003). However, this mutant monomer was unlikely to ever be capable of associating as a homodimer as there is an obvious steric clash and positive charge repulsion (Boulanger and Kantrowitz 2003).

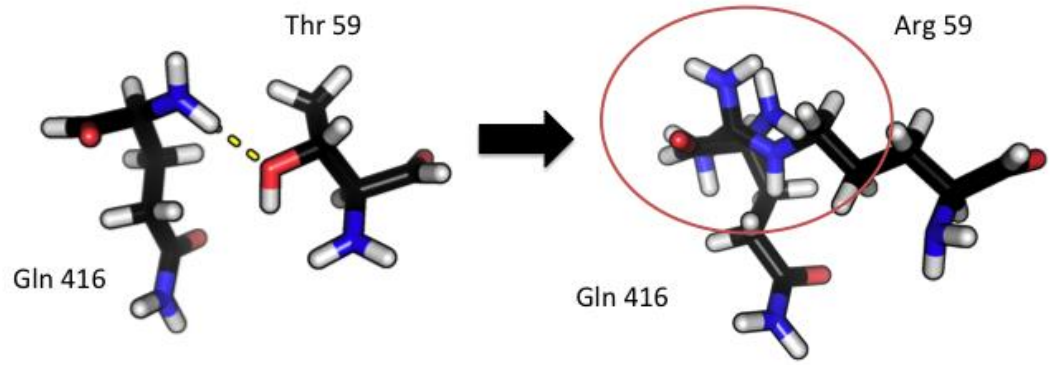

Figure 1.19 A schematic of the T59R mutation.

Left; in wild type AP, the hydrogen bond between the side chains of Thr 59 and Gln 416 is shown as a dashed line. Right; when mutated to Arg 59 the large side chain sterically clashes with Gln 416, highlighted with a red circle

Sucrose density gradient analysis showed wild type AP and T59A to be dimeric, and T59R to be monomeric. Size exclusion chromatography showed similar retention times for wild type and T59A, whereas T59R had a longer retention time. The Stokes radii were calculated as 3.41 nm for wild type, 3.35 nm for T59A, and 2.93 nm for T59R. The kinetics data for wild type, T59A and T59R were compared and k_{cat} values were 74.7 s^{-1}, 56.3 $s^{-1}$and 2.1 x10^{-4} s^{-1} respectively, demonstrating that wild type and T59A are similar whereas the T59R cat aonstant was reduced by a factor of ca. 3 x 10^{6}. The K_m values were 21.8 μM, 24.9 μM and 39.2 μM respectively indicating that substrate can bind but catalytic turnover is compromised in the T59R enzyme. Circular dichroism (CD) studies on the three enzymes showed that they have almost identical secondary structure. CD was also used to indicate thermal stability by monitoring ellipticity at 222 nm and revealed that wild type and T59A have a T_m in excess of 90°C whereas T59R had a T_m of only 43°C. Finally, the metal content of the three enzymes was investigated and indicated that wild type and

T59A have a normal content of zinc and magnesium, with T59R having only a trace amount of both metals (Boulanger and Kantrowitz 2003).

1.5.4 Current Uses of alkaline phosphatase

In molecular biology, ECAP is a valuable tool for the removal of terminal mono-esterified phosphate from both ribo- and deoxyribo-oligonucleotides. For example, removing phosphates from a vector helps prevent its re-ligation, thus reducing vector-only background during cloning experiments. ECAP is used in laboratory assays as a reporter enzyme, often fused to an antibody or other protein of interest. These fusions can be used in epitope mapping, histochemistry, immunoblotting, and ELISA (Sambrook, *et al.* 1989).

1.5.5 Substrates of *E. coli* alkaline phosphatase.

ECAP has many substrates as it hydrolyses a wide variety of phosphomonoesters and also catalyzes transphosphorylation reaction by transferring a phosphoryl group to alcohol groups in the presence of certain phosphate acceptors (Garen and Levinthal 1960).

1.5.5.1 Chromogenic substrates

Typically, para-nitrophenyl phosphate (pNPP) is used for chromogenic detection of alkaline phosphatase (Coleman 1992). It is a colourless substance which turns yellow when the phosphate is removed. This colour change can be observed visually, but accurate measurements are made using a spectrophotometer at 405 nm.

1.5.5.2 Electrochemical substrates

4-amino-1-naphthyl phosphate (4ANP) can be used as a substrate for alkaline phosphatase and detected electrochemically. Alkaline phosphatase releases the phosphate, giving 4-amino-1-naphthol-HCl (4AN), 4AN is oxidised to produced 1,4-naphthoininoquinone (4NIQ). The product, 4NIQ releases 2 electrons which can be detected using cyclic voltammetry (Masson, *et al*. 2004).

1.6 Aims of this work

The overall aim was to create a novel, electrochemically active split-enzyme for use in a biosensor. This was to be achieved through a series of investigations, including:

- Splitting β-lactamase and producing purified N- and C-terminal fragments, then exploring whether these fragments can be functionally associated in an *in vitro* assay.
- Mutational studies on the dimeric interface of alkaline phosphatase in order to create a stable monomeric alkaline phosphatase, followed by exploring whether the monomers can be brought back together and catalyse substrate turnover.
- Preparing relevant Affimers that can bind a target molecule at two separate epitopes. Generating fusions between the split enzyme monomers and investigating if this interaction can be used to regenerate a functional enzyme.

Splitting β-lactamase was a proof of concept as it had been used in previous protein complementation assays. **Chapter 3** describes how the β-lactamase coding fragments were cloned, produced, and purified and used in basic assays to assess functional reconstitution.

Chapter 4 deals with alkaline phosphatase and details the residues at the dimer interface that were selected for alteration with the intention of generating a stable monomer. Starting with the known mutant T59R, which forms a stable monomer but cannot interact to dimerise, this residue was further investigated by a saturation mutagenesis approach. A modest alanine substitution library of residues along the dimeric interface was also created. R10, R24, T59, and T81 were all included as they have been shown to increase instability in the enzyme. Bioinformatics analysis was also used to select D28, R34, R62, and Y98. Single and double mutants of these alanine substitutions were created and assayed for activity. One particular residue, R62, was investigated further as it showed promise when mutated to alanine. Saturation mutagenesis was

used to investigate possible residues to determine whether any variants were more stable than the leading double mutant from the alanine library studies.

Chapter 5 describes further characterisation of the most promising mutants from the work reported in Chapter 4. Initially, CD and Optim instruments were used to assess the stability of the proteins, followed by size exclusion chromatography (SEC) and analytical ultracentrifugation (AUC) to assess their monomeric or dimeric state. Complementary coiled-coil sequences fused to the N-terminal of the mutant protein were used to drive association of the mutant forms of the monomers. Further investigations were undertaken into the stability and the secondary structure of the coiled-coil mutant forms.

Chapter 6 describes how Affimers directed to two different epitopes on the model protein GFP were produced. The Affimers were characterised and used in ELISA and sandwich ELISA to show that they can be used with alkaline phosphatase and that two distinct binding sites were recognised. The split alkaline phosphatase was also tested using these two model proteins.

Finally, in **Chapter 7**, future directions for this research are discussed.

Chapter 2
Materials and Methods

2.1 Standard Buffers, Reagents, and Media.

2.1.1 Buffers/reagents

2.1.1.1 Tris-acetate-EDTA (TAE)

40 mM Tris-acetate,
1 mM ethylenediaminetetraacetic acid (EDTA),
made up as a 50 x stock, pH 8.0

2.1.1.2 Tris-borate-EDTA (TBE)

220 mM Tris pH 8.3
180 mM Borate
5 mM EDTA

2.1.1.3 Buffers for chemically competent cell preparation

TFB1	TFB2
3 mM potassium acetate,	10 mM $RbCl_2$
100 mM $RbCl_2$	75 mM $CaCl_2$
50 mM $MnCl_2$	10 mM MOPS,
10 mM CaCl2	15% (v/v) glycerol
15% (v/v) glycerol	

TFB1 pH adjusted to 5.8 with acetic acid and filter sterilised through a 0.2 µm membrane**.** TFB2 pH was adjusted to 6.5 with potassium hydroxide and filter sterilised through a 0.2 µm membrane),

2.1.1.4 IMAC buffers for Affimer and Alkaline Phosphatase purification

LYSIS buffer:

Affimers	Alkaline phosphatase
50 mM NaH_2PO_4, pH 7.4	50 mM Tris pH 8.0
300 mM NaCl	300 mM NaCl
20 mM Imidazole,	20 mM Imidazole

WASH BUFFER:

Affimers	Alkaline phosphatase
50 mM NaH_2PO_4, pH 7.4	50 mM Tris pH 8.0
500 mM NaCl	300 mM NaCl
20 mM Imidazole	20 mM Imidazole

ELUTION BUFFER

Affimers	Alkaline phosphatase
50 mM NaH_2PO_4 pH 7.4	50 mM Tris pH 8.0
500 mM NaCl	300 mM NaCl
300 mM Imidazole,	300 mM Imidazole

2.1.1.5 Buffers for Zif- Alkaline Phosphatase purification

Lysis buffer:	Binding buffer:
500 mM Tris pH 8.0	500 mM Tris pH 8.0
300 mM NaCl	300 mM NaCl

Elution Buffer	Regeneration buffer
50 mM Tris pH 8.0	50 mM Tris pH 8.0
300 mM NaCl	300 mM NaCl
2.5 mM desthiobiotin	1 mM HABA

2.1.1.6 SDS PAGE Buffers

SDS PAGE gel loading buffer (4x)

200 mM Tris-HCl pH 6.8
20% (v/v) glycerol
8% (w/v) SDS
0.4% (w/v) bromophenol blue
20% (v/v) β-mercaptoethanol

15% resolving gel

15% (v/v) acrylamide (Severn Biotech Ltd.),
375 mM Tris-HCl, pH 8.8
0.1% (w/v) SDS
0.1% (w/v) ammonium persulfate (APS)
0.04% (v/v) N,N,N',N',-tetramethylethylenediamine (TEMED)

5% SDS PAGE stacking gel

5% (v/ v) acrylamide (Severn Biotech Ltd.)
125 mM Tris-HCl, pH 6.8
0.1% (w/v) SDS
0.1% (w/v) APS
0.1% (v/v) TEMED

SDS-PAGE running buffer

25 mM Tris pH 8.3
250 mM glycine
0.1% (w/v) SDS

2.1.1.7 Buffer for western blots

Transfer buffer

0.1 M Tris
0.192 M Glycine
20 % Methanol

Tris buffered saline with Tween (TBST)

50 mM Tris
150 mM NaCl
0.1% Tween 20

adjusted to pH 8.0 with hydrochloric acid, filter sterilised through a 0.2 µm membrane

2.1.2 Media

2.1.2.1 LB & LB Agar

Tryptone (10 g/L)
Yeast extract (5 g/L)
NaCl (10 g/L)

2.1.2.2 2TY & 2TY Agar

Tryptone (16 g/L)
Yeast extract (10 g/L)
NaCl (5 g/L)
Agar (12g/L)

2.1.2.3 SOC

Tryptone (20 g/L),
Yeast extract (5 g/L)
NaCl (0.5 g/L)
10 ml 1 M $MgCl_2$ (0.1 M),
10 ml $MgSO_4$ (0.1 M)
1 ml 2 M D-glucose (20 mM).

2.1.2.4 Terrific Broth (TB)

Tryptone (12.0 g/L)
Yeast Extract (24.0 g/L)
Potassium phosphate, Dibasic = 9.4g Potassium phosphate, Monobasic = 2.2 g Final pH 7.2 ± 0.2 at 25°C

2.1.2.5 Super Broth (SB)

Tryptone (35 g/L)
Yeast extract (20 g/L)
NaCl (5 g/L)
1 M NaOH (5 ml/L)

The ingredients above were dissolved in deionised water, (for agar recipe -12 g/L agar was added) and the volume adjusted before the solution was autoclaved at 121 °C, 15 psi for 20 min. After autoclaving, the solution was cooled in a 50 °C water bath for 30 min before addition of antibiotic to the appropriate concentration. For plates the agar was dispensed into

approximately 20 ml per petri dish. For TB and SOC the salt and glucose were added after autoclaving

2.2 Bacterial strains

Different *E. coli* strains were used for replication, purification of DNA and protein production, depending on the protein being produced.

2.2.1 XL-1-Blue

Genotype: *recA1 endA1 gyrA96 thi-1 hsdR17 supE44 relA1 lac [F´ proAB lacIqZ ⊿M15* Tn10 (Tetr)] Source: Agilent

XL1-blue cells were used for DNA manipulation because they are *recA* deficient which improves insert stability and *endA* deficient, which is an endonuclease, thus improves the quality of the miniprep DNA. The *hsdR* mutation also prevents cleavage of cloned DNA by the *EcoK* endonuclease system. Termination of translation is reduced by the *supE44* mutation. The other mutations in the genotype were not necessary, as blue/white selection was not used in this study.

2.2.2 One shot BL21 (DE3) Star

Genotype: F- *ompT hsd*S_B *(*$r_B^-m_B^-$*) gal dcm rne131* (DE3) Source: ThermoFisher

BL21 Star (DE3) cells were used for general protein expression because they are engineered to reduce the degradation of recombinant proteins. The cells also carry the gene for T7 RNA polymerase, therefore, can be used with a T7 promoter. The mRNA is more stable due to a mutation in the RNaseE gene (*rne131*). The levels of endogenous RNases are reduced, which in turn increases the stability of mRNA, making the transcripts more available for the ribosome.

2.2.3 SHuffle T7 Express

Genotype**:** F´ lac, pro, $lacI^q$ / Δ(ara-leu)7697 araD139 fhuA2 lacZ::T7 gene1 Δ(phoA)PvuII phoR ahpC* galE (or U) galK λatt::pNEB3-r1-cDsbC ($Spec^R$, $lacI^q$) ΔtrxB rpsL150(Str^R) Δgor Δ(malF)3 Source: NEB

Shuffle T7- Express cells were used for alkaline phosphatase expression as they have been optimized by a number of mutations. This strain is engineered to promote disulphide bond formation in the cytoplasm as it constitutively expresses a chromosomal copy of the disulfide bond isomerase DsbC. DsbC promotes the correction of mis-oxidized proteins into their correct form. Furthermore, this strain is deficient in the phoA gene and therefore does not produce any endogenous alkaline phosphatase.

2.2.4 ArcticExpress (DE3)

Genotype: *E. coli* B F^- ompT hsdS (r_8^- m_8^-) dcm^+ Tet^r gal λ(DE3) endA [cpn 10 cpn 60 Gent'] source: Agilent

ArcticExpress cells were used to produce a mutant (T59A-R62A) alkaline phosphatase which was fused to a zinc finger ($zifAP_{T59AR62A}$). The cells were derived from *E. coli* B which naturally lacks the Lon protease and are engineered to remove the OmpT protein which is also a protease; this reduces the degradation of recombinant proteins, similar to that in BL21 (DE3) cells. Transformation efficiency was increased by the presence of the Hte phenotype. Cpn10 and Cpn60 are constitutively expressed from a plasmid that contains a gentamycin-resistance gene. These are the *antarctica* chaperonins which help proteins fold at temperatures of 4-12 ^oC. The other mutations in the genome were not necessary for this study.

2.3 Production of competent *E. coli* cells

A LB agar plate containing an appropriate antibiotic was streaked with a commercial stock of the appropriate bacterial strain and incubated overnight in a static incubator at 37 °C. A single colony was picked and used to inoculate 5 ml 2TY broth that was incubated overnight at 37 °C with shaking at 220 rpm. A 1 ml aliquot of the overnight culture was used to inoculate 50 ml pre-warmed 2TY broth that was then incubated in a shaking incubator at 37 °C with shaking at 220 rpm until an OD_{600} of 0.4 - 0.6 was reached. The cells were then transferred to a sterile 50 ml Falcon tube and chilled on ice for 5 min. After centrifugation at 4 °C for 10 min at 4000 x g in a Hermle Z400 K centrifuge with a 220 97 VO2 rotor, the cell pellet was resuspended in 20 ml ice-cold TFB1

buffer and chilled on ice for 5 min. The cells were then centrifuged again for 10 min at 4000 x g, the supernatant discarded, and the tube wiped dry with tissue. The cells were resuspended in 2 ml ice-cold TFB2 buffer chilled on ice for 15 min and then 200 µl aliquots pipetted into sterile pre-chilled 1.5 ml microcentrifuge tubes. The aliquots were flash frozen in liquid nitrogen and stored at -80 °C.

2.4 Transformation of *E. coli* competent cells

A 50 µl aliquot of competent cells (Section 2.2.4) was defrosted on ice for at least 10 min before addition of 10-50 ng plasmid DNA in a total volume of no more than 5 µl. The mixture was gently mixed and incubated on ice for 30 min before transfer to a 42 °C water bath for 45 s. The microcentrifuge tube was then transferred immediately to ice for a minimum of two min before addition of 1 ml 2TY broth, pre-warmed to 37 °C. The culture was then placed in a shaking incubator at 37 °C with shaking at 220 rpm to permit recovery and expression of the antibiotic resistance protein. After one hour, a 100 µl aliquot was plated onto an agar plate containing the appropriate antibiotic and the remaining culture was centrifuged at 4000 rpm for 4 min in a microcentrifuge. All but 100 µl of the supernatant was discarded and the remaining broth used to resuspend the bacterial pellet which was then plated out onto a second agar plate containing the appropriate antibiotic. Both plates were incubated at 37 °C in a static incubator overnight.

2.5 Molecular Biology

2.5.1 Cloning

2.5.1.1 TEM-1 β-lactamase fragment cloning

Fragment A of the coding region of the β-lactamase gene was amplified using PCR. The PCR reaction contained 50 ng of template DNA, 2.5 µl 10x Phusion buffer (NEB), 2 µl of 10 mM dNTPs, 2 µl of 10 nM forward and reverse primer, 200 U Phusion polymerase (NEB), and double distilled water (ddH_2O) to 25 µl. The PCR products were digested for 3 h with NdeI and EcoRI, according to the manufacturer's instructions (New England Biolabs - NEB). A 2 µl aliquot of digested DNA was analysed on an agarose gel to check for a correct size product. The remaining DNA was purified using a QIAGEN PCR purification kit. The digested fragment insert was ligated into a pET28c vector digested with appropriate restriction enzymes and treated with Antarctic phosphatase (NEB). The ligation reaction contained 40 ng of linearised, phosphatase-treated pET28c, a 3-fold molar excess of the fragment insert, 1 µl 10x T4 DNA ligase buffer (Roche), 200 U T4 DNA ligase (Roche), and ddH_2O to 10 µl. The reaction was incubated at 16°C for 16 h, followed by transformation into XL-1 Blue competent cells and screening using colony PCR, followed by agarose gel electrophoresis. The identity of clones was confirmed by DNA sequencing

The PCR reaction for fragment B contained 50 ng of template DNA, 5.0 µl 10x KOD buffer (Novagen), 5 µl of 0.2 mM dNTPs, 5 µl of 10 nM forward and reverse primer, 0.02 U KOD polymerase (Novagen), and ddH_2O to 50 µl. The PCR products were digested for 3 h with NcoI and XhoI, according to the manufacturer's instructions (NEB). 2 µl of digested DNA were run on an agarose gel to check for a correct size band. The remaining DNA was purified using a QIAGEN PCR purification kit. The digested fragment was ligated into a pET28c vector digested with appropriate restriction enzymes and treated with Antarctic phosphatase (NEB). The ligation reaction contained 40 ng of linearised, phosphatase-treated pET28c, a 10-fold molar excess of the insert fragment, 1 µl 10x T4 DNA ligase buffer (Roche), 200 U T4 DNA ligase (Roche), and ddH_2O to 10 µl. The reaction was incubated at 16°C for 16 h, followed by transformation into XL-1 Blue competent cells and resulting

colonies screened by colony PCR, followed by agarose gel electrophoresis. The identity of clones was confirmed by DNA sequencing

2.5.1.2 Site-directed mutagenesis

To introduce a point mutation(s), two complementary oligonucleotide primers containing the mutation(s), and designed to bind to complementary strands of the plasmid, were synthesised. Using the pECAP-sort plasmid (see Figure 4.1) as a template, a linear amplification temperature cycling was carried out with KOD DNA polymerase to extend the two primers. Typical conditions were:

Step 1	95°C	Initial denaturation	2 minutes
Step 2	95°C	Denaturation	1 minute
Step 3	55°C	Annealing	1 minute
Step 4	70°C	Extension	1minute/kb
Step 5	Cycle back to step 2 29 times (30 cycles total)		
Step 6	70°C	Final extension	10 minutes

Following temperature cycling, the methylated template DNA which did not contain the mutation was digested by DpnI leaving the non-methylated nicked plasmid containing the introduced mutation(s) on both strands. This was then transformed into XL-1 Blue cells, the resulting plasmid DNA purified from transformants, and the mutation confirmed by DNA sequencing. The following primers were used to introduce mutations during these studies.

T59X alkaline phosphatase

T59A FOR	5′ GATAGCGAGATT**GCA**GCAGCGCGCAATTAC 3′
T59A REV	5′ GTAATTGCGCGCTGC**TGC**AATCTCGCTATC 3′
T59D FOR	5′ GATAGCGAGATT**GAT**GCAGCGCGCAATTAC 3′
T59D REV	5′ GTAATTGCGCGCTGC**ATC**AATCTCGCTATC 3′
T59E FOR	5′ GATAGCGAGATT**GAA**GCAGCGCGCAATTAC 3′
T59E REV	5′ GTAATTGCGCGCTGC**T**TCAATCTCGCTATC 3′
T59F FOR	5′ GATAGCGAGATT**TTT**GCAGCGCGCAATTAC 3′
T59F REV	5′ GTAATTGCGCGCTGC**AAA**AATCTCGCTATC 3′
T59G FOR	5′ GATAGCGAGATT**GGC**GCAGCGCGCAATTAC 3′
T59G REV	5′ GTAATTGCGCGCTGC**GCC**AATCTCGCTATC 3′
T59H FOR	5′ GATAGCGAGATT**CAT**GCAGCGCGCAATTAC 3′
T59H REV	5′ GTAATTGCGCGCTGC**ATG**AATCTCGCTATC 3′
T59I FOR	5′ GATAGCGAGATT**ATT**GCAGCGCGCAATTAC 3′
T59I REV	5′ GTAATTGCGCGCTGC**AAT**AATCTCGCTATC 3′
T59K FOR	5′ GATAGCGAGATT**AAA**GCAGCGCGCAATTAC 3′
T59K REV	5′ GTAATTGCGCGCTGC**TTT**AATCTCGCTATC 3′
T59L FOR	5′ GATAGCGAGATT**CTG**GCAGCGCGCAATTAC 3′

T59L REV 5′ GTAATTGCGCGCTGC**CAG**AATCTCGCTATC 3′
T59M FOR 5′ GATAGCGAGATT**ATG**GCAGCGCGCAATTAC 3′
T59M REV 5′ GTAATTGCGCGCTGC**CAT**AATCTCGCTATC 3′
T59N FOR 5′ GATAGCGAGATT**AAC**GCAGCGCGCAATTAC 3′
T59N REV 5′ GTAATTGCGCGCTGC**GTT**AATCTCGCTATC 3′
T59P FOR 5′ GATAGCGAGATT**CCG**GCAGCGCGCAATTAC 3′
T59P REV 5′ GTAATTGCGCGCTGC**CGG**AATCTCGCTATC 3′
T59Q FOR 5′ GATAGCGAGATT**CAG**GCAGCGCGCAATTAC 3′
T59Q REV 5′ GTAATTGCGCGCTGC**CTG**AATCTCGCTATC 3′
T59R FOR 5′ GATAGCGAGATT**CGC**GCAGCGCGCAATTAC 3′
T59R REV 5′ GTAATTGCGCGCTGC**GCG**AATCTCGCTATC 3′
T59S FOR 5′ GATAGCGAGATT**TCT**GCAGCGCGCAATTAC 3′
T59S REV 5′ GTAATTGCGCGCTGC**AGA**AATCTCGCTATC 3′
T59V FOR 5′ GATAGCGAGATT**GTG**GCAGCGCGCAATTAC 3′
T59V REV 5′ GTAATTGCGCGCTGC**CAC**AATCTCGCTATC 3′
T59W FOR 5′ GATAGCGAGATT**TGG**GCAGCGCGCAATTAC 3′
T59W REV 5′ GTAATTGCGCGCTGC**CCA**AATCTCGCTATC 3′
T59Y FOR 5′ GATAGCGAGATT**TAT**GCAGCGCGCAATTAC 3′
T59Y REV 5′ GTAATTGCGCGCTGC**ATA**AATCTCGCTATC 3′

R62X alkaline phosphatase

R62A FOR 5′ GATTACCGCAGCG**GCC**AATTACGCCG 3′
R62A REV 5′ CGGCGTAATT**GGC**CGCTGCGGTAATC 3′
R62D FOR 5′ GATTACCGCAGCG**GAT**AATTACGCCG 3′
R62D REV 5′ CGGCGTAATT**ATC**CGCTGCGGTAATC 3′
R62E FOR 5′ GATTACCGCAGCG**GAA**AATTACGCCG 3′
R62E REV 5′ CGGCGTAATT**TTC**CGCTGCGGTAATC 3′
R62F FOR 5′ GATTACCGCAGCG**TTT**AATTACGCCG 3′
R62F REV 5′ CGGCGTAATT**AAA**CGCTGCGGTAATC 3′
R62G FOR 5′ GATTACCGCAGCG**GGC**AATTACGCCG 3′
R62G REV 5′ CGGCGTAATT**GCC**CGCTGCGGTAATC 3′
R62H FOR 5′ GATTACCGCAGCG**CAT**AATTACGCCG 3′
R62H REV 5′ CGGCGTAATT**ATG**CGCTGCGGTAATC 3′
R62I FOR 5′ GATTACCGCAGCG**ATT**AATTACGCCG 3′
R62I REV 5′ CGGCGTAATT**AAT**CGCTGCGGTAATC 3′
R62K FOR 5′ GATTACCGCAGCG**AAA**AATTACGCCG 3′
R62K REV 5′ CGGCGTAATT**TTT**CGCTGCGGTAATC 3′
R62L FOR 5′ GATTACCGCAGCG**CTG**AATTACGCCG 3′
R62L REV 5′ CGGCGTAATT**CAG**CGCTGCGGTAATC 3′
R62M FOR 5′ GATTACCGCAGCG**ATG**AATTACGCCG 3′
R62M REV 5′ CGGCGTAATT**CAT**CGCTGCGGTAATC 3′
R62N FOR 5′ GATTACCGCAGCG**AAC**AATTACGCCG 3′
R62N REV 5′ CGGCGTAATT**GTT**CGCTGCGGTAATC 3′
R62P FOR 5′ GATTACCGCAGCG**CCG**AATTACGCCG 3′
R62P REV 5′ CGGCGTAATT**CGG**CGCTGCGGTAATC 3′
R62Q FOR 5′ GATTACCGCAGCG**CAG**AATTACGCCG 3′
R62Q REV 5′ CGGCGTAATT**CTG**CGCTGCGGTAATC 3′
R62S FOR 5′ GATTACCGCAGCG**TCT**AATTACGCCG 3′
R62S REV 5′ CGGCGTAATT**AGA**CGCTGCGGTAATC 3′
R62T FOR 5′ GATTACCGCAGCG**ACC**AATTACGCCG 3′
R62T REV 5′ CGGCGTAATT**GGT**CGCTGCGGTAATC 3′
R62V FOR 5′ GATTACCGCAGCG**GTG**AATTACGCCG 3′
R62V REV 5′ CGGCGTAATT**CAC**CGCTGCGGTAATC 3′
R62W FOR 5′ GATTACCGCAGCG**TGG**AATTACGCCG 3′

R62W REV 5′ CGGCGTAATT**CCA**CGCTGCGGTAATC 3′
R62Y FOR 5′ GATTACCGCAGCG**TAT**AATTACGCCG 3′
R62Y REV 5′ CGGCGTAATT**ATA**CGCTGCGGTAATC 3′

Point mutation for alkaline phosphatase

R10A FOR 5′ GTGCTGGAGAAT**GCG**GCAGCGCAGGGTG 3′
R10A REV 5′ CACCCTGCGCTGC**CGC**ATTCTCCAGCAC 3′
R24A FOR 5′ GGTGGCGCACGT**GCG**CTGACCGGCGACC 3′
R24A REV 5′ GGTCGCCGGTCAG**CGC**ACGTGCGCCACC 3′
D28A FOR 5′ CTGACCGGC**GCC**CAAACCGCGGC 3′
D28A REV 5′ GCCGCGGTTTG**GGC**GCCGGTCAG 3′
R34A FOR 5′ CGCGGCACTG**GCC**GACAGCCTGA 3′
R34A REV 5′ TCAGGCTGTC**GGC**CAGTGCCGCG 3′
T81A FOR 5′ GCTCTGCCTCT**GGC**GGGTCAGTATACC 3′
T81A REV 5′ GGTATACTGACCC**GCC**AGAGGCAGAGC 3′
Y98A FOR 5′ CAAACCGGAT**GCT**GTTACGGATAG 3′
Y98A REV 5′ CTATCCGTAAC**AGC**ATCCGGTTTG 3′

Double point mutation for alkaline phosphatase

T59A-R62A FOR 5′ GATAGCGAGATT**GCA**GCAGCG**GCC**AATTACGCC 3′
T59A-R62A REV 5′ GGCGTAATT**GGC**CGCTGC**TGC**AATCTCGCTATC 3′

Addition of a cysteine for alkaline phosphatase

E407C FOR 5′ GGTAATAGCGAA**TGT**GATAGCCAAGAGC 3′
E407C REV 5′ GCTCTTGGCTATC**ACA**TTCGCTATTACC 3′

2.5.1.3 Introducing the K4 coiled coil into pECAP-Sort.

A plasmid containing the genetic information for the K4 coiled coil was supplied by the Wälti laboratory and was used as a template to amplify a ‘megaprimer’. This ‘megaprimer’ was generated using K4 For and K4 Rev primers and contained a coiled coil coding region:

K4 For: 5′ CCCCGGTGACCAAGGCACGTGGTGGTCAGAAACTGG 3′
K4 Rev: 5′ CAGCACCGGCATCTCAGGGGTACCACCTTTGATAGCAGC 3′

The ‘megaprimer’ contains overlapping regions with the pECAP coding sequence to facilitate insertion of the K4 coiled coil DNA into the pECAP plasmid. This resulted in a plasmid with the DNA encoding the coiled coil being introduced between a linker region and the alkaline phosphatase gene. The Quikchange™ method described for single point mutation introduction was

used. The introduction of the coiled coil sequence was confirmed by DNA sequencing. The resulting plasmid was called pK4_ECAP-sort.

2.5.1.4 Subcloning Affimers from pDHIS into pET11 and pET11AP

pDHIS phagemids containing the open reading frame of each of the Affimers were transformed into XL-1 Blue cells and were cultured for 16 h at 37°C. These colonies were used to inoculate 5 ml each of 2TY with ampicillin (amp) in a 50 ml falcon tube, and incubated for ca. 16 h at 37°C with shaking (220 rpm). Small-scale isolation of the plasmid DNA was performed using a QIAGEN miniprep kit. The plasmid DNA was digested for 3 h with NotI and NheI according to the manufacturer's instructions (NEB). The digested DNA was separated on an agarose gel and the correct size band was excised and purified using a QIAGEN gel extraction kit. The Affimer insert was ligated into a pET11a vector, which had previously been modified to include extra restriction sites, digested with NotI and NheI, and treated with Antarctic phosphatase. The ligation reaction contained 40 ng of linearised, phosphatase-treated pET11a, a 3-fold molar excess of the Affimer insert, 1 µl 10x T4 DNA ligase buffer (Roche), 200 U T4 DNA ligase (Roche), and ddH_2O to 10 µl. The reaction was incubated at 16°C for 16 h, followed by transformation into XL-1 Blue competent cells. Both 50 µl and 250 µl aliquots of the transformation reaction were plated onto each of two 2TY/amp agar plates, then incubated at 37°C for 16 h. Plasmid DNA was prepared from several colonies using a QIAGEN miniprep kit and the clones were screened for successful ligation by colony PCR followed by agarose gel electrophoresis. The recombinant clones were confirmed by DNA sequencing.

2.5.2 Agarose gel electrophoresis of DNA

The agarose gel was prepared and operated using an HU6 Mini or HU10 Mini-Plus horizontal gel unit (Scie-Plas, Harvard Bioscience). The gel was prepared by combining the appropriate volume of TAE with agarose in a 250 ml flask, and heating in a microwave for 2 min until the agarose completely dissolved. The agarose solution was cooled under running cold water with agitation before addition of the 1:10000 volume of SYBRsafe DNA gel stain (Invitrogen).

The molten agarose was then poured into the casting tray in a casting unit, a comb added and the gel left to set at room temperature.

For use, the casting tray containing the agarose gel was removed from the casting unit and placed into the gel running chamber. The comb was removed and TAE buffer was added until the gel was submerged. DNA samples were prepared by addition of 6 x gel loading dye (NEB) and then loaded into the wells of the agarose gel. A 1 µl aliquot of the appropriate DNA size ladder was also combined with 1 µl 6 x gel loading dye and added to a well. Either 1 kb or or 100 bp DNA size ladders (NEB) were used.

Once samples were loaded, the running chamber was connected to the power unit and a voltage of 70 V applied for 40 min. After completion, DNA was either visualised under UV light and photographed, or, if it was to be used for downstream applications, was visualised using a Safe Imager (Invitrogen), which is a blue light transilluminator and does not lead to DNA damage as does UV light, allowing excision of bands from the gel.

2.5.2.1 Gel extraction and ethanol precipitation

The DNA was isolated by gel extraction using the dialysis tube/electrophoresis method due to the low levels of product and potential 50% losses seen for product recovery from gel extraction kits. In this method, DNA was loaded into a 0.7 % agarose gel and separated using a HU6 Mini or HU10 Mini-Plus horizontal gel unit. The gel was visualised on a Safe Imager with Safe Imager glasses and a piece of agarose with the correct band of DNA was cut out using a sterile scalpel, and placed in a piece of dialysis tubing with 0.5 ml TAE. The ends of the dialysis tubing were sealed and placed back in the HU6 Mini or HU10 Mini-Plus horizontal gel unit and a voltage of 70 V was applied for 20 min. The gel was visualized again to make sure that the DNA had migrated out of the gel and into the solution. The DNA was then desalted and concentrated by ethanol precipitation. A 10 % volume of 3 M sodium acetate (pH 5.2) and a 200 % volume of absolute ethanol were added to the eluted DNA solution and the mixture was incubated on ice for 15 min. This was followed by centrifugation at 13,000 x g for 30 min at room temperature. The supernatant was carefully discarded and the DNA pellet was rinsed with 200

µl 70% ethanol followed by centrifugation at 13,000 x g for 15 min. The supernatant was discarded again and left to air dry for 10 min, and then the pellet was dissolved initially in 30 µl of water.

2.5.3 Colony PCR screening of bacterial colonies or cultures

It is possible to directly analyze colonies to determine whether they contain a desired recombinant plasmid, and, at the same time, to set up overnight cultures from the colonies to allow isolation of recombinant plasmids for further study.

3 ml aliquots of SOC medium containing the appropriate antibiotic in 50 ml falcon tubes were prepared. 100 µL aliquots of sterile water were pipetted into 0.2 ml PCR tubes. Using a toothpick, a colony was collected from the agar plate and swirled gently in the sterile water aliquot; the toothpick was then used to inoculate a tube containing SOC medium. This was repeated for each of the colonies to be screened.

Table 2-1 Colony PCR premix

Component	Vol (µl)	Final concentration
5X Green GoTaq Flexi buffer	5	1X
$MgCl_2$ (25 mM)	2	2 mM
PCR nucleotide mix (10 mM each)	0.5	0.2 mM each
Primer (10 pmol/µl)	0.5	0.2 pmol/µl
Primer (10 pmol/µl)	0.5	0.2 pmol/µl
GoTaq Hotstart polymerase (5 U/µl)	0.125	0.025 U/µl
dH_2O	15.375	
TOTAL	24	

The tubes containing the water and dispersed bacterial suspension were placed in a thermal cycler and heated to 99 ^{o}C for 5 min, and then cooled to 20 ^{o}C, followed by centrifugation for 5 min at 13,000 *g* in a microcentrifuge to pellet the cell debris. A 24 µL aliquot of the PCR premix, as detailed in Table 2-1, was added to a PCR tube together with 1 µL of the DNA solution from the bacterial colony. The PCR was performed using the following conditions;

- 94^{o}C, 5 min initial denaturation
- 94 ^{o}C, 30 sec;
- 55 ^{o}C, 30 sec;
- 72 ^{o}C, 2 min

} for 30 cycles

- 72 ^{o}C, 5 min

A 5 µL sample was analysed on an agarose gel whilst the inoculated cultures were placed in an orbital incubator at 37 ^{o}C to allow growth for the culture for subsequent plasmid isolation from PCR positive colonies.

2.5.4 QIAgen miniprep

The QIAprep Spin miniprep kit (Qiagen) was used to purify DNA from *E. coli* cultures. A single colony containing the plasmid to be purified was used to inoculate 5 ml 2TY broth containing the appropriate antibiotic, then incubated overnight at 37 °C in a shaking incubator at 220 rpm. The cells were harvested by centrifugation at 7500 x g for 5 min in a Hermle Z400 K centrifuge with a 220 97 VO2 rotor and the supernatant drained by inverting the tube. The pellet was completely resuspended in 250 µl buffer P1 (50 mM Tris-HCl, pH 8.0, 10 mM EDTA, 100 µg/ ml ribonuclease A, 1 µl/ ml LyseBlue reagent), using a vortex, before being transferred to a 1.5 ml microcentrifuge tube. A 250 µl aliquot of lysis buffer P2 (200 mM NaOH, 1% (w/v) SDS) was added and the solution mixed by inversion until a homogeneous blue colour was achieved. Then 350 µl neutralisation buffer N3 (4.2 M guanidinium chloride, 0.9 M potassium acetate, pH 4.8) was added and immediately mixed by inversion until all the blue colour had disappeared indicating that the SDS had precipitated and the solution had been neutralised. The tube was then centrifuged at 13000 rpm in a microcentrifuge for 15 min to pellet all of the cell debris. The supernatant was applied to a QIAprep spin column, which contains

a silica gel membrane that can bind up to 20 µg DNA in the presence of high concentrations of chaotropic salts, such as guanidinium chloride, and centrifuged for 45 s. The flow-through was discarded and the silica gel membrane was washed to remove impurities by addition of 750 µl buffer PE (10 mM Tris-HCl, pH 7.5, 80% (v/v) ethanol) and centrifuged for 45 s. The flow-through was discarded and the spin column with DNA was centrifuged for a further 60 s to remove any residual ethanol which would prevent loading of the sample onto an agarose gel and inhibit any future enzymatic reactions. The column was transferred to a sterile 1.5 ml microcentrifuge tube, 50 µl of deionised water were carefully pipetted onto the membrane and after 60 s the column was centrifuged for 2 min to elute the DNA, which was then stored at -20 °C.

2.6 Protein Production

In the work described in Chapter 3 there were only three proteins of interest: β-lactamase and two different β-lactamase fragments. In the work described in Chapter 4 there were over one hundred proteins produced due to several small mutagenesis libraries of alkaline phosphatase mutants. Chapter 6 includes several Affimers and three different targets. Each set of proteins was produced differently and the different protocols are detailed in the sections below.

2.6.1 β-lactamase and β-lactamase fragments

β-lactamase was provided in pET28c and was transformed into BL21 star (DE3) cells. The newly cloned, pET28cFragB, C-terminal fragment of β-lactamase (fragment B) was transformed into BL21 star (DE3) cells. A single colony was used to inoculate 5 ml of 2TY medium supplemented with 60 ng/ml kanamycin. This culture was used to inoculate 400 ml of 2TY medium, for both full-length and fragment B, then incubated at 37ºC with shaking until an OD_{600} of 0.6 was reached. 0.5 mM IPTG was added and incubated for a further 8 h. The cells were pelleted by centrifugation at 3600 g for 10 min at 4ºC.

The newly formed pET28cFragA was used for β-lactamase fragment A expression. This vector was transformed into BL21 star (DE3) cells. A single colony was used to inoculate 5 ml of 2TY medium supplemented with 60 ng/ml kanamycin. This culture was used to inoculate 500 ml of auto TB medium (Formedium) and incubated at 25 ºC for 48 hrs. The cells were pelleted by centrifugation at 3600g for 10 min at 4ºC.

2.6.2 Alkaline phosphatase and Alkaline phosphatase mutants

pECAP-sort, pECAP-sort incorporating a mutation, and pK4_ECAP-sort, were transformed into *E. coli* SHuffle competent cells. A single colony was used to inoculate 5 ml of 2TY medium supplemented with 60 ng/ml kanamycin and grown overnight at 37 ºC with shaking at 220 rpm to produce a booster culture. A 5 ml aliquot of the booster culture was used to inoculate 500 ml of 2TY medium, then incubated at 25 ºC with shaking until an OD_{600} of between 0.4 and 0.8 was reached. Rhamnose was added to 0.01 % and incubated for a further 4 h, 6 h or overnight. The cells were pelleted by centrifugation at 3600g for 10 min at 4ºC and frozen for storage.

2.6.3 Zinc-finger alkaline phosphatase fusion protein

pZifAP or pZifAP$_{T59A\text{-}R62A}$ were transformed into ArcticExpress cells. A single colony was used to inoculate 1 ml aliquots of LB broth containing 20 ng/ml of gentamycin (to maintain the chaperone proteins: Cpn10 and Cpn60 which are constitutively expressed), and 50 ng/ml carbenicillin. These cultures were incubated at 37°C with shaking at 220 rpm overnight. A 50 µl aliquot of this culture was added to 50 ml of LB broth containing no selection antibiotics, and incubated at 30°C with shaking at 220 rpm for 3 h. Next, the culture was transferred to 10 °C and incubated with shaking at 220 rpm for approximately 10 min to equilibrate the culture, IPTG was added to each flask to a final concentration of 1 mM and incubated at 10 °C, with shaking at 220 rpm, for 24 h. The cells were pelleted by centrifugation at 3600 g for 10 min at 4ºC and frozen for storage.

2.6.4 Affimers

The pET11a plasmid containing the coding region for the Affimer was transformed into BL21 Star (DE3) cells. A single colony was used to inoculate

5 ml of 2TY medium supplemented with 50 ng/ml carbenicillin and incubated overnight at 37 ºC with shaking (220 rpm). A 1 ml aliquot of this booster culture was used to inoculate 400 ml TB auto-induction media (Formedium) supplemented with 50 ng/ml carbenicillin, 1 x lactose (LAC), and 25 mM succinate. This culture was incubated for approximately 48 h at 25ºC with shaking (220 rpm). The cells were pelleted at 3600 g for 10 min at 4ºC.

2.7 Purification of Proteins

Several protocols for purification of the different proteins used in this study are detailed.

2.7.1 β-lactamase

The *E. coli* pellet from 50 ml of culture was re-suspended in 10 ml of lysis buffer (section 2.1.1.5). The suspension was vortexed for 5-10 min and left to lyse at 4ºC whilst rolling for 1.5 h. The soluble fraction of the sample was separated by centrifugation at 25000 g for 30 min. The supernatant was filtered (0.22 µm) and poured onto a HisPur Ni-NTA column which had been equilibrated with binding buffer (section 2.1.1.5) at 4 ºC followed by 5 column volumes of wash buffer (section 2.1.1.5), and then eluted with 2 column volumes of β-lactamase elution buffer (section 2.1.1.5).

2.7.1.1 Purifying N terminal fragment of β-lactamase (fragment A)

The N-terminal fragment of β-lactamase is insoluble. An inclusion-body prep was carried out by first thawing the cell pellet on ice, followed by re-suspension in 20 ml re-suspension buffer. The cells were lysed by sonication – 6x1 min bursts with 1 min cooling on ice in between each sonication. The insoluble fraction was pelleted (25000 g, 30 min, 4 °C) and the supernatant was discarded. The insoluble pellet was re-suspended in 20 ml detergent wash buffer and incubated for 1 h at room temperature on a see-saw rocker. The insoluble fraction was pelleted (25000 g, 30 min, 4 °C) and the supernatant was discarded. The pellet was washed twice by resuspending in 50 mM Tris.HCl pH 8.0 and incubated for 1 hour at room temperature on a see-saw rocker. The purified inclusion bodies were pelleted (25000 g, 30 min, 4 °C) and stored at -20 °C.

Purification and re-folding of the N-terminal fragment was accomplished on a Ni^{2+}NTA column (Pierce). The column was equilibrated with equilibration buffer. The inclusion bodies were re-suspended in re-suspension buffer and incubated for 1 hour at 4^{o}C, followed by filtration (0.22 µm) to remove large impurities. This was poured onto the equilibrated column, followed by 10 column volumes (CV) re-suspension buffer. Then 50 CV of wash buffer were added, and, since the wash buffer does not contain denaturant, the protein should re-fold on the column. The fragment was eluted in 3 CV of elution buffer.

2.7.1.2 Purifying the C terminal fragment of β-lactamase (fragment B)

The C-terminal fragment was, at least in part, in the soluble fraction. The pellet was lysed using lysis buffer followed by centrifugation of 25000 x g for 35 min. The resin was equilibrated with 5 CV of wash buffer and the filtered supernatant (0.22 µm) added to the column. Then 10 CV of wash buffer were added to the column and the protein was eluted in 3 CV of elution buffer.

2.7.2 Alkaline phosphatase and alkaline phosphatase mutants

The cell pellet containing alkaline phosphatase, or alkaline phosphatase mutant, was thawed at room temperature and mixed with 10 ml of lysis buffer (section 2.1.1.4) per gram of cells. The lysate was pelleted at 25000 x g at 4 ^{o}C for 30 min. The supernatant was filtered (0.22 µm) and then incubated with Ni^{2+} NTA resin (Amintra) for 40 min before being poured into a Pierce, disposable plastic column and washed with 20 ml of wash buffer (section 2.1.1.4), or until the OD_{280} was less than 0.1. The protein was eluted in 0.5 ml fractions with elution buffer until the OD_{280} stabilised.

2.7.3 ZifAP and zifAP Mutants

The cell pellet containing Zif-alkaline phosphatase, or a Zif-alkaline phosphatase mutant, was thawed at room temperature and mixed with 10 ml of lysis buffer (section 2.1.1.4) per gram of cells, for 40 min. The streptavidin resin and buffers were equilibrated to room temperature, during the lysis incubation, and then packed into a column. The column was equilibrated with three column volumes of binding buffer. The sample was added to the column and allowed to enter the resin bed, and was left to exit the column by gravity flow. The flow-through was put through the column a further two times. The column was washed with 10 CV of binding buffer (section 2.1.1.4), and the last CV was kept for analysis. The bound protein was an eluted sample with 3 CV of elution buffer (section 2.1.1.4), collected in 0.5-1 ml fractions. After analysis on SDS PAGE gels, the protein was immediately desalted or dialyzed. The column was regenerated with 5 CV of regeneration buffer followed by 5 CV of binding buffer. If the column needed to be stored this was done in 20% ethanol.

2.7.4 Affimers

E. coli pellets from 400 ml of culture were suspended in 40 ml lysis buffer (Section 2.1.1.4) supplemented with 2 mg/ml lysozyme, cOmplete protease inhibitor tablet (Roche) and 200 U OmniCleave (Epicenter), and incubated at room temperature whilst rolling for 2 h. The cell lysate was then incubated at 50 ^{o}C for 20 min followed by centrifugation at 25000 x g for 35 min. The supernatant was then filtered (0.22 µm) to remove any large impurities. The soluble fraction of the cell lysate was incubated for 1.5 h with HisPur Ni-NTA resin (Pierce) whilst rolling at room temperate. The cell lysate and resin mix were then put through an empty column to collect the resin and leave the flow through. The resin was removed from the column and incubated with 10 ml of wash buffer for 10 min whilst rolling at room temperature. The wash buffer (section 2.1.1.4) was removed and the resin was further washed with 20 column volumes of wash buffer followed by elution with 6 column volumes of elution buffer. These were collected in 6x1 ml fractions.

2.8 Modification of Proteins

Proteins can be modified chemically, often at the thiol on a cysteine residue.

2.8.1 Reduction of disulfides on cysteines

A Tris [2-carboxyethyl] phosphine hydrochloride (TCEP) disulfide reducing gel (Thermo Scientific) was used to reduce the thiol on cysteine residues. A volume of between 100-500 µl of TCEP reducing gel slurry was added to a microcentrifuge tube and centrifuged at 1000 × g for 1 min so that the supernatant was removed. An equal volume of protein (1 mg/ml) was added to the gel, and the tube vortexed and incubated with agitation for 1 h. The tube was centrifuged at 1000 x g for 1 min. The supernatant containing the reduced protein was recovered and used immediately in a biotinylation reaction.

2.8.2 Biotinylation

EZ-link BMCC-biotin (Thermo Scientific) was used to biotinylate the reduced protein. An 8 mM stock solution of BMCC-Biotin was prepared by dissolving 2.1 mg in 500 µl of DMSO. 2 µl of 8 mM stock solution were added to 50 µl of reduced protein (1 mg/ml) and incubated at room temperature for 2 h. The labelled protein was purified from non-reacted BMCC-Biotin by desalting or dialysis.

2.9 Protein characterisation

2.9.1 SDS PAGE Analysis

Protein samples were separated according to their size by SDS-polyacrylamide gel electrophoresis (PAGE). To make sure protein samples were denatured, and for easy loading, soluble samples were mixed with gel loading buffer (section 2.1.1.6) and heated at 95 °C for 3 min. The insoluble fraction was resuspended in 20 % lysis buffer and incubated for 20 min at room temperature, with agitation, and centrifuged at 13000 rpm in a microcentrifuge for 5 min. The supernatant was discarded and the pellet resuspended again

in 20% lysis buffer. The pellet was resuspended in 4 x loading buffer then heated at 95 °C for 3 min.

A 15% resolving gel was poured between Bio-Rad PROTEAN casting plates and allowed to polymerise. To ensure a flat interface between the resolving and stacking gel it was overlaid with water. A 5% stacking gel (section 2.1.1.6) was added to the top of the resolving gel, followed by a comb to create wells. Protein samples were loaded along with either PageRuler Unstained Protein Size Ladder (Fermentas) or Pageruler Prestained Protein Ladder (Fermentas). Gels were run at 150 V in SDS-PAGE running buffer (Section 2.1.1.6) for 55 min.

2.9.2 Protein concentrations

The concentration of an enzyme is central to enzyme activity assays. To ensure accuracy, two different methods for calculating protein concentration were employed: Absorbance at 280 nm and a colourimetric assay; either BCA or Bradfords assay.

2.9.2.1 Absorbance of proteins

The absorbance at 280 nm is based on Beer-Lambert equation: $A= \varepsilon cl$, where A is the absorbance value, ε is the molecular extinction coefficient, c is the analyte concentration in moles/litre or molarity (M) and l is the path length in centimetres. Protein concentrations were determined using a NanoDrop Lite Spectrophotometer (Thermo Scientific), which gives the absorbance reading at 1 cm absorbance equivalent, therefore the path length is 1. A 3 μl aliquot of ddH_2O was loaded onto the instrument and 'blank' was selected from the menu, followed by a repeat with ddH_2O. A 3 μl aliquot of the protein buffer was then measured. If the absorbance was less than 0.04 AU at 280 nm then a 3 μl aliquot of the sample protein was used for the measurement. The molecular extinction coefficients were calculated using the ExPASy protparam tool. For β-lactamase the coefficient is 27880 M^{-1} cm^{-1} and for alkaline phosphatase it is 32890 M^{-1} cm^{-1}. To determine the concentration, the absorbance was divided by the molecular extinction coefficient. To convert to units of mg/ml of enzyme, the molar concentration was multiplied by the

molecular weight, because concentration (moles per litre) x molecular weight (grams per mole) = grams per litre.

2.9.2.2 Bicinchoninic acid (BCA) assay

The reduction of Cu^{2+} ions from the copper(II) sulfate to Cu^{+} by the peptide bonds is proportional to the amount of protein present in a sample. Each Cu^{+} ion is chelated by two molecules of Bicinchoninic acid (BCA) forming a complex that strongly absorbs light at 562 nm and is purple in colour.

A micro BCA protein assay kit from Thermo Scientific was used to examine the concentration of protein samples. Mixing 24 parts of reagent MA with 24 parts of reagent MB, and 1 part reagent MC, prepared a working reagent. 150 µl of each standard, or unknown sample, were pipetted into a 96 well plate. 150 µl of the working reagent were added to each well and incubated at 37 °C for 2 h. The plate was left to cool to room temperature and the absorbance was measured at 562 nm on a Tecan Spark (Tecan) plate reader. The average absorbance measurement of the blank standard was subtracted from all the standard and unknown sample replicates. A standard graph was prepared by plotting the average absorbance for each BSA standard vs. its concentration in µg/ml, and a linear equation for the line was established. This was used to calculate the protein concentration of each unknown sample.

2.9.2.3 Bradford Assay

The Bradford assay was performed with a Coomassie (Bradford) Protein Assay Kit. When Coomassie dye binds with a protein there is an immediate shift in absorption from 465 nm to 595 nm with a colour change from brown to blue.

50 µl of each standard or unknown sample was added to a 1 ml cuvette, and 950 µl of the Coomassie reagent was added to each cuvette. These were mixed and incubated for 10 min at room temperature. Using a UV-2401PC spectrophotometer (Shimadzu), controlled by UV Probe v.2.2 software set to 595 nm, the instrument was zeroed on a cuvette filled only with water. The absorbance of all the standards and samples were measured. The average measurement for the blank replicates was subtracted from the measurements of all standard and unknown samples, and a standard curve was prepared by

plotting the average measurement for each BSA standard vs. its concentration in µg/ml. A linear equation for the line was established which was then used to calculate the protein concentration of each of the unknown samples.

2.9.3 Kinetics analysis of enzyme activity

Enzyme kinetic parameters were used to assess if the newly produced recombinant enzymes in this study were as active as previously reported in the literature, as well as to assess mutants of the enzymes

2.9.3.1 β-lactamase and fragments

In order to measure the kinetic parameters for β-lactamase and β-lactamase fragments, a nitrocefin assay was carried out in which nitrocefin turns from yellow to red upon hydrolysis of the β-lactam ring. Hydrolysed nitrocefin has a λmax of 492 nm. A working solution of 0.5 mg/ml (968 µM) nitrocefin was prepared by adding 5 mg of nitrocefin to 500 µl of DMSO and 1.9 ml of 200 mM phosphate buffer. 50 µl of β-lactamase or β-lactamase fragments at an appropriate concentration were added to a cuvette with nitrocefin, and made up to 1 ml with 200 mM phosphate buffer. The cuvette was immediately covered with Parafilm, inverted, and then placed into a UV-2401PC spectrophotometer (Shimadzu). Absorbance at 492 nm was measured for 60 s using the UV Probe v.2.2 software and the plot of A_{486} against time was used to determine the rate in absorbance units per s. The extinction coefficient of hydrolysed nitrocefin 492 nm is 20500 M^{-1} cm^{-1}, the rate in absorbance units per s was divided by 20500 and then multiplied by 10^6 to convert the units to µM per s.

2.9.3.2 Alkaline phosphatase and alkaline phosphatase mutants

To determine the kinetic parameters for alkaline phosphatase, and alkaline phosphatase mutants, p-nitrophenyl phosphate (pNPP) (NEB) was used. 15 nM enzyme was added to a cuvette with pNPP and made up to 1 ml with either 50 mM Tris buffer pH 8.0 or 1 M Tris buffer pH 8.0. The cuvette was

immediately covered with Parafilm, inverted, and then immediately placed into the UV-2401PC spectrophotometer (Shimadzu). Absorbance at 405 nm was measured for between 30 s and 10 min using the UV Probe v.2.2 software and the plot of A_{405} against time was used to determine the rate in absorbance units per s. The extinction coefficient of hydrolysed nitrocefin at 405 nm is 18000 M^{-1} cm^{-1}, so the rate in absorbance units per s was divided by 18000 and then multiplied by 10^6 to convert the units to µM per s.

Kinetic parameters for all enzymes were determined by measuring activity over a range of substrate concentrations and fitting the plot of rate against substrate concentration to the Michaelis-Menten equation using non-linear regression in OriginPro 9.0: Rate = (Vmax[S])/ (K_M+[S]). Where V_{max} (µM hydrolysed nitrocefin/sec) is the maximum rate of the enzyme, [S] (mM) is the substrate concentration and the Michaelis constant, K_M (mM) is the [S] at half V_{max} and can give an indication of the affinity of the enzyme for the substrate. The turnover number, k_{cat} (s^{-1}) was determined using the equation: $k_{cat} = V_{max} / E_T$ where E_T is the total amount of enzyme.

2.9.3.2.1 Alkaline phosphatase specific activities

Specific activities were used as a high-throughput approach to assess a large number of mutants. The assay to determine specific activities of the mutants was performed in the same way as kinetic analysis (section 2.9.3.2) but only one measurement at one substrate concentration was taken. The rate was divided by the mg of alkaline phosphatase added and then divided by 1000 ml to convert to units of µmol pNP /min/mg alkaline phosphatase.

2.9.3.2.2 Activity Assays

Assay to examine changes before and after addition of a mediator using the activity level of an enzyme is a common theme in this thesis.

2.9.3.2.3 Coiled coil activity assay

The activity of K4-AP and K4-AP mutants at a final concentration of 0.4 nM in 1 M Tris pH 8.0 was detected using pNPP (2 mM final concentration) and the assay was stopped after 30 min with 50 µl 5 M NaOH. The resulting absorbance values were converted to a percentage of wild-type activity.

2.9.3.2.4 Coiled coil inhibition assay

A final concentration of 0.4 nM K4-T59A-R62A protein was incubated with K4 peptide in a concentration range from 25 pM to 20 nM for 2 h in 1 M Tris pH 8.0. The activity was detected using 100 µl (2 mM final concentration) of pNPP, and the assay was stopped after 5 min with 50 µl 5 M NaOH. The A_{405} was converted to the product amount using the Beer-Lambert law as described in Section 2.9.3.2. The amount of product (pNP) was plotted against the Log_{10} of the concentration of K4 peptide

2.9.4 Circular dichroism

Far UV CD was used to analyse the secondary structure of the mutants. The activity of alkaline phosphatase mutants was performed in 1 M Tris-HCl pH 8.0, and it was important to know what was happening with the secondary structure in this buffer. Buffers which contain chloride ions absorb light strongly below 200 nm (Kelly, *et al.* 2005), and therefore the data were processed between 200 nm to 260 nm. Wild-type alkaline phosphatase was investigated as a positive control and it was expected to be folded correctly, and therefore the spectra could be used as a comparison.

CD experiments were performed on a Jasco J715 spectropolarimeter and the spectra were recorded in a 0.02-cm path length using a scan speed of 50 nm/min, a time constant of 0.5 s, and a bandwidth of 2 nm. 3 scans were performed. The Jasco J715 spectropolarimeter gives its raw output in ellipticity, with the symbol θ measured in millidegrees (mdeg). To compare the data with those of others, θ was converted to molar ellipticity, this is given the symbol [θ] and is in units of degrees.cm^2 per decimole. Hence, $[\theta] = \theta / (10 \times c \times l)$ where c is the molar concentration of the sample and *l* is the path length in cm.

To investigate the thermal stability of the T59A-R62A mutant, both with and without the K4 coiled coil, a thermal melt experiment using CD was performed. The intensity of the CD signal at 220 nm was recorded. A 0.02-cm path length cuvette was used with a scan speed of 50 nm/min, a time constant of 0.5 s, and a bandwidth of 2 nm. Three repeats were performed.

2.9.5 Static light scattering and intrinsic fluorescence (Optim)

Simultaneous SLS and intrinsic fluorescence measurements were conducted using an Optim 1000 (Avacta Analytical) to analyse the rate of aggregation of the Affimer and give an indication of their stability. Colloidal stability was measured using SLS at 266 nm, and the data output was given as the onset of aggregation temperature (T_{agg}). Thermal stability was assessed by measuring the intrinsic fluorescence of Tryptophans, which were excited at 266 nm, and extrinsic fluorescence was measured at a range from 300 to 400 nm. The data were reported as a barycentric mean (BCM), The melting temperature (T_m) was calculated using the BCM as a function of temperature. A stepped thermal ramp program was used, set between 20 ^oC and 95 ^oC using 1 °C increments, with an equilibration time of 30 s. Aliquots of 8.8 µl of each protein (1 µg/ml) were measured in triplicate, and the analysis software provided with the Optim 1000 was used to process the data.

2.9.6 Oligomerisation

2.9.6.1 Size Exclusion Chromatography (SEC)

Preparative SEC was performed on a HiPrep 16/60 Sephacryl S-100 HR preparative column, so the protein could be recovered for other assays. The flow rate of buffer was set to 0.5 ml/min in an isocratic fashion on a ÄKTA FPLC and the eluent was collected in 2 ml fractions for 1.25 column volumes. To begin with, five protein standards: β-amylase, alcohol dehydrogenase, albumin, carbonic anhydrase, and *cytochrome c,* were separated on the SEC column for calibration purposes. The sample proteins were loaded onto the column after their first step in purification in as high a concentration as possible.

2.9.6.2 Analytical SEC

A Superdex 200 10/300 GL column was used to analyse the multimeric state of Affimers. The column was equilibrated with PBS with 10% glycerol and 1.2 ml of 2 mg/ml Affimers were added separately to the column. This was eluted in an isocratic fashion using PBS with 10 % glycerol. The flow rate of buffer was set to 0.5 ml/min in an isocratic fashion on a ÄKTA FPLC and the eluent was collected in 0.5 ml fractions.

2.9.6.3 Analytical Ultracentrifugation (AUC)

All of the protein had an A_{280} of between 0.3 and 0.5, and were exhaustively dialysed against 50 mM Tris pH 8.0 using 4 buffer changes, the first two after 2 h each and then changed for overnight incubation, followed by a further change and being left for a further 2 h the next day. A XL-I machine from Beckman Coulter was used, and after the AUC cells were filled and assembled, a centrifugation scan from 3000 rpm to 30000 rpm was run to indicate if any of the cells were leaking. A continuous scan from 5.8 to 7.3 cm at 30000 rpm was set up and data were recorded for every third scan. 200 scans were recorded in total at a constant temperature of 19.8 ^{o}C. The data were fitted using the SEDPHAT and SEDFIT programs (Schuck 2000). SEDPHAT was used to calculate the density and viscosity from the buffer ingredients. The partial specific volume 'v bar' was calculated using the same software for each of the proteins from the amino acid sequence. The 200 data scans were loaded into the SEDFIT program, continuous c(S) distribution was selected and the parameters calculated from the SEDPHAT program were entered. The SEDFIT program was used to fit the data using the Marquardt Levenberg algorithm. To check the fitting, SEDFIT was used to fit the data again using a Simplex algorithm. If the root mean square deviation (rmsd) was =< 0.05, and the Z (stddev) =< 15, this was considered a reliable fit.

2.9.7 Distance dependence of Zif-AP

2.9.7.1 TEV cleavage

20 µg of the fusion protein in 1M Tris pH 8.0 and 10 units of TEV protease were incubated at 30 ^{o}C for 2 h. The protein was analysed by SDS PAGE.

2.9.7.2 Annealing DNA

The zinc finger 'Zif 268' has three fingers and each finger binds a specific sequence of DNA. The recognition sequence for Zif 268 is:

```
5′ GCG TGG GCG T 3′
3′ CGC ACC CGC A 5′
```

Each coloured highlight represents where each of the fingers binds. Single-stranded DNA oligonucleotides were designed to incorporate two binding

sites, with a spacer in between of zero, 5 and 10 base pairs. In each case reverse oligos were designed as a whole oligo or in two parts; thus, a nick would be introduced once the three pieces of DNA were annealed together. Each of the oligos is listed below:

Zif_H2H_0_Fwd	5′ GTGAACTGCGTGGGCGTACGCCCACGCGACGAGC 3′
Zif_H2H_0_Rev_Whole	5′ GCTCGTCGCGTGGGCGTACGCCCACGCAGTTCAC 3′
Zif_H2H_0_rev_nick1	5′ GCTCGTCGCGTGGGCGT 3′
Zif_H2H_0_rev_nick2	5′ ACGCCCACGCAGTTCAC 3′
Zif_H2H_5_Fwd	5′ GTGAACTGCGTGGGCGTGCTCAACGCCCACGCGACGAGC 3′
Zif_H2H_5_Rev_Whole	5′ GCTCGTCGCGTGGGCGTTGAGCACGCCCACGCAGTTCAC 3′
Zif_H2H_5_Rev_nick1	5′ GCTCGTCGCGTGGGCGTTGAG 3′
Zif_H2H_10_Fwd	5′ GTGAACTGCGTGGGCGTGCTCAGTTCAACGCCCACGCGACGAGC 3′
Zif_H2H_10_Rev_Whole	5′ GCTCGTCGCGTGGGCGTTGAGCTGAGCACGCCCACGCAGTTCAC 3′
Zif_H2H_10_Rev_nick1	5′ GCTCGTCGCGTGGGCGTTGAGCTGAGC 3′

Different 20 nM samples of single stranded of DNA were mixed together in a PCR tube in a total volume of 60 µl, which was heated to 95 ^{o}C for 10 min and brought back down to room temperature in 1 ^{o}C steps per min. The resulting duplex DNA was analysed on 4% agarose gels (NuSieve GTG -Lonza) made with TBE buffer.

2.9.7.3 Zinc Finger Assay

Zinc finger-enzyme fusion protein (15 nM) and 15 nM of oligo were added to a 96 well plate. Wild-type alkaline phosphatase was used as a positive, and T59R as a negative control. pNPP was added to 2 mM and the absorbance at 405 nm was measured after 24 h.

2.9.8 Protein – Protein Interactions

2.9.8.1 Bilayer interferometry analysis (BLItZ)

Bilayer interferometry was used to measure binding affinity. The software fits a trend line to the on and off rate, and calculates a dissociation constant (K_D). The chips used on the BLItz system (fortéBIO) are streptavidin chips and so the proteins required biotinylation. The protein was biotinylated using (+)-Biotin N-hydroxysuccinimide ester (Pierce). The biotin linker was dissolved in

DMSO (5 mg/ml). A 100 µl aliquot of dissolved biotin linker was mixed with 100 µl of protein (1 mg/ml) and incubated for 2 h at room temperature followed by desalting on a Zeba column with a MWCO of 7 kDa (Thermo scientific). The streptavidin chips were hydrated in PBS for 10 min and a baseline was taken for 30 s. The biotinylated protein was loaded onto a chip by incubating the chip with the biotinylated protein for 2 min, followed by another 30 s baseline. Association was then calculated for 2 min by incubating with the binding partner. Finally, dissociation was calculated for 2 min by incubation in PBS

2.9.8.2 Enzyme-linked immunosorbent assay (ELISA)

ELISA is a technique for detecting the presence of molecules such as proteins. In an ELISA, a protein is immobilized on a solid surface, usually in a 96 well plate. Then, an antibody that is linked to an enzyme is incubated with the protein of interest. Detection is accomplished by enzyme activity with a substrate to produce a measurable signal. Variations of a simple ELISA included in this study are a phage ELISA, and a sandwich ELISA.

2.9.8.2.1 Sandwich Phage ELISA

In a 96-well Nunc plate, 50 µl of Adhiron 21 (1 µg/ml) was placed in 32 (columns 1-4) of the 96-well plates, another 32 (columns 5-8) were left blank and incubated at 4 ^{o}C overnight. The plate was then washed twice with PBS, blocking buffer was added to each of the wells and incubated overnight at 25^{o}C. 50 µl of mGFP (1 µg/ml) was then added to columns 1-4 and incubated at 4 ^{o}C overnight. The plate was washed twice with PBS, 10 µl of blocking buffer and 40 µl of the supernatant from the phage growth was added to each well. This was incubated at room temperature for 1 hour followed by a single wash with PBS. The enzyme-linked antibody was added, followed by 10 washes with PBS and finally 50µl 3,3',5,5'-Tetramethylbenzidine (TMB) was added and the colour change observed.

2.9.8.3 Enzyme-Linked Affimer assay

Biotinylated Affimers were immobilized onto strep-activated plates (Pierce) at a concentration of 100 µg/ml in phosphate buffered saline (PBS) and incubated at 4 °C overnight. Alternatively, Polysorp microtiter plates (Nunc) were coated with Affimers at 37 °C for 2 h. Plates were washed three times with PBS before blocking non-specific sites with 5% skimmed milk in PBS overnight at 4 ^{o}C. Plates were then washed three times with PBS with 0.05% Tween-20 (PBST). Dilutions of the target protein (GFP) were prepared in 1% skim milk/PBST, added to wells in duplicate and incubated for an additional hour at room temperature, followed by 6 more washes with PBST. The alkaline phosphatase linked Affimer was added and incubated for 2 h at room temperature and washed 6 times with PBST. Activity was measured after incubation with 100 µl of pNPP (2 mM final concentration) for 30 min at room temperature. The reaction was halted by the addition of 50 µl, 3 M NaOH, and the absorbance read at 405 nm.

Chapter 3
Split β-lactamase

3.1 Introduction – split β-lactamase:

Split β-lactamase was generated for use in protein complementation assays (PCA) (Galarneau, *et al*. 2002, Wehrman, *et al*. 2002) to measure the interaction of two proteins through the restoration of beta-lactamase enzymatic activity (Galarneau, *et al.* 2002, Wehrman, *et al.* 2002). The DNA sequences encoding N- and C-terminal fragments of β-lactamase (Figure 3.1) were fused to coding regions for interactive protein partners and the resulting plasmids were co-transfected into Cos-7 or HEK 293 cells. Proof of principle experiments were carried out by (Galarneau, *et al.* 2002) who used Bad and Bcl2, two apoptotic proteins with high affinity for each other. These two proteins were both fused to the N-terminal and C-terminal fragments of β-lactamase. Galarneau *et al* also repeated this experiment showing that the PCA principle could be used with a coiled coil interaction between GCN4 leucine zipper, and the homodimerisation domain of Smad3. Wehrman *et al* (2002) did some similar experiments but used the Fos and Jun coiled-coils to bring the enzyme fragments together. The Bad/Bcl2 or Fos/Jun interactions facilitated association of the fragments of β-lactamase, and subsequent turnover of a chromogenic substrate was detected.

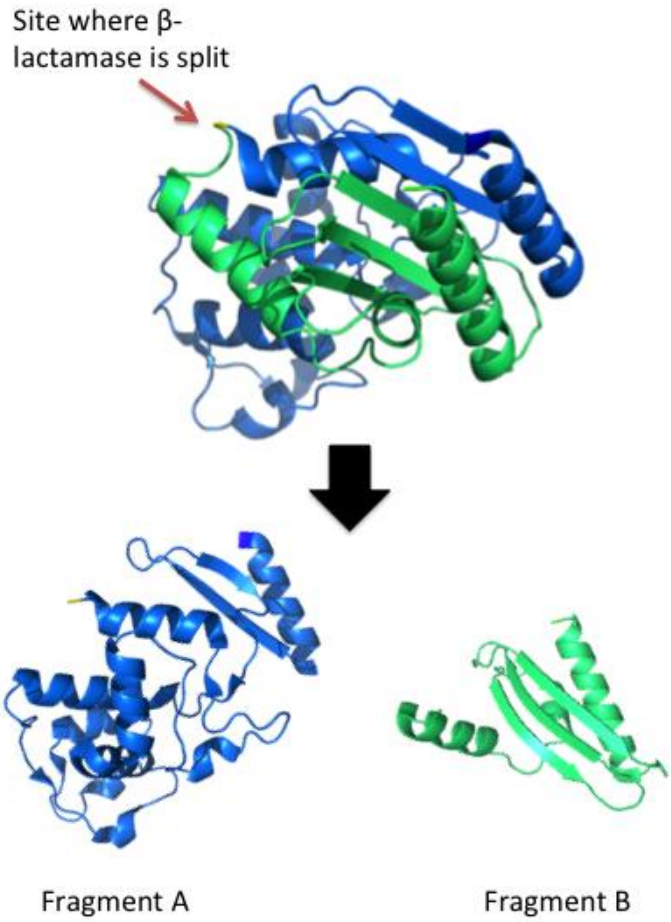

Figure 3.1 The β-lactamase (PDB ID 1ZG4) structure shown in a ribbon format.

The complementing fragments A (N-terminal; blue) and B (C-terminal; green) are shown with the red arrow indicating the position of the split site.

Figure 3.2 highlights the loop (red arrow) that was effectively split by cloning two DNA fragments to create the two β-lactamase fragments, both in literature and in this study. In this study, as a control, a full length functional mature β-lactamase protein, without the signal sequence, was expressed and purified. Furthermore, two β-lactamase fragments, one comprising the N-terminal fragment and one comprising the C-terminal fragment, needed to be cloned, expressed and purified. It is important to note that the majority of split-β-Lactamase assays are performed in fixed cells or cell lysates (Remy, *et al*. 2007). In order to use split β-lactamase in this study it was necessary to determine if the enzyme fragments could be produced and purified for use in an *in vitro* assay. There was a single article reporting that purified fragments

could complement *in vitro*. In this study (de las Heras, *et al.* 2008), purified fragments of β-lactamase. The fragments had His tags at appropriate sites for nickel or anti-His antibody binding, which would bring the fragments back into association with one another, as described in Chapter 1 Section 1.4.3. This study demonstrated that an *in vitro* approach should prove feasible and that the association could be mediated by distinct moieties; ionic nickel and an anti-His antibody (de las Heras, *et al*. 2008).

3.1.1 Full length β-Lactamase

The full-length gene for β-lactamase in the expression vector pET28a was kindly provided by the Radford laboratory (University of Leeds). The pET28awtBla plasmid containing mature full-length β-lactamase without a signal sequence was used as a template to generate the various DNA fragments. To confirm the identity of plasmid pET28awtBla the β-lactamase coding region was confirmed by DNA sequence analysis and a diagram of the plasmid is shown in Figure 3.2.

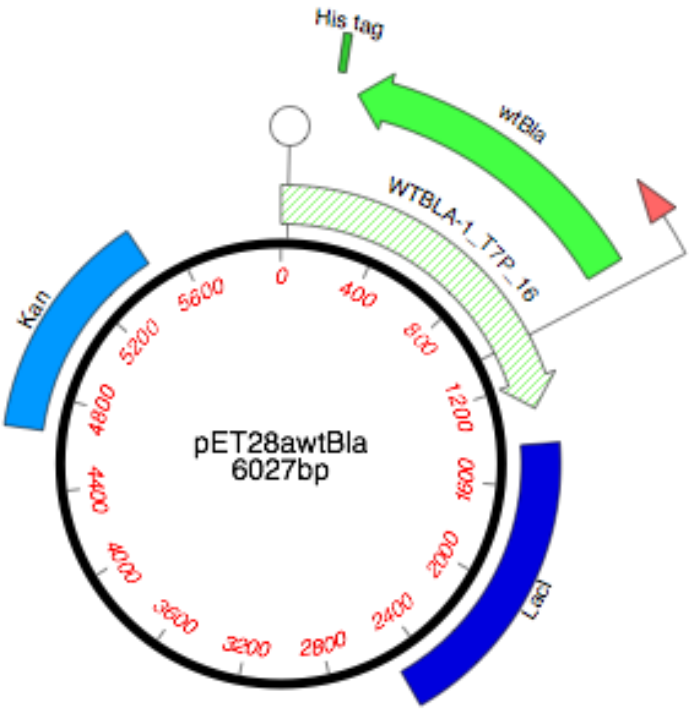

Figure 3.2 Vector map of pETawtBla plasmid containing wild type β-lactamase.

A schematic diagram of pET28awtBla, showing the alignment of wtBLA-1_T7P_16 gene (green strip arrow) with a reference wtBla (solid green arrow). The wtBla gene produces the enzyme. Kan confers kanamycin resistance for bacterial selection and the lac I gene produces the lac repressor which represses wtBla expression until an inducer is added. The red arrow indicates the position of the T7 promoter and the solid green arrow the β-lactamase coding region and direction of transcription/translation, while the white circle represents the transcription terminator.

The pET28awtBla plasmid was used to produce β-lactamase protein and was also used as a template DNA to PCR amplify the coding region fragments for subcloning into pET28c. The fragments were amplified by PCR and appropriate restriction enzyme sites were added by 5' extensions on the PCR primers. The N-terminal β-lactamase encoding peptide was designated fragment A, and the C-terminal encoding fragment was designated fragment B.

3.1.2 β-Lactamase fragments

Figure 3.3 illustrates the approach for the amplification of the β-lactamase fragments. Each of the fragments was amplified from the full-length coding region using primers which introduced 5' restriction sites. Block arrows represent the β-lactamase gene and gene fragments, and the primers are represented by coloured arrows. The restriction sites added to fragment A were 5' Nde I and 3' Eco RI, and for fragment B were 5' Nco I and 3' Xho I. The pET28c vector and PCR gene fragments were digested with the appropriate restriction enzymes, and then ligated. As different enzymes were used at the 5' and 3' ends, the PCR product could be directionally cloned into the vector.

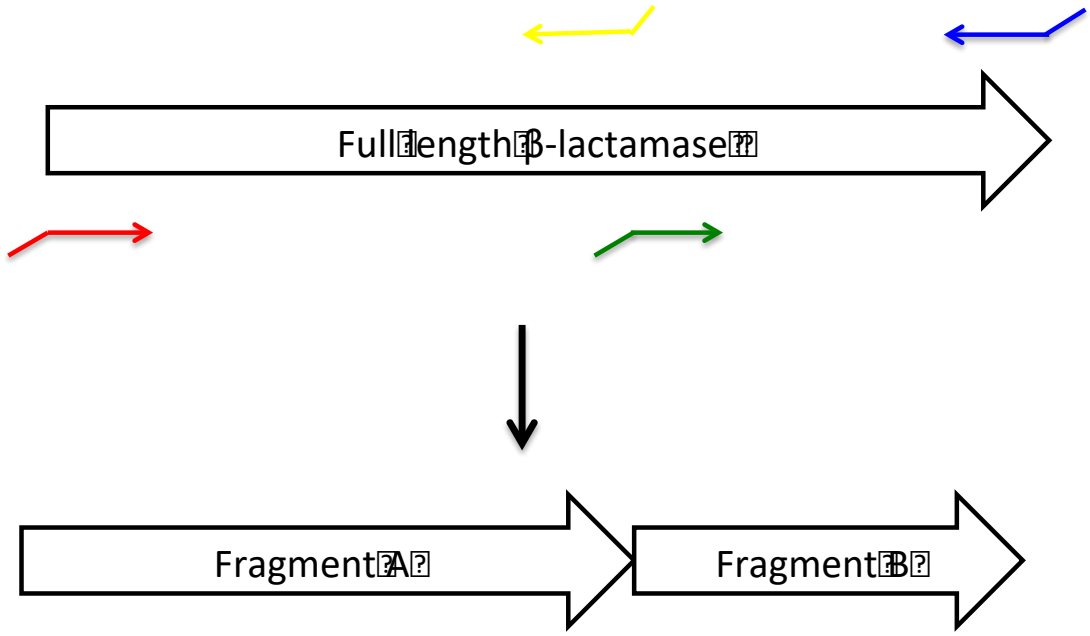

Figure 3.3 Schematic of the strategy for the amplification of the fragments of β-lactamase.

The red and yellow arrows represent primers for fragment A and the green and blue arrows represent the primers for fragment B.

3.1.2.1 PCR amplification

Figure 3.4 shows the PCR products for fragment A and B, which were calculated to be 513 and 273 base pairs respectively. Figure 3.4A shows that fragment A was amplified successfully in good yield, whereas little amplification was observed for fragment B indicating that it was not well amplified. Both fragments were used for ligation reactions and transformed into competent *E. coli* cells. Plasmid DNA was isolated from colonies picked from the Fragment A transformation. Unfortunately, there were no colonies from the fragment B transformation, therefore PCR amplification was optimised. Three different proof reading DNA polymerases: Pfu Turbo, KOD and Phusion were used. An annealing temperature gradient from 57 ^{o}C to 69 ^{o}C was used to investigate the best annealing temperature (Figure 3.4B).

Figure 3.4B shows that Turbo did not produce any products of the correct size. KOD produced products of the correct size, which increased in yield with temperature, although a downside of this is that at higher temperatures a second larger product appears. The PCR using Phusion also produced two products at all the temperatures tested. There is an increase in intensity with temperature, which then decreases after 65^{o}C. The highest intensity of the correct size product was at 65 ^{o}C and 69 ^{o}C, with KOD polymerase

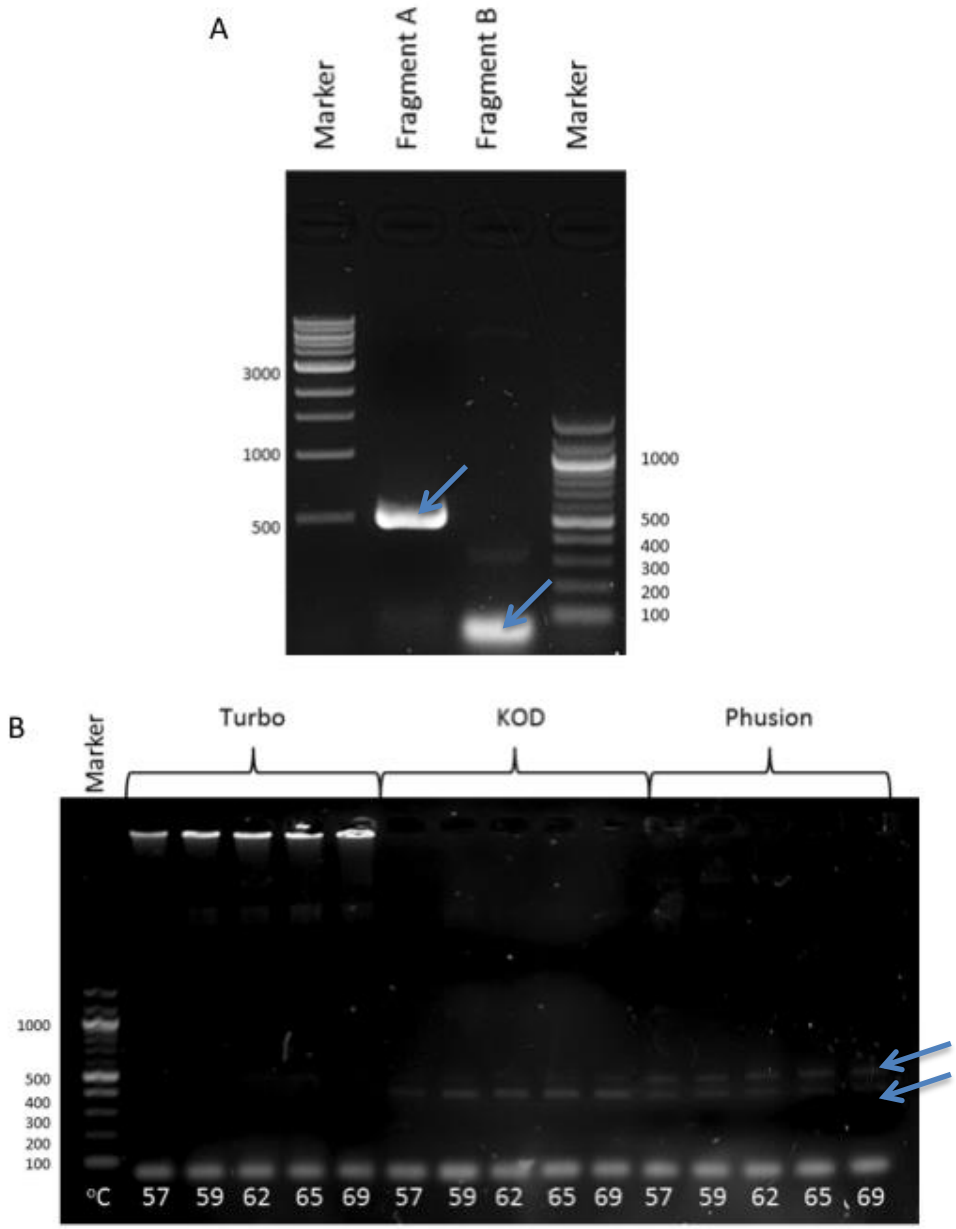

Figure 3.4 Agarose gel (1%) analysis of PCR products for fragment A and fragment B of β-lactamase.

(A) Fragment A showed good yield compared with Fragment B. Two different markers were used; a 100 bp ladder and 1000 bp ladder. The numbers at the side of the gel indicate the size in bps of that band (B). Optimisation of PCR of fragment B over annealing temperatures of 57 to 69 ^{o}C with three different DNA polymerases: Turbo, KOD and Phusion. Using Turbo did not result in any correct size bands. KOD and Phusion show that there are two product bands; the bottom band is the correct size for Fragment B. The marker used was 100 bp ladder and the number on the side of the gel refers to the approximate size in bp.

The conditions chosen for a larger scale amplification were 65ºC with KOD polymerase. The reaction was set up as 5 X 50 µl aliquots giving 250 µl in total. The PCR amplification products were separated on a 1.2% agarose gel, which is a higher than usual percentage, to aid separation of the two products. The lower band was then gel purified.

3.1.2.2 Ligation optimisation

Fragment B was digested with Nde I and Eco RI for 3 h at 37 ºC and a ligation reaction with pET28 was set up at 16ºC overnight. This ligation reaction was then introduced into competent *E. coli* XL-1 blue cells by transformation. However, no colonies grew over a 16 h period. There was sufficient digested vector and insert to set up further ligation reactions, therefore, several ligation conditions were tested to find optimal conditions.

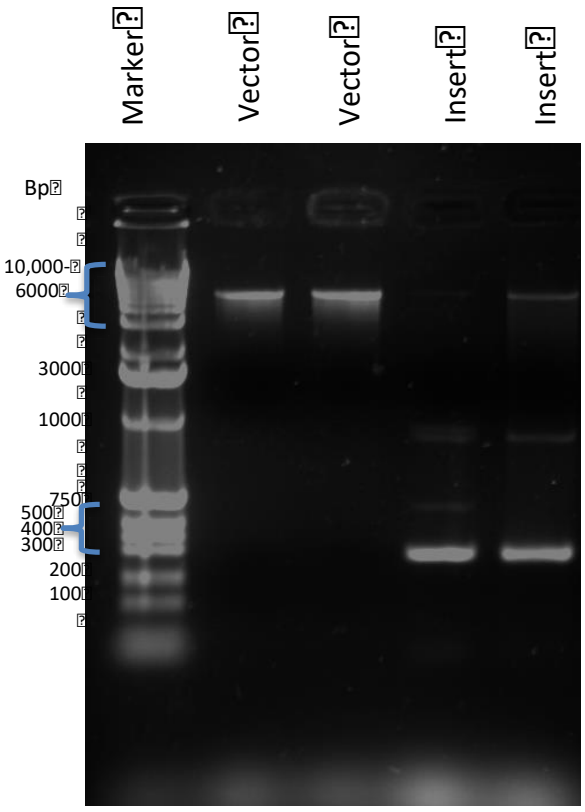

Figure 3.5 Vector (pET28c) and fragment B insert for the ligation reaction. Two separate vector purification and digestion reactions were set up and separated in the two lanes labelled vector. Two separate samples of digested PCR products were also separated in the lanes labelled insert.

The absorbance at 260 nm was used to determine the vector and insert concentrations. Each of the two aliquots of insert and vector were also separated on an agarose gel at the same amount of DNA to ensure the intensities were approximately the same as shown in Figure 3.5. Table 1 displays the different conditions used to ligate fragment B insert and pET28c vector. Both the ratio of insert to vector and the temperature was varied.

Table 3-1 Ligation reaction conditions tested to ligate fragment B of β-lactamase into the pET28c vector. Each ligation reaction was incubated over a 16-hour period.

Temperature	Ratio of Insert to Vector	Ratio of Insert to Vector	Ratio of Insert to Vector
4^{o}C	1:1	3:1	10:1
16^{o}C	1:1	3:1	10:1
20-25 ^{o}C	1:1	3:1	10:1

There were several colonies recovered from the transformation of the ligations conducted at 16 ^{o}C. Whilst colonies grew for samples from all three ratios, the greatest difference between vector only and the test sample was on the 10:1 plate that showed 6 and 50 colonies respectively. Five colonies were picked and colony PCR was performed to identify a colony that contained a recombinant plasmid. Figure 3.6 confirms that all 5 colonies contained recombinant plasmids with an insert of approximately the correct size. The positive control used pET28wtBla (Figure 3.2) while the negative control used pUC19 as the template.

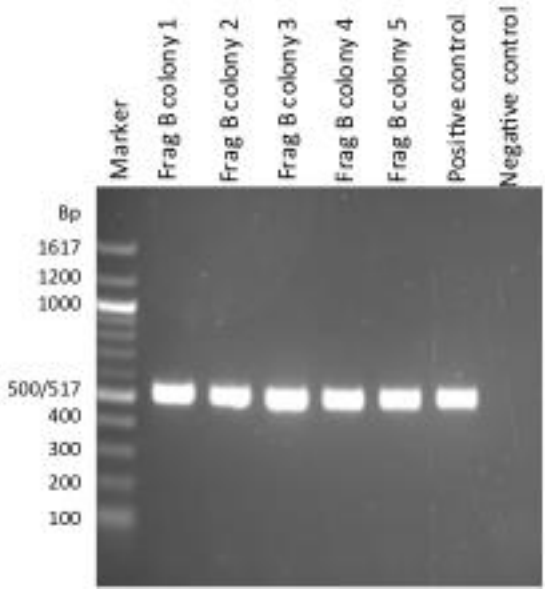

Figure 3.6 Colony PCR to identify correctly cloned fragment B of β-lactamase in pET28c.

The DNA for fragment A or fragment B cloned into pET28c was subjected to DNA sequence analysis to confirm their integrity, and the corresponding amino acid sequences are shown in Figure 3.7. This plasmid was used to produce the recombinant proteins of β-lactamase fragments A and B.

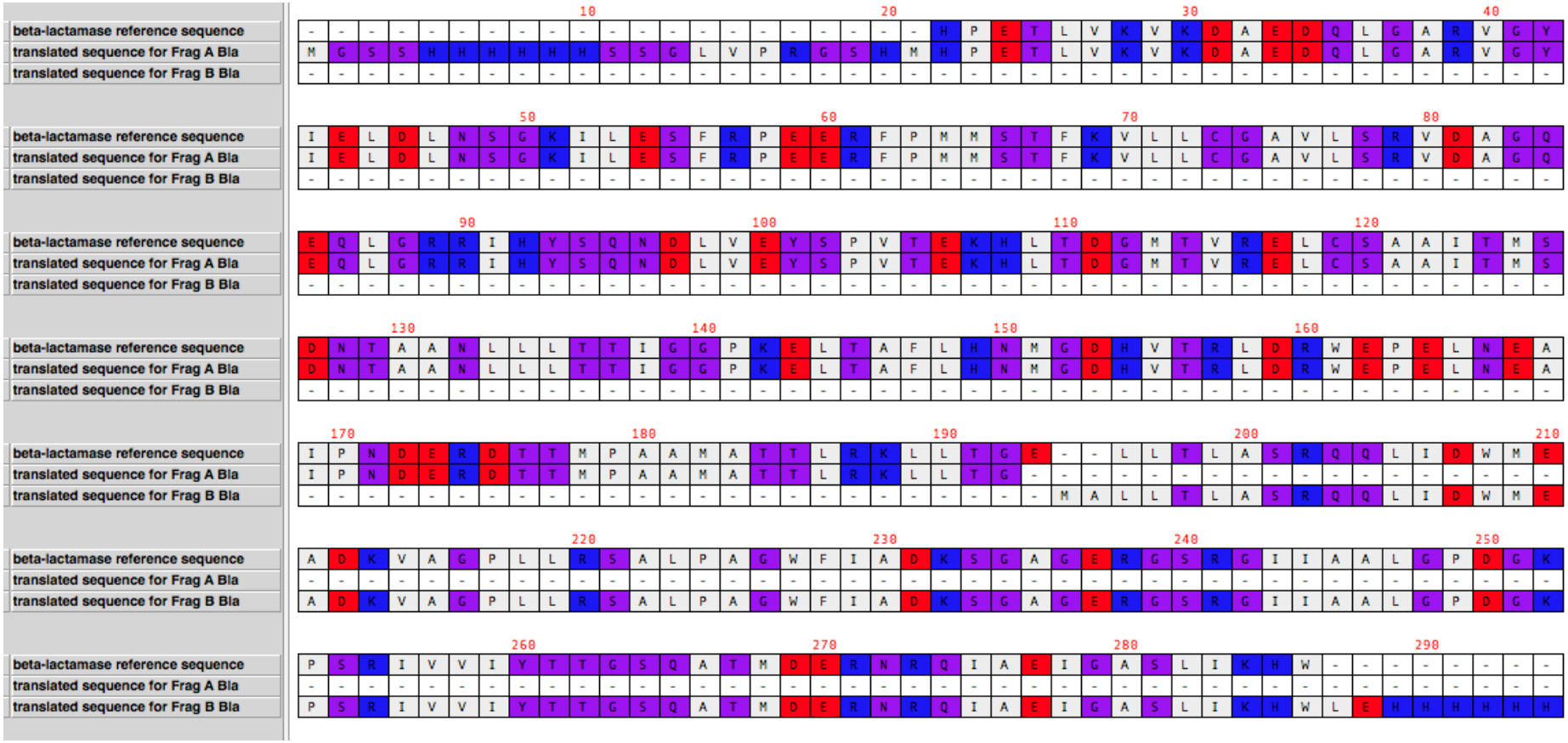

Figure 3.7 Amino acid sequence alignment for fragment A and B of β-Lactamase.

The DNA sequences were translated into a protein sequence for both fragment A and B and aligned against the full-length sequence of β-Lactamase. Fragment A has a N-terminal His tag followed by a small linker region and fragment B has a C-terminal His tag, with three preceding amino acids used as a small linker. White residues are aliphatic, red residues are negatively charged amino acids, blue residues are positively charged amino acids and purple resides are polar amino acids. All the sequences align correctly.

3.2 Protein production of β-Lactamase and β-Lactamase fragments

The vector pET28AwtBla (Figure 3.2) has a T7 promoter, and therefore 0.5 mM IPTG was used to induce expression of full-length β-lactamase in *E. coli* BL21 (DE3) star cells as described in Chapter 2 Section 2.2.2. Samples were taken before induction, then after 4, 8 and 16 h. The samples are shown in Figure 3.8A and indicate β-lactamase was expressed in the soluble fraction. It expressed at the highest yield after 8 h and did not improve further after 16 h. There was sufficient protein for further studies and so the expression was not optimised further.

Several attempts were made to obtain Fragment A in the soluble fraction. Three different *E. coli* cell strains were tested: BL21(DE3) Gold, BL21(DE3) Star and SHuffle; these did not show any difference, and there was a band representing the protein of interest only in the insoluble fraction. Lower induction temperatures of 30^{o}C, 25 ^{o}C, 20^{o}C and 18 ^{o}C were tested in four different media, LB, 2TY, TB and SB. In each case a small band was observed in the insoluble fraction, but again there was nothing present in the soluble fraction. Finally, auto-induction was tried using auto LB, auto TB and auto SB media. Once again, the protein produced was only in the insoluble fraction. However, there was a large band shown on the insoluble protein gel, with auto TB producing the most protein. These expression trials were conducted in 2 ml volumes in a 24 well plate. Fragment A expression was reproduced in a 500 ml volume, and again, as expected, the protein fragment expressed almost completely in the insoluble fragment as shown in Figure 3.8B. It was decided to purify from the insoluble fraction.

Fragment B was expressed using 0.5 mM IPTG induction in BL21(DE3) star *E. coli* cells. Figure 3.8C shows fragment B was expressed mainly in the insoluble fraction, as there is a larger band in this insoluble fraction lane. However, there was a small band in the soluble fraction. This was not further optimised as there was sufficient soluble protein for functional complementation testing.

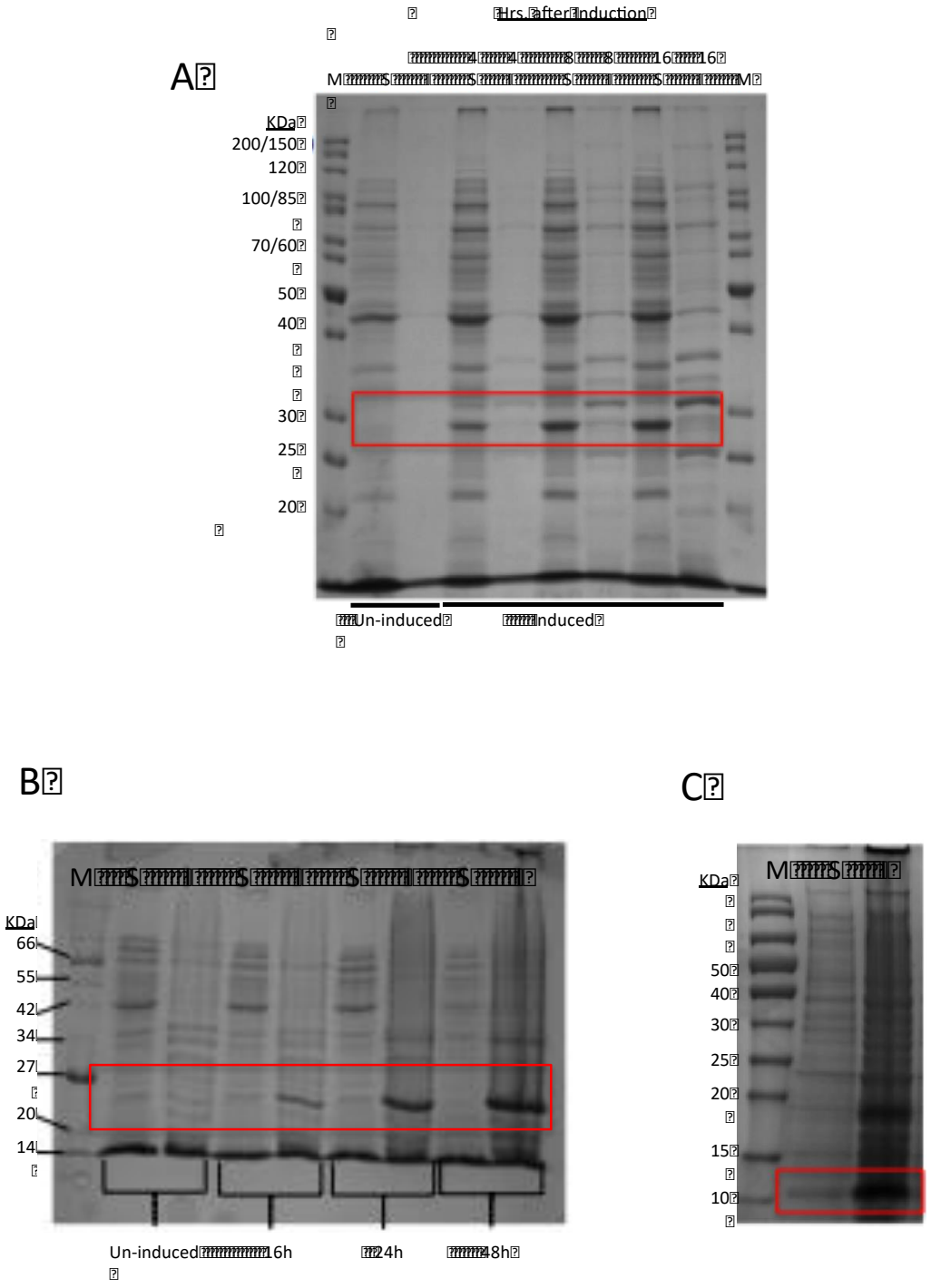

Figure 3.8 β-lactamase expression analysed by SDS PAGE.

The red boxed bands are the correct size bands for each of the β-lactamase protein or protein fragments. A) Full-length β-lactamase is expressed in the soluble fraction. B) Fragment A is expressed in the insoluble fraction. C) Fragment B of β-lactamase has some protein in both fractions.

3.3 Protein purification of β-Lactamase and β-Lactamase fragments

Purification of full-length β-lactamase was performed by affinity chromatography. There was a His tag present and therefore, immobilised nickel on agarose beads was used to purify the protein by affinity chromatography as described in Chapter 2 Section 2.7.1. The cell lysate was loaded on to the column, and a sample of the flow through was collected. The column was then washed with 10 CV of wash buffer and a sample from the last CV was collected. The protein was eluted with elution buffer and collected in two 1 ml samples. Figure 3.9 shows all the samples and a molecular weight ladder. The protein was then dialysed into a PBS with 20 % glycerol, flash frozen in liquid nitrogen and stored at -80ºC until it was used in downstream experiments.

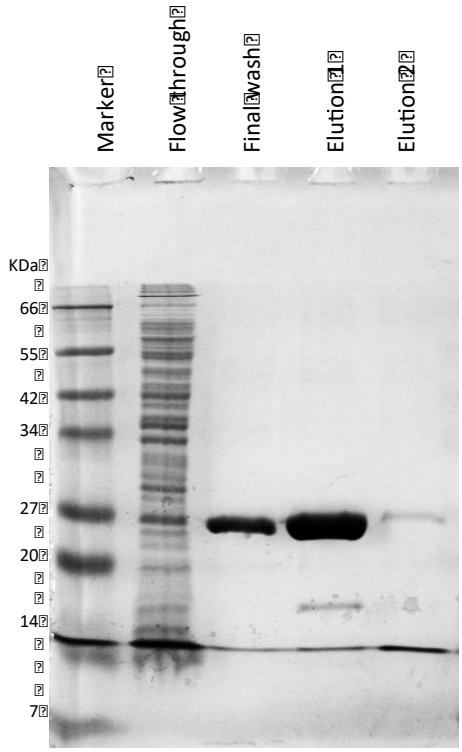

Figure 3.9 Purification of full-length β-lactamase.

Nickel affinity chromatography was used to purify β-lactamase. A sample of the flow through, final wash and two elutions were collected, and analysed. The marker is shown in the very left lane and the numbers down the left side of the gel are molecular weights in kDa.

Fragment A was purified from inclusion bodies as it was in the insoluble fraction, as shown in Figure 3.10. This involved a two-step purification, initially isolating the inclusion bodies in denaturing conditions, followed by nickel chromatography. The denaturing conditions meant that fragment A unfolded, and therefore required refolding into a functional protein. See Chapter 2 Section 2.7.1.1 for a detailed description.

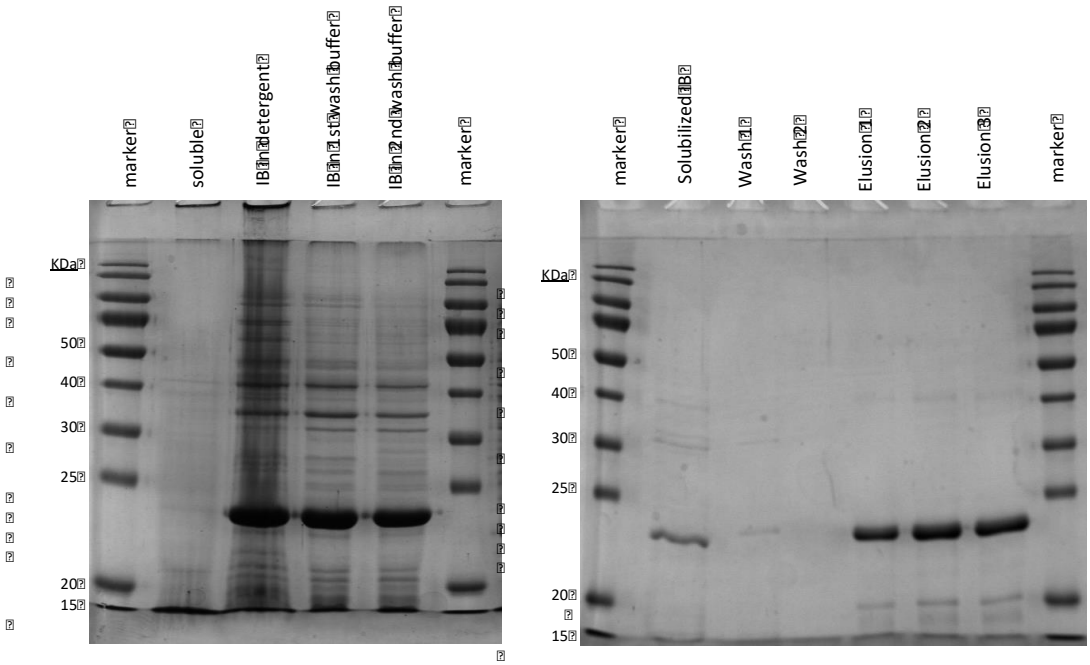

Figure 3.10 Purification analysis of fragment A.

The gel on the left shows the various stages of the inclusion body preparation. The first lane is the molecular weight marker, followed by the inclusion bodies in detergent. The next two lanes are subsequent wash steps to clear the detergent. The large band is the correct size for fragment A. The gel on the right shows the inclusion bodies being further purified using a nickel IMAC column. The first lane is the same as the final lane on the left gel (solubilised inclusion bodies) but at 5X lower concentration. This is followed by two wash samples, three elution samples and a repeat of the marker. All of these purification steps were done under denaturing conditions in 8 M urea.

The pellet from the expression of fragment A was thawed on ice and resuspended in 50 mM Tris buffer pH 8.0. The cells were lysed by sonication, the insoluble fraction was pelleted and the supernatant was discarded. The insoluble pellet was then re-suspended in a detergent wash buffer and incubated for 1 h at room temperature on a see-saw rocker. The insoluble fraction was pelleted and the supernatant discarded. The pellet was washed twice by resuspending in 50 mM Tris.HCl pH 8.0 and incubated for 1 h at room temperature on a see-saw rocker. The purified inclusion bodies were pelleted and stored at -20 °C. The inclusion bodies were then purified on a Ni^{2+} NTA column under denaturing conditions (8 M urea). Once eluted, the protein needed to be refolded.

Initially, serial dialysis with lower and lower concentrations of urea was carried out in an attempt to refold the protein. In this initial trial, the reduction in urea was in 1 M concentration steps each equilibrating for a minimum of 8 h. However, the protein fragment precipitated between 4 M and 3 M urea. A second attempt was made with the increments reduced to 0.25 M steps after 4 M urea. The protein precipitated again between 4 M and 3.75 M. On column folding was tried next, as described in the methods section. In short, purification and refolding of the N-terminal fragment was accomplished on a Ni^{2+}NTA column. The inclusion bodies were resuspended and poured on to the equilibrated column, followed by 10 CV re-suspension buffer. 50 CV of wash buffer were added and as the wash buffer does not contain denaturant, the protein should re-fold on the column. The fragment was eluted in 3 CV of elution buffer. There was no visible precipitate either associated with the column or in the elution fraction. The pooled and dialysed fractions were flash frozen in liquid nitrogen and kept at -80 ^{o}C until required.

Initially, fragment B was also purified from inclusion bodies as there was a much larger amount of fragment B in the insoluble fraction. Unfortunately, this did not result in any protein in the elution fractions. Another attempt was made using the soluble fraction and a small amount (0.55 μg) of protein was purified. Further optimisation of expression of fragment B would be prudent, but as time was restricted and there was enough to proceed with, the expression was not further optimised. A second purification of a larger expression of the protein

was completed to have enough protein to determine kinetic parameters of the protein fragments both on their own and together.

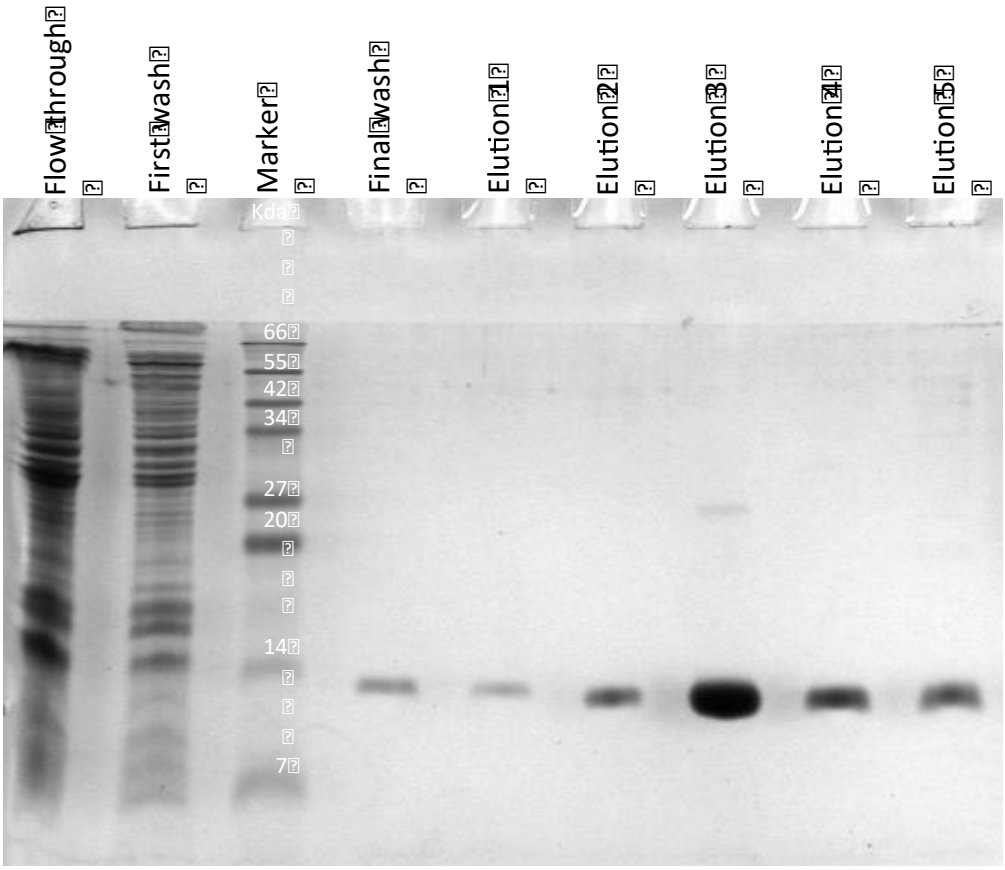

Figure 3.11 Purification of fragment B.

A 500 ml culture was lysed and the soluble fraction was purified. The flow through or unbound protein are in the first lane followed by the first wash. The final wash only contains a band equal to the size of the protein. Elutions 1-5 were pooled and dialysed into PBS with 20 % glycerol.

3.4 Reconstruction of an active protein from two fragments

To investigate if the purified fragments of β-lactamase could be brought together, they were incubated with nickel ions in the form of nickel sulphate. These ions should be able to coordinate the His tags from each fragment located precisely where the loop was before β-lactamase was split. Figure 3.12 shows how the nickel ion could coordinate two polypeptide chains with His tags on them. As the two His tags are brought into close proximity the hypothesis is that the two protein fragments would come together and regain activity. Nickel has a variety of coordination numbers and geometries (Eaton and Zaw 1972). For example, when the coordination number is 4, both tetrahedral and square planar complexes can be found, and for a coordination number 5, both square pyramid and trigonal bipyramid complexes are formed (Eaton and Zaw 1972). An equilibrium of each of these different forms exists (Eaton and Zaw 1972).

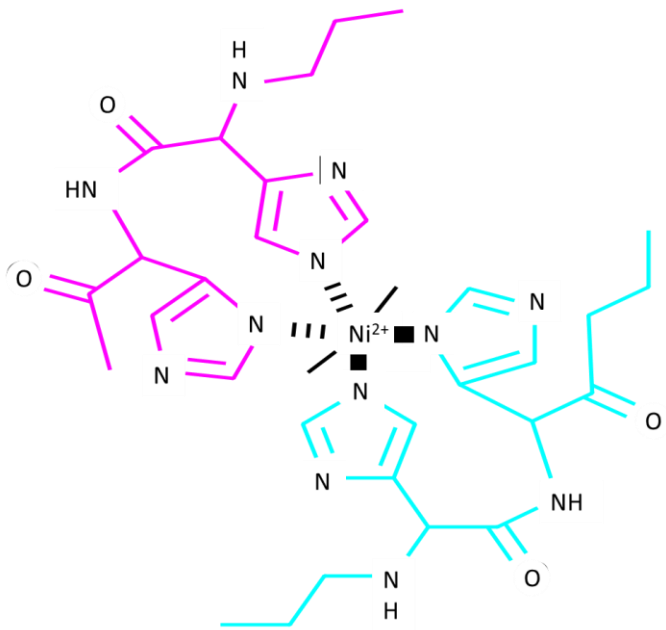

Figure 3.12Nickel ion coordinating histidine residues.

Nickel has a variety of coordination numbers and geometries. For example, when the coordination number is 4, both tetrahedral and square planar complexes can be found, and for a coordination number 5, both square pyramid and trigonal bipyramid complexes are formed.

Detection of active β-lactamase can be performed in a number of ways. First, in a survival based assay using any β-lactam antibiotic, such as ampicillin. Second, with a coloured assay using nitrocefin as a substrate which, when turned over by β-lactamase, turns from a yellow substrate to a red product and can be quantified by measuring absorbance at 482 nm. Finally, a fluorescent assay can also be performed using CCF2 as a substrate. CCF2 is a derivative of cephalosporin which has two additional fluorescent groups attached (Qureshi 2007). This split β-lactamase a very versatile protein.

CCF2 AM is a fluorescent substrate that requires a cytoplasmic esterase and therefore can only be used in certain eukaryotic cell types. After the cytoplasmic esterase has processed CCF2, β-lactamase hydrolyses the product and fluorescence is detected. In addition to the restriction of cell type, CCF2 was prohibitively expensive for use in this study. Nitrocefin is a chromogenic substrate for β-lactamase that is yellow in colour, but when hydrolysed turns a red colour, as shown in

Figure 3.13.

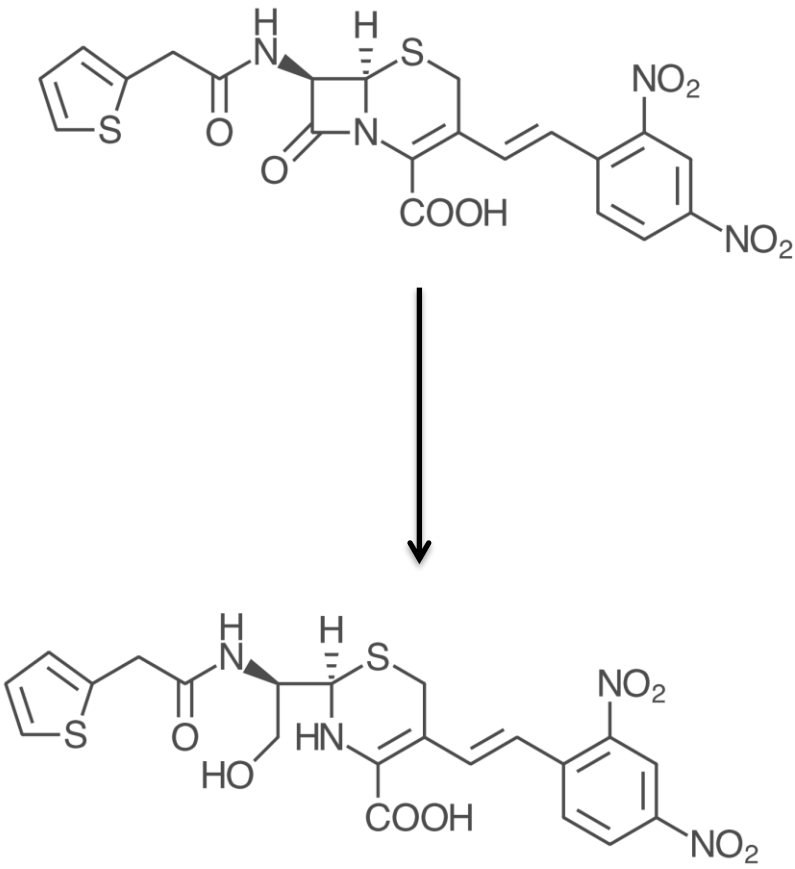

Figure 3.13 Hydrolysis of nitrocefin by a β-lactamase

The hydrolysis of nitrocefin involves hydrolysing the β-lactam ring with the associated colour change from yellow to red. The β-lactam ring is shown in black.

Traditionally, nitrocefin has been utilised in several different ways:

- Slide Surface Assay: a single colony is added to a drop of 0.5 mg/ml nitrocefin on the surface of a clean glass slide. If the solution changes to red, β-lactamase is present (Parr, Pai *et al.* 1984).
- Direct Contact Assay: one drop of 0.5 mg/ml nitrocefin is placed directly on the surface of a colony. If the colony changes to red, β-lactamase is present. (Brook and Gober 1984).
- Broth Suspension Assay: 3-5 drops of 0.5 mg/ml nitrocefin is added to 1 ml of broth suspension, and if β-lactamase is present the suspension changes to a red colour (Brook and Gober 1984).
- Lysed Cell Assay: 3-5 drops of 0.5 mg/ml nitrocefin is added to 1 ml of lysed cells and if the lysate turned red then β-lactamase is present (Parr, Pai *et al.* 1984).

- Filter Paper Assay: add 3-5 ml of 0.5 mg/ml nitrocefin to filter paper and smear isolated colonies over the paper, if β-lactamase is present the area where the smear is located will turn red (Parr, *et al.* 1984).

In each of these cases, the appearance of red colour within 20-30 min indicates β-lactamase activity and gives a present/absent result. A more quantitative assay was needed to measure the activity of β-lactamase, in order to compare different levels of activity. This involved measuring the absorbance of product formation at 500 nm. Nitrocefin is a chromogenic substrate that turns from yellow to red upon hydrolysis. Looking at the spectra, the λ max was checked for both intact and hydrolysed nitrocefin. After a sample of nitrocefin was hydrolysed, both the hydrolysed and intact nitrocefin spectra were recorded.

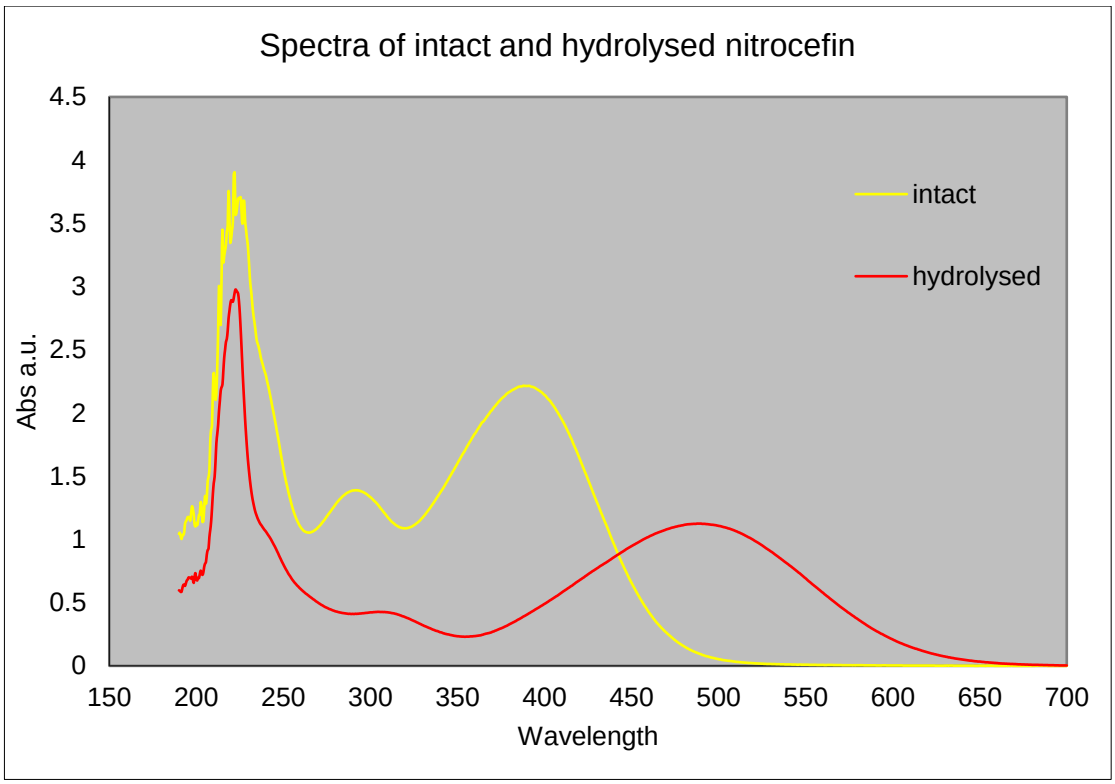

Figure 3.14 Spectra of Intact and hydrolysed nitrocefin.

The yellow spectrum is for intact nitrocefin as it is yellow in colour. The red spectrum is for hydrolysed nitrocefin as it is red in colour. The λmax shifts from 380 nm to 500 nm. Reading the absorbance at 500 nm would indicate the amount of product produced from a β-lactamase assay.

To investigate the association of the fragments into a functional protein, many experimental controls were required. Recombinant full-length β-lactamase was used as a positive control, indicating the substrate is turning over correctly. Recombinant full-length β-lactamase with nickel ions was also included as a second positive control to ensure the nickel ions did not interfere with the normal turnover of the enzyme. Each of the fragments, both with and without nickel, were included in this experiment to indicate their individual levels of turnover. Finally, as a negative control, the assay was set up without the enzyme, again both with and without nickel. Purified β-lactamase and β-lactamase fragments were produced as described in Section 3.2.

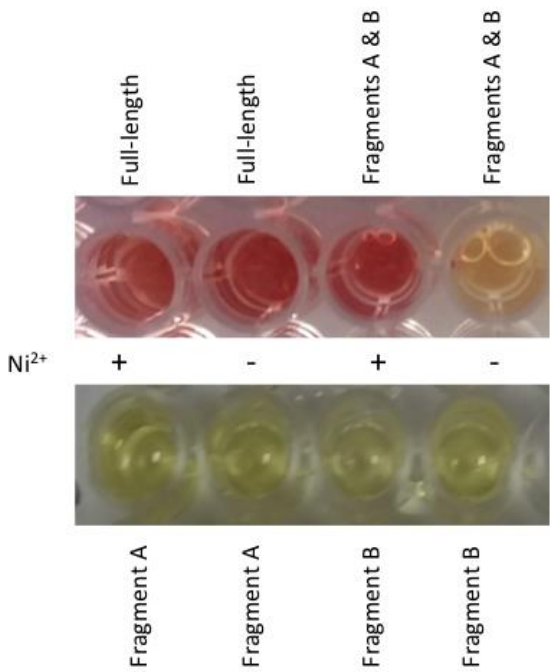

Figure 3.15 Nitrocefin Assay for the recombination of the β-lactamase fragments.

The photographs were taken after a 16-hour incubation. The top row has full-length β-lactamase in the first two wells, both with and without nickel, indicated with a '+' or '-'. The third and fourth wells on the top row contain both fragments of β-lactamase, with and without nickel. Each of the fragments on their own are shown on the bottom row. A red colour indicates turnover of the substrate nitrocefin, and a yellow colour indicates the substrate was not turned over.

Figure 3.15 shows the full-length β-lactamase in the first two wells on the top row. Both are red, indicating the nitrocefin substrate was turned over. The only difference in the two samples was the presence and absence of nickel ions respectively, thus indicating that the nickel does not make a difference to the nitrocefin being turned over. The next two wells on the top row contained both fragments of β-lactamase. The sample with nickel has turned red, whereas the sample without nickel has a slightly orange colour. This suggests that the fragments on their own do turn over the substrate but only at a very low level, and will add to the background. The sample with the nickel is red rather than orange indicating that when the fragments are held together with nickel the turnover rate is higher.

The bottom row contains samples of the fragments of β-lactamase individually, again with and without nickel. All the samples remained yellow inferring that the fragments do not turn over the substrate without their partner fragment. Figure 3.15 shows recombinant β-lactamase, that was used as a positive control, started to decolourise, as shown by the faded colour in the first well on the top row. Furthermore, it is more clear on Figure 3.16 where there is an obvious decrease in absorbance after about 15 h. It was necessary to investigate this further, because a value for the positive control could be reducing when the two fragments with nickel were increasing, thereby giving skewed results.

3.5 Nitrocefin time course

Figure 3.16 shows a time course of the measurement of the hydrolysis of nitrocefin in each of the following conditions: Full-length recombinant β-lactamase, Fragment A of β-lactamase, Fragment B of β-lactamase, Fragment A & B of β-lactamase. All of these sets of proteins were assayed both with and without nickel.

To process the data shown in Figure 3.16 the absorbance for nitrocefin alone was subtracted from each of the assay mixes without nickel. The absorbance for nitrocefin with nickel was subtracted from each of the assay mixtures with nickel. The reason being that, in each of the assay mixtures containing nickel,

a small amount of precipitate was observed. A precipitate would cause light to scatter and give a false reading of a higher than actual absorbance. The absolute values were small and did not reach an absorbance higher than 0.5 at 492 nm. The error bars are not displayed on the main graph for clarity. The insert graph shows the error bars for full-length β-lactamase. The largest error was introduced when the batch of nitrocefin was changed.

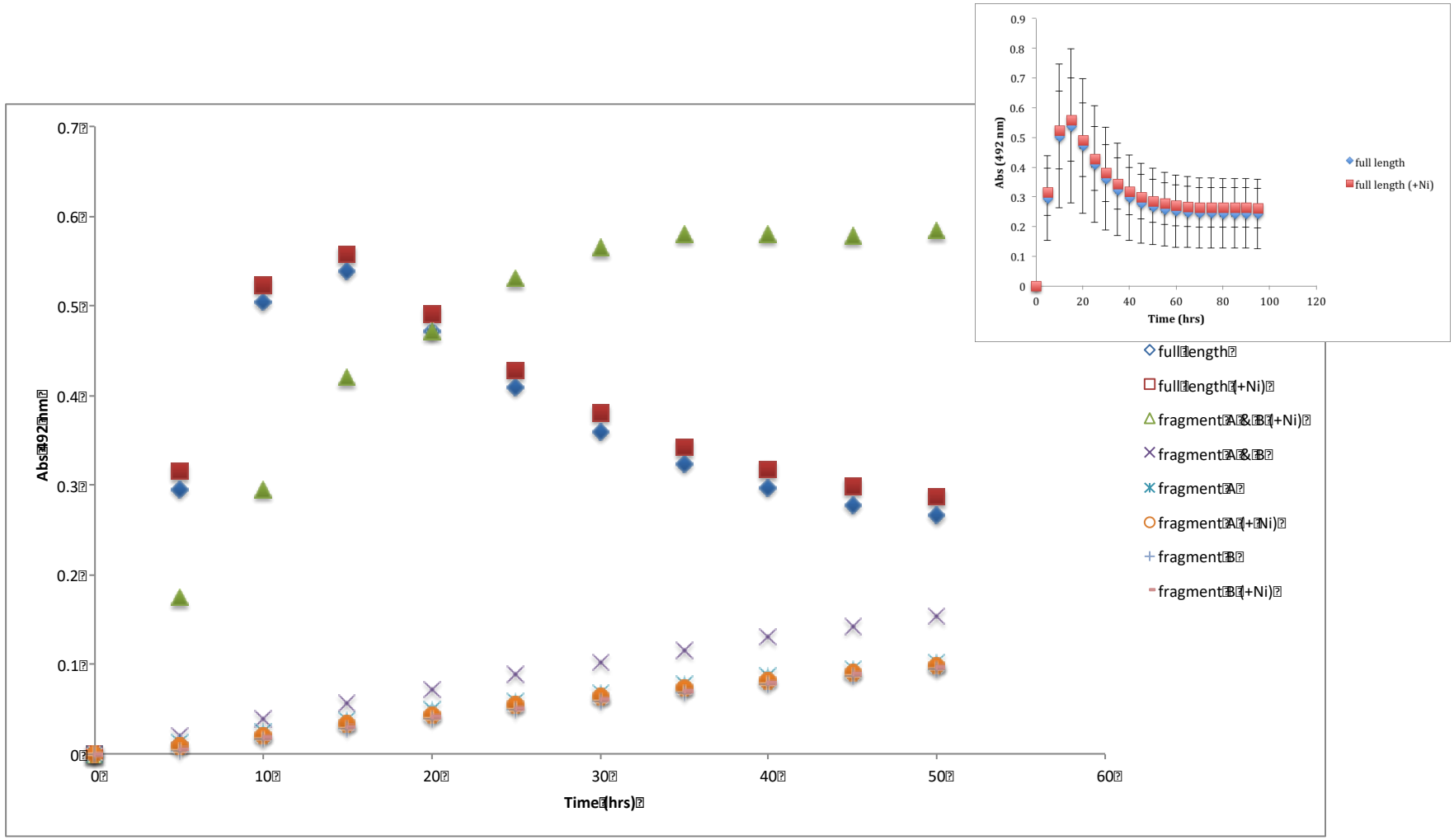

Figure 3.16
Nitrocefin assay time course. Absorbance at 492 nm over several hours for full-length β-lactamase, and for β-lactamase fragments both with and without nickel ions.

Full-length recombinant β-lactamase both with and without nickel shows a high rate of product formation in the first hour followed by a reduction in absorbance. This is not the product reducing, because hydrolysis of a cephalosporin is a one way reaction (Page and Proctor 1984). The most plausible explanation is a bleaching effect as the mixture is exposed to light. However, the same effect did not happen for the fragment A and B in the presence of nickel, even after 50 hours. It is encouraging that in both cases, with and without nickel, the hydrolysis rate remains similar and has the same pattern, as shown by the red squares and blue diamonds in Figure 3.16.

Fragment A and fragment B of β-lactamase, both with and without nickel, seem to show a very low level of product formation over time, which could be an effect of the instrument heating up over time. Effectively, this looks like a baseline, but slightly higher than each of the fragments on their own.

In absorbance measurements, the intensity was less than 0.1 at 492 nm after 50 h. When fragments A and B were mixed together there was an increase over each of the fragments on their own, and after 50 h an absorbance of 0.2 was almost reached. When nickel was present to hold the two fragments together, the absorbance reached 0.5 after 20 h. Each of the assays exhibited different rates and this seemed to be the best way to show the differences objectively for each of the different assay conditions.

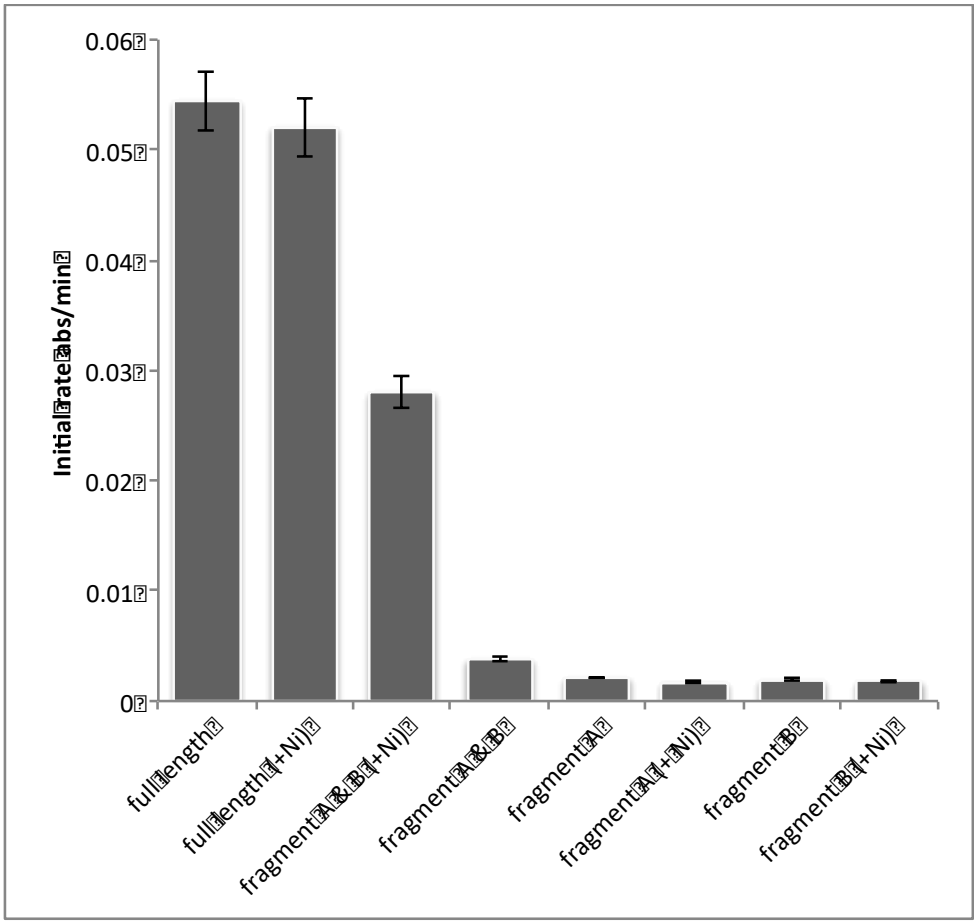

Figure 3.17 Nitrocefin assay of β-lactamase and β-lactamase fragments displayed as a rate.

The first 20 minutes of the nitrocefin assay were recorded and the initial rates were determined and shown in a bar chart.

There is an obvious difference between the fragments of β-lactamase when nickel was introduced. In the absence of nickel the rate for fragment A and B was only 0.0038 absorbance units/min, and after addition of nickel the rate went up to 0.028 absorbance units/min; representing a more than 7-fold increase.

3.6 Kinetic parameters

The substrate nitrocefin was used to calculate the kinetic parameters for recombinant TEM-1 β-lactamase and fragments of TEM-1 β-lactamase in the presence and absence of nickel ions. The absorbance of hydrolysed nitrocefin at 492 nm was used to determine the amount of product produced. However,

it should be noted that nitrocefin is light sensitive and these assays were performed on the bench top. Therefore, some variability was expected. Published data for TEM-1 β-lactamase quote the K_M to be around 61 μM and the k_{cat} to be about 122 s^{-1} (de las Heras, *et al.* 2008).

Table 3-2 Kinetic parameters for β-lactamase and β-lactamase fragments.

β-lactamase variant	K_M (μM)	k_{cat} (s^{-1})
Recombinant β-lactamase	89 ± 9	65 ± 10
Fragment A and B with Ni^{2+}	36 ± 3	3.2 ± 0.3
Fragment A and B only	68 ± 8	0.31 ± 0.06

The kinetic results do show a small difference in the K_M, between the β-lactamase fragments in the presence and absence of nickel, but the interesting difference is in the k_{cat}. Recombinant β-lactamase has a turnover rate of 65 s^{-1} which is reduced to only 0.31 s^{-1} for the β-lactamase fragments on their own. When the fragments were brought together with nickel ions the turnover rate increased, some 10-fold, to 3.2 s^{-1}. This demonstrates that in theory an enzyme can be split and brought back together in a functional purified format, although there is an obvious question about the efficiency with which high levels of activity can be restored.

3.7 Discussion

TEM-1 β-lactamase was expressed and purified, and an N-terminal and C-terminal fragment of β-lactamase was cloned, expressed and purified. These fragments were brought back together in a functional format in an *in-vitro* experiment using nickel ions. This indicates that a split enzyme could work in a completely purified system, for example in a biosensor type assay, although there are clearly challenges associated with this process. These include the ability to produce sufficient quantities of fragments ideally without refolding, and also the extent to which intact enzyme activity can be restored in the split enzyme system.

Natively purified β-lactamase is reported in literature to have a k_{cat} of 960 s^{-1} (de las Heras, *et al*. 2008). In the de las Heras study there was a significant drop in turnover from 960 sec^{-1}, for natively purified β-lactamase, to 122 s^{-1} for recombinant β-lactamase (de las Heras, *et al.* 2008). Values in the current study are within an agreeable level of those for recombinant TEM-1 β-lactamase. The rate of turnover for recombinant full-length β-lactamase was 65 s^{-1}. A further 20-fold drop in turnover down to just 3.2 s^{-1} was recorded when the fragments were brought back together in close proximity with nickel ions. This compared well with what was reported in literature as 6.5 s^{-1} (de las Heras, *et al.* 2008). A background was reported in the literature (de las Heras, *et al.* 2008) but quantitative data was not given. The background in this study was due to a turnover rate of 0.31 sec^{-1}. There was a difference between the signal and noise, and this could be further improved, by further optimisation of the fragments.

Improvements could be made to this system to make it more effective. The addition of the mutation M182T is known to disrupt an inactive molten intermediate of the full-enzyme and this should give fragment A more stability and higher activity (Galarneau, *et al.* 2002).

The addition of a tri-peptide Asn-Gly-Arg at the C-terminal of fragment A could also improve the split β-lactamase assay. In a study by Wehrman *et al* (Wehrman, *et al*. 2002) it was noted that the antibiotic resistance was improved by the addition of this tripeptide.

However, as the recombinant β-lactamase activity is already significantly reduced before the protein was even split, it was decided to investigate a different enzyme. Furthermore, the stability of nitrocefin was questionable. Instability of nitrocefin in light, moisture and temperature make this system less than optimal. The activity data show that one batch of nitrocefin was so sensitive to light that after several hours it lost the red colour. Moreover, the batch to batch variance was substantial for this split β-lactamase to be used in a reliable colorimetric biosensor. The reduced activity of the β-lactamase protein could be due to inefficient refolding as it needed to be purified from the insoluble fraction.

Ideally, a dimeric protein, which can be expressed as a functional recombinant protein, without affecting the activity, would be best suited to the proposed diagnostic application. An enzyme with potential from this perspective is alkaline phosphatase, which is a routinely used enzyme within biochemistry laboratories.

Chapter 4

Mutational studies on the dimer interface of alkaline phosphatase

4.1 Introduction

For a protein complementation system, an enzyme should be split into two fragments which, by themselves, do not turn over the substrate, but when brought into close proximity can interact and gain the ability to turn over substrate to generate a measurable signal. In a biosensor, it is envisaged that this signal amplification would arise from the binding of two Affimer proteins to separate epitopes on a single target protein. This binding would bring the enzyme fragments together to allow multiple substrate turnover events. A major problem with some split enzyme systems is that the level of recovery of enzyme activity, relative to wild-type activity, can be quite low; meaning the signal generated from the split enzyme would be relatively weak. Another option to consider is the use of a dimeric enzyme where the dimer interface is engineered to prevent spontaneous monomer association, but still retaining the ability of the two subunits to associate and form a functional enzyme. *E. coli* alkaline phosphatase is a good model enzyme for investigating subunit interactions in homodimeric enzymes as it exhibits cooperativity (Garen and Levinthal 1960). In this study, it is also a good candidate for use as an amplification tool in a biosensor

E. coli alkaline phosphatase does not turnover substrate when in a monomer form but only functions as a dimer indicating some form of cooperativity between the subunits, although this is poorly understood. So, in order to create a stable monomer, and to understand the mechanism of control and regulation of AP achieved by the subunits' interactions, several mutants of the enzyme have been constructed in previous studies (Martin, *et al*. 1999, Boulanger and Kantrowitz 2003, Orhanovic, *et al*. 2006).

Four positions on the dimeric interface have been previously investigated: R10, R24, T59 and T81 that when mutated to an alanine were found to have a small negative effect on substrate turnover. These mutations did, however, show a notable effect on the stability of the protein (Martin, *et al*. 1999, Boulanger and Kantrowitz 2003, Orhanovic, *et al.* 2006). However, the only mutation to successfully result in a stable monomer was at T59 when mutated to arginine. (Martin, *et al.* 1999, Boulanger and Kantrowitz 2003). Chapter 1

Figure 1.19 shows why the T59R monomers are unlikely to form a dimer due to steric hindrance and charge repulsion. The T59R mutant was generated in this study to confirm lack of dimer formation and to provide a negative control in stability, activity, and structural assays.

R10, R24, and T59 are all situated on the dimer interface (Martin, *et al.* 1999). The mutational variants R10A, R24A, and T59A were all described as having an effect upon protein stability and a small negative effect on substrate turnover. The largest effect was due to R10A that showed a reduction in k_{cat} from 69.5 ± 4.5 s^{-1} to 53.9 ± 3.4 s^{-1}. The stability of the dimer or monomer forms were also investigated, as was that of the double mutant R10A-R24A that showed instability similar to that of the single mutants. At pH 5 all of the mutant proteins were a mixture of both dimeric and monomeric forms, whereas at pH 4 all were monomeric (Martin, *et al.* 1999). The pH optimum for wild type alkaline phosphatase is approximately pH 8.0 although it displays reasonable activity at even higher pH values and thus, to be used in a biosensor, the enzyme must exist as a monomer at basic pH values.

The T81A mutation is also at the subunit interface and has a small negative effect on substrate turnover, with k_{cat} reduced from 61.8 s^{-1} to 36.9 s^{-1} at pH 8. The thermostability of this variant was reduced compared to wild type, indicating an effect on the stability of the dimer in 1 M Tris pH 8.0 (Orhanovic, *et al*. 2006). Figure 1.18 in Chapter 1 shows the R10, R24, T59, and T81 residues and their interactions with the nearest residues on the other chain of the dimer. In each case, only one set of interactions is shown for simplicity.

4.2 Producing wild-type alkaline phosphatase

Figure 4.1 shows a map of an expression plasmid pECAP-T81A-Sort containing a mutant version of alkaline phosphatase that was available in the lab. It contained the point mutation T81A and a sortase tag. Mutagenesis was used to revert the mutant alkaline phosphatase back to a wild type Thr version, while the sortase tag was retained as it had no bearing on the function of the protein. Primers were designed to introduce the A81T change into pECAP-T81A-Sort as detailed in Chapter 2, Section 2.5.1.2 creating the plasmid pECAP-Sort.

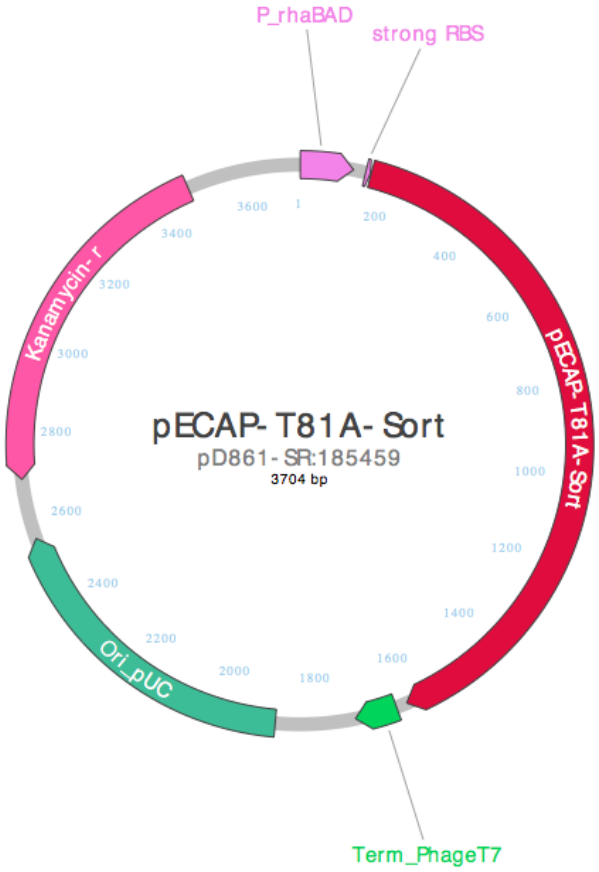

Figure 4.1 Vector diagram of pECAP-T81A–Sort containing T81A (taken from DNA 2.0 gene synthesis report).

Features include a P_rhaBAD promoter which is rhamnose inducible, a strong ribosome binding site (RBS) and a kanamycin resistance marker. The pUC ori is a mutated form of origin of replication derived from *E. coli* plasmid pBR322 which allows production of greater than 500 copies of plasmid per cell.

DNA sequencing confirmed successful mutagenesis and the new vector, pECAP, was used for wild type alkaline phosphatase protein production. The protein was produced in SHuffle cells that are deficient in the *phoA* gene, so there is no endogenous alkaline phosphatase and they are designed to allow the formation of disulfide bonds in proteins within the cytoplasm. For more details see Chapter 2 Section 2.2.3.

The rhamnose promoter makes this expression system tunable by varying the amount of rhamnose used to induce protein production. A range of rhamnose concentrations from 0.001 % to 0.2 % were tested and samples were taken 6 h post-induction.

Figure 4.2 shows that the amount of protein produced varies depending upon the amount of rhamnose added. The proportion of protein in the insoluble fraction increases to appreciably more than that in the soluble fraction at 0.1 % rhamnose. This suggests that at 0.1 % rhamnose protein production is so rapid that protein folding is compromised. In the soluble fraction, the quantity of protein produced is approximately the same between rhamnose concentrations of 0.005 % to 0.01 %. Thus 0.01 % rhamnose was used for further production of protein, including mutant forms, from this vector.

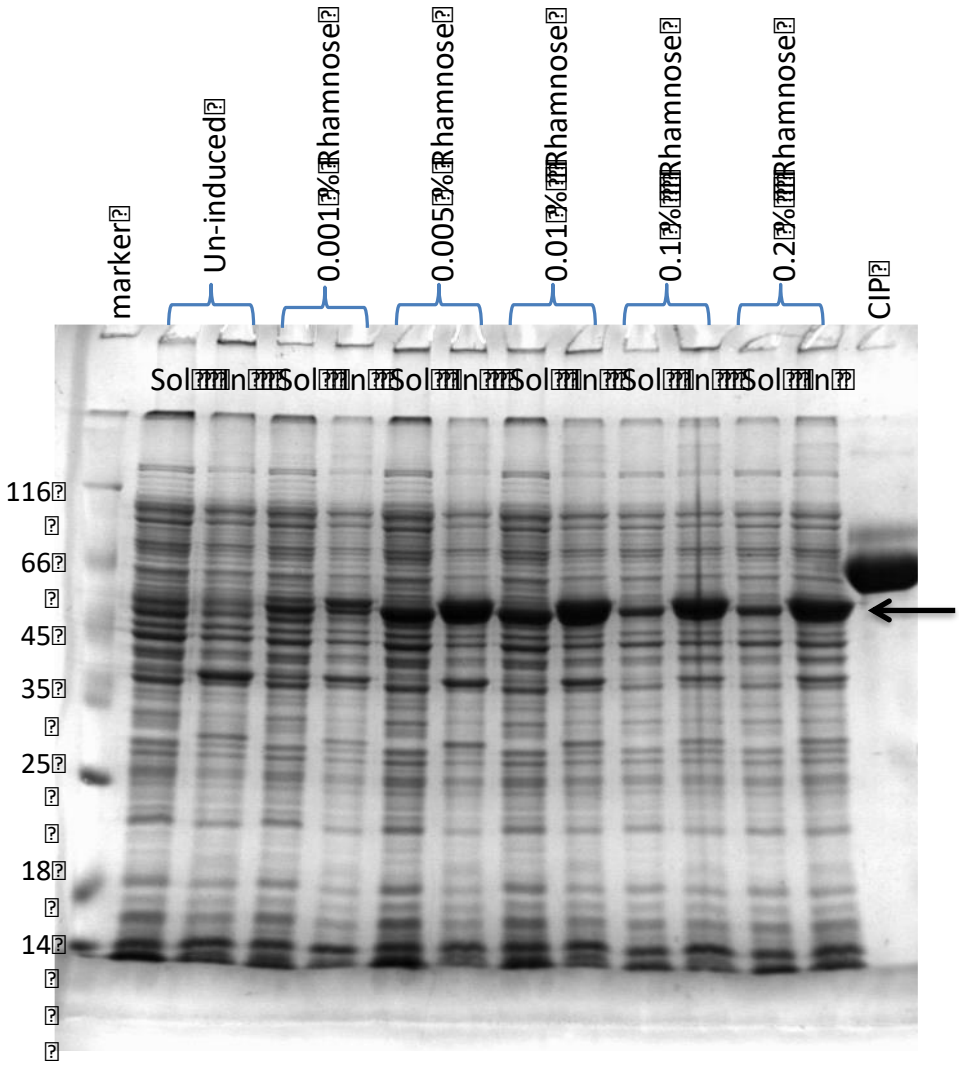

Figure 4.2 Expression of wild-type alkaline phosphatase at different concentrations of rhamnose inducer.

The marker lane shows molecular mass markers and their sizes in kDa are indicated to the left. Two lanes are shown per concentration. Sol; soluble protein, In; insoluble protein. The samples have been induced with 0%, 0.001%, 0.005%, 0.01%, 0.1%, and 0.2 % rhamnose. The lane marked CIP is calf intestinal phosphatase (70 kDa), CIP is larger than *E. coli* alkaline phosphatase (48 kDa).

Figure 4.3 shows an SDS PAGE gel of levels of protein production at different induction times. Samples were taken before induction (uninduced) and at various times post induction with 0.01 % rhamnose; 50 µl of each of the samples were normalised by reducing the OD_{600} to 0.5. There was little obvious difference between 4, 6, and 16 h levels. Following quantification, using a BCA assay as described in Chapter 2 Section 2.9.2, the amount of wild type protein produced at 4 and 6 h was determined to be between 9 and 10 mg/L. Overnight incubation resulted in a decrease to between 5 and 7 mg/L. However, for different experiments conducted during this study, either 4 h, 6 h or overnight grow ups were used for convenience.

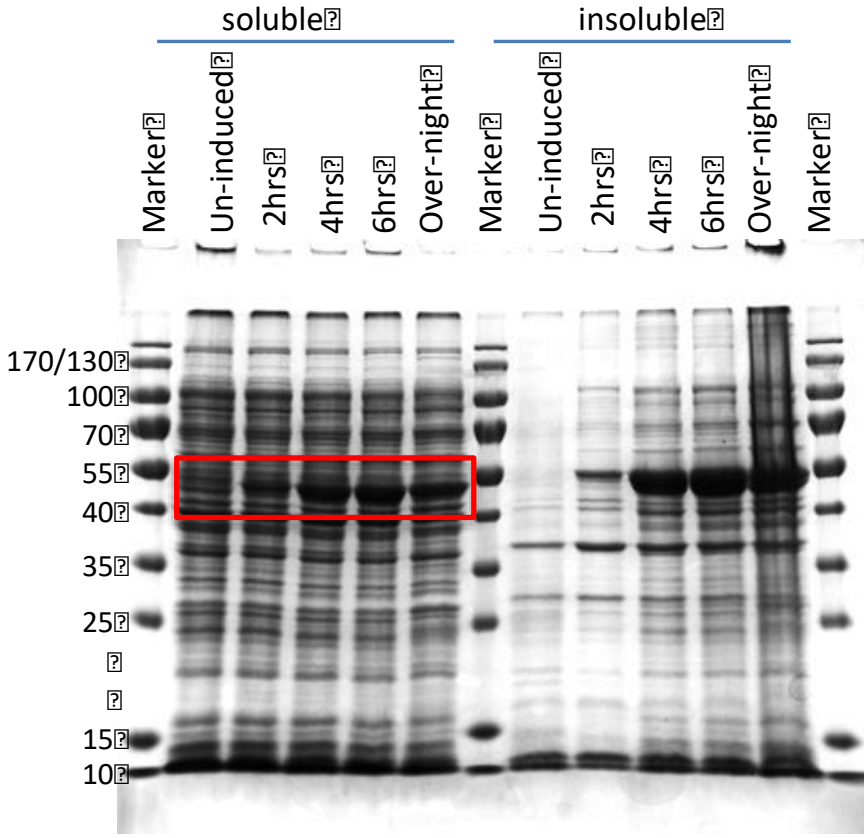

Figure 4.3 Expression of wild type alkaline phosphatase: optimizing the length of time for induction.

Marker lanes show molecular mass markers with the size noted in kDa. Soluble and insoluble fractions are shown as uninduced and then 2, 4, 6, and 16-hour post-induction samples. The soluble AP is highlighted by the red box.

Wild-type alkaline phosphatase was purified using IMAC chromatography with nickel NTA beads, as described in Chapter 2, Section 2.7.2. Briefly, after the induction phase, the cells were harvested by centrifugation and frozen at -80 ^{o}C for storage. For protein purification, the cell pellet was thawed at room temperature and mixed with 10 ml of lysis buffer per gram of cells. The lysate was clarified, and the soluble fraction was incubated with Ni^{2+} NTA beads for 40 mins before being poured into a Thermo Scientific, Pierce, disposable plastic column, then washed with 20 ml of wash buffer, or until the OD_{280} was less than 0.1. The protein was eluted in 0.5 ml fractions of elution buffer until the OD_{280} stabilised. Samples from the soluble fraction, flow through, wash steps, and elution fractions were analysed by SDS PAGE. Figure 4.4 shows a 15 % SDS PAGE gel of fractions of a purification. Elution fractions 1 to 3 were pooled and after dialysis, as described in Section 4.2.1, the concentration was determined using both a BCA assay and by absorbance at A_{280} using an extinction coefficient of 32890 M^{-1} cm^{-1}.

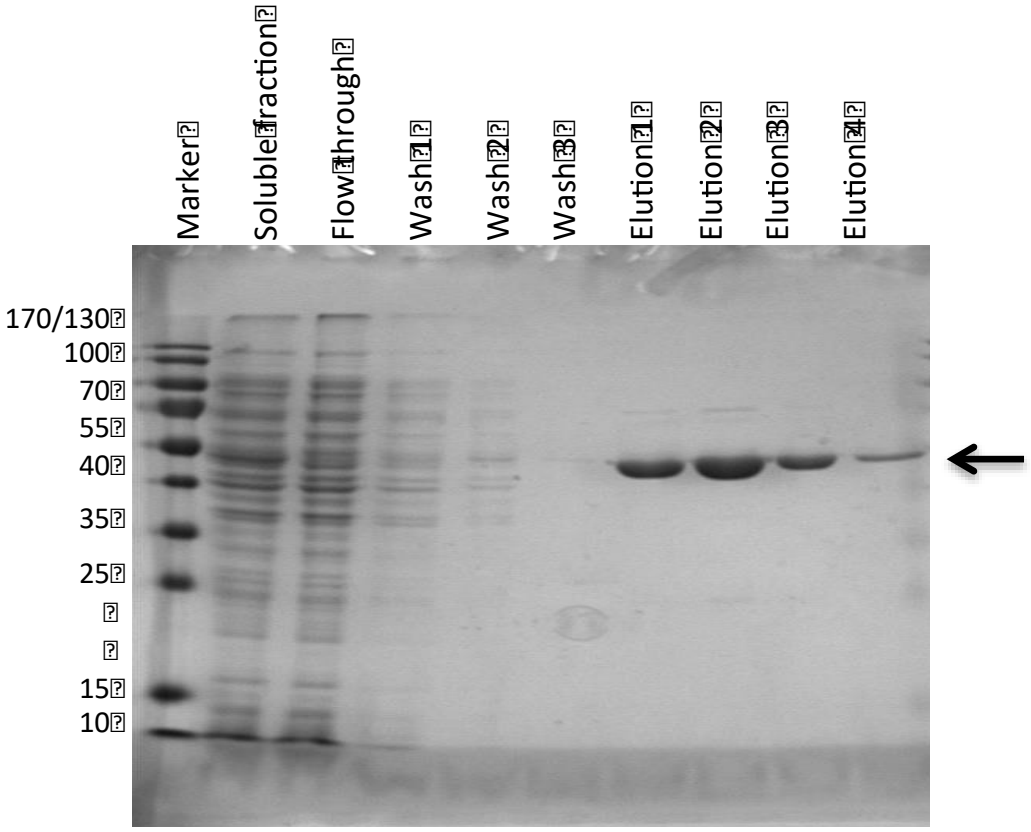

Figure 4.4 Purification of wild-type alkaline phosphatase. M, molecular mass markers with sizes shown in kDa.

From left to right, the lanes contain the soluble fraction loaded onto the column, the flow-through showing unbound material, three wash steps, and then four elution fractions. The arrow indicates the position of alkaline phosphatase.

Traditionally, alkaline phosphatase from *E. coli* is produced using phosphate deficient media (Garen and Levinthal 1960). The protein produced is a natural product and is present in sufficient amounts to enable characterisation. The aims of this project included investigating numerous mutants of alkaline phosphatase, many of which were thought to be inactive. Thus, using phosphate deficient media as an approach to produce the mutants would not work as this method relies upon the production of phosphate from endogenous

active alkaline phosphatase. Moreover, the conventional approach for purification is ammonium sulfate precipitation followed by ion exchange chromatography. Mutations would change the properties of the enzyme and potentially require tailoring of the purification protocol for each mutant.

The approach used here involves IMAC, in this case, nickel NTA, and only requires a His tag to be associated with the recombinant protein, making protein isolation facile, fast and essentially independent of the physicochemical properties of the protein, including any mutational variants. The potential drawback of producing and purifying alkaline phosphatase in this way is that the kinetic parameters could be affected when alkaline phosphatase is produced in the reducing environment of the cytosol. Alkaline phosphatase has two disulfide bridges in each chain between Cys-168 and Cys-178, and between Cys-286 and Cys-336 (Sone, *et al.* 1997). The SHuffle cells used for alkaline phosphatase production are deficient in endogenous alkaline phosphatase and facilitate cytoplasmic disulfide bond formation. The kinetic parameters for wild-type AP were, therefore, determined and compared with those previously reported.

4.2.1 Dialysis of alkaline phosphatase.

Stringent dialysis of alkaline phosphatase is required. Reasons for this include the fact that alkaline phosphatase is inhibited by imidazole, which is present in all the buffers used to purify the protein, and also, because if zinc is not present in the active site, the protein is inactive. To overcome both issues the protein was rigorously buffer exchanged; firstly into 50 mM Tris-HCl pH 8.0 for 2-4 hrs, then into the ion addition solution (50 mM Tris-HCl pH 8.0, 1 mM $ZnSO_4$ 0.1 mM MgCl) for 2-4 h, and then finally into 1 M Tris-HCl pH 8.0 overnight at 4 ^{o}C.

4.3 Determination of kinetic parameters for wild-type alkaline phosphatase.

A general assay to investigate alkaline phosphatase enzyme activity is through turnover of the colourless substrate pNPP that upon catalytic hydrolysis of the phosphate results in *p*-nitophenol, a chromogenic product that can be monitored spectrophotometrically at 405 nm.

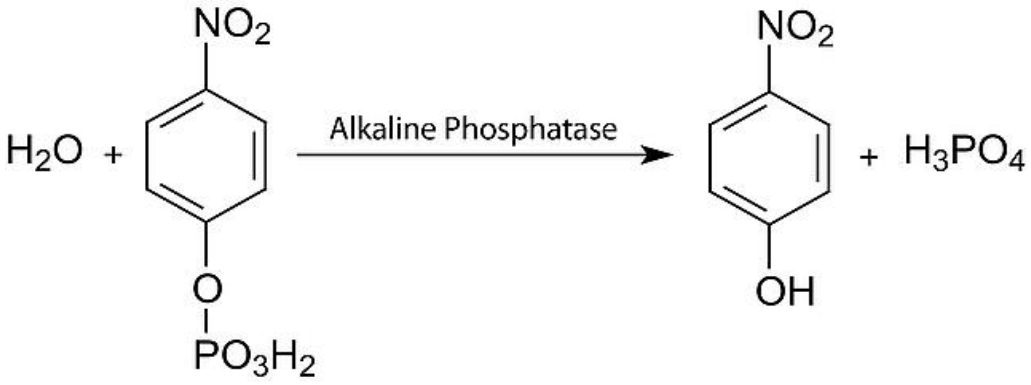

Figure 4.5 Assay for alkaline phosphatase activity

***p*-nitrophenyl phosphate is dephosphorylated to produce *p*-nitrophenol, a chromogenic (yellow) product that can be monitored spectrophotometrically at 405 nm.**

The k_{cat} of recombinant wild type alkaline phosphatase is reported to be between 26 - 80 s^{-1} and the K_m is between 7.3 - 160 µM. Temperature and buffer composition affect the enzyme activity and contributes to the variability reported in the literature (Garen and Levinthal 1960, Garen and Garen 1963, Coleman 1992, Martin, *et al*. 1999, Boulanger and Kantrowitz 2003, Orhanovic, *et al.* 2006). In this study, the k_{cat} of recombinant alkaline phosphatase was determined to be 49 ± 4 s^{-1} with a K_m of 34 ± 12 µM. These experimental data fall within the published range of values, indicating that the approach used for production and purification of the protein (Section 4.2) is appropriate.

4.3.1 Optimisation of specific activity assays

To ascertain the appropriate quantities of enzyme and substrate for specific activity assays, a range of enzyme concentrations, and two concentrations of *p*NPP, were investigated. The concentration range for the enzyme was varied from 1 mg/ml to 5 µg/ml with substrate at 2 mM and 0.5 mM. The results of this preliminary test are shown in Figure 1.8. The assay was allowed to continue for 2 mins and stopped with 50 µl of 5 M NaOH. The conditions determined for subsequent assays were 2 mM substrate with enzyme concentrations of 0.6 mg/ml and 0.25 mg/ml**.**

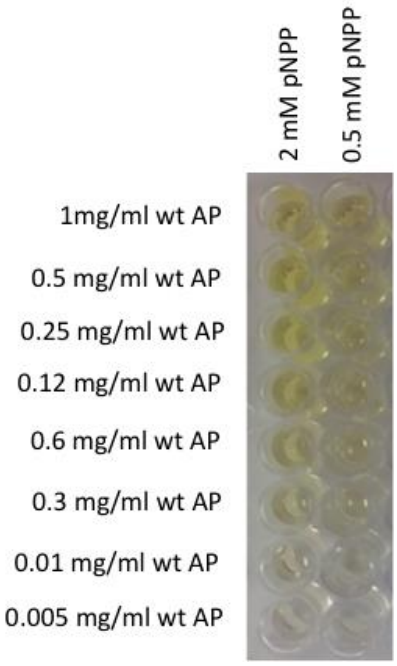

Figure 4.6 Optimisation of specific activity assay.

A range of concentrations of wild type alkaline phosphatase from 0.005 to 1 mg/ml were tested for activity at two concentrations of pNPP: 2 mM and 0.5 mM. The assay was allowed to continue for 2 mins and stopped with 50 µl of 5 M NaOH.

4.4 pH Optimum of wild-type alkaline phosphatase

Previous studies have reported different pH optima (Garen and Levinthal 1960, Torriani 1960) using various buffers, but the buffer composition may also affect enzyme activity. In the present study, a tri-buffer system was used to buffer the reaction from pH 6.5 to pH 11.5 without changing the buffer composition. Table 4-1 specifies the buffer components and their individual buffering range.

Table 4-1 Buffer composition of a three-component buffer system used to determine the pH optimum of wild-type alkaline phosphatase.

Buffer component	pKa of buffer	Useful pH range
N-2-aminoethane sulfonic acid (ACES)	6.9	6.1 - 7.4
Tris (hydroxymethyl) aminomethane (Tris)	8.0	7.0 - 9.0
N-cyclohexyl-3-aminopropanesulfonic acid (CAPS)	10.4	9.7 - 11.1
1 M sodium chloride (NaCl)		
5 M hydrochloric acid (HCl)	Used to change pH	
5 M sodium hydroxide (NaOH)	Used to change pH	

ACES can buffer from 6.4 to 7.4 overlapping with Tris, which buffers well up to pH 9.0, and CAPS buffers to pH 11.1. In fact, the assays were performed up to pH 11.5 which is beyond the buffering capability of this system. To test the integrity of the tri-buffer system, experiments were also performed with each of the buffers individually. The differences between these sets of data are shown in Figure 4.7, where both the single and tri-buffer system show a similar trend, although there is less variation in the tri-buffer system.

Sodium chloride at 1 M was added to ensure a high ionic strength, minimising the influence of other components, that are present at lower concentration, on the ionic strength. 1 M NaCl is far from the typical ionic strength at which the reaction takes place, furthermore, the addition of excess neutral salt means the introduction of additional ions, that can interfere with the enzyme reaction. To examine if there was indeed an effect of the high concentration of NaCl on the reaction, assays were conducted across a range of NaCl concentrations

from 50 mM to 1 M in 50 mM steps, and no difference was observed on the activity of wild type alkaline phosphatase indicating that 1 M NaCl was appropriate for establishing a constant ionic strength.

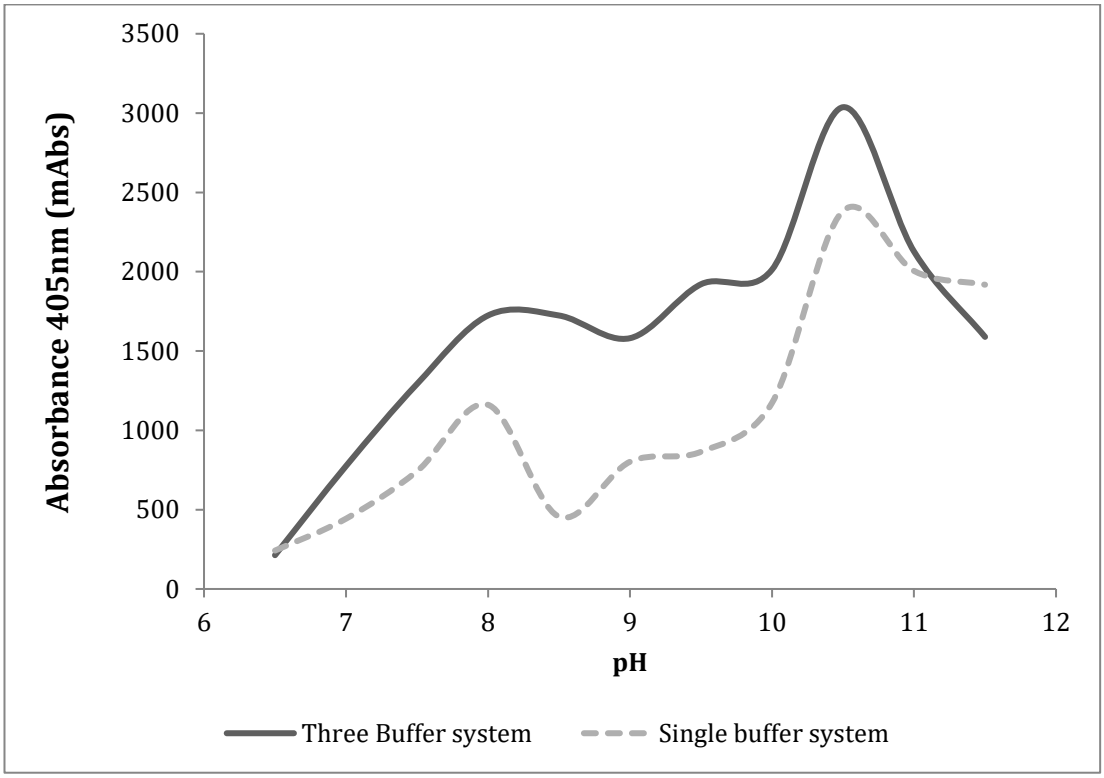

Figure 4.7 Measurement of pH optimum for wild type recombinant alkaline phosphatase.

The solid line are data for the three-component buffer system and the dashed line is generated from each of the single buffers.

These sets of data suggest that there are two optima in the pH series, at pH 8 and pH 10.5, but that for highest enzyme activity, the optimum pH is 10.5. However, as previous studies on some of the mutational variants were investigated at pH 8 (Martin, *et al.* 1999, Boulanger and Kantrowitz 2003, Orhanovic, *et al.* 2006), assays in this study were also performed at pH 8.0 to allow direct comparison with published data.

4.5 Saturation Mutagenesis at position Thr59

T59R results in a stable monomer showing no enzyme activity (Boulanger and Kantrowitz 2003), but as shown in Figure 1.19 it is expected that steric hindrance prevents the production of a stable functional dimer. In order to explore whether any other amino acid at position 59 would lead to a monomer that could nonetheless engage in intersubunit complementation, a saturation mutagenesis experiment was performed. A series of primer pairs were designed to replace the threonine at position 59 with every other amino acid, except cysteine as this could potentially result in disulfide bonds. A disulfide bridge at the dimer interface would be expected to stabilise the dimeric form of the enzyme, which is not compatible with the requirements for a split alkaline phosphatase.

The Quikchange™ mutagenesis reactions (Section 2.5.1.2) were set up in parallel and Dpn I was added to destroy the parental template DNA which should leave predominantly mutated DNA products for transformation into *E. coli* (Section 2.4). Figure 4.8 shows products of the mutagenesis reactions and the size of the expected product is 3704 bp. Initially T59Q and T59W reactions generated an incorrect product, but these were successfully repeated (Figure 10C).

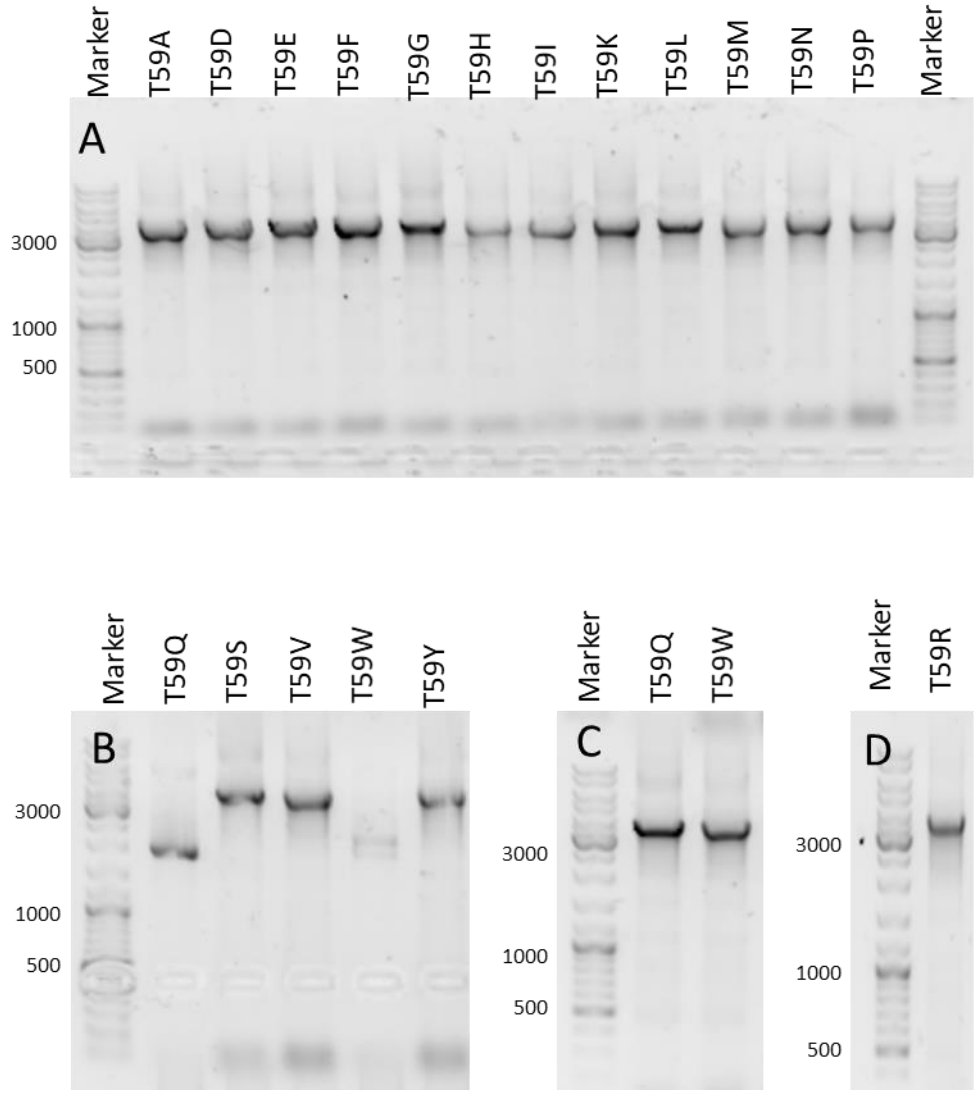

Figure 4.8 Quikchange™ mutagenesis products after Dpn I digestion from saturation mutagenesis of T59.

Gel A contains the products for T59A, T59D, T59E, T59F, T59G, T59H, T59I, T59K, T59L, T59M, T59N, and T59P, which display a band at the expected size. Gel B contains products for T59Q, T59S, T59V, T59W, and T59Y, unfortunately, T59Q and T59W have bands at an incorrect size. These were repeated and are shown on gel C. Gel D contains the PCR products of T59R.

The DNA was transformed into XL-1 blue cells and, after overnight growth, five colonies for each variant were cultured in 5 ml of LB medium and the plasmid DNA extracted using a QIAGEN mini prep kit (Section 2.5.4). The mutations were confirmed by DNA sequencing and a single clone for each was selected for protein production.

The variant proteins were produced using the same protocol as for wild type alkaline phosphatase (Section 4.2). Briefly, the plasmid DNA was transformed into SHuffle expression cells. A 5 ml starter culture in 2TY with 30 µg/ml kanamycin was inoculated with a single colony and grown overnight. 1 ml was used to inoculate 50 ml 2TY/ kan 30 µg/ml medium for 4-6 h at 25^{o}C. Protein was purified from the cultures, dialyzed as described in section 4.2.1, and the concentration of protein determined by a BCA assay. This process was successful for all variants except T59P that was not produced in the culture and therefore could not be studied further. The purified proteins are collectively referred to as T59X variants.

4.6 T59X variant protein activity

The specific activities for each of the T59X variants was determined using 17 nM of three independent preparations for each protein. A sample of wild type was also produced for comparative assays. The data are reported as percentage of the wild-type activity in Figure 4.9.

The specific activities of most of the variants was greater than 75 % of wild type activity, the exceptions being T59K, T59W and T59Y and, as expected, T59R showing essentially no activity.

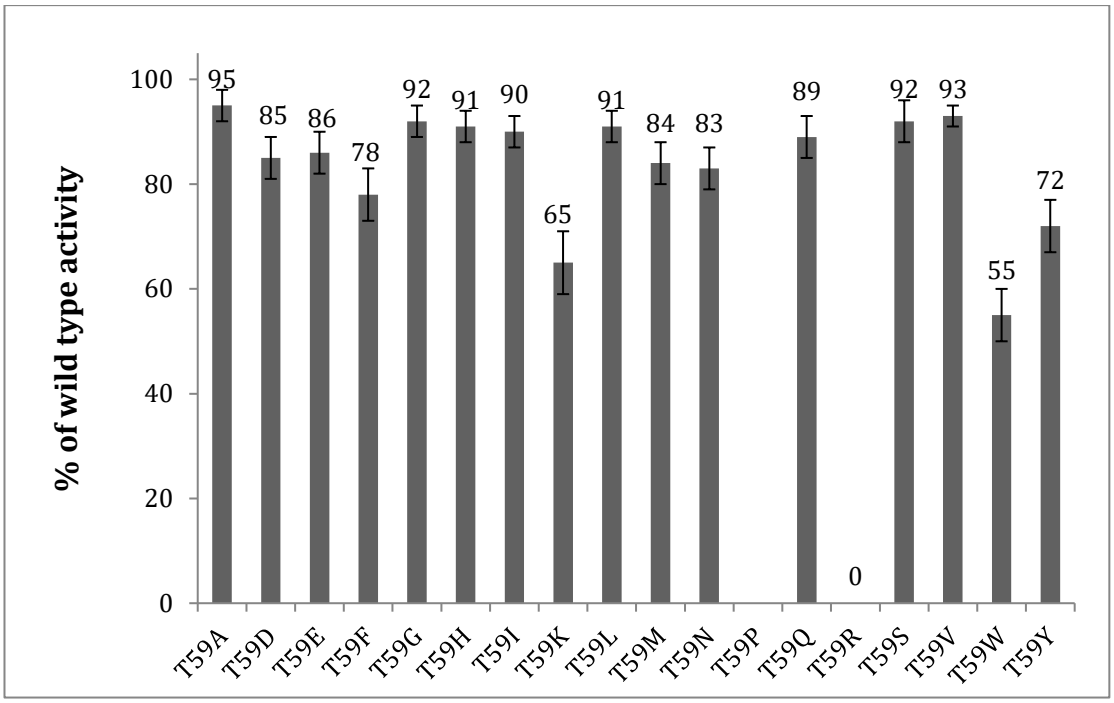

Figure 4.9 Relative specific activity levels of the T59X variants shown as % of wild type activity.

The values measured are shown above each bar.

Thr 59 is situated in the centre of an alpha helix at the dimeric interface. As noted, T59P did not produce protein and as a proline would distort the alpha helix this likely affects normal protein folding. T59K and T59R introduce large positively charged side chains. As previously discussed, mutation to arginine was reported to eradicate activity (Boulanger and Kantrowitz 2003). Lysine in this position also reduces activity to 65 % of wild type but this is not as drastic as Arg, perhaps due to the greater flexibility of the lysine side chain, which presumably adopts a conformation that still allows enzyme dimerization, although apparently not as efficiently as wild-type. T59Y and T59W both introduce aromatic side chains which are bulky and probably lead to some steric hindrance, albeit with 72 % and 55 % activity retained respectively, and are not as deleterious as Arg. With the exception of T59R, none of these variants alone resulted in a sufficient level of monomerisation and associated loss of activity to be used for this project. Thus, investigations into further mutations at the dimer interface were undertaken.

4.7 PDBSum analysis to identify important residues at the dimer interface

PDBSum (Laskowski, *et al.* 1997, Laskowski 2001) is a program that describes the inter- and intra-molecular interactions of a protein from the coordinates in a PDB file. This program was used to specifically investigate the interactions at the dimer interface. The PDBSum results for *E. coli* alkaline phosphatase, from PBD accession code 1ALK, were 504 non-contact bonds, such as van der Waals or hydrophobic interactions, 49 hydrogen bonds, and no other electrostatic interaction between 80 residues on chain A and 82 residues on chain B. Non-contact bonds cannot be overcome by a mutation as they are not specific to a side chain. Hydrogen bonds form between a hydrogen atom and an electronegative atom, usually oxygen, in a protein. Such bonds can involve both backbone and side chains, and for the purposes of protein engineering, only bonds involving side chains are amenable to modification, unless unnatural compound incorporation is used, which was not the case in these studies.

The 49 hydrogen bonds were investigated further and the 4 residues mentioned previously: R10, R24, T59, and T81 were included in this group. To reduce the number of interactions, for experimental investigation, first duplicate interactions in the form of mirroring interactions where the same residues on chain A interact with chain B and vice versa, were removed. Next, those where the interactions did not involve the amino acid side group were also removed. Thus, remaining interactions could potentially be manipulated through mutagenesis as shown in Figure 4.10. In addition to R10, R24, T59, and T81, the residues D28, R34, R62, and Y98 were investigated further. These all have at least one hydrogen bond interaction between their R-group and another residue (Figure 4.10). Thus, initially, each residue was mutated to an alanine, which, with a methyl side chain, cannot form side chain hydrogen bonds. The stability of the dimer interface interaction should be reduced as the number of hydrogen bonds holding the two peptide chains together is reduced. Hopefully, decreasing some of these interface interactions would convert the dimer into a monomer state.

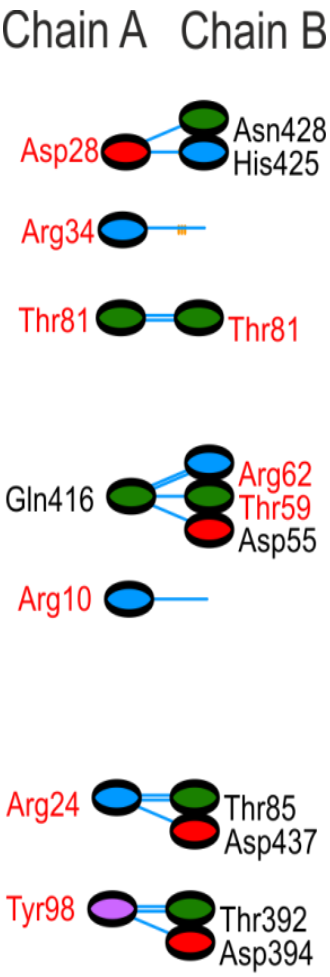

Figure 4.10 Hydrogen bonds formed between Chain A and Chain B of *E. coli* alkaline phosphatase.

The Figure is adapted from PDBsum output. The residues highlighted in red have been mutated to an alanine in this study. Only one set of interactions has been shown for simplicity. Arg34 and Arg10 interact with the backbone of the peptide and therefore their interacting partners are not shown.

Asp 28 was chosen because it was proposed that when mutated to an alanine it would remove interactions to Asn 428 and His 425. Arg 34 was proposed to interact with the backbone of chain B, but this would also be prevented by an alanine mutation. As T59A has already been shown to reduce the stability of alkaline phosphatase (Martin, *et al.* 1999, Boulanger and Kantrowitz 2003), R62 was theorized to increase the instability as it is part of the same interacting group and forms two hydrogen bonds to Gln 416. Finally, Tyr 98 was chosen as mutating it would prevent hydrogen bonds with Thr 392 and Asp 394.

T59A and T59R had been produced in the T59X saturation mutagenesis. The R10, R24, and T81 residues were reported in literature to destabilize the dimer interface (Martin, *et al.* 1999, Boulanger and Kantrowitz 2003, Orhanovic, *et al.* 2006), and so were also mutated to Ala. A further four residues indicated from the PDBSum data to potentially influence dimer interface stability, namely D28, R34, R62, and Y98, were also mutated to Ala.

4.8 Creating point mutations on the dimer interface

The mutagenesis reactions were not as straightforward as for the saturation mutagenesis at T59 and some reactions had to be optimized. Figure 4.11 shows a 1% agarose gel of the initial reaction for each of the single point mutations. R10A, R34A, and Y98A reactions contained DNA of the correct size, and were transformed into XL-1 blue cell. Colonies were cultured in 5 ml of LB medium and the plasmid DNA isolated using a QIAGEN mini prep kit.

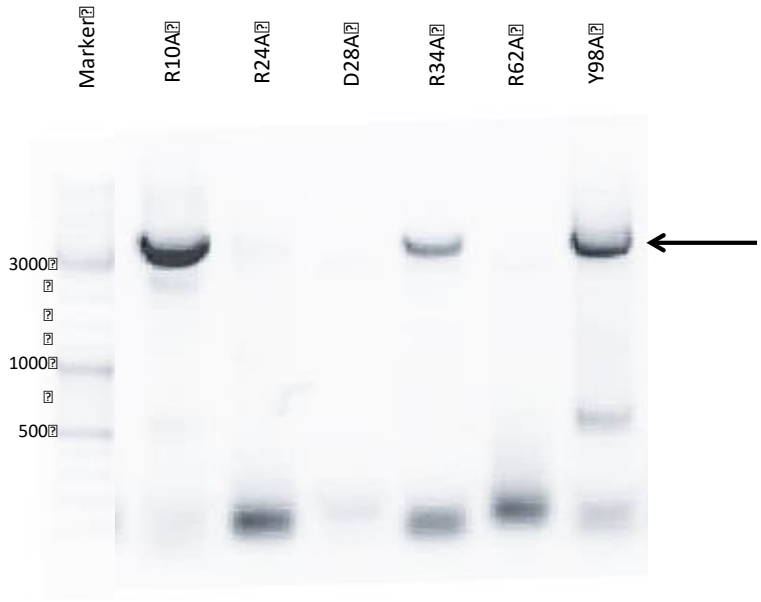

Figure 4.11 Mutagenesis reaction after Dpn I digestion from point mutagenesis reactions for R10A, R24A, D28A, R34A, R62A, and Y98A.

The expected products for R10A, R34A, and Y98A are indicated by the black arrow. Marker: molecular size markers with sizes in base pairs.

The mutagenesis reactions for R24A, D28A, and R62A had failed according to the results shown in Figure 1.15. The primers for R24A, D28A, and R62A were used to set up mutagenesis reactions at a range of annealing temperatures in order to ascertain the appropriate annealing temperature. The resulting gel contained two bands; one at approximately 3704 bp, that was likely to be the expected product, and one at approximately 4000 bp that was not expected. The DNA from the 3704 band was isolated by gel extraction by using the dialysis tube/electrophoresis method due to the low levels of product and potential 50% losses seen for product recovery from gel extraction kits (Chapter 2 Section 2.5.2.1).

The DNA was transformed into XL-1 blue cells, 5 colonies were cultured, plasmid DNA was isolated and, following DNA sequence analysis, the correct sequences were confirmed. Protein production, protein purification, concentration, and activity assays were performed as previously described in Section 4.2 and 4.6. Figure 4.12 shows the specific activities of the mutant forms of alkaline phosphatase relative to wild type alkaline phosphatase. Most of the specific activities are above 68 % of wild type activity, with the exception of R62A. The activity level of R62A was only 15 % of wild type, which is a notable reduction in activity. However, further improvements were sought by combining this point mutation into a small double mutant library, and by saturation mutagenesis at the R62 position.

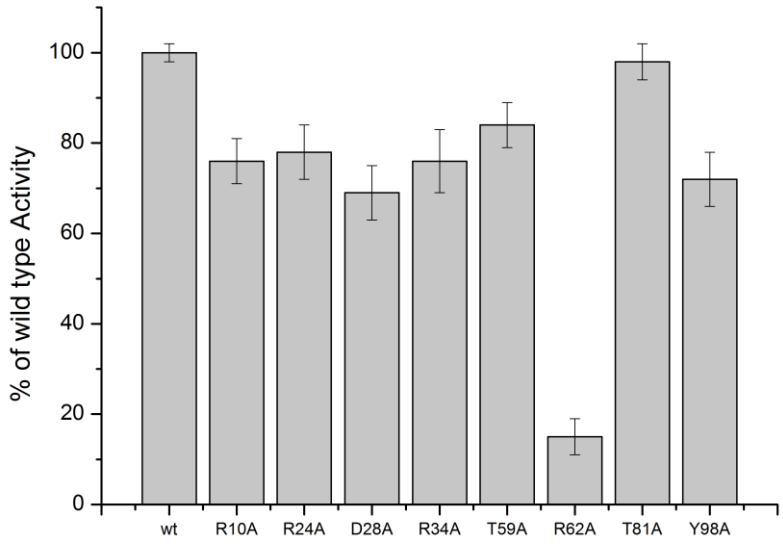

Figure 4.12 Relative specific activities of mutant forms of alkaline phosphatase

The values are showns as a percentage of wild type activity with 2 mM pNPP. The standard errors (n=3) are shown on the bar chart.

4.9 Combining the alanine mutations into a small double mutant library

Each of the single point mutants were used as a template, coupled with the primers for each of the other mutations, to create a small double mutant library as shown in Figure 4.13. As T59A and R62A are close together in the sequence, new primers were designed to introduce both mutations simultaneously. Mutagenesis was straightforward as the conditions for each set of primers had been optimised (Section 4.8), with the exception of T59A-R62A, but this proved successful using the same conditions as for the R62A primers. Once the mutations had been confirmed by DNA sequencing, protein production, protein purification, concentration, and activity assays were executed as previously described in Sections 4.2 and 4.6

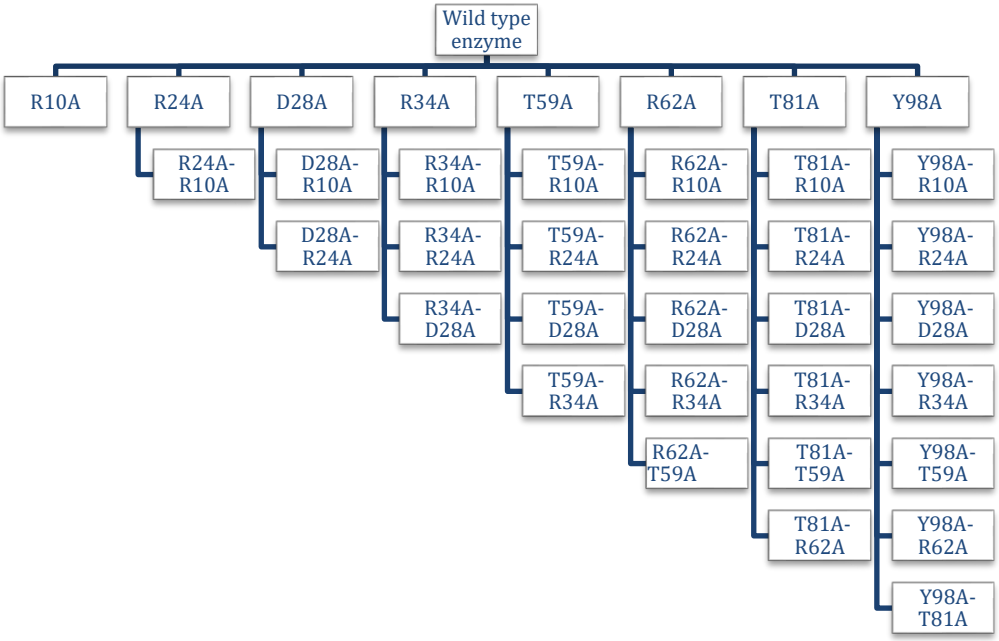

Figure 4.13 A schematic of the double mutant forms of AP produced in this study.

Each of the coding regions for single mutants were used as a template together with appropriate primers to introduce a second mutation, with the exception of T59A-R62A for which new primers were designed.

4.9.1 Enzymatic activity of double mutant forms

As alkaline phosphatase is not active as a monomer, in order to provide an indicator that the mutations affected dimerisation the specific activities of the double mutant forms were again measured and recorded as a percentage of wild-type activity.

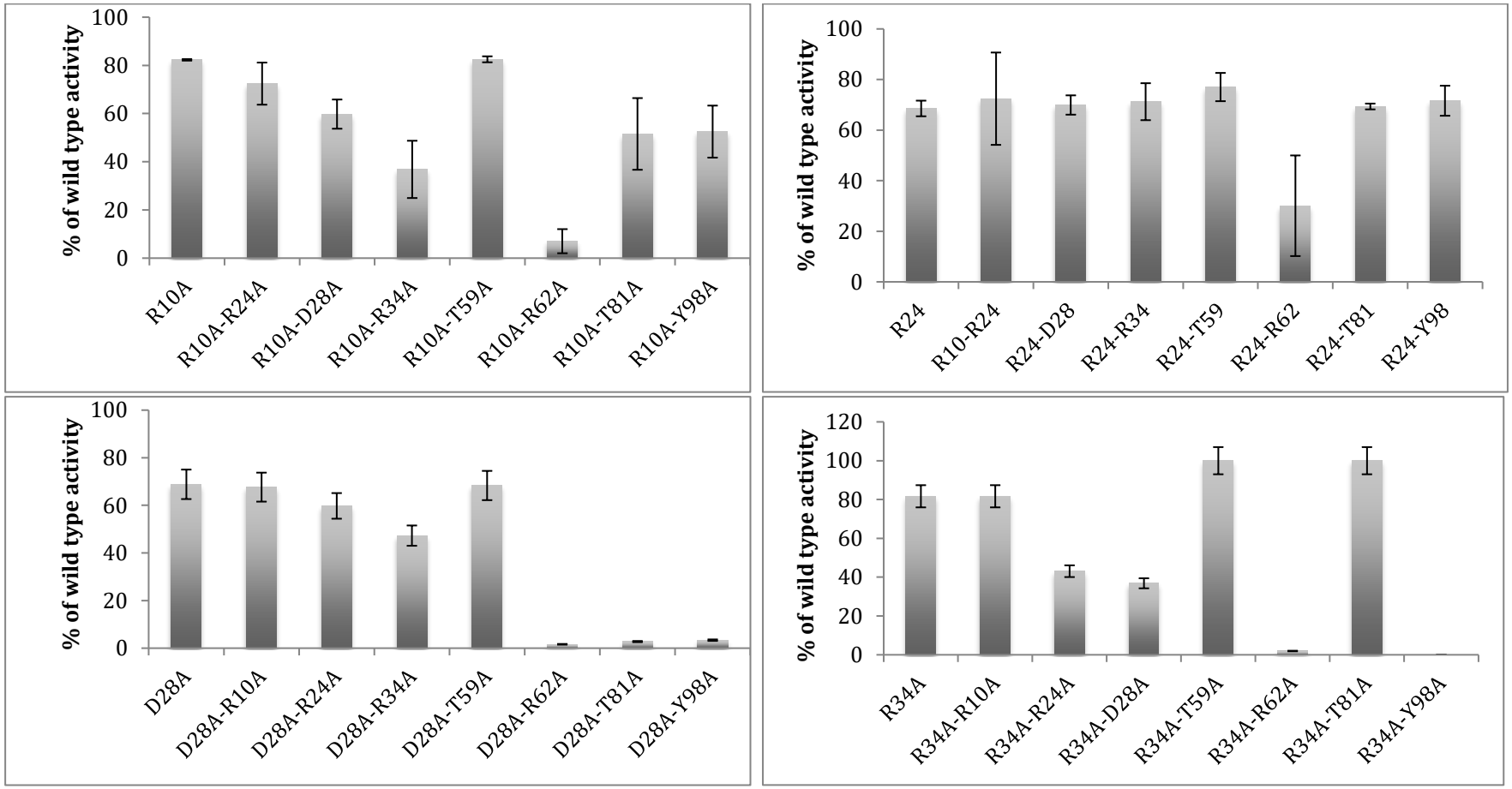

Figure 4.14 Relative specific activity as a percentage of wild-type activity of double mutant forms of R10A, R24A, D28A, and R34A.

The single mutant forms were also measured for comparison.

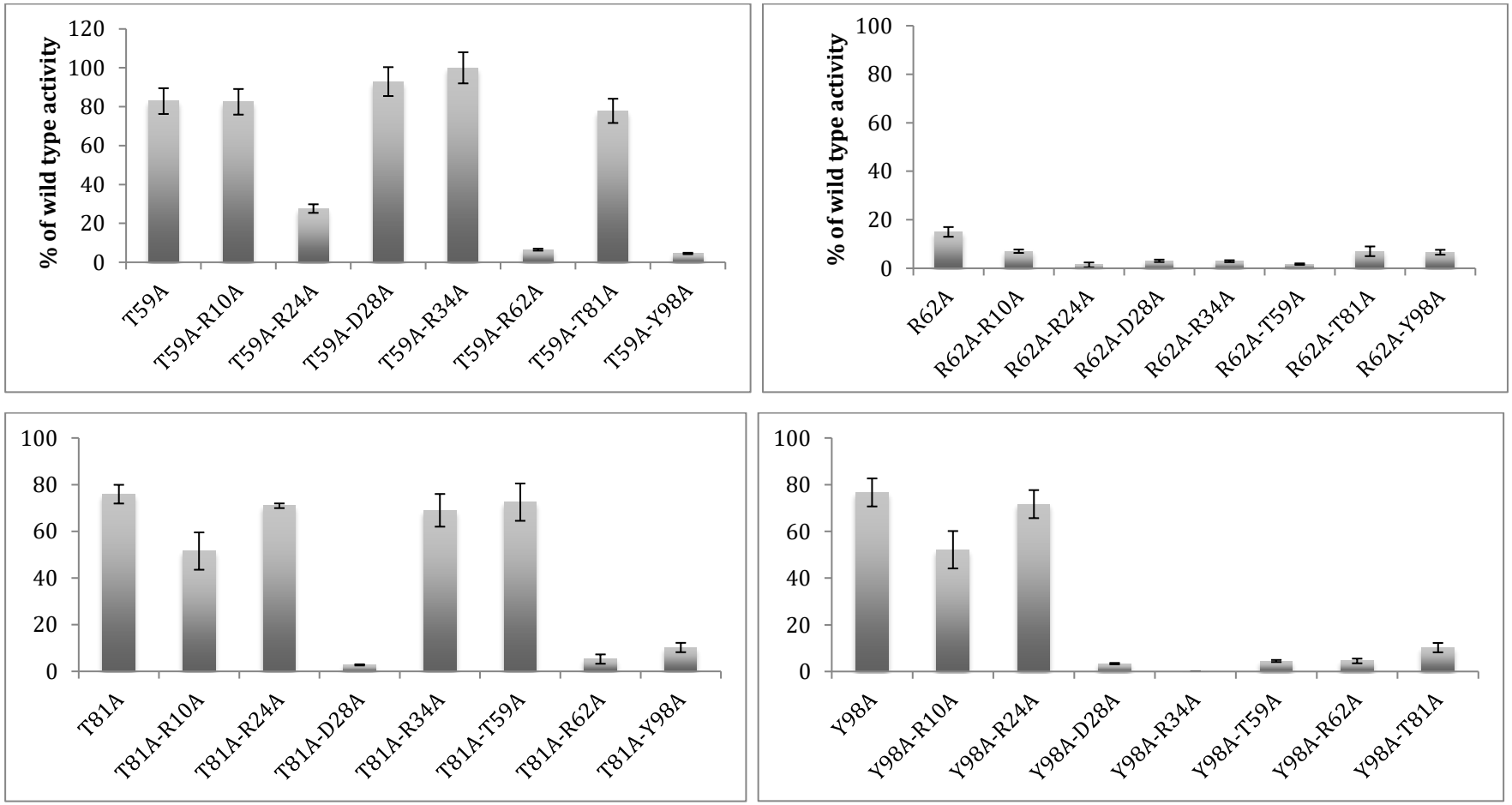

Figure 4.15 Relative specific activity as a percentage of wild-type activity of double mutant forms of T59A, R62A, T81A, and Y98A.

The single mutant forms were also measured for comparison.

Figure 4.14 and Figure 4.15 show the specific activity, relative to wild type, for of all the double mutants. Mutants of interest have reduced activity because a reduction in activity is an indicator of the enzyme being, at least in part, in a monomeric form. Table 4-2 lists all of the mutants with activity of less than 10 %. The R62A group is of particular interest as all double mutants show less than 7 % wild-type activity. In fact, the majority of mutant enzymes, seven out of eleven with reduced activity, contain the R62A mutation. The R34A-Y98A mutant did not express.

Table 4-2 Specific activity of low-level mutant alkaline phosphatase relative to wild type.

Mutant	Activity (% of wild type)	Mutant	Activity (% of wild type)
R10A-R62A	7.0 ± 0.7	T59A-R62A	1.7 ± 0.3
R24A-R62A	1.4 ± 1.0	T59A-Y98A	4.5 ± 0.5
D28A-R62A	3.1 ± 0.5	R62A-T81A	7.0 ± 2.0
D28A-T81A	1.5 ± 0.2	R62A-Y98A	6.6 ± 1.1
D28A-Y98A	3.4 ± 0.3	T81A-Y98A	10.0 ± 2.1
R34A-R62A	2.9 ± 0.4		

All of the variants listed in Table 4-2, together with wild-type and T59R, were investigated further to ascertain whether they would be good candidates for use in a split enzyme biosensor, as described in Chapter 5.

4.10 R62X saturation mutagenesis

When Arg 62 is mutated to alanine it has a dramatic effect on the activity of the enzyme, as shown in Figure 4.12, resulting in 15 % of wild type activity. A database search for similar sequences to *E. coli* alkaline phosphatase was performed using Basic Local Alignment Search Tool (BLAST) (Altschul, *et al*. 1990), the parameters of which are shown in Table 4-3.

Table 4-3 Search parameters for BLAST search.

Search Parameter Name	Search Parameter Value
Program	Blastp
Word size	6
Expected value	10
Hitlist score	100
Gapcost	11,1
Matrix	BLOSUM62
Filter string	F
Genetic Code	1

The algorithm returns a ranked order of scores with the highest indicating more similar sequences. The sequences with high similarity were confirmed to be alkaline phosphatases originating from several different organisms. These sequences were aligned using the Clustal W (Larkin, *et al.* 2007) software to perform a multiple sequence alignment that illustrates identity and similarity between the sequences. This analysis shows the equivalent of Arg62 to be conserved across a wide range of organisms, as shown in Figure 4.16, indicating that it is a key residue for either structural stability or biological function such as dimerization.

4.10.1 BLAST search & multiple sequence alignment

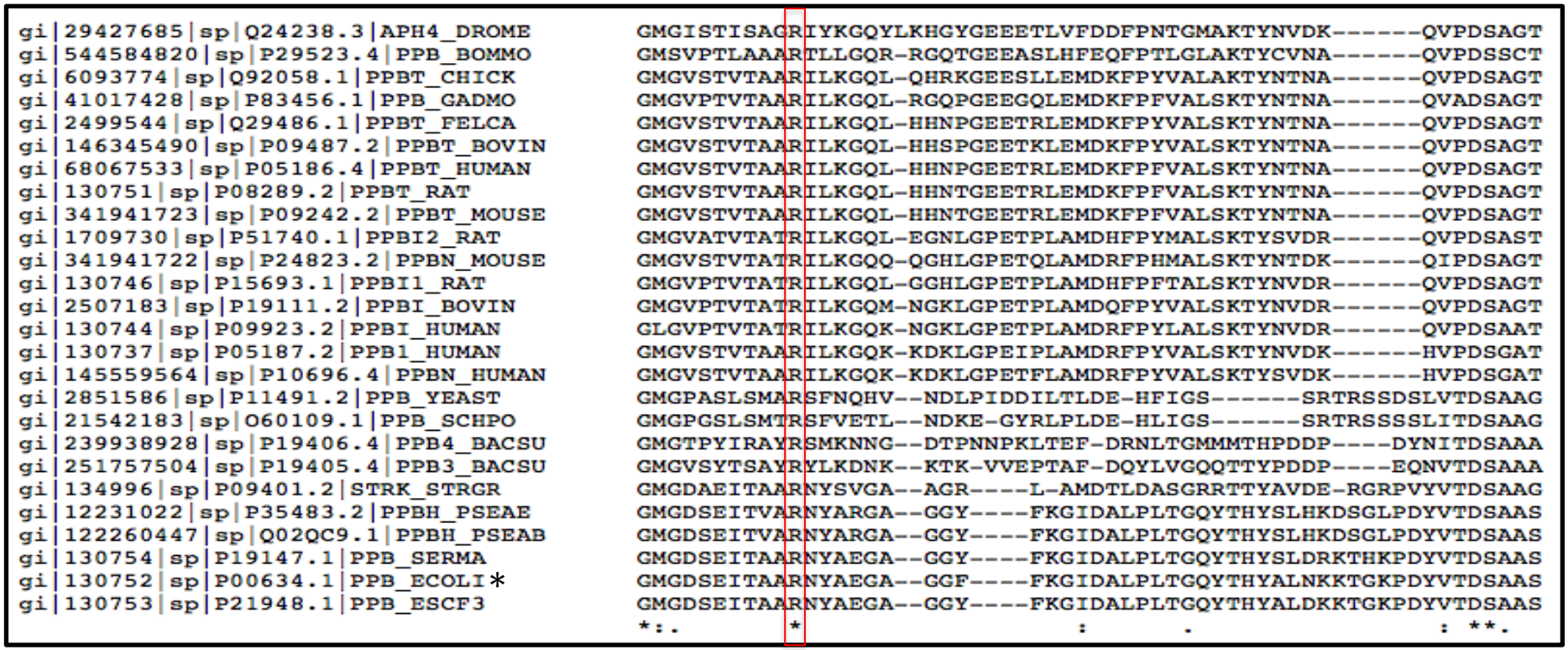

Figure 4.16 A multiple sequence alignment for several different alkaline phosphatases.

The species range from human (several isotypes) to *E. coli*. The red box shows the arginine conserved throughout the different proteins.

To investigate R62 further, saturation mutagenesis was performed with arginine being mutated to every amino acid, except cysteine, to avoid disulfide bridge formation at the dimer interface, as described in Chapter 2 Section 2.5.1.2. Each mutation was confirmed by DNA sequencing and the protein was produced as described in Section 4.2 and 4.6. The concentration of each of the R62X proteins was determined using a BCA assay and then the enzyme activity was investigated.

4.10.2 R62X specific activity

Figure 4.17 shows the specific activity for each of the R62X mutants. For clarity the values are shown above each data point. The presence of any other amino acid in place of arginine has a detrimental effect on enzyme activity. Changing to lysine has the least effect, with the R62K mutant retaining 82.8 % of wild-type activity. R62A, R62H, and R62P also had greater than 12 % activity so these three variants were also disregarded.

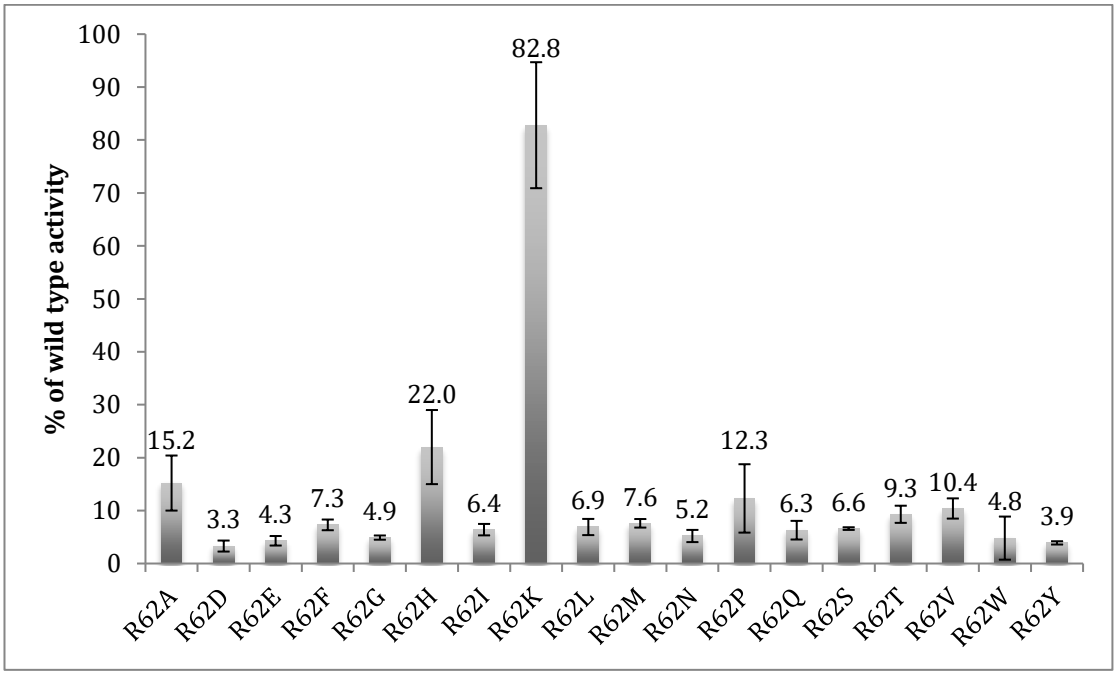

Figure 4.17 Specific activities of R62X mutants of alkaline phosphatase. The activity was determined as a percentage of wild-type at 2 mM pNPP. The standard errors (n=3) are also shown.

Further investigation of a subset of the variants with low activity R62D, R62E, R62G, R62I, R62L, R62M, R62N, R62Q, and R62Y was undertaken together with an analysis of the 11 variants identified from the double mutant pool. This analysis is described in Chapter 5.

4.11 Discussion

Monomeric alkaline phosphatase from *E. coli* does not turn over the substrate, but in the homodimeric form it turns over several different phosphate esters (Heppel, *et al.* 1962). A monomeric form of alkaline phosphatase was required for use as a split enzyme. In order to explore the creation of a stable monomer, residues at the dimer interface of alkaline phosphatase were mutated. A reduced specific activity was used as an indicator that the enzyme may be predominantly monomeric. There are a number of mutations of residues along the dimer interface that are reported in the literature to reduce the stability of the dimer, and it has also been reported that monomeric formation is possible. These mutations are R10A, R24A, T59A, T59R, and T81A (Boulanger and Kantrowitz 2003, Orhanovic, *et al.* 2006). T59R was a stable monomer (Boulanger and Kantrowitz 2003) but steric hinderance would prevent association of these monomers into a functional dimer. The various reported point mutations were included in this study, along with D28A, R34A R62A, and Y98A, based on bioinformatic data that indicated that mutations at these positions may affect the stability of the dimeric interface.

Saturation mutagenesis of positions T59 and R62 was carried out to determine whether an alternative side chain could create a stable monomer. The T59X group of mutants did not yield any further interesting variants other than the already established T59R. However, the R62A mutant appeared of interest, because of its reduction in activity and, from double mutant libraries, 11 variants with substantial reductions in activity were identified. These were; R10A-R62A, R24A-R62A, D28A-R62A, D28A-T81A, D28A-Y98A, R34A-R62A, T59A-R62A, T59A-Y98A, R62A-T81A, R62A-Y98A, and T81A-Y98A.

These variants all include R62A, T81A, or Y98A, and, with the exception of the R62A double mutant group, do not include R10A, R24A, and R34A. A study

by Tyler-Cross *et al.* (Tyler-Cross, Roberts *et al.* 1989) reveals that deleting 9 amino acids from the N-terminal end of alkaline phosphatase does not affect the turnover of the enzyme. The point at which amino acid deletion began to impact upon the enzyme was upon removal of R10, whilst removing a further 24 residues to position 36 did not result in any further change. This study along with that of Tyler-Cross *et al.* (Tyler-Cross, *et al.* 1989) indicate that the R10A, R24A, D28, and R34A mutations do not contribute to the same extent as other residues to the stability at the dimer interface.

The large reduction in activity of R62A to just 15% of wild type indicates that this residue is important. Furthermore, the fact that the residue is highly conserved throughout many different species indicates it is important for the function of the enzyme. Saturation mutagenesis of R62 showed that mutating this residue to any other amino acid, with the exception of lysine, has a marked effect on the activity of the enzyme. R62K had the least effect, retaining over 80 % of wild-type activity. Both arginine and lysine have positively charged side chains, indicating that a positive amino acid in this position is required for optimal function. The pKa of the side chains of arginine and lysine are 12.48 and 10.53 respectively. The activity measurements were performed in a Tris buffer at pH 8.0, therefore, the dominant form of these amino acids would be positively charged.

The pyrrole ring in histidine has a pKa of 6.0, and therefore at pH 8.0 the dominant form would be neutral. R62H retained 22 % of wild type activity, which is a marked reduction and is indicative of the dominant neutral form at pH 8.0. The level of activity could be due to an equilibrium between neutral and charged species. All other mutants gave rise to a marked reduction in activity.

The saturation mutagenesis libraries omitted mutating to a cysteine because it would for a disulphide bridge and would not come apart. Although it could be argued that because the enzyme is destabilised, when the subunits are brought back together would you get a S-S bond which might actually lead to a stable signal.

A subset of these mutants: R62D, R62E, R62G, R62I, R62L, R62M, R62N, R62Q, and R62Y were further characterised along with the 11 double mutants in Chapter 5.

Chapter 5
Characterising Alkaline Phosphatase Variants

5.1 Introduction

The alkaline phosphatase variants from Chapter 4 that showed a low enzyme activity were:

R10A-R62A	R34A-R62A	T81A-Y98A	R62L
R24A-R62A	T59A-R62A	R62D	R62M
D28A-R62A	T59A-Y98A	R62E	R62N
D28A-T81A	R62A-T81A	R62G	R62Q
D28A-Y98A	R62A-Y98A	R62I	R62Y

These include 11 double mutants and 9 R62X mutants chosen from the R62X saturation mutagenesis group. It was necessary to characterise whether any of these would be suitable for use, initially in a split enzyme assay, and subsequently in a split enzyme biosensor. This analysis process required the re-reconfiguration of the variants.

5.2 Re-activation of Split- Alkaline Phosphatase

The underlying principle of a split enzyme assay is that the two parts of the split enzyme can undergo intramolecular complementation if they are brought together by suitable molecular interactions. It was therefore necessary at this stage to provide a suitable mechanism for the stabilisation of the variant subunits in order to restore enzyme activity. A schematic of alkaline phosphatase is shown in Figure 5.1(a). The two monomers in the dimer form are shown, with the N-terminus indicated by a green circle, and the C-terminus by a red circle. Figure 5.1(b) shows the presence of a mutation at the dimeric interface. The experimental approach was designed to re-stabilise the mutationally destabilised parts by associating them via a coiled coil interaction. The DNA sequence encoding the K4 coiled coil (De Crescenzo, *et al.* 2003) was cloned into the vector pECAP-Sort to generate an N-terminal fusion with alkaline phosphatase pK4-ECAP-Sort. The coiled coil used is shown in Figure 5.1(c) and is called ‘K4’ as it is 4 repeats of a lysine-rich heptad sequence and it is shown as a schematic coiled coil structure. To give the coil directionality, two asparagine residues were used since buried polar interactions on the

interface of the coiled coils can orient the coiled coils in a particular way (Oakley and Kim 1998). Figure 5.1(d) presents a schematic of each of the mutated alkaline phosphatase subunits, with the K4 coiled coil holding them together.

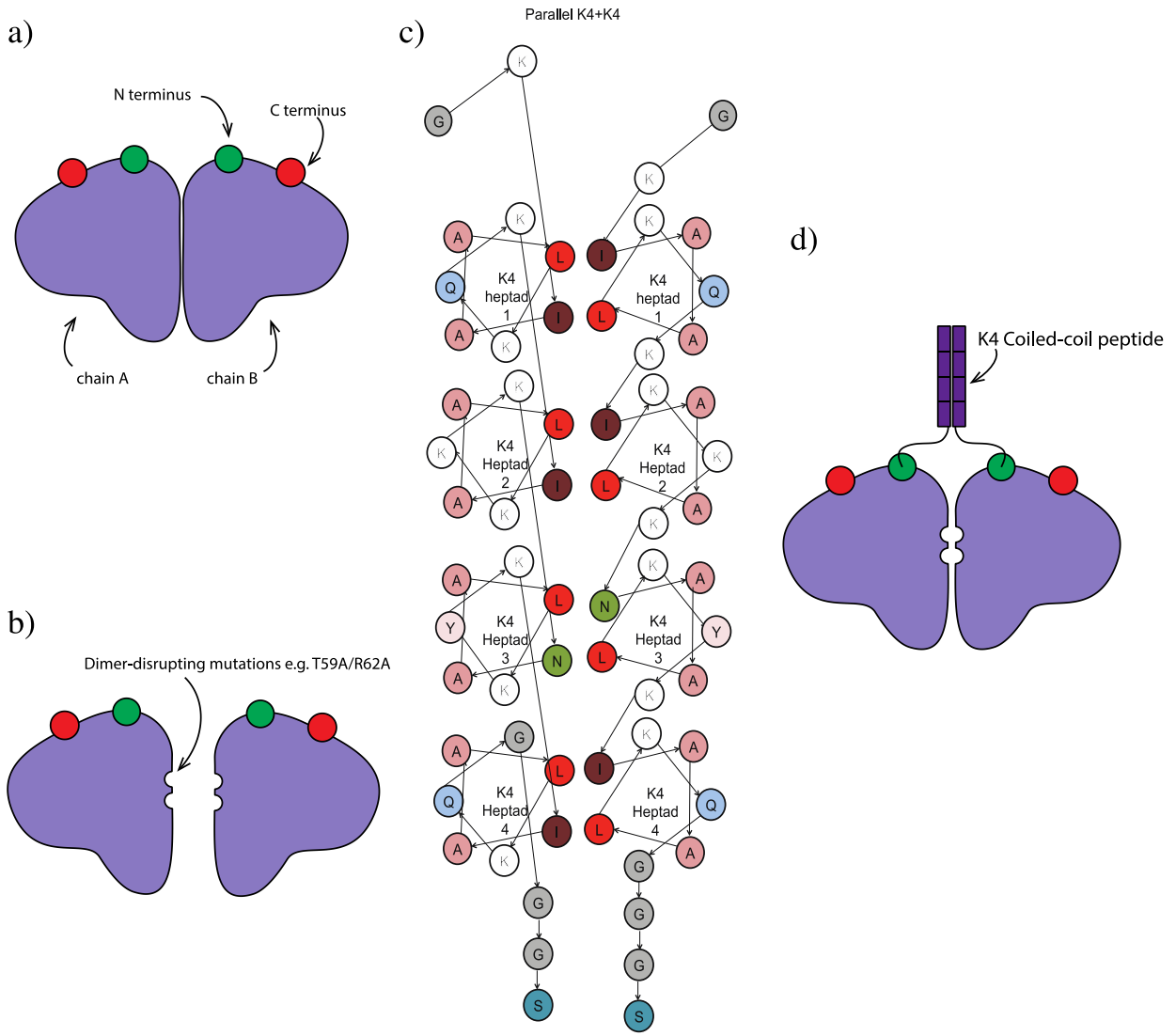

Figure 5.1 Introduction of the K4 coiled coil at the N-terminus of alkaline phosphatase to test whether the monomer association can lead to restored enzyme activity.

a) A schematic of alkaline phosphatase, with the N-terminus shown as a green circle, and the C-terminus as a red circle. b) A schematic of alkaline phosphatase with the dimer interface disrupting mutations. c) The K4 coiled coil showing the residue interactions designed to facilitate association of the two coils d) A schematic of alkaline phosphatase with the K4 coiled coils attached and associated.

5.2.1 K4 coiled coil – alkaline phosphatase fusion protein.

A plasmid; pE4-K4 which contained the coding region for the K4 coiled coil, was kindly supplied by the Wälti laboratory (University of Leeds) and this was used as a template for PCR amplification of the coiled coil coding region. The result of this amplification was the production of a megaprimer, as shown in Figure 5.2

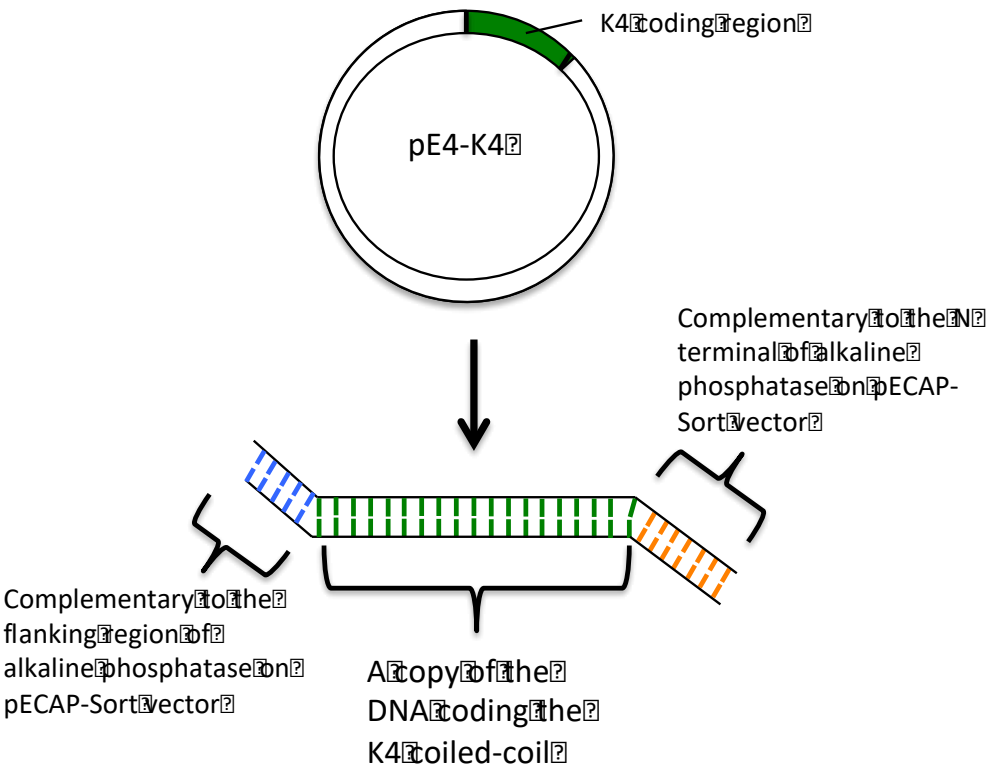

Figure 5.2 Mega primer amplification.

Primers to amplify the K4 coding region from pE4-K4 were used in a PCR reaction to produce a K4 megaprimer. The primer was designed to include the flanking region of alkaline phosphatase and the N-terminal of alkaline phosphatase on pECAP-Sort

The megaprimer was then used to insert the K4 coding region into the pECAP-Sort plasmid. The result was a plasmid encoding a fusion protein with the coiled coil, a linker region and then alkaline phosphatase.

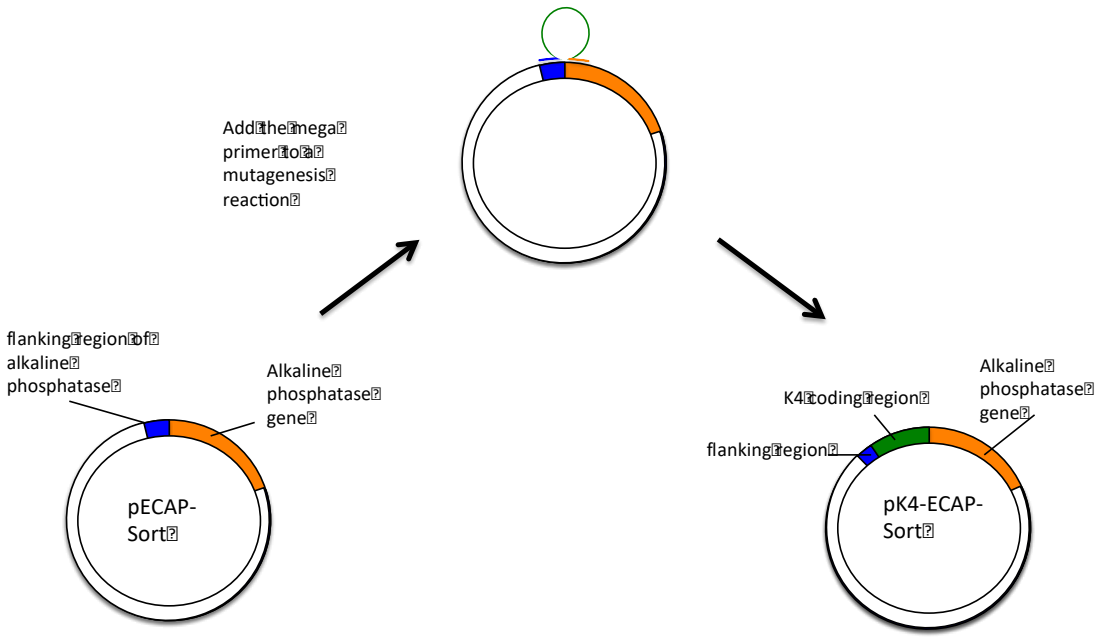

Figure 5.3 Megaprimer mutagenesis of pECAP-Sort.

A K4 megaprimer was used as the primers for a mutagenesis reaction to add the K4 coding region to the alkaline phosphatase gene.

This was done by introducing overlapping ends, which are complementary to regions flanking the position where the K4 coiled coil was introduced, using the Quikchange™ method described in Chapter 2 Section 2.5.1.3. The introduction of the coiled coil was confirmed by DNA sequencing and the resulting plasmid was called pK4-ECAP-Sort. There was a stutter introduced between the K4 coiled coil and alkaline phosphatase: 3' ggtggtacccctgagatgccggtgctggctgctatcaaaggtggt 5'. This extra DNA translated into 15 amino acids: G G T P E M P V L A A I K G G. Several attempts were made to remove the extra DNA, but this was unsuccessful, and at the same time the K4 – alkaline phosphatase fusion protein was produced from pK4-ECAP-Sort. It was decided that if the protein behaved the same as the wild type form then the experiment could continue with this construct and the extra 15 amino acids would be considered a linker region.

5.2.2 Protein production

The pK4_ECAP- Sort vector was transformed into competent Shuffle cells and then protein was produced in the same way as wild type alkaline phosphatase, as described in Chapter 2 Section 2.6.2. Each mutation was introduced into this plasmid by using the previously successful Quikchange^{TM} approach but using K4_ECAP rather than pECAP as the template. Purification of the K4-wild type protein resulted in a yield of around 2-3 mg/L, which is markedly lower than achieved for wild type alkaline phosphatase (10-15 mg/L) The mutant versions of the alkaline phosphatase with the K4 coil proved even more difficult to produce with yields of 0.1 - 0.25 mg/L. To generate sufficient protein for the planned experiments, 6 litre cultures were used to produce the proteins with purification performed in the same way as for wild type alkaline phosphatase, as described in Chapter 2 Section 2.7.2

5.2.3 Assays of coiled coil containing variants

Enzyme assays to measure the specific activity of each of the K4-AP variants and the corresponding variants lacking the K4 were undertaken. This was expected to ascertain whether any of the mutants displaying low activity would show an increase in enzyme activity in the coiled coil format.

5.2.3.1 Wild type and T59R

Wild type alkaline phosphatase and K4 wild type were compared to establish whether the addition of the coiled coil adversely affected enzyme activity. T59R and K4_T59R were also tested to ascertain whether this mutant could be stabilised in a functional dimer despite the steric hindrance discussed in Chapter 4.

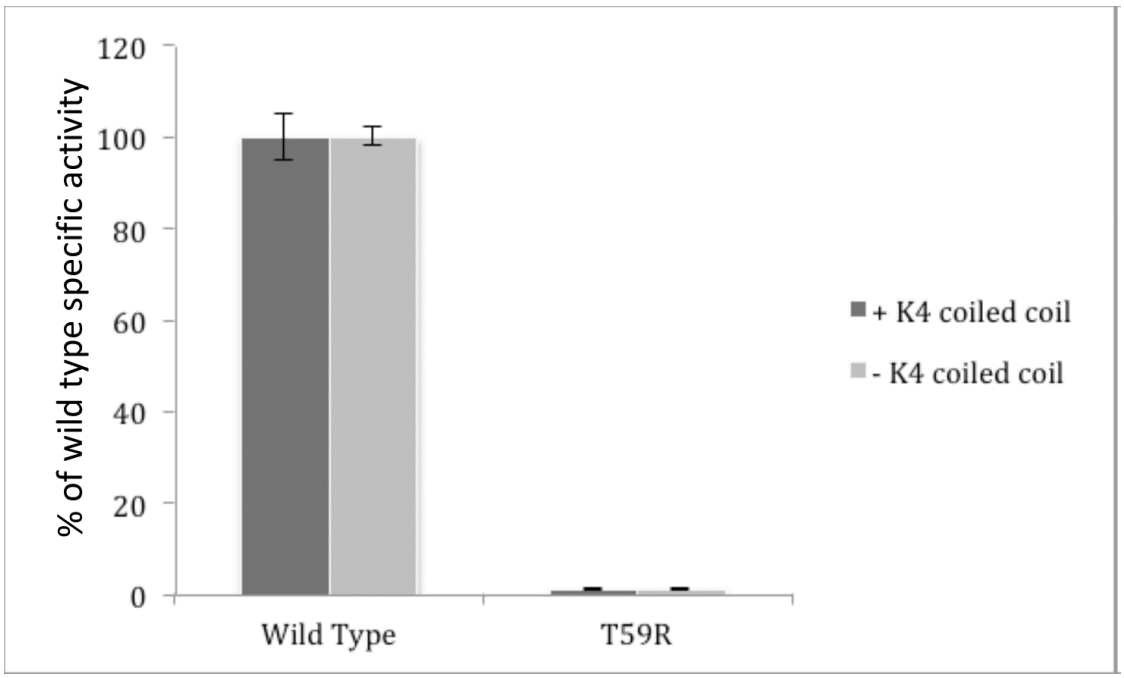

Figure 5.4 Activity of wild type alkaline phosphatase and a T59R mutant with and without K4 coiled coil attached.

With the coiled coil is displayed in dark grey and without the coiled coil is displayed in light grey.

Figure 5.4 shows that the addition of the K4 coiled coil does not affect the activity of either wild type or the T59R mutant. T59R could thus be used as a negative control in future activity experiments. There were three different protein preparations and these were measured three times with each of the protein preps. There was good agreement between the three repeats of wild type alkaline phosphatase.

Table 5-1 Absorbance (405 nm) results for specific activity of wild type and T59R

Wild Type			
	batch 1	batch 2	batch 3
repeat 1	1.14	1.11	1.26
repeat2	1.20	1.19	1.22
repeat3	1.26	1.14	1.30

K4 Wild Type			
	batch 1	batch 2	batch 3
repeat 1	1.23	1.16	1.22
repeat2	1.20	1.21	1.20
repeat3	1.17	1.18	1.25

T59R			
	batch 1	batch 2	batch 3
repeat 1	0.02	0.02	0.02
repeat2	0.02	0.02	0.02
repeat3	0.01	0.01	0.02

K4 Wild Type			
	batch 1	batch 2	batch 3
repeat 1	0.03	0.03	0.02
repeat2	0.02	0.03	0.03
repeat3	0.03	0.02	0.03

Table 5-1 shows the results for wild type and T59R. The average of these three repeats was taken as 100% wild type activity, and the activities of all mutants were compared to this activity. As a control, wild type activity was measured every time a batch of proteins containing mutations was tested, to confirm the correct assay parameters for wild type activity.

5.2.3.2 Specific activities of double mutants

The relative specific activity of each double mutant, with and without the K4 coiled, is shown in Figure 5.5. These were each tested alongside wild type and T59R and two repeats of each were averaged.

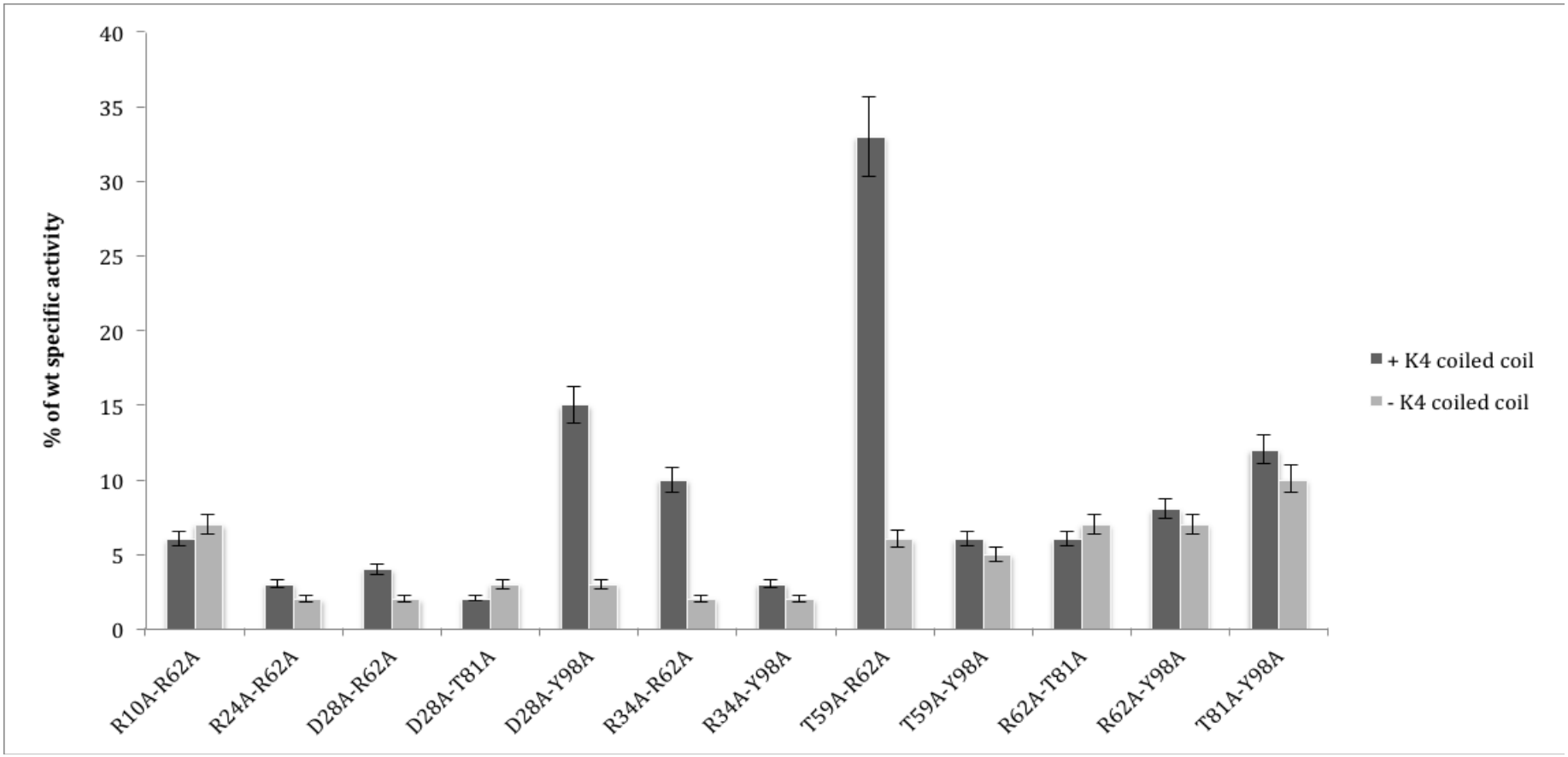

Figure 5.5 Specific activity of the double mutants.

The dark grey shows the activity of the mutant with the addition of the K4 coiled coil. The light grey shows the activity of the mutant without the coiled coil. The data are presented as a percentage of wild type activity.

Figure 5.5 indicates that three of the double mutants showed a significant K4 associated increase in activity; D28A-Y98A, R34A-R62A, and T59A-R62A. R34A-R62A increased by 8% of wild type activity; D28A-Y98A increased by 12% of wild type activity. Out of these three, T59A-R62A shows the largest increase, with an increase of 27% of wild type activity. When the data are analysed as the magnitude of the increase in activity as a ratio of +K4/-K4, the order doesn't change. R34A-R62A activity increased 3.5 fold; D28A-Y98A activity increased 4.2 fold, and T59A-R62A shows the largest increase, with an activity increase of 5.5 fold.

5.2.3.3 R62X mutants

The eight R62X mutants that displayed low specific activity were also investigated alongside the versions incorporating the K4 coiled coil. There were two different protein preparations and these were measured three times with each of the protein preps. R62G, R62I, and R62N all have increased activity as presented in Figure 5.6.

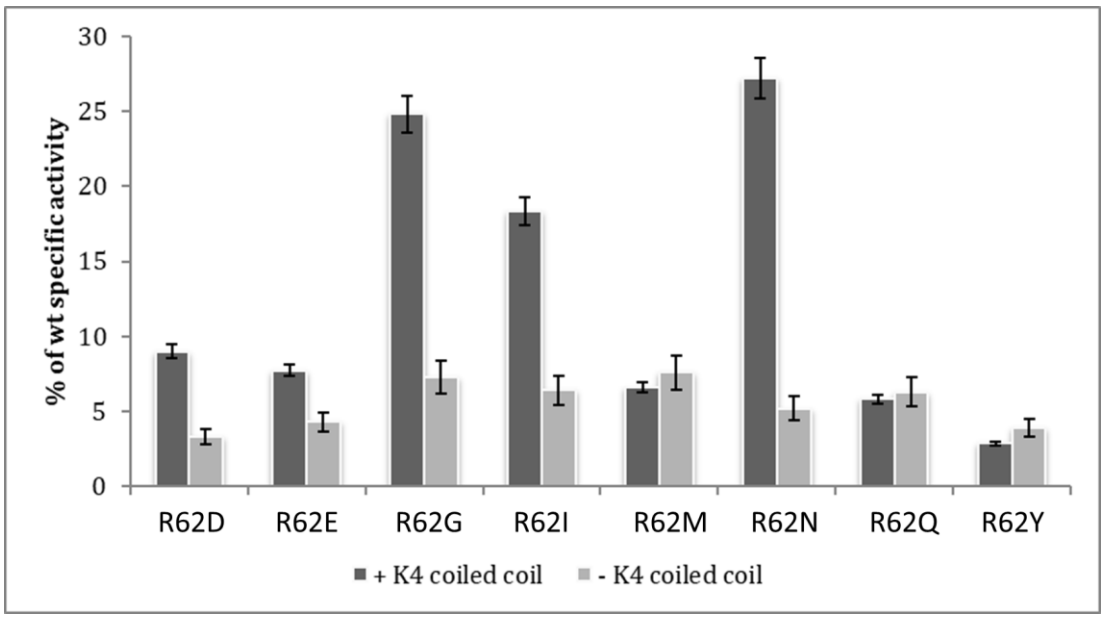

Figure 5.6 Activity of the R62X mutants.

The dark grey shows the activity of the mutant with the addition of the K4 coiled coil. The light grey shows the activity of the mutant without the coiled coil. The data are presented as a percentage of wild type activity

Figure 5.6 shows that R62I and R62G increased in activity to 18% and 25% of wild type activity respectively, although the greatest increase was for R62N, which increased from 5 to 27% of wild type activity.

5.3 Secondary structure analysis of alkaline phosphatase mutants.

The secondary structure of the alkaline phosphatase double mutants and R62X mutants was investigated by far UV CD to determine whether the proteins were likely to be folded correctly. As the activity of alkaline phosphatase mutants was measured in 1 M Tris-HCl pH 8.0, it was important to check whether the secondary structures were affected in this buffer. Buffers that contain chloride ions absorb light strongly below 200 nm (Kelly, *et al.* 2005), and therefore the data were analysed between 200 nm to 260 nm. Wild type alkaline phosphatase was investigated as a positive control and as it showed the expected level of enzyme activity it should be folded correctly, allowing comparison with the spectra of variants.

5.3.1 CD analysis of wild type and T59R proteins

CD experiments were performed on a Jasco J715 spectropolarimeter and the spectra were recorded in a 0.02-cm path length using a scan speed of 50 nm/min, a time constant of 0.5 s and a bandwidth of 2 nm. Three scans of each sample were performed. The Jasco J715 spectropolarimeter reports its raw output in ellipticity (θ) measured in millidegrees (mdeg). To compare the data across samples, θ was converted to Molar Ellipticity ([θ]) in units of degrees/cm^2/decimole. Hence, $[\theta] = \theta / (10 \times c \times l)$ where c is the molar concentration of the sample and *l* is the path length in cm.

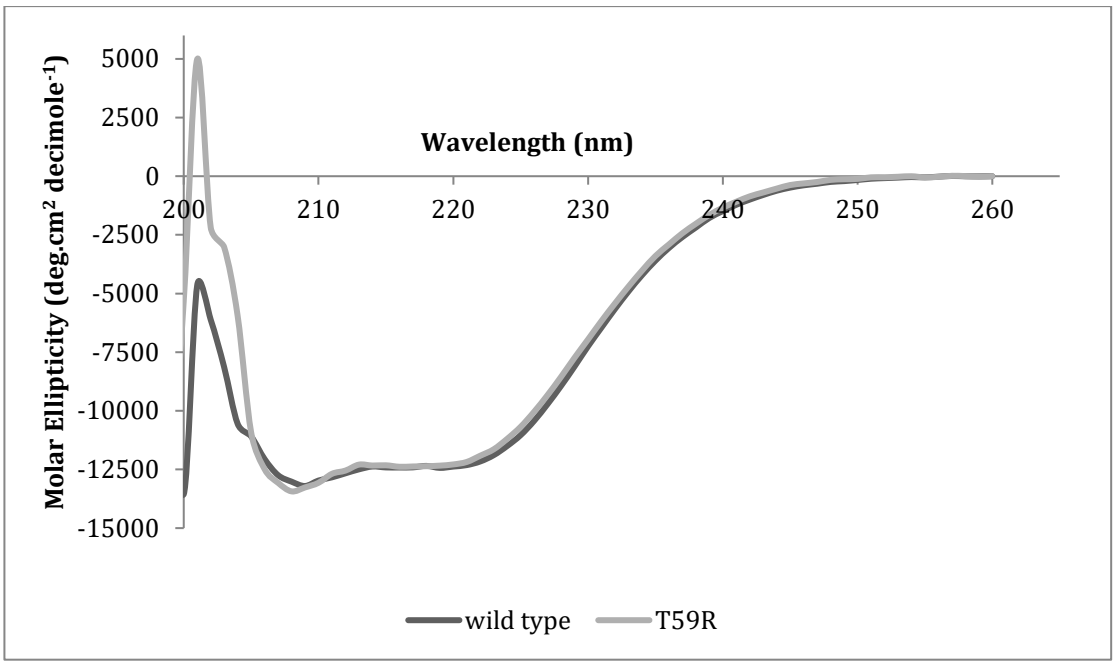

Figure 5.7 Far UV CD spectra of wild type (dark grey line) & T59R (light grey line) alkaline phosphatase.

The spectra show that there is little change in secondary structure between wild type and the T59R mutant

The CD spectra of wild type alkaline phosphatase and T59R overlay directly between 205 and 260 nm, as shown in Figure 5.7. The shape of the curves gives an indication of secondary structure and therefore suggests the proteins are folded correctly. The shape is indicative of α-helix secondary structure (Kelly, *et al*. 2005) and also indicates that there is a high degree of similarity between wild type and T59R secondary structures.

5.3.2 CD analysis of double mutant proteins

Figure 5.8 shows the CD spectra of the double mutant proteins: R10A-R24A, D28A-R62A, D28A-Y98A, R34A-Y98A, T59A-R62A, R62A-T81A, R62A-Y98A, and D28A-T81A. These spectra are very similar to the wild type shown in Figure 5.7, which indicates that these proteins have essentially identical secondary structure profiles to the wild type and can therefore be considered to be correctly folded. By contrast the CD spectra shown in Figure 5.9 indicate that the low enzyme activity measured for R24A-R62A, T59A-Y98A, and T81A-Y98A are likely due to the protein being in an abnormal folded state.

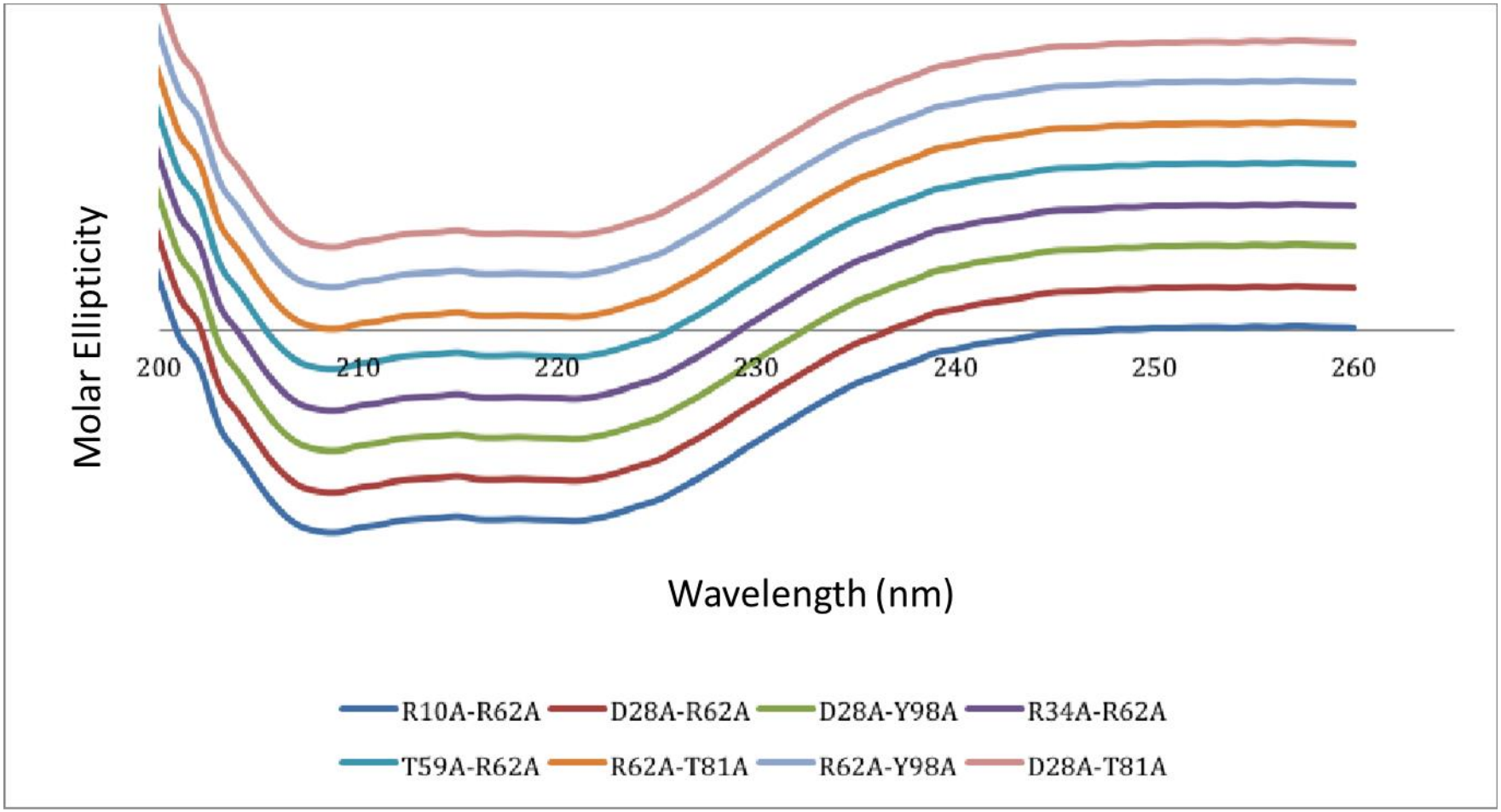

Figure 5.8 Far UV CD spectra of alkaline phosphatase double mutants.

R10A-R24A - dark blue, D28A-R62A - red, D28A-Y98A – green, R34A-Y98A – purple, T59A-R62A – light blue, R62A-T81A – orange, R62A-Y98A - lilac, D28A-T81A - salmon. The spectra shows that there is little change in secondary structure between each of the mutants. The spectra are stacked for clarity.

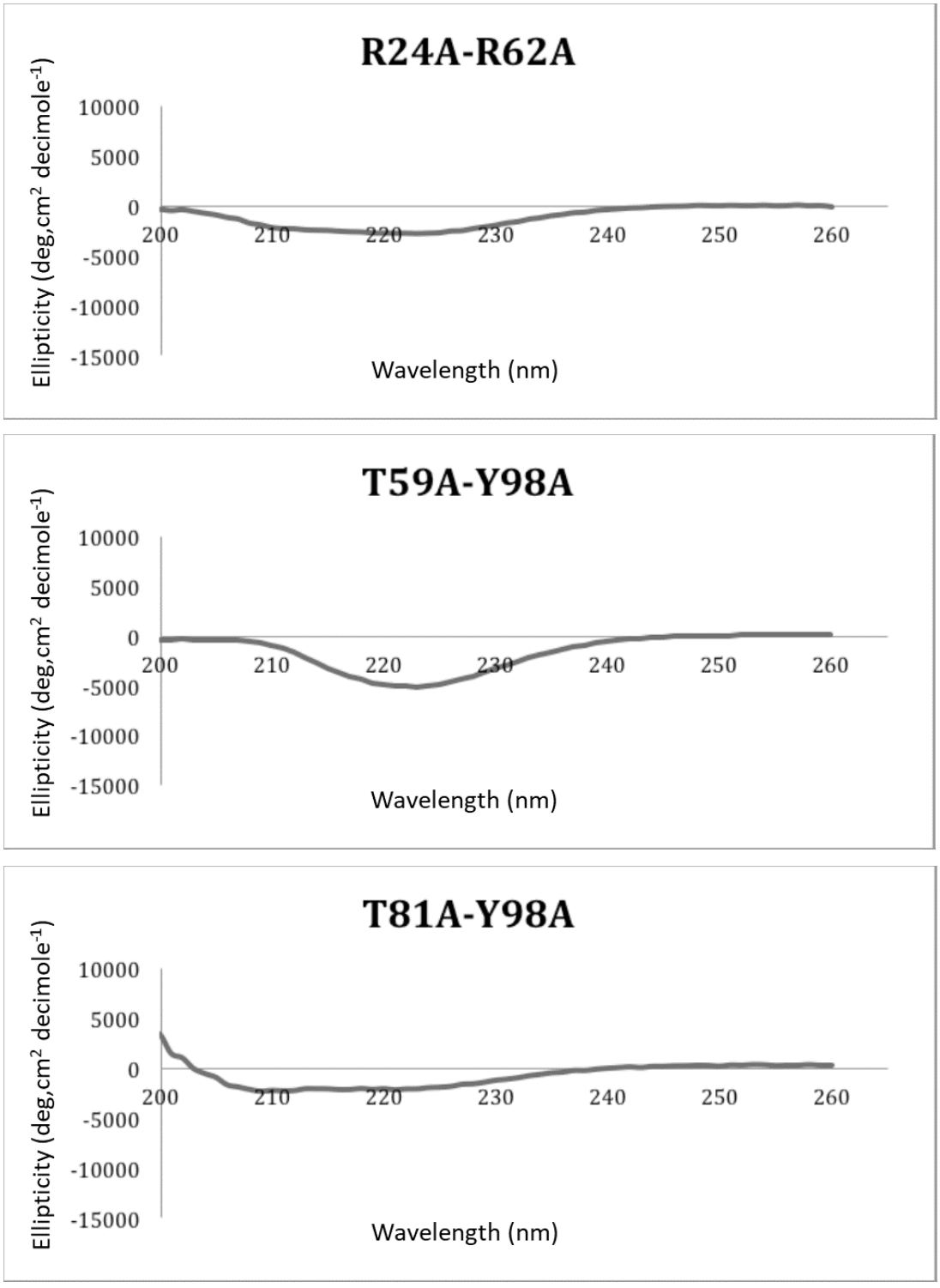

Figure 5.9 Far UV CD spectra of the double mutants not showing secondary structure.

R24A-R62A – top, T59A-Y98A – middle and T81A-Y98A bottom. All appear to show secondary structures distinct from the wild type.

5.3.3 R62X mutants

The R62X mutants all have similar spectra to wild type as shown in Figure 5.10, indicating that the proteins are correctly folded.

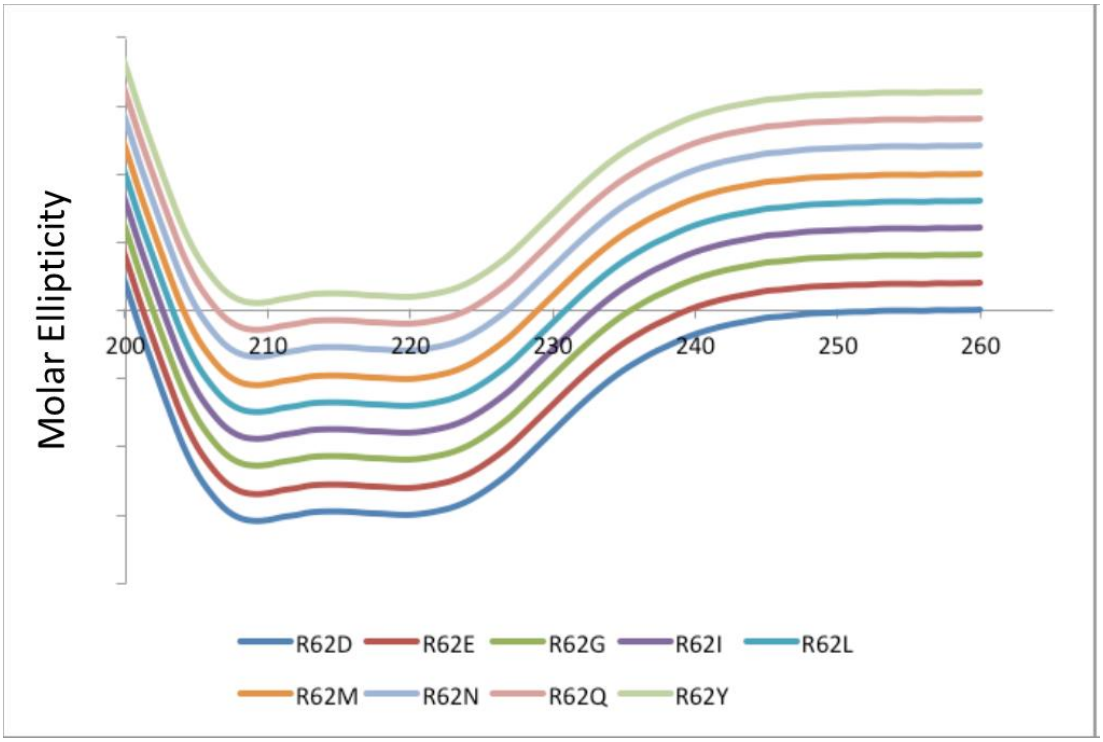

Figure 5.10 Far UV CD spectra of alkaline phosphatase point mutants. R62D - dark blue, R62E - red, R62G – green, R62I – purple, R62L – light blue, R62M – orange, R62N - lilac, R62Q – salmon R62Y – light green. The spectra show secondary structures essentially identical to wild type. The spectra are stacked for clarity.

5.4 Colloidal and thermal stability of alkaline phosphatase mutants

In a thermal ramp experiment with CD, the signal from a particular secondary structure element, such as the alpha helices, reduces as the protein melts. To look at the stability of a wide range of mutants, Optim can give a large amount of protein stability information using an 8.8 µl sample at 0.5 mg/ml protein.

5.4.1 Optim data

Optim (AVACTA analytical) experiments detect the shift in intrinsic fluorescence from tryptophan residues and, to a lesser extent, tyrosine residues present in the protein. When tryptophan and tyrosine move from an internal folded non-polar environment to an exposed polar environment, their fluorescence changes and is taken as indicative of protein unfolding. Colloidal stability can also be investigated in the same experiment. Light scatter gives information on the protein's propensity to aggregate.

5.4.1.1 Optim analysis of wild type and T59R

The thermal stabilities of wild type alkaline phosphatase and T59R were investigated by measuring the barycentric mean (BCM). These data allow for an estimate of the melting temperature of the protein.

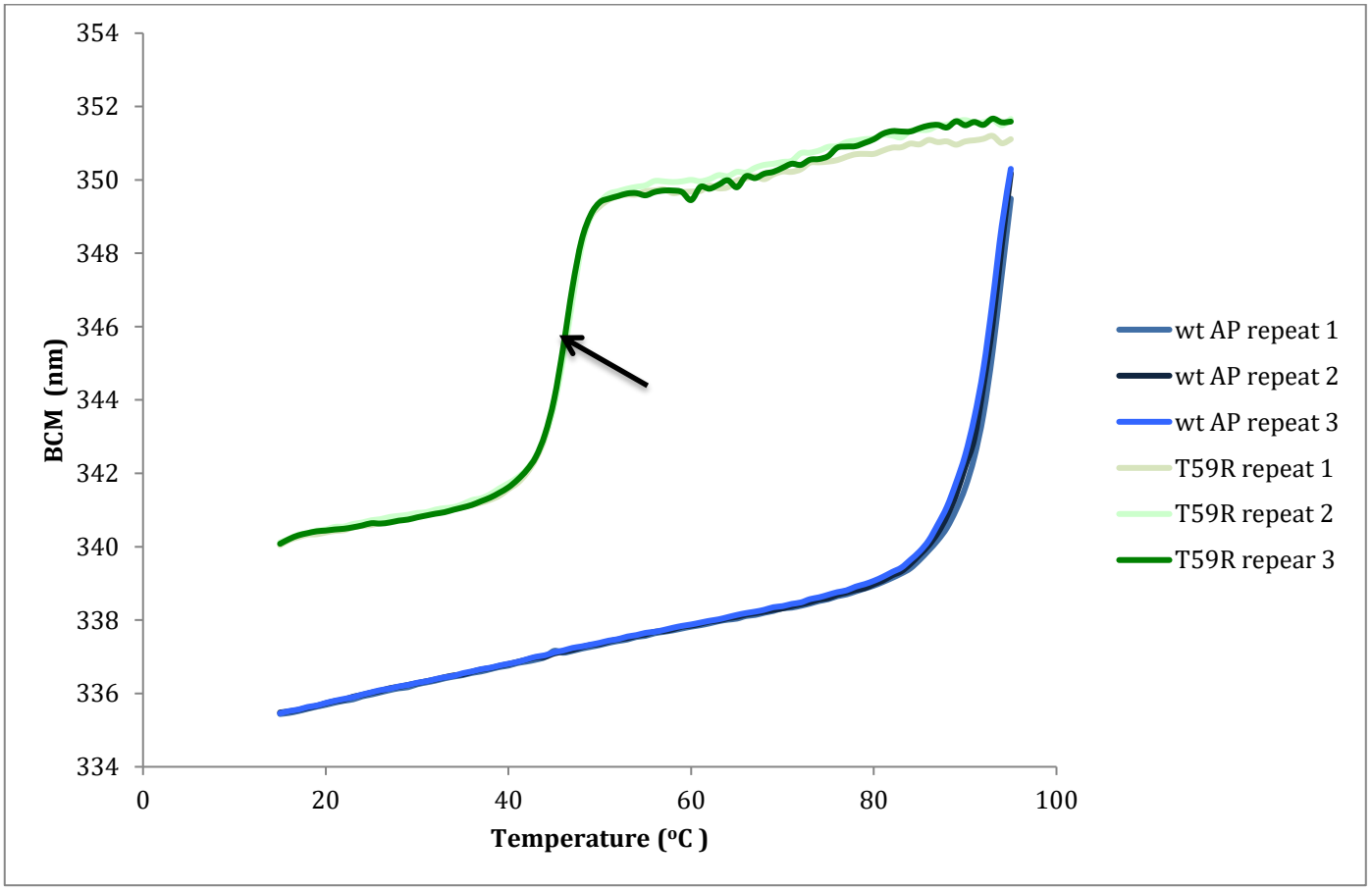

Figure 5.11 BCM analysis of wild type alkaline phosphatase and the T59R mutant.

Blue lines show the three repeats of wild type alkaline phosphatase, Green lines show the repeats of T59R. The Tm is calculated from the mid-point of the transition on a sigmoidal curve shown here by an arrow on the T59R data.

Figure 5.11 shows the BCM vs temperature for wild type alkaline phosphatase and T59R. T59R shows a sigmoidal curve that begins relatively flat, then increases through the transition to a plateau. The arrow points to the midpoint of the transition on this curve that represents the melting temperature. The melting temperature for T59R is approximately 47°C. Wild type alkaline phosphatase does not reach a plateau by the maximum temperature measured and thus an accurate Tm cannot be determined. Wild type alkaline phosphatase begins to unfold at about 85 °C, and therefore the melting temperature is greater than 85 °C.

5.4.1.2 Analysis of double mutants

Each of the double mutants was investigated for their thermal and colloidal stability. There are three repeats of each protein, the average of the melting temperature (T_m) and the temperature at the onset of aggregation (T_{agg}) are displayed in Figure 5.12.

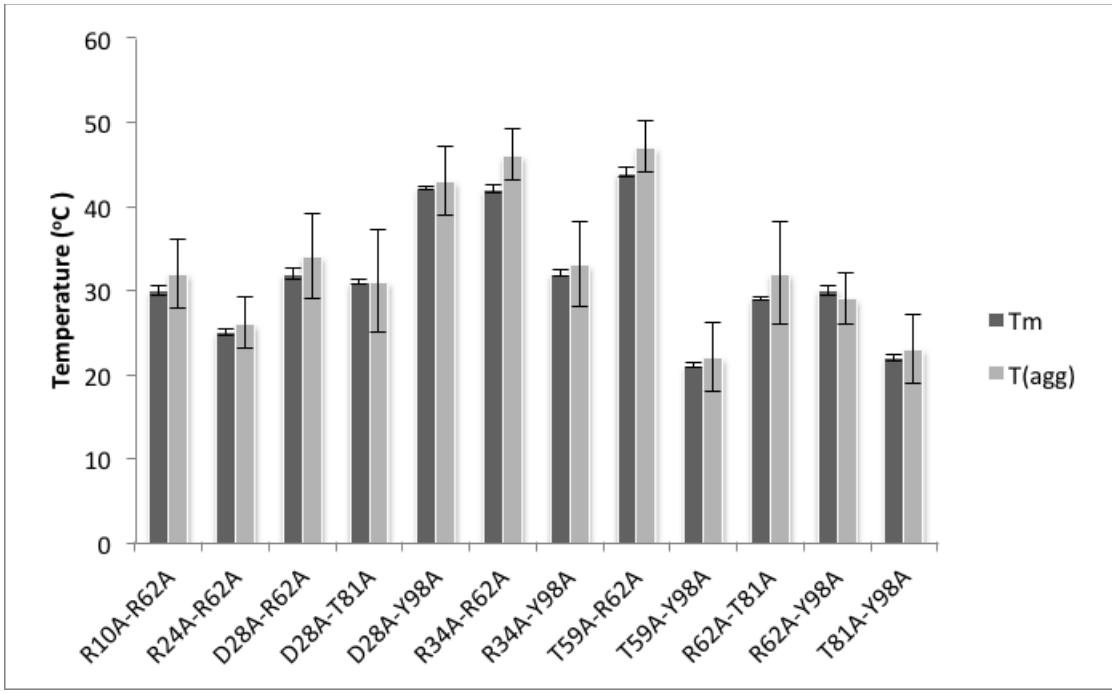

Figure 5.12 T_m and T_{agg} of all of the double mutants that demonstrated low enzyme activity.

For all the double mutants, the melting temperature was followed closely by the onset of aggregation. The highest thermal stabilities were shown by D28A-Y98A, R34A-R62A, and T59A-R62A. R24A-R62A, T59A-Y98A, and T81A-

Y98A have a T_m of 25 ^oC, 21 ^oC, and 22 ^oC respectively which is near room temperature.

5.4.1.3 Analysis of R62X mutants

The melting temperature and the onset of aggregation were investigated using Optim.

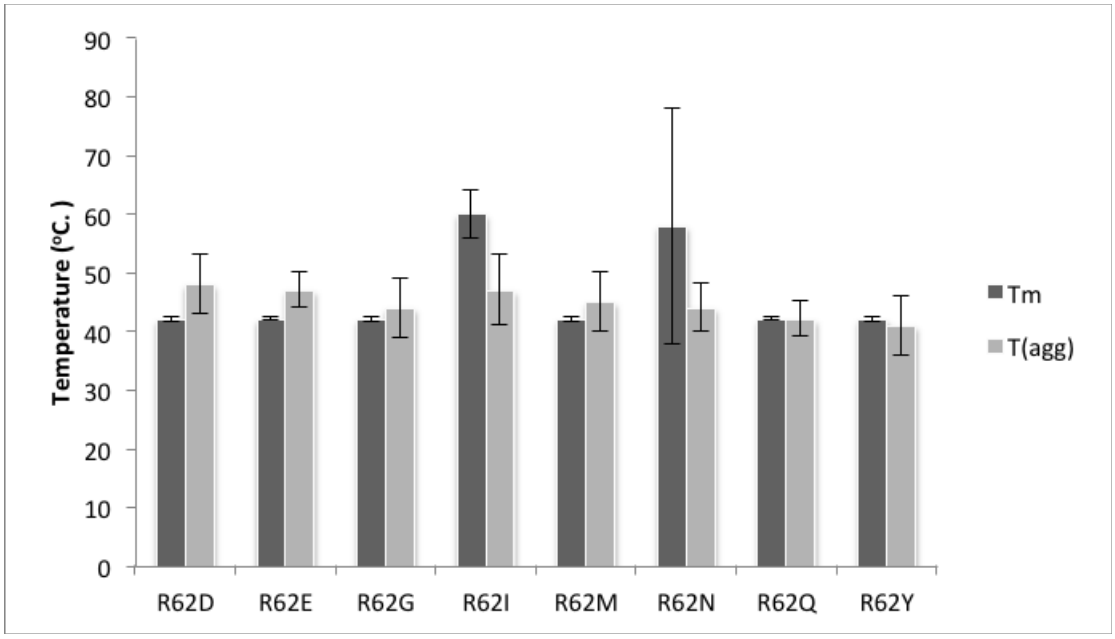

Figure 5.13 T_m and T_{agg} of a subset of the R62X mutants that demonstrated low activity.

The melting temperature of R62D, R62E, R62G, R62M, R62Q, and R62Y are all just over 42 ^oC with aggregation following shortly afterward. R62I and R62N appear to have higher T_m values. However, on further analysis of the primary data as shown in Figure 5.14, it is clear that this is not the case. The beginning of the change in BCM is the same for R62I, R62N and R62M. The difference between R62I, R62N and R62M is that the transition is longer, suggesting that the beginning of unfolding provides more reliable data.

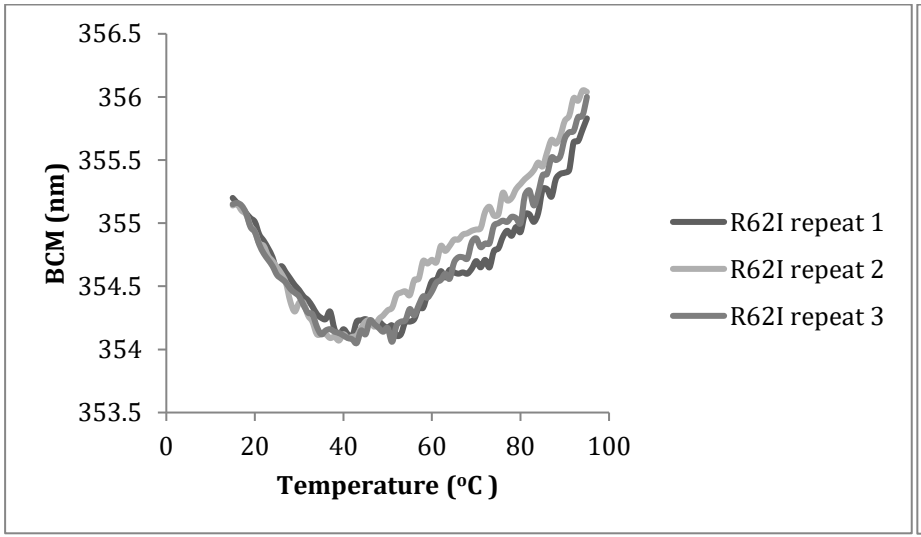

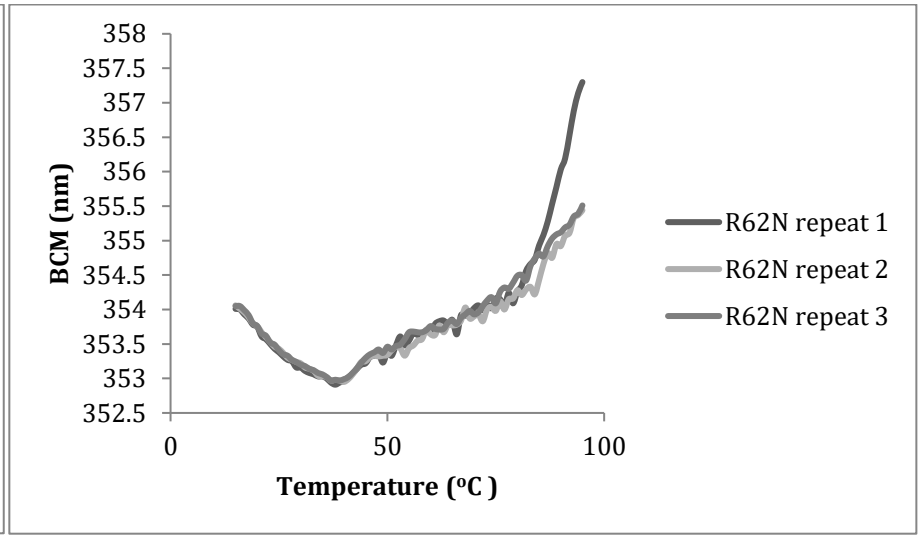

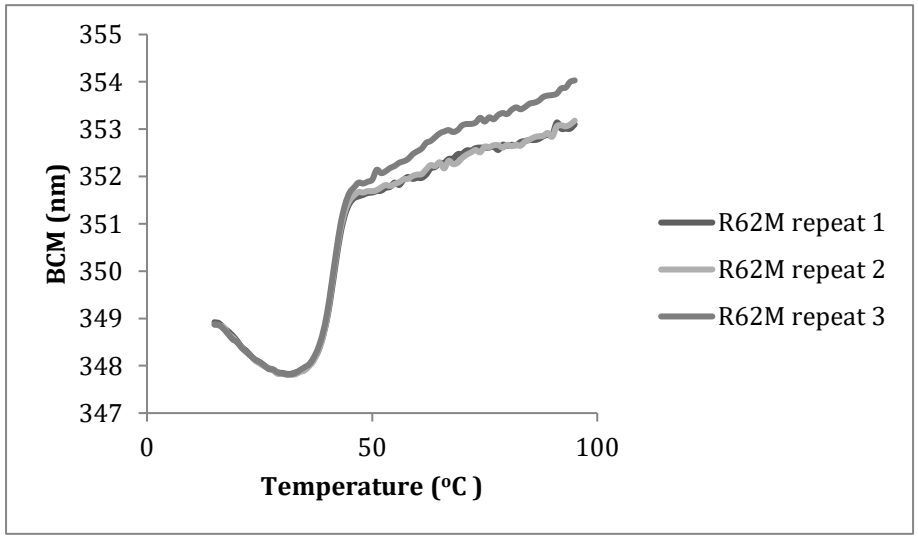

Figure 5.14 BCM primary data for R62I, R62N, and R62M. Each graph displays three repeats of each protein.

The best performing variant was T59A-R62A and so this was characterised further to ascertain the stability of this mutant when held together with the K4 coiled coil. Further analysis was completed to investigate whether the mutant exists in a monomeric form. Additionally, inhibition studies of the K4-T59A-R62A activity by addition of excess K4 peptide were performed to establish whether it was the K4 coiled coil that was responsible for mediating the dimer association. Finally, pH and temperature shift assays were completed to further investigate the K4-T59A-R62A interaction.

5.5 Characterisation of T59A-R62A

The double mutant T59A-R62A showed the largest increase in enzyme activity, from 6 to 33% of wild type, between the original protein and the K4 coiled coil version. The initial analysis measured the secondary structure of the mutant with the addition of the K4 coiled coil for comparison with the earlier CD data of this mutant without a coiled coil. Next, information on the thermal stability was analysed by measuring the melting temperature using CD.

5.5.1 Secondary structure

Figure 5.15 shows the CD spectra of the T59A-R62A mutant with and without the K4 coiled coil. These CD experiments were performed in the same way as described in section 5.3.1. There are some differences between the two spectra, but both show secondary structure similar to wild type. All the spectra show an overall α-helical structure. Some differences were to be expected as the addition of a coiled coil itself gives an α-helical signal which would change the overall spectra of the fusion protein.

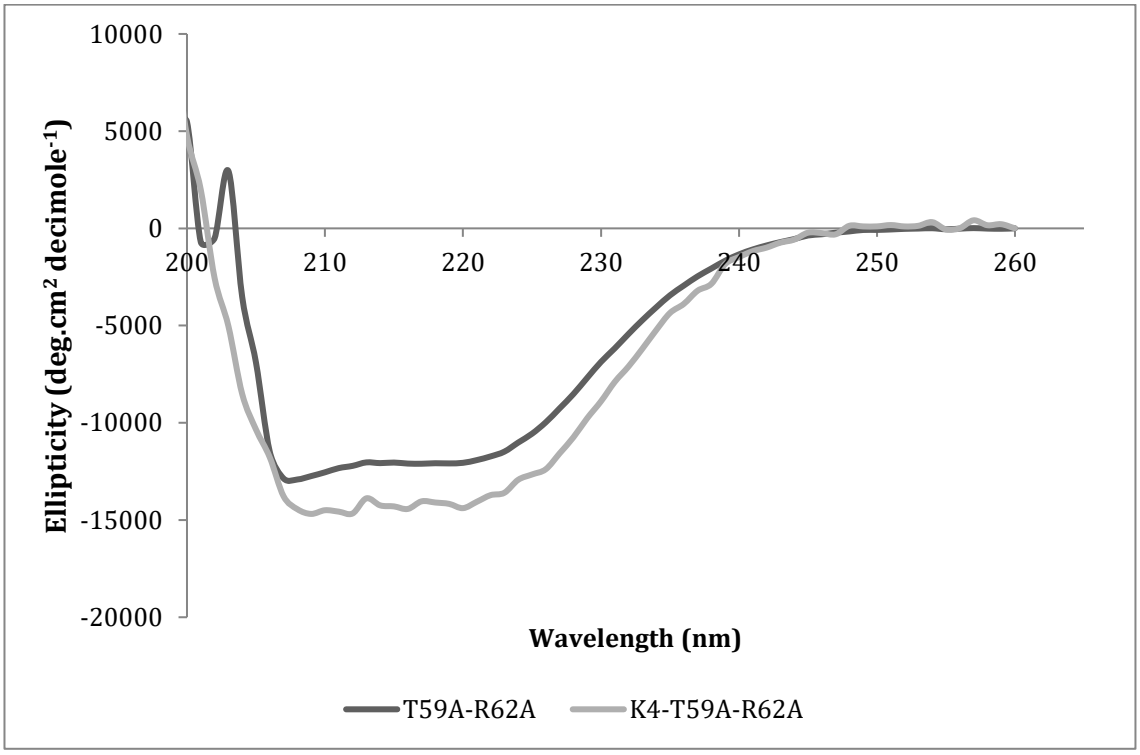

Figure 5.15 Far UV CD spectra of T59A-R62A (dark grey line) & K4-T59A-R62A (light grey line) alkaline phosphatase.

The spectra show that there are some differences in secondary structure between the two proteins, but both appear folded.

5.5.2 Thermal stability

To investigate the thermal stability of the T59A-R62A mutant, both with and without the K4 coiled coil, thermal melt experiments using CD were performed. CD experiments were performed on a Jasco J715 spectropolarimeter and the intensity of the CD signal at 220 nm was recorded. A 0.02-cm path length cuvette was used with a scan speed of 50 nm/min, a time constant of 0.5 s, and a bandwidth of 2 nm. Three repeat measurements were performed for each sample.

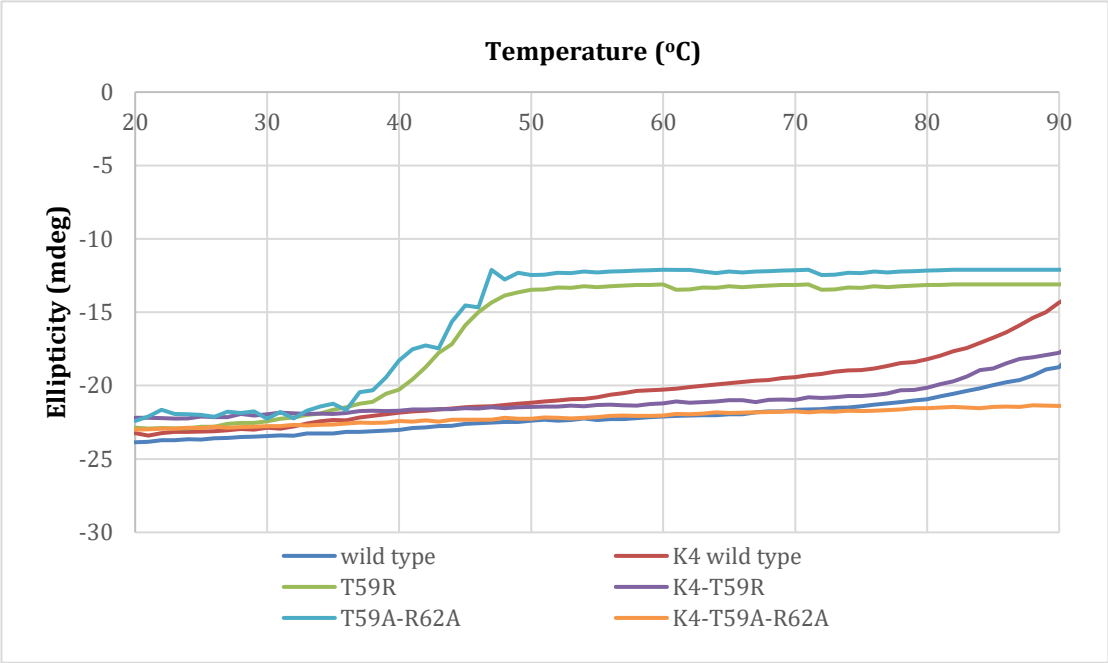

Figure 5.16 Thermal melt experiment at 220 nm, indicating the melting temperatures of the proteins.

Wild type is in dark blue, T59R is in green, T59R-R62A is in light blue, K4 wild type is in red, K4 T59R is in purple and K4-T59A-R62A is in orange. The T_m of T59R and T59A-R62A is approximately 43 °C. The T_m of wild type is higher than 90 °C. The addition of a K4 coiled coil increases the T_m in line with wild type.

Figure 5.16 indicates that the T_m of the two mutants; T59R and T59A-R62A, is approximately 43 °C. The T_m of wild type is higher than 90 °C, although the exact experimental value cannot be established with this technique. The addition of the coiled coil seems to reduce the stability of wild type, but this could be due to baseline differences. The addition of the K4 coiled coil

increases the T_m of T59A-R62A, in fact K4-T59A-R62A seems much more stable than even the wild type enzyme as it remains as almost a flat line at 90 ^oC.

5.6 Inhibition assays of K4-R62A-T59A

To validate that the K4 coiled coil mediates the dimerization of the monomer form of alkaline phosphatase, leading to the increase in enzyme activity, the interaction was inhibited by the addition of free K4 peptides as outlined schematically in Figure 5.17

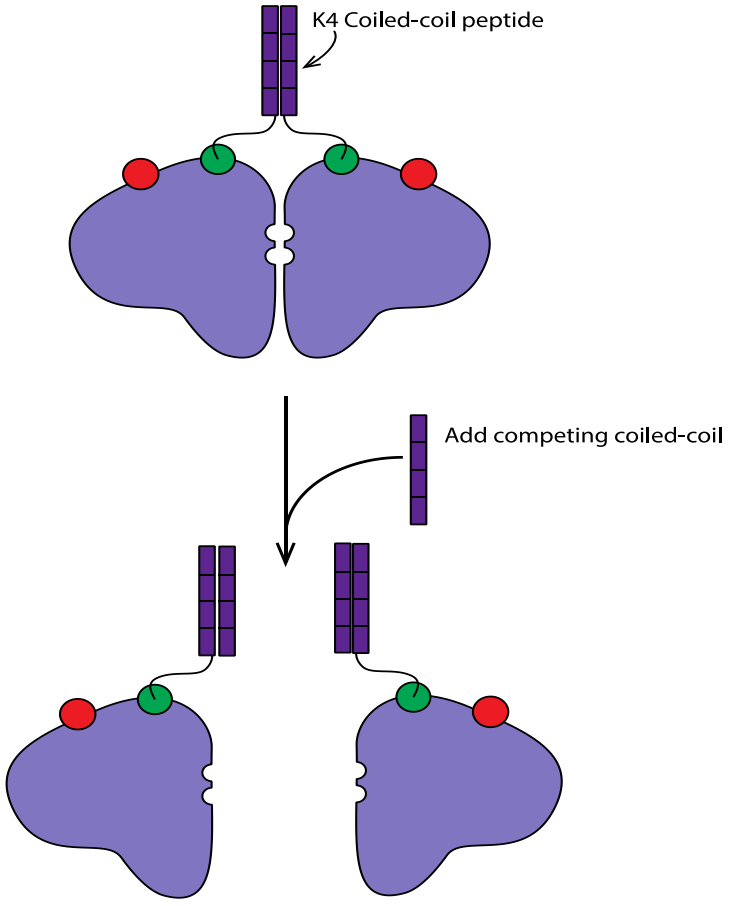

Figure 5.17 A schematic of the K4-T59A-R62A mutant before and after addition of free K4 peptide.

The protein is held in a dimeric state (top) by the K4 coiled coil, and this association is disrupted by competition with free K4 coiled coil peptide (bottom).

A final concentration of 0.4 nM K4-T59A-R62A protein was incubated with K4 peptide over a concentration range from 0 pM to 20 nM for 2 h in 1 M Tris pH 8.0. Enzyme activity was measured by addition of 100 µl (2 mM final concentration) of pNPP, and the assay was stopped after 5 min with 50 µl 5 M NaOH. The A_{405} values were converted to amount of product produced per unit time by using the Beer Lambert law as described in Chapter 2 Section 2.9.3.2. The concentration of pNP was plotted against the Log_{10} of the concentration of K4 peptide. The resulting IC_{50} value was 0.4 ± 0.1 nM, which indicates a 1:1 interaction of the coiled coil and the protein, as shown in Figure 5.18. This reduction in enzyme activity with increasing competitor concentration indicates that the inactive monomers are indeed being held together by the K4, and the addition of the free K4 peptide disrupts this interaction.

K4-T59R was incubated with 25 pM to 20 nM K4 peptide but, as expected, no change in absorbance was observed when pNPP was introduced. K4 wild type was also investigated in the same manner and, again as expected, the absorbance remained at the initial level and did not reduce with increased concentration of K4 peptide. This indicates that the K4 plays no part in the stable association of the wild type monomers.

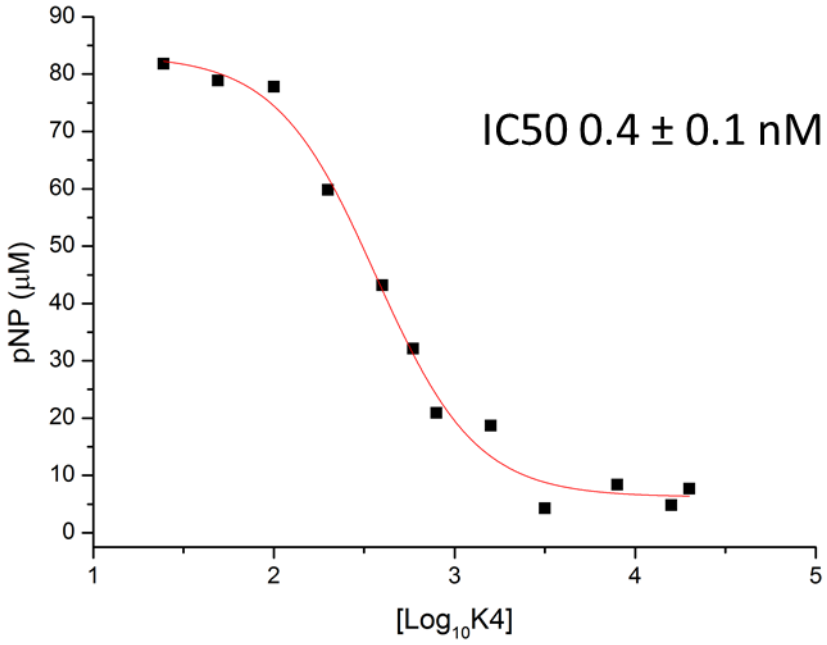

Figure 5.18 IC_{50} of K4-T59A-R62A mutant enzyme with the free K4 coiled coil.

K4-T59A-R62A protein was incubated with 25 pM to 20 nM K4 peptide for 2 h in 1 M Tris pH 8.0. The activity was detected at 405 nm using 2 mM final concentration of pNPP.

5.7 pH/temp shift assay of T59A-R62A

The thermal stability of the K4 coiled coil increased with pH, and as the K4 peptide was attached to alkaline phosphatase it would be interesting to investigate whether the attachment of the coiled coil affected the enzyme activity in the same manner. The T59A-R62A protein and wild type both with and without the K4 peptide were examined. Further controls included assay mix only and T59R, both with and without the K4 peptide. Each of these purified proteins was split into two batches and buffer exchanged into Tris /ACES/ CAPS tri-buffer as described in Chapter 4 Section 4.4. One batch of each sample was exchanged into buffer at pH 8 and the other into buffer at pH 11. Aliquots of both batches were then incubated at either 20 ^{o}C or 50 ^{o}C for 1 h. Then 100 µl (10 µg) samples of enzyme and 100 µl (2 mM final concentration) of pNPP was added to a 96 well plate and after 5 mins the assay was stopped by addition of 50 µl 5 M NaOH

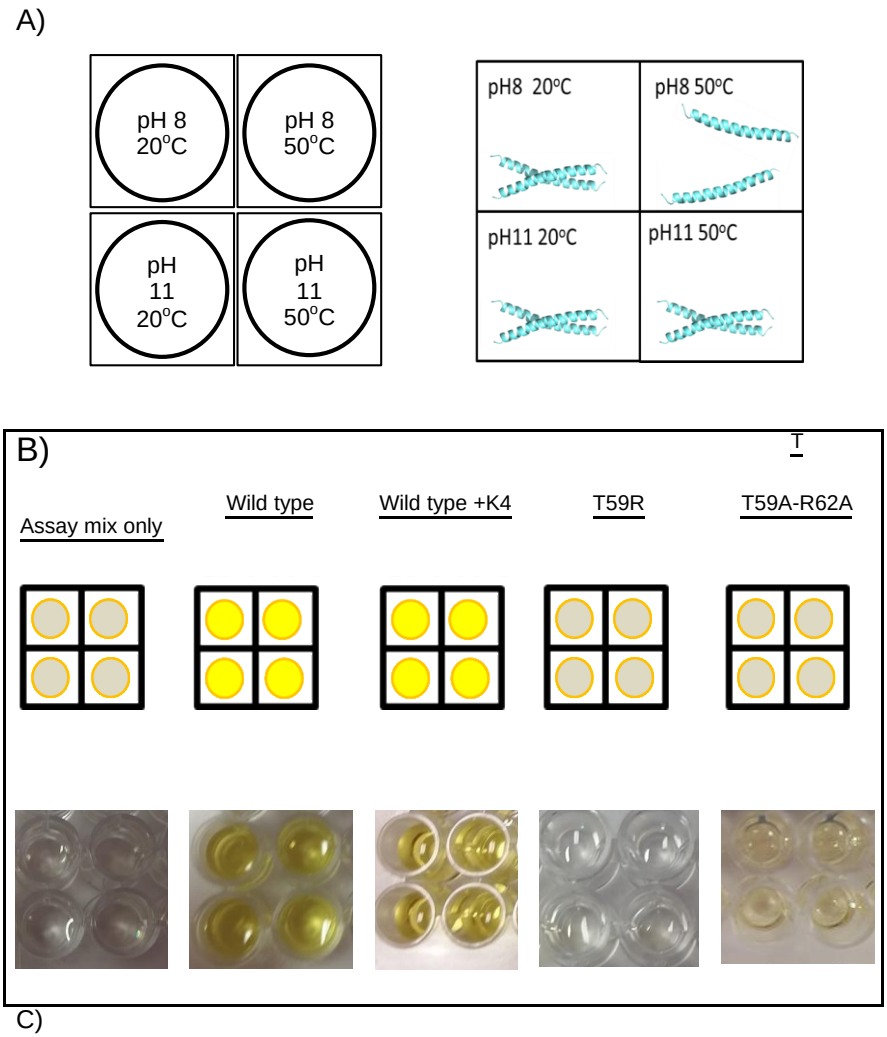

Figure 5.19 Temperature and pH shift assay for alkaline phosphatase with a K4 coiled coil.

A) shows the different pH and temperature in each of the four wells and a schematic of what was expected from the K4 coiled coil interactions under the different temperature and pH conditions. B) Control reactions including buffer only, wild type, T59R, with and without a K4 coiled coil. C) K4-T59A-R62A mutant under the same conditions. All activity was measured with pNPP (2 mM final concentration).

The assay mix did not show any activity in any of the 4 conditions. The wild type alkaline phosphatase could turn over substrate in all of the conditions; both with and without the K4 coiled coil attached. T59R did not turn over substrate in any condition. Interestingly, when T59A-R62A had the K4 peptide attached, it turned over substrate at pH 8 and pH 11 when incubated at 20 ^{o}C. It also turned over substrate at pH 11 when incubated at 50 ^{o}C but did not turn over substrate at pH 8 when incubated at 50 ^{o}C. This is consistent with the melting temperature of the K4 coiled coil; the expected coiled coil formations are shown at the top of Figure 5.19.

5.8 Oligomerisation of alkaline phosphatase R62A-T59A

The assumption that low activity in a mutant is due to destabilisation of the dimeric interface required further examination. Size exclusion chromatography (SEC) and analytical ultracentrifugation (AUC) were used to investigate whether the various proteins existed in predominantly the monomeric or dimeric state. The retention time on a SEC column gives an indication of the hydrodynamic radius, and, when used with protein standards, can indicate the size of the protein.

5.8.1 Size Exclusion Chromatography

Size exclusion chromatography was performed on a 120 ml, HiPrep 16/60 Sephacryl S100HR preparative column so that the protein could be recovered for subsequent assays. The flow rate was set to 0.5 ml/min on an ÄKTA FPLC and the eluate was collected in 2 ml fraction for 1.25 column volumes. To begin with, five protein standards: β-amylase, alcohol dehydrogenase, albumin, carbonic anhydrase and *cytochrome c*, were separated on the SEC column. The sizes in kDa and retention in ml of each of these proteins are shown in Table 5-2

Table 5-2 Approximate molecular weight of protein standards used in size exclusion chromatography.

Protein standard	Approximate molecular weight (kDa)	Retention (ml)
β-amylase	200	42.1
alcohol dehydrogenase	150	45.1
albumin	66	47.5
carbonic anhydrase	29	62.5
cytochrome c	12.4	82.6

The size of alkaline phosphatase in its native dimer state is 98 kDa and so would be expected to elute after albumin at 47.4 ml but before alcohol dehydrogenase at 45.1 ml. The monomer form of alkaline phosphatase should elute between carbonic anhydrase at 62.5 ml and albumin at 47.5 ml. Figure 5.20 shows wild type eluted at approximately 44.9 ml and T59R, the monomer version of alkaline phosphatase, eluted at 49.0 ml. This was in reasonable agreement with the expected result supporting the occurrence of wild type AP as a dimer and T59R as a monomer. The blue trace on Figure 5.20 representing T59A-R62A has several peaks. The two peaks at approximately 36 and 38 ml are probably some form of larger associations or aggregates as they elute considerably before the 200 kDa marker at 42.1 ml. The other two peaks are at 45.3 ml and 49.5 ml, which indicates a mixed population of monomer and dimer.

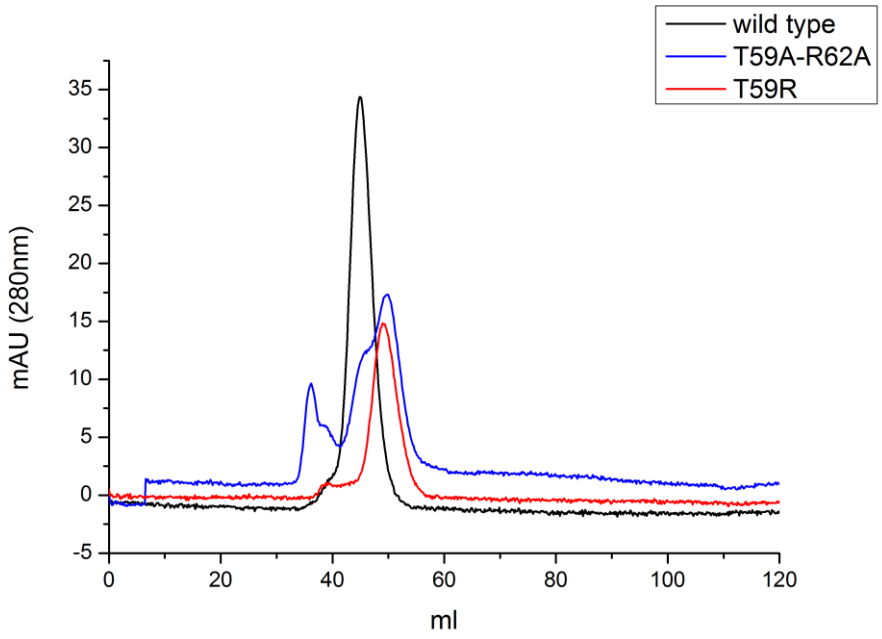

Figure 5.20 Absorbance data for the elution of alkaline phosphatase from a size exclusion column.

Wild type (black) alkaline phosphatase eluted at 44.9 ml. T59R (red) a known monomer eluted, at 49 ml. The blue trace indicates T59A-R62A, which has a double peak corresponding with both dimer and monomer sizes.

5.8.2 Analytical Ultracentrifugation (AUC)

In AUC the sedimentation coefficient (S) is a good indicator of the size and multimeric state of proteins. All of the AP proteins had an A_{280} value of between 0.3 to 0.5, and were exhaustively dialysed against 50 mM Tris pH 8.0, using four buffer changes; the first two after 2 h each, followed by overnight incubation, followed by a further 2 h the next day. A XL-I AUC instrument (Beckman Coulter) was used. After the AUC cells were filled, a quick centrifugation step from 3,000 to 30,000 rpm was performed to ensure the cells were not leaking. A continuous scan from 5.8 to 7.3 cm at 30000 rpm was set up and data were recorded every third scan. 200 scans were recorded at a constant temperature of 19.8 ^{o}C. The data were fitted using the SEDFIT and SEDPHAT programmes (Schuck 2000). For full details on how the AUC data were fitted, please see Chapter 2 Section 2.9.6.3.

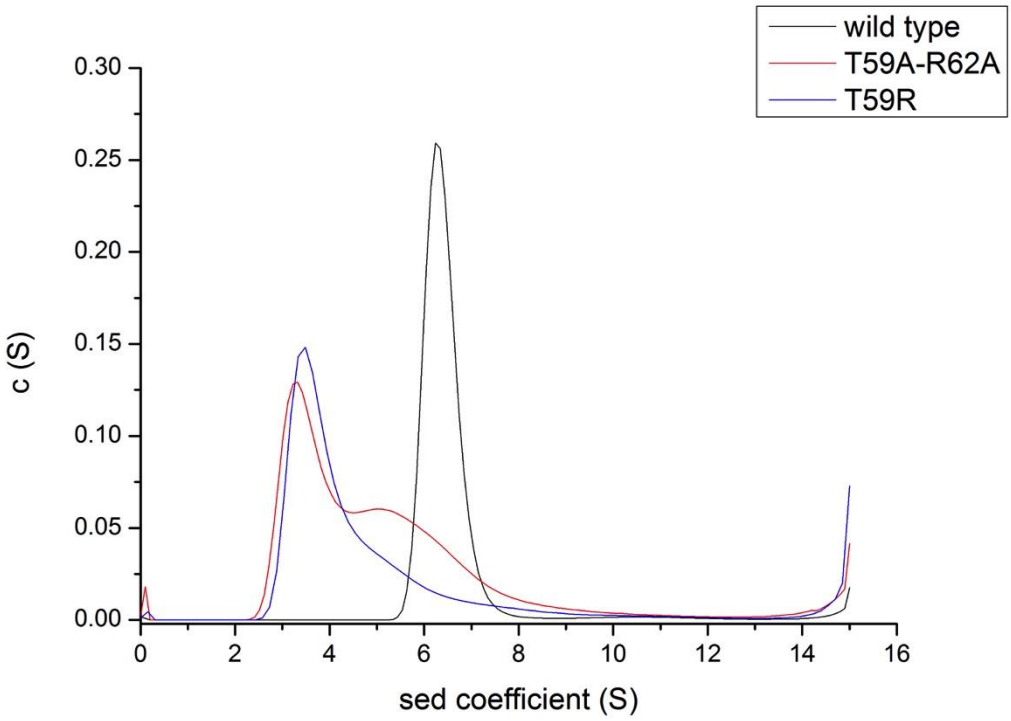

Figure 5.21 Sedimentation coefficient distributions derived from sedimentation velocity profiles

Wild type (black), T59R (blue) and T59A-R62A (red). The raw sedimentation signals acquired at different time points with absorbance at 280 nm, a rotor speed of 30000 rpm and a temperature of 19.8 °C

Figure 5.21 shows a clear difference between the sedimentation coefficient of wild type shown in black and T59R shown in blue. T59A-R62A shown in red shows a mixture of species, probably monomer and dimer, which agrees reasonably with the SEC data. The SEC and AUC data suggest that the predominant form of T59A-R62A is monomer, with potentially with some dimer, but this has minimal activity.

5.9 Zinc incorporation

Alkaline phosphatase requires two zinc ions to function; both coordinate one of the phosphate oxygens. Two points of the tetra-coordinated Zn1 and one point of the penta-coordinated Zn2 are coordinated by the imidazole nitrogens of histidines as shown in Figure 5.22 (Kim and Wyckoff 1991). The coordination of zinc in the active site is described in detail in Chapter 1 Section 1.5.2.1. To investigate the amount of zinc in the active site of the mutant enzymes a zinc binding assay was used.

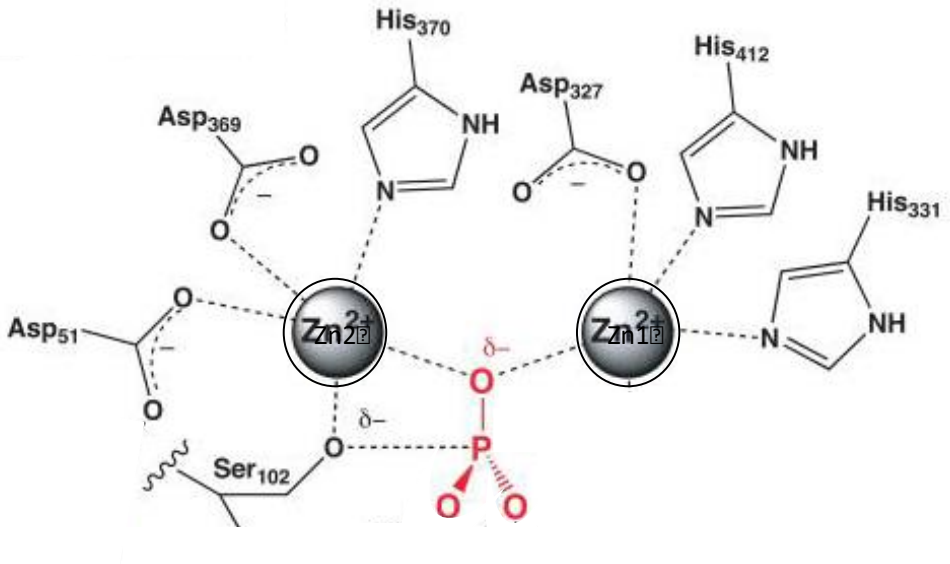

Figure 5.22 Zinc coordination in the active site of alkaline phosphatase. Zn1 is tetra-coordinated by His 412, His 331, Asp 327 and phosphate. Zn2 is penta-coordinated by His 370, Asp 360, Asp 51, Ser 103 and phosphate. Figure adapted from (Bobyr, *et al*. 2012).

5.9.1 Zinc binding assay with 4-(2-Pyridylazo) resorcinol

4-(2-Pyridylazo) resorcinol (PAR) is a chemical that displays an altered absorbance spectrum upon binding to zinc, as shown in Figure 5.23. When zinc is present there is an increase in absorbance at 500 nm that is proportional to the amount of zinc present.

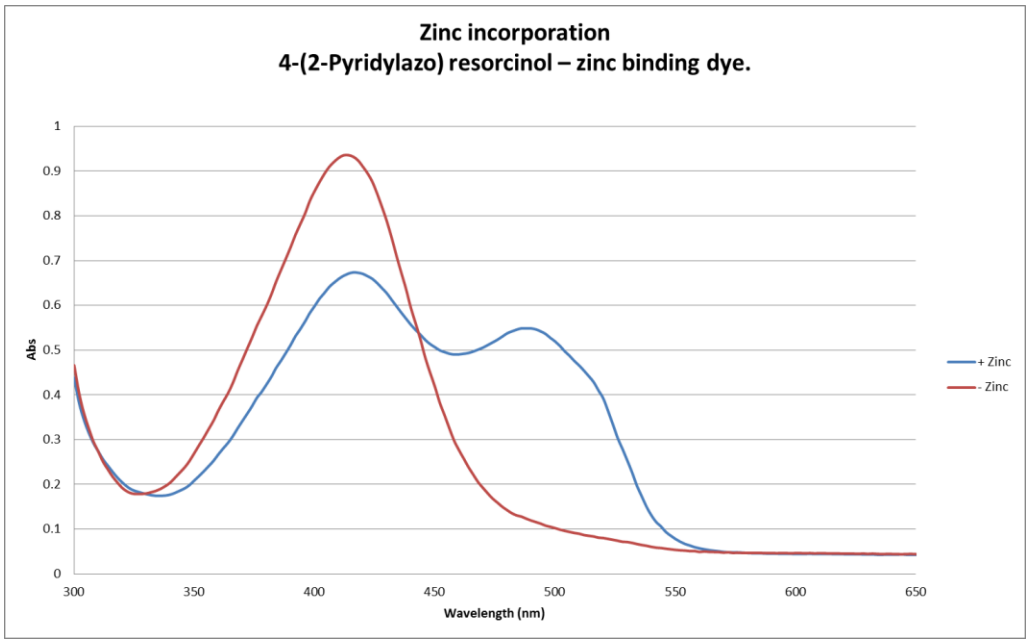

Figure 5.23 PAR spectrum with (red line) and without (blue line) zinc. Note the increase at 500 nm when zinc is present

To investigate the amount of zinc present in wild type alkaline phosphatase, T59R, and T59A-R62A, 100 µl aliquots of 100 µM PAR were dispensed into a 96 well plate. $ZnSO_4$ (100 µl) solutions were added at concentrations from 20 mM to 1 µM to create a calibration curve.

Diethyl pyrocarbonate (DEPC) was used to dissociate zinc from its histidine ligands. DEPC binds with high affinity to histidine, preventing interaction with zinc which is released into solution. 100 µl aliquots of 0.5 mg/ml wild type, T59R, or T59A-R62A in 1 M Tris, was added to 100 µl of 100 µM PAR in 1 M Tris containing 1% DEPC, and the absorbance at 500 nm was measured after a 2 h incubation at room temperature. The quantity of zinc was then calculated from the calibration curve. Wild type had 2 (± 0.3) zinc molecules per monomer, whilst T59R showed a negligible amount of zinc present. T59A-R62A has 2 (± 0.4) molecules of zinc per monomer. In addition to these three proteins, T59A-Y98A was also investigated and had 0.4 (± 0.4) molecules of zinc per monomer.

5.10 Distance dependence of dimerization interactions

When the K4 coiled coil interacts to associate the alkaline phosphatase subunits, there is, in effect, no distance between the two coils. Although the distance between the subunits of variants of alkaline phosphatase, would be determined by the linker length between the N-terminal residue of alkaline phosphatase and the start of the coiled coil. A starting point needed to be established to begin investigating the distance permissible between two epitopes on a target molecule. In order to investigate the distance dependence of the T59A-R62A interaction, an experiment was devised whereby DNA would be used as a molecular ruler.

Zinc finger motifs that bind to DNA were used to ascertain the permissible distance between two alkaline phosphatase monomers. Fusion proteins were designed to fuse a zinc finger motif to alkaline phosphatase. DNA oligos with the binding site for the zinc fingers were also designed. Several pairs of oligo were designed as described in Chapter 2 Section 2.9.7.2 with the binding site being moved along the DNA as shown in Figure 5.24.

.

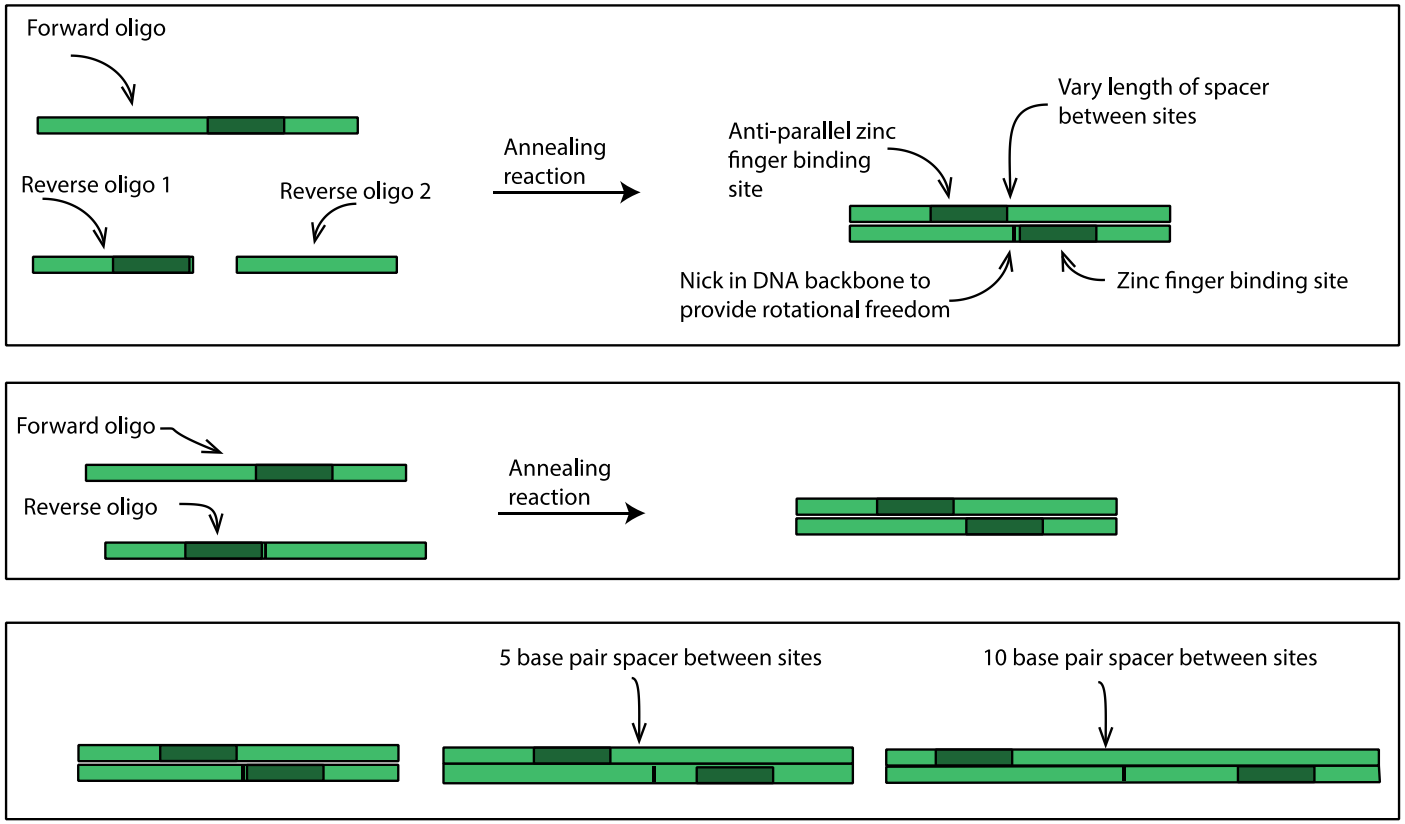

Figure 5.24 DNA template for zinc finger binding assay.

Three oligos were mixed together in an annealing reaction to create a duplex DNA construct capable of binding a zinc finger motif. The binding site for the zinc finger was moved further apart by 5 and 10 base pairs thereby introducing distance between the binding sites.

It was hypothesised that an oligo construct without any base pairs in between the zinc finger binding sites would hold the monomers of alkaline phosphatase together and eventually at a critical juncture would hold them apart as exhibited in Figure 5.25.

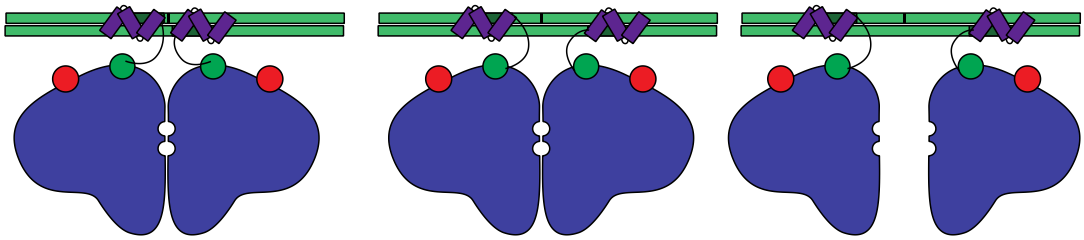

Figure 5.25 Schematic showing zinc finger motif moving the subunits of alkaline phosphatase along double-stranded DNA.

The green bars represent DNA, the purple zig-zag on the DNA represents the zinc fingers. Note as the zinc finger moves along the DNA from left to right this holds the subunits of alkaline phosphatase apart.

The vector pzifAP was designed, as shown by the schematic in Figure 5.26 to include GST to enhance solubility, followed by a TEV site to enable removal of the GST. The zinc finger protein, 268, was designed to be fused to the N-terminal of alkaline phosphatase via a colicin linker in between. A strep tag is present after the C-terminal of alkaline phosphatase so that StrepTactin resin can be used to purify the protein.

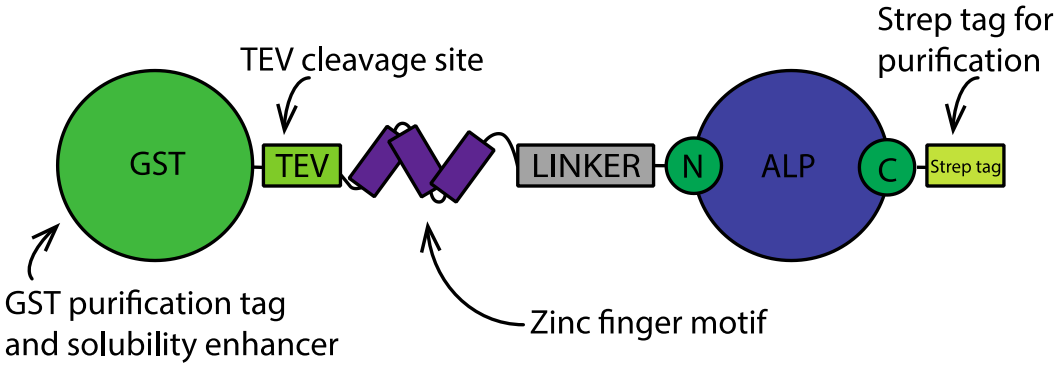

Figure 5.26 Schematic of the protein construct designed for the zinc finger distance dependence experiments.

GST was used to enhance solublity, the TEV site was used to cleave off the GST, and the zinc finger motif bound DNA in a specific manner. This was followed by a linker and the alkaline phosphatase (ALP), and finally a strep tag which was used for purification.

5.10.1 Mutagenesis and protein production

T59A-R62A and T59R were introduced into the pzif vector using a site-directed mutagenesis approach as previously described in Chapter 2 Section 2.5.1.2. The vectors: pzifAP, pzifAP$_{T59A-R62A}$ and pzifAP$_{T59R}$ were introduced into competent ArcticExpress cells, as these cells can be gown between 4 and 12 ^{o}C, giving the recombinant protein time to fold correctly. A single colony was used to inoculate 1 ml aliquots of LB broth containing carbenicillin These cultures were incubated at 37°C with shaking at 220 rpm overnight. A 50 µl aliquot of this culture was added to 50 ml of LB broth containing no selection antibiotics, as described by the manufacturer and incubated at 30°C with shaking at 220 rpm for 3 h. The culture was transferred to 10 °C and incubated with shaking at 220 rpm for approximately 10 minutes to equilibrate the culture, IPTG was then added to 1 mM to each flask and the culture incubated at 10 °C, with shaking at 220 rpm for 24 h. For full details see Chapter 2, Section 2.6.3

The protein was purified using Streptavidin agarose resin from Pierce. Full details are in Chapter 2 Section 2.7.3. Briefly, this comprised equilibrating the streptavidin column with three column volumes of binding buffer, adding the

sample to the column, then washing with 10 CV of binding buffer. The bound sample was eluted with 3 CV of elution buffer and collected in 0.5 – 1 ml fractions.

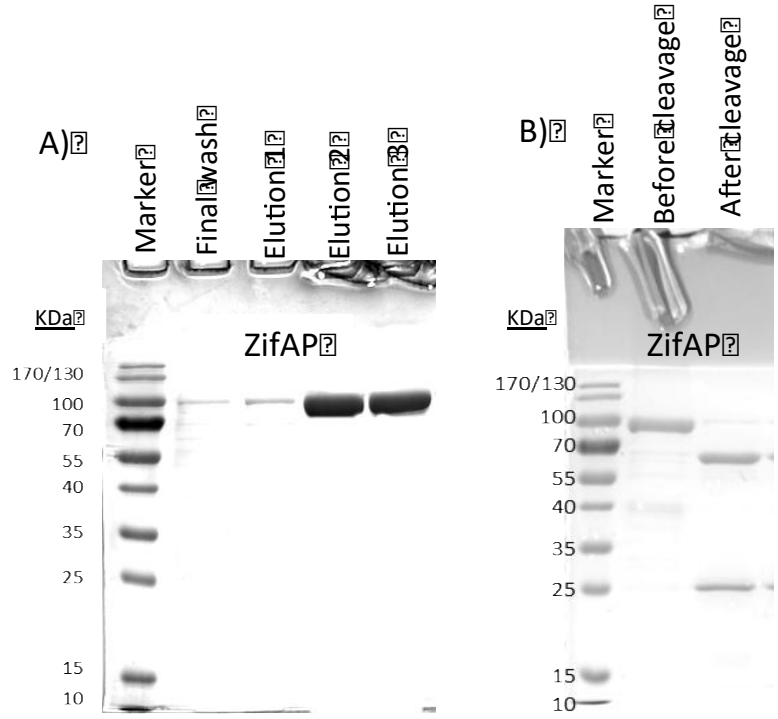

Figure 5.27 Purification and cleavage of zifAP.

Gel A shows the molecular weight markers, noted in kDa on the left of the gel, followed by the final wash and elution fractions 1 to 3. Fractions 2 and 3 were pooled. Gel B shows the cleavage of GST from zifAP. The molecular weight markers are shown in kDa, followed by the zifAP protein before and after cleavage with TEV.

5.10.2 DNA oligonucleotides

The DNA oligos were supplied by Integrated DNA Technology as single-stranded DNA and were annealed to produce duplex DNA for zifAP and zifAP mutants to bind. For full details see Chapter 2 Section 2.9.7.2. Briefly, 20 nM single strand DNA samples were mixed together in a PCR tube, which was heated to 95 ^{o}C for 10 mins and brought back down to room temperature in 1 ^{o}C per minute steps. Figure 5.28 shows each of the DNA duplex reactions on 4% agarose gels.

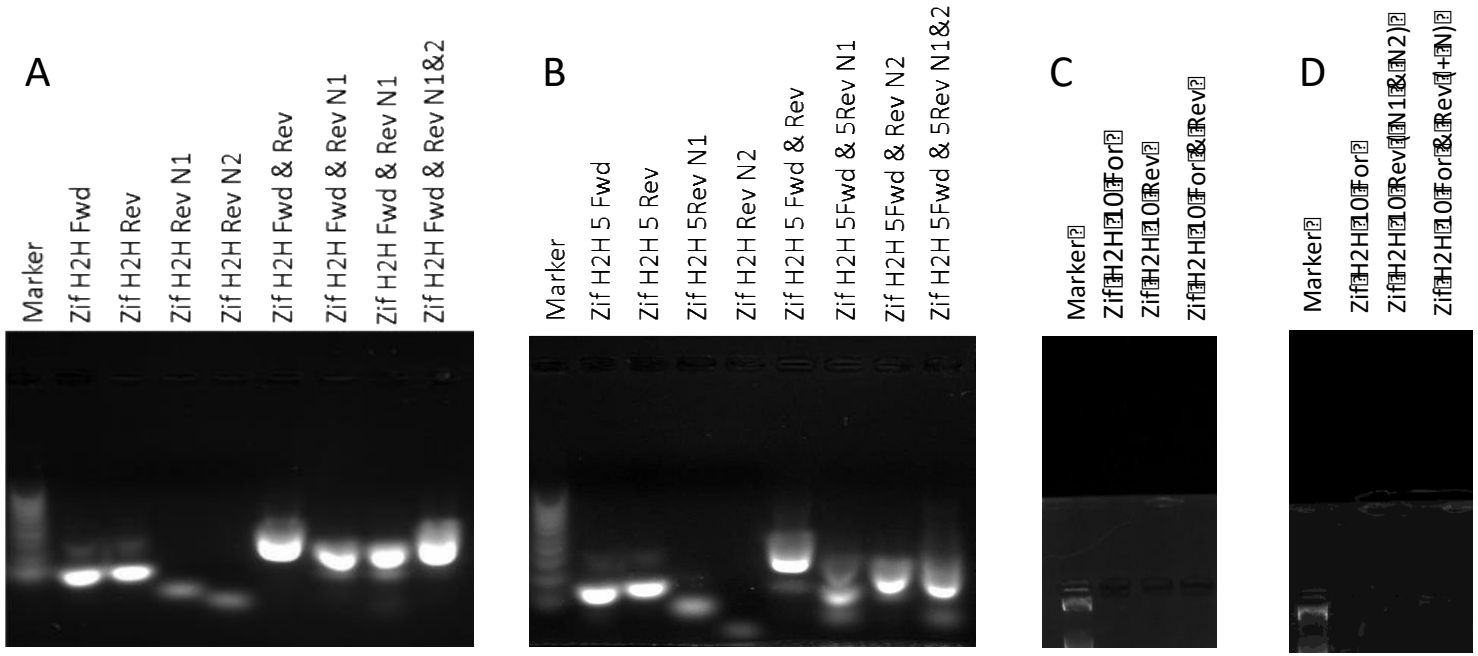

Figure 5.28 Agarose gels showing duplex DNA.

The marker for gel A and B is a 10 bp marker from fermentas, and the marker for gel C & D is a 10 bp marker from NEB. Gel A shows the DNA in various combinations for duplex DNA without a space in between the zinc finger binding sites. Gel B shows the DNA in various combinations for duplex DNA with a 5 bp gap in between the zinc finger binding sites. Gel C shows the same for duplex DNA with a 10 bp spacer and D is the same but with a nick in the DNA.

Duplex DNA without a spacer, and with a 10 bp spacer, presents on the gels as expected. The 5 bp duplex DNA without a nick also looks as expected, but when a nick is introduced into the construct then there appears to be a problem with how the DNA was annealed, as shown in Figure 5.28, gel B. This construct was omitted from the assay

5.10.3 Zinc finger activity assay

To determine the permissible gap for T59A-R62A, 15 nmol enzyme and 15 nmoles oligo were added to a 96 well plate. Wild type was used as a positive control and T59R as a negative control. 100 µl pNPP (2 mM final concentration) was added and reactions containing wild type alkaline phosphatase turned yellow immediately. All of the other reactions initially remained clear. After 24 h, absorbance at 405 nm was measured and a difference was observed for T59A-R62A. Wild type remained high at an absorbance of over 3.4 absorbance units, and the absorbance for T59R remained negligible. The absorbance for T59A-R62A changed depending upon the oligo present.

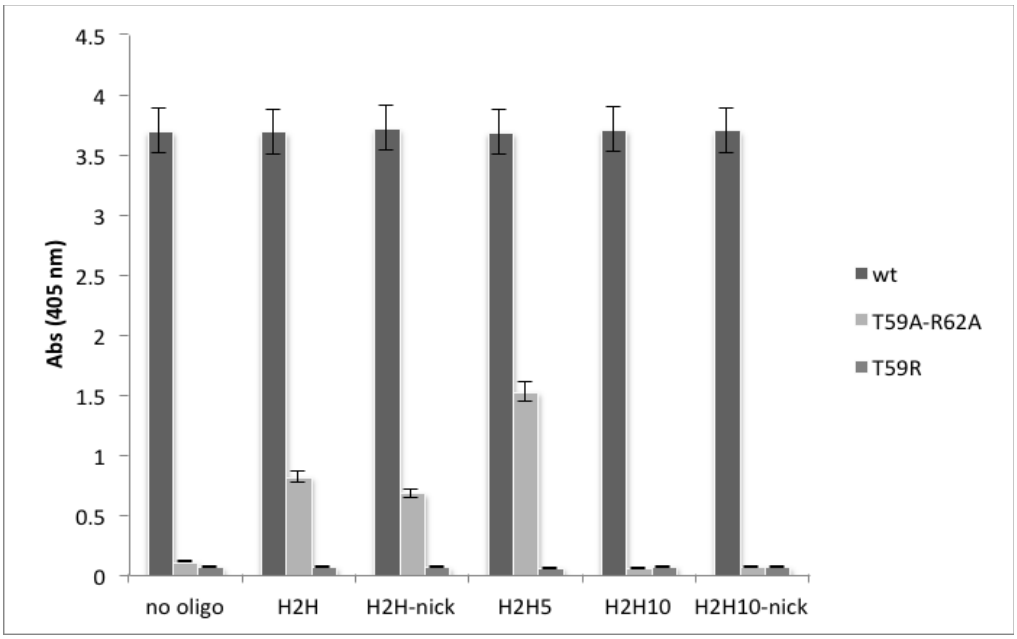

Figure 5.29 Zinc finger activity assay.

The activity of 15 nM of the enzyme with 15 nM of oligo and 2 mM pNPP was investigated after a 24-hour incubation period. The absorbance at 405 nm was recorded. The same batch of protein was assayed with a N=2 sample size.

As presented in Figure 5.29, when the DNA oligo was absent, the absorbance from the product remained negligible. When DNA without a spacer was present there was an increase in absorbance to over 0.8 absorbance units. The same DNA, but with a nick present remained at a similar level; 0.7 absorbance units. A 5 bp spacer appeared to increase the absorbance to 1.5 absorbance units. However, when the spacer increased to 10 bp the absorbance reduced again to a negligible level. These initial data suggest that the distance dependence is between 5 and 10 base pairs; as DNA has a distance between base pairs of 3.4 Å (Voet, *et al*. 2008) this is between 17 to 34 Å.

5.11 Discussion

Eleven double mutants and nine R62X mutants were investigated initially by looking at the re-activation of the mutants by inserting a coiled coil. In this scenario several of the mutants showed an increase in activity upon re-activation. Three double mutants: D28A-Y98A, R34A-R62A, and T59A-R62A, and three R62X mutants: R62G, R62I, and R62N.

The secondary structure was investigated for all 20 of the mutants and three of the mutants lacked secondary structure: R24A-R62A, T59A-Y98A, and T81A-Y98A. This is a satisfactory explanation as to why these three mutants did not re-gain activity when held in place with the coiled coil. It does not explain why other mutants have secondary structure but do not have activity when held in place with a coiled coil. The investigation into the colloidal and thermal stability of all 20 mutants revealed small variations in stability for the double mutants. The 3 mutants with highest colloidal and thermal stability: D28A-Y98A, R34A-R62A, and T59A-R62A were the three mutants that gained activity. The thermal stability for the R62X mutants was essentially the same at 42 ^{o}C and analysis of the primary data explained the shift in Tm for R62I and R62N. The largest increase in activity when coupled with a coiled coil was seen for the double mutant T59A-R62A.

The distance between the linker and the coiled-coil was an arbitrary length, and optimisation of the length, and type, of the linker would warrant further

investigation. It is well documented that a linker contributes to the overall stability and function of proteins (Chen, *et al*. 2013). It could be that a rigid linker would hold the alkaline phosphatase chains in place better than the flexible linker used in the construct in this study. Also, in this investigation, only homodimers were investigated; it would be interesting to explore the many combinations of heterodimer and see if there is a winning combination, which would provide a higher signal when stabilised into the dimer form of the enzyme.

T59A-R62A was characterised further by looking at the thermal stability of the mutant both with and without the coiled coil present. The coiled coil gave the mutant a near wild-type level of thermal stability. This was established by inhibiting the coiled coil interaction by addition of further coiled coils that were free in solution; it was found that the coiled coil mediating the increase in stability and increase in activity. Furthermore, the coiled coil also helped stabilise the mutant alkaline phosphatase at pH 11. T59A-R62A was shown to be a mixture of monomer and dimer at pH 8.0 by SEC and AUC, with the majority being in the monomer form. A zinc-binding assay indicated T59A-R62A has a full complement of zinc, which is required for functionality (Ma, *et al.* 1995). It would be interesting to investigate the amount of bound zinc in all of the 20 mutants taken forward for characterisation. This could give an explanation for the other nonfunctional, folded mutants.

Initial data show the distance dependence of T59A-R62A is between 17 and 34 Å. Optimising the zif interaction, including the linker length and experimental parameters, such as concentrations and incubation time, would be advantageous. These initial data are promising. However, further information on the distance dependence of different constructs would be valuable information towards the design of a diagnostic device.

Chapter 6

Affimers as a biosensor recognition element

6.1 Introduction

In this study, the Affimer was chosen as a molecular recognition element. An Affimer is a scaffold protein that behaves like an antibody molecule but it is only 12-14 KDa, and can be produced in *E. coli* in 3 days as opposed to raising antibodies in an animal. Some antibody fragments can be produced in *E. coli,* but all Affimers can be produced in this way. The target to demonstrate the split enzyme concept needed to be over 20 KDa; large enough to have two epitopes for two different Affimers to bind. A model protein, modified GFP (mGFP), was selected, as it is a 27 KDa protein and would be expected to have several epitopes for Affimer binding. Several Affimers had been raised against mGFP for a previous study and were supplied in a pDHis phagemid vector.

6.1.1 Sub-cloning into an expression vector

The Affimer coding regions were sub-cloned into pET11 by PCR amplification from the pDHIS vector. The primers were designed to introduce a 5' Nhe I site and a C-terminal cysteine and 3' restriction site for Not I. The amplified DNA was digested for 3 h with Not I and Nhe I (New England Biolabs - NEB) before separation on a 10 % agarose gel. The DNA was gel purified as described in Chapter 2 Section 2.5.1.4. The Affimer insert was then ligated into a modified pET11a vector digested with Not I and Nhe I and then treated with Antarctic Phosphatase. The ligation reaction contained 40 ng of linearised, phosphatase-treated pET11a, a 3-fold to 7-fold molar excess of the Affimer insert, which is 6-15 ng of DNA, 1 µl 10x T4 DNA ligase buffer (Roche), 200 U T4 DNA ligase (Roche), and ddH_2O to 10 µl. The reaction was incubated at 16 °C for 16 h, followed by introduction into XL-1 Blue competent cells. Aliquots of 50 µl and 250 µl of this transformation mix were spread onto each of two 2TY/carbenicillin (50 µg/ml) agar plates and incubated inverted at 37°C for 16 h. Plasmid DNA was prepared using a QIAGEN miniprep kit from 5 colonies, and analysed for successful ligation by colony PCR followed by agarose gel electrophoresis, for full details see Chapter 2 Section 2.5.2. The clones containing an insert were confirmed by DNA sequencing.

6.1.2 Affimer protein production and purification

The pET11a plasmids containing the coding regions for the Affimers were introduced into BL21 Star (DE3) cells. A single colony was then used to inoculate 5 ml of 2TY medium supplemented with 50 ng/ml carbenicillin and incubated overnight at 37 ^{o}C with shaking (220 rpm). A 1 ml aliquot of this culture was used to inoculate 400 ml TB auto-induction medium (Formedium) supplemented with 50 ng/ml carbenicillin, 0.2% w/v lactose and 25 mM succinate. This culture was incubated for ca. 48 h at 25 ^{o}C with shaking (220 rpm). The cells were pelleted at 3600 x g for 10 min at 4 ^{o}C for full details see Chapter 2 Section 2.7.4.

Cell pellets from 400 ml of culture were added to 40 ml of lysis buffer, supplemented with 2 mg/ml lysozyme, a cOmplete protease inhibitor tablet (Roche), and 200 U OmniCleave (Epicenter), then incubated at room temperature with agitation for 2 h. Affimers are stabile to over 50 ^{o}C , therefore, the cell lysate was then incubated at 50 ^{o}C for 20 min to denature proteins which are not stable upto 50 ^{o}C, followed by centrifugation at 25,000 x g for 35 min. The supernatant was then filtered (0.22 µm) to remove any large impurities. The soluble fraction of the cell lysate was then incubated for 1.5 h with 160 µl HisPur Ni-NTA resin (Pierce) with agitation at room temperate. The cell lysate and resin mix were then loaded into an empty disposable 2 ml column (Pierce) to collect the resin and let the liquid flow through. This ensured all of the resin was captured. The resin was removed from the column and incubated with 10 ml of wash buffer for 10 min while rolling at room temperature. The wash buffer resin mix was then loaded into a disposable 2 ml column and the resin was further washed with 20 column volumes of wash buffer followed by elution with 2.5 ml of elution buffer, in five 0.5 ml fractions. Samples were taken from the flow through, the final wash, and fractions 1, 3 and 5, and were analysed by SDS PAGE as shown in Figure 6.1

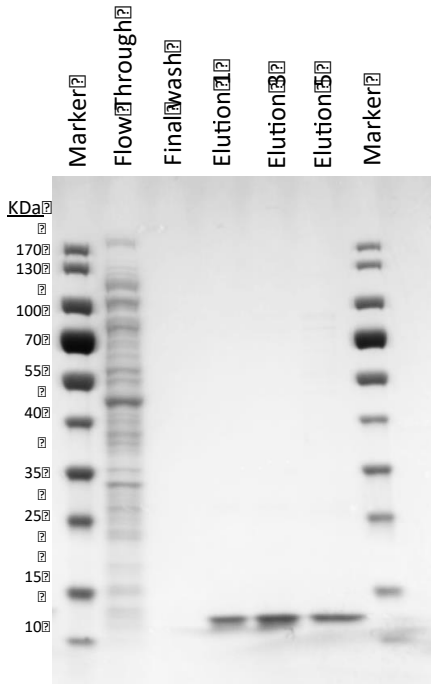

Figure 6.1 Purification of GFP Affimers.

The PA gel shows the molecular weight markers, noted in kDa on the left of the gel, followed by the flow through, final wash and elution fractions 1, 3 and 5 loaded in equal amounts of protein. Fractions 1-5 were pooled.

The C-terminal cysteine on each of the Affimers was biotinylated to allow oriented binding to streptavidin chips in a BLItz experiment. Any intermolecular disulfide bonds were reduced using a TCEP reducing gel (Thermo Scientific) and biotinylated with EZ-link BMCC biotin (Thermo Scientific). Full details are in Chapter 2 Section 2.8.2.

6.1.3 Characterisation of Affimers

One Affimer; mGFP21, was chosen at random to determine the K_D of the Affimer for mGFP, using Bilayer interferometry (BLItz). The experimental parameters for the BLItz experiment can be found in detail in Chapter 2 Section 2.9.8.1. Briefly, the streptavidin chip was incubated in PBS buffer for the first 30 seconds to obtain a baseline. The biotinylated Affimer was loaded onto the streptavidin chip for 2 min, which can be seen in real time, followed by another 30 second baseline.

The loaded chip was then exposed to the target, in this case mGFP, and an association curve was produced, followed by a dissociation curve when incubated with buffer. The BLItz software then creates a fit to obtain an association (k_{on}) and a dissociation (k_{off}) rate as well as calculating a K_D. Figure 6.2 demonstrates an example of the fit, which is not very accurate even after many optimisation experiments.

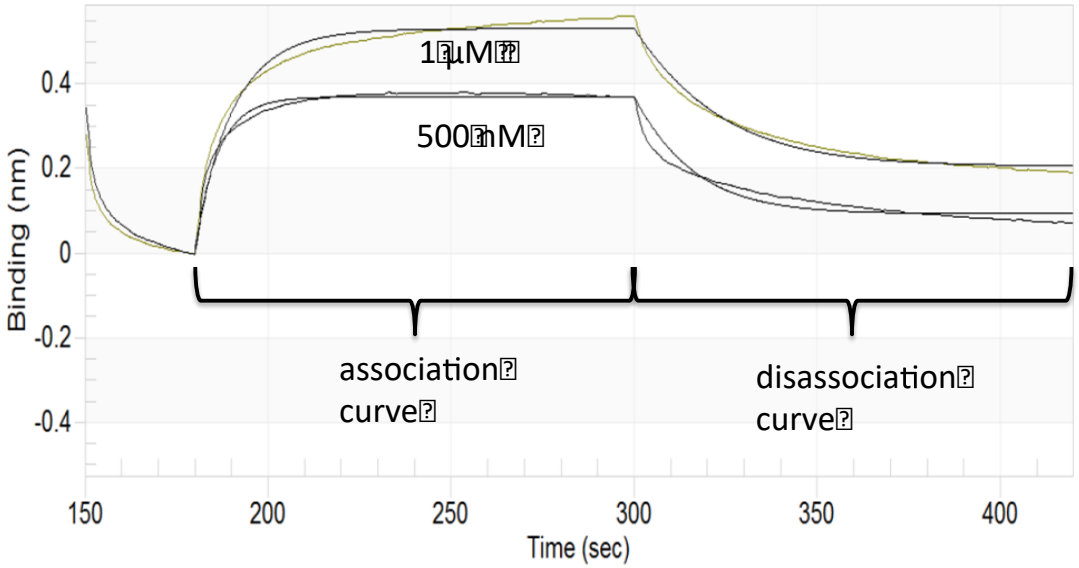

Figure 6.2 An example of a fit for the association and dissociation curves produce by BLItz software.

Here the Affimer, mGFP21, was challenged with mGFP to create the association curve, and then incubated with PBS buffer to create the dissociation curve. Two different concentrations of mGFP were used: 1 µM, and 500 nM.

Initial BLItz data indicated a K_D value of approx. 8.8 nM for mGFP21. The pool of mGFP Affimers were then used in an experiment to investigate dual binding to mGFP. The binding of two separate epitopes was key to future work, and therefore a sandwich phage ELISA assay was performed to ascertain if the mGFP Affimers could indeed bind mGFP at two separate epitopes. There was over 1 g of mGFP21 Affimer available from the first expression. It showed a high signal in the initial phage ELISA and was consequently chosen as the initial binding partner.

In a 96-well Nunc Maxisorp plate, 50 µg of Affimer mGFP 21 was placed in the first 4 columns, while the second four columns were left blank. The plate was incubated for 16 h at 4^{o}C followed by two washes with 250 µl PBS. 200 µl of 1 X blocking buffer (Sigma) was added to each of the wells and incubated for 16 h at 25^{o}C. 10 µg of mGFP was added to all 8 columns and was incubated for 2 h at room temperature. The plate was washed twice again with PBS, followed by 10 µl of 1 X blocking buffer, and 40 µl of the supernatant from the phage growth containing each of the mGFP Affimers were added to each well. The same set in each of the 4 columns, so the sample columns and the blank columns had the same phage in each of the wells. This was incubated at room temperature for 1 hour followed by a single wash with PBS. The enzyme-linked anti-pIII antibody was added followed by 10 washes with PBS and 50 µl TMB was added to give the colour change. For full details see Chapter 2 Section 2.9.8.1. Figure 6.3 shows the results from the phage ELISA. The sample plate is labelled ‘A’ and the control plate is labelled ’C’. The annotated plate, labelled ‘B’ is the exact same plate as A with annotated numbers on it. Each of the wells contains an Affimer from the original pool of mGFP Affimers. These were all sequenced, and the number on the annotated plate represents the Affimer in the well. Affimer mGFP21 was in the pool as a control. Where mGFP 21 was present this should not produce a signal as it should not be able to bind, because the binding site(s) for mGFP21 should all be taken. Wells labelled 21 in Figure 6.3 are those containing mGFP21 phage and as expected showed no binding signal. The control plate ‘C’ does not contain mGFP. Therefore, the Affimers in the three wells that show colour development on the control plate presumably bind to the well, and these Affimers were discarded.

Within the pool some other Affimers were expected to bind to the same or similar areas as mGFP21, and some were expected to bind elsewhere on mGFP. If the Affimer bound in the same or similar position then there would not be a signal produced, but where there was binding at a separate site then a signal would be given. Three repeats of mGFP20 were negative suggesting that Affimer 20 binds the same or an overlapping epitope as mGFP21. Three replicate wells tested with mGFP18 phage all show a strong positive result, as

do two repeat wells for both mGFP32 and 33. Thus Affimers 18, 32 and 33 seem likely to bind a distinct epitope to mGFP21.

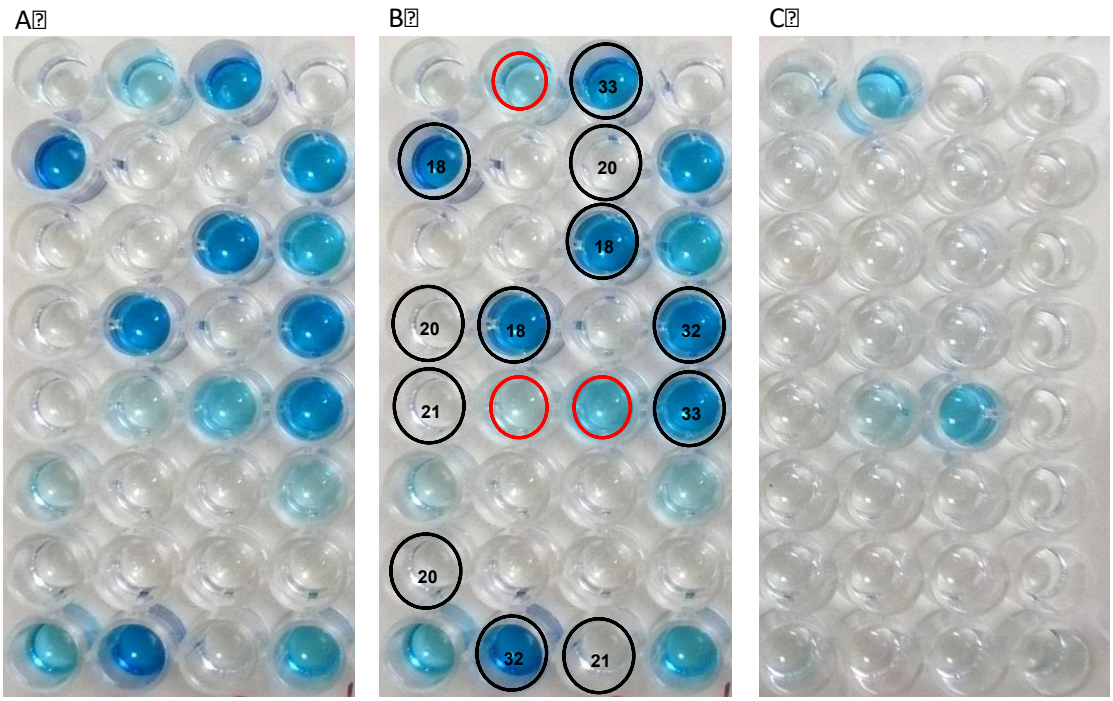

Figure 6.3 mGFP sandwich phage ELISA.

The sample plate is labelled 'A' and the control plate is labelled 'C'. The annotated plate, labelled 'B' is the exact same plate as A with annotated numbers on it. Each of the wells contains an Affimer from the original pool of mGFP Affimers. These were all sequenced, and the number represents the Affimer in the well. The two '21' circled wells on the plate show two samples of MGFP21, which cannot bind due to the binding site for MGFP21 already being bound, and they are clear. Affimer 18, 32 and 33 circles all show a strong positive result. Affimer 20 demonstrates a negative result. Plate C shows the blank control, with three positive results. These three samples indicated on the annotated plate with red circles were discarded as the Affimer probably binds to the plate.

In the phage pool of mGFP Affimers, there were 20 unique Affimers that bound mGFP. In this phage ELISA experiment 13 of these failed to bind mGFP21 immobilised mGFP indicating that they likely bind the same or overlapping

epitope as mGFP21. By contrast mGFP Affimers 18, 32 and 33 gave a good positive signal and Affimer mGFP32 was arbitrarily chosen as the binding partner for Affimer mGFP21.

6.1.4 Colloidal Stability

mGFP21 and mGFP32 were buffer exchanged from the elution buffer into PBS but a white precipitate was observed in the dialysis tubing. The protein concentration in the solution was quantified using the BCA assay and was confirmed using a Bradford assay (see Chapter 2 Section 2.9.2). The concentration of protein was between 1 and 2 mg/ml. A second batch of mGFP21 was buffer exchanged into PBS with the addition of 10% glycerol resulting in a concentration of 10 mg/ml of protein in solution, and a lower level of white precipitate was observed.

This result was corroborated by light scattering data using an Optim 1000 (Avacta Analytical). A stepped thermal ramp program was used with the temperature setting being staged between 20 ^{o}C and 95 ^{o}C in 1 °C increments. An 8.8 µl aliquot of each protein (1 mg/ml) was measured in triplicate, and Optim 1000 software was used to process the data. Colloidal stability was measured by monitoring SLS at 266 nm against temperature. A transition associated with protein aggregation was observed as shown in

Figure 6.4.

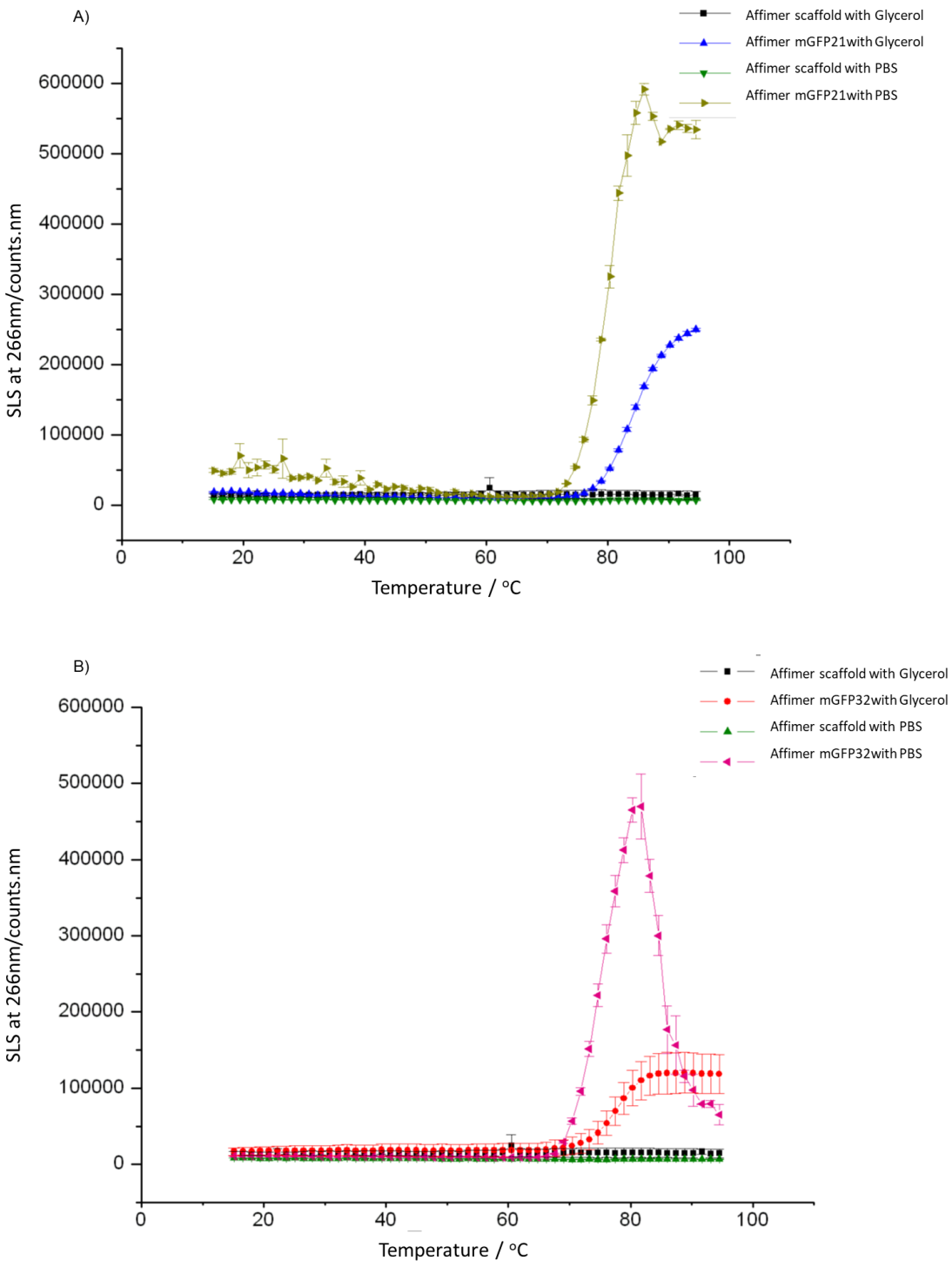

Figure 6.4 Static light scattering (SLS) data at 266 nm over a range of temperatures for Affimers mGFP21 and mGFP32.

The SLS data are also shown for the Affimer scaffold as a comparison. The Affimer scaffold does not aggregate at temperatures up to 95 °C, the highest temperature measurable in the Optim 1000. The mGFP Affimers started aggregating at lower temperatures while addition of glycerol delayed this onset and magnitude.

For mGFP21 the absorbance reading started to increase at around 72 ^{o}C in PBS and reached approximately 600,000 counts. By contrast, the absorbance did not rise until around 80^{o}C and only reached 250,000 counts. This indicates that mGFP21 is less prone to aggregation in the presence of 10% glycerol. A similar pattern was observed with mGFP32. The Affimer scaffold did not exhibit a high-level of light scattering in either PBS or PBS with 10% glycerol, indicating that it does not precipitate, in agreement with the lack of observable precipitate during dialysis.

6.1.5 Monomeric or Dimeric Affimer

A Superdex 200 10/300 GL column was used to analyse the multimeric state of mGFP21 and mGFP18. The column was equilibrated with PBS containing 10 % glycerol before a 1.2 ml aliquot of 2 mg/ml Affimer was added to the column. This was eluted in an isocratic fashion using PBS with 10 % glycerol. The flow rate was set to 0.5 ml/min on a ÄKTA FPLC and the eluate was collected in 0.5 ml fractions.

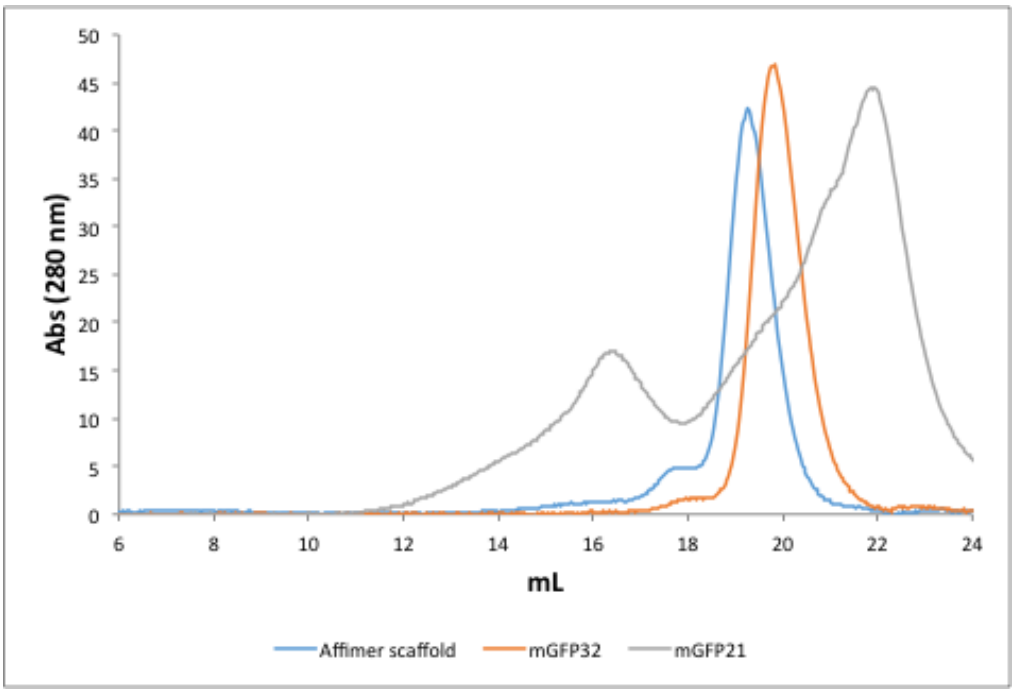

Figure 6.5 Affimer SEC spectra.

The elution profile for the Affimer scaffold (blue), mGFP32 (orange) and mGFP21 (grey) were monitored at 280 nm. Affimer scaffold and mGFP32 show a single peak characteristic of monomer. By contrast mGFP21 has two broad peaks suggesting a mixed population of monomer and dimer.

The Affimer scaffold and mGFP32 behave similarly on the SEC column, suggesting these proteins are principally monomeric. By contrast mGFP21 shows two broad peaks suggesting a mixed population of molecular species. To investigate the nature of the protein in these peaks, a HiPrep 16/60 Sephacryl S-100 HR preparative size exclusion column was used with mGFP21, so that protein fractions could be recovered for further analysis.

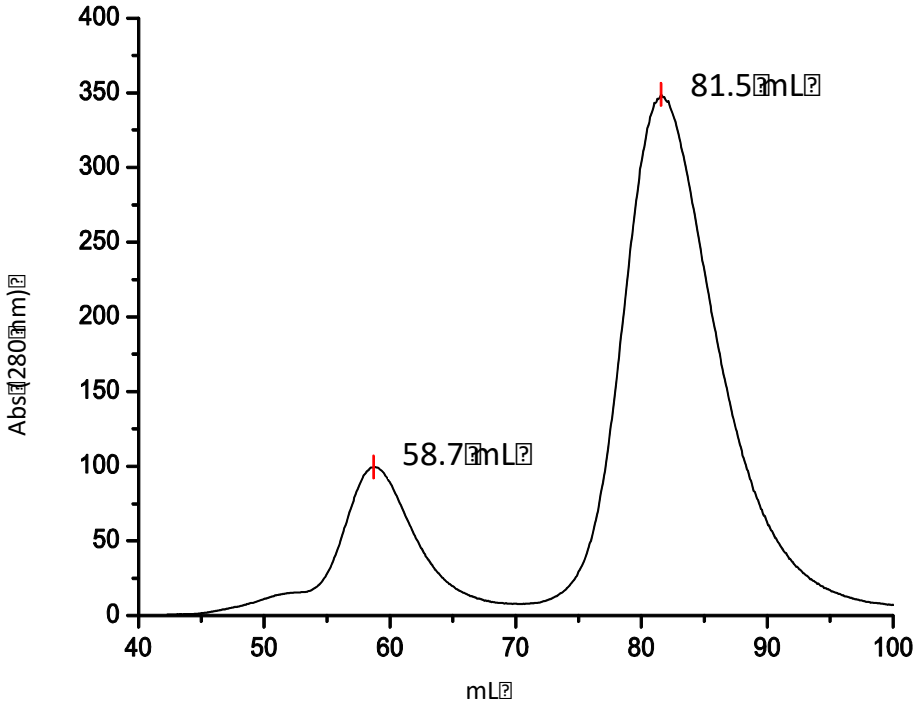

Figure 6.6 SEC profile showing separation of mGFP 21 species.

As expected Figure 6.6 shows two peaks for mGFP21, suggesting the presence of monomer and dimer. The peak eluting at 58.7 ml has an integrated area of 776 au, whilst the peak at 81.6 ml has an integrated area of 3227 au. The ratio is approximately 1:4, suggesting 4 times more of the smaller species. Two samples from each peak were analysed on a native gel along with the Affimer scaffold, a mixture of mGFP21 and Affimer scaffold, and mGFP21 that had not been separated by SEC.

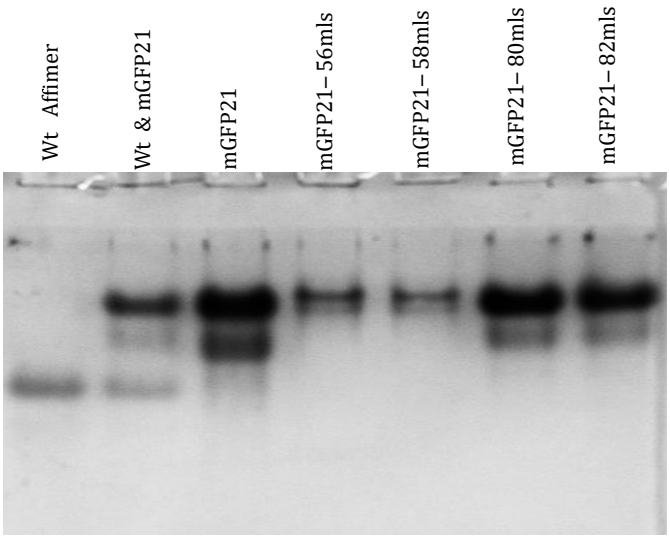

Figure 6.7 Native 10% polyacrylamide gel of mGFP21.

The samples are shown above the lanes. The right hand 4 lanes are fractions from the SEC (Figure 1.7) taken at 56 and 58 ml from the first peak and 80 and 82 ml from the second peak.

The native gel in Figure 6.7 shows one band for the Affimer scaffold, two bands for mGFP21, and three bands for the mixture. The overall charge on the Affimer scaffold is -1 while for mGFP21 it is +1. This partly explains for the faster migration of the Affimer scaffold towards the anode. The two samples from the second peak have two bands in the same migration pattern as the mGFP21 sample that was not on a SEC, although the second band is smaller. This suggests the monomer – dimer formation is in equilibrium, the SEC trace in Figure 6.6 suggests 20% putative dimer and 80% putative monomer, although the samples from the dimer peak do not have a monomer band. This could suggest that once an Affmer is in a dimer form, it remains in the dimer form. However, another explanation based on the data from SEC and the native gel showing mGFP21 is that the upper band is the monomer not the dimer because of the relative intensities of the bands. As native gels separate on the basis of hydrodynamic radius and charge. Whilst it was expected that the dimer would migrate more slowly, the dimer could be compact and the positive charge might be masked by dimer formation, leading to the dimer migrating more rapidly. If this is the case then the data suggests that the

samples for the 56 and 58 ml which were originally dimeric have reached a new monomer dimer equilibrium that favours the monomer, as the sample is more dilute coming off the column than when it went on.

6.2 Crosslinking alkaline phosphatase with Affimers

To facilitate simple cross-linking between an Affimer and other molecules, Affimers with a C-terminal cysteine were used. To ensure the thiol group on the cysteine residue of each Affimer was reduced, the sample was treated with TCEP reducing gel (Thermo Scientific) according to Chapter 2 Section 2.8.1. Alkaline phosphatase was buffer exchanged by dialysis into PBS containing 1 mM EDTA to avoid the presence of Tris that interferes with the chemical crosslinking reaction. Alkaline phosphatase was mixed with 1 $SM(PEG)_2$ (Pierce) a PEGylated SMCC cross-linker. $SM(PEG)_2$ has two reactive groups, a NHS ester and a maleimide, therefore it is reactive towards amino and sulfhydryl groups respectively. The PEG spacer arm gives a flexible linker of about 17.7 Å.

0.1 mM Alkaline phosphatase was mixed with 1 mM cross-linker and the reaction was incubated at room temperature for 1 hour before desalting using dialysis. The derivatised enzyme was then mixed with 0.1 mM reduced Affimer and incubated at room temperature for a further hour. To examine whether the crosslinking reaction was successful, samples were separately run on a 15% SDS PAGE gel. Figure 6.8 shows samples of mGFP21 and alkaline phosphatase flanking samples taken from two independent cross-linking reactions. Although the cross-linking samples do not show a distinct single species, the presence of higher molecular mass species than alkaline phosphatase together with the reduced level of monomeric Affimer, confirm that crosslinking has occurred. There is a high concentration of non-crosslinked alkaline phosphatase and the conditions for cross linking could be refined to increase cross linking efficiency.

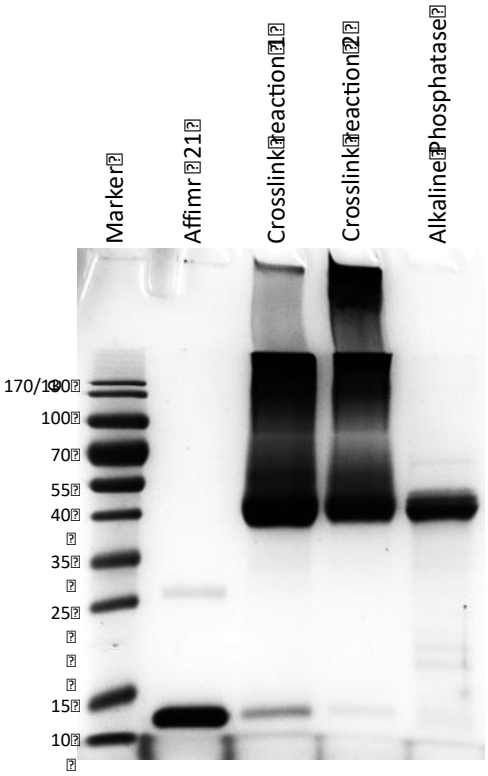

Figure 6.8 Crosslink reaction SDS PAGE gel.

Molecular weight markers are noted in kDa on the left of the gel. The cross-linked reaction samples show high molecular mass species, indicating that cross-linking has occurred.

The cross-linked Affimer-AP samples were not purified further, but were desalted and buffer exchanged as described previously (Chapter 4 Section 4.2.1).

6.3 Enzyme-linked Affimer assay

Dilutions of biotinylated mGFP were immobilized onto streptavidin-activated plates (Pierce) in triplicate at concentrations between 10 - 0 µg/ml in 200 µl PBS and incubated at 4 °C overnight. Plates were washed three times with PBS before blocking non-specific sites with 5% skimmed milk in PBS overnight at 4 °C. Plates were then washed three times with PBS/0.05% Tween-20 (PBST). The alkaline phosphatase linked mGFP21 was added and incubated for 2 h at room temperature and then washed six times with PBS. Enzyme activity was measured following addition of 100 µl of pNPP (2 mM final

concentration) for 30 min at room temperature. The reaction was stopped by the addition of 50 µl 3 M NaOH and the absorbance reading measured at 405 nm (Figure 6.9).

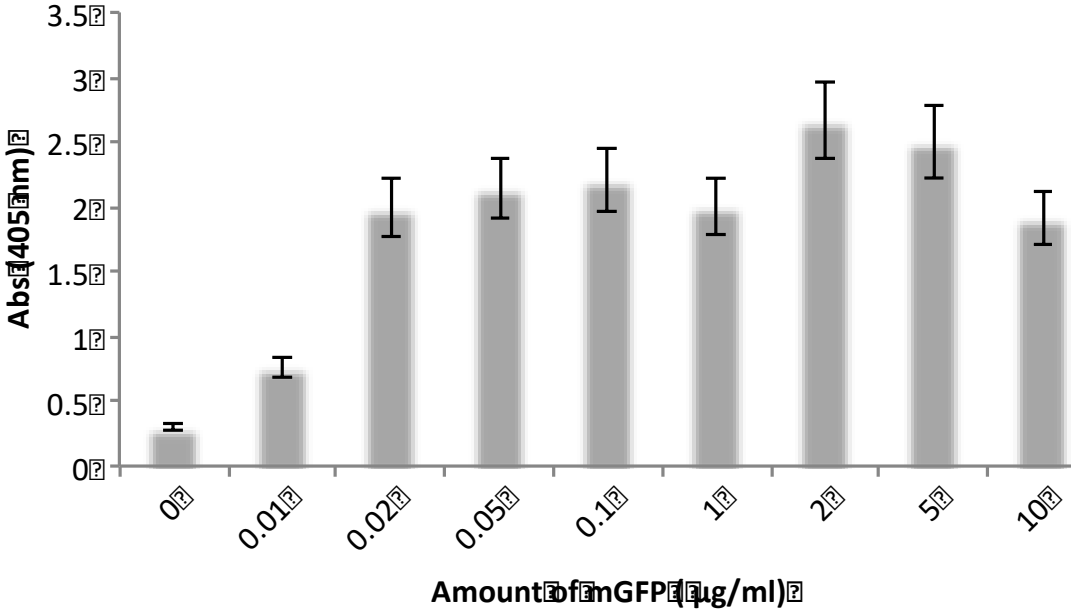

Figure 6.9 Enzyme-linked Affimer assay for mGFP with alkaline phosphatase linked mGFP21.

Three repeats of 0-10 µg of GFP were incubated on plates and detected with enzyme-linked mGFP21 Affimer. Concentrations above 0.02 µg/ ml of GFP were reliably detected

The background reading of 0.3 absorbance units is shown on the graph where the amount of mGFP added is zero. 0.01 µg/ml shows a slight increase in signal above the background to 0.8 absorbance units. The data reading from 0.02 to 10 µg/ml of GFP incubated on the plates shows an increase in absorbance to over 2 absorbance units. There is not a correlation between increase in concentration from 0.02 µg/ml to 10 µg/ml and an increase in absorbance. This could be because at 20 ng/ml the plate surface has reached saturation. This experiment shows that 20 ng/ml or more mGFP can be reliably detected by the enzyme-linked mGFP21 Affimer.

6.4 Enzyme-linked sandwich Affimer assay

Biotinylated mGFP32 was immobilized onto strepavidin-activated plates (Pierce) at a concentration of 10 µg/ml in PBS and incubated at 4 °C overnight. Plates were washed three times with PBS before blocking non-specific sites with 5% skimmed milk in PBS overnight at 4 °C. Plates were then washed three times with PBST. 200 µl dilutions of mGFP from 0 to 10 µg/ml were prepared in 1% skimmed milk/PBST, added to duplicate wells and incubated for an additional hour at room temperature, followed by six further washes with PBST. The alkaline phosphatase linked mGFP21 was added and incubated for 2 h at room temperature, and washed 6 times with PBST. Enzyme activity was measured as described in chapter 2 Section 2.9.3.2 and the data are shown in Figure 6.10.

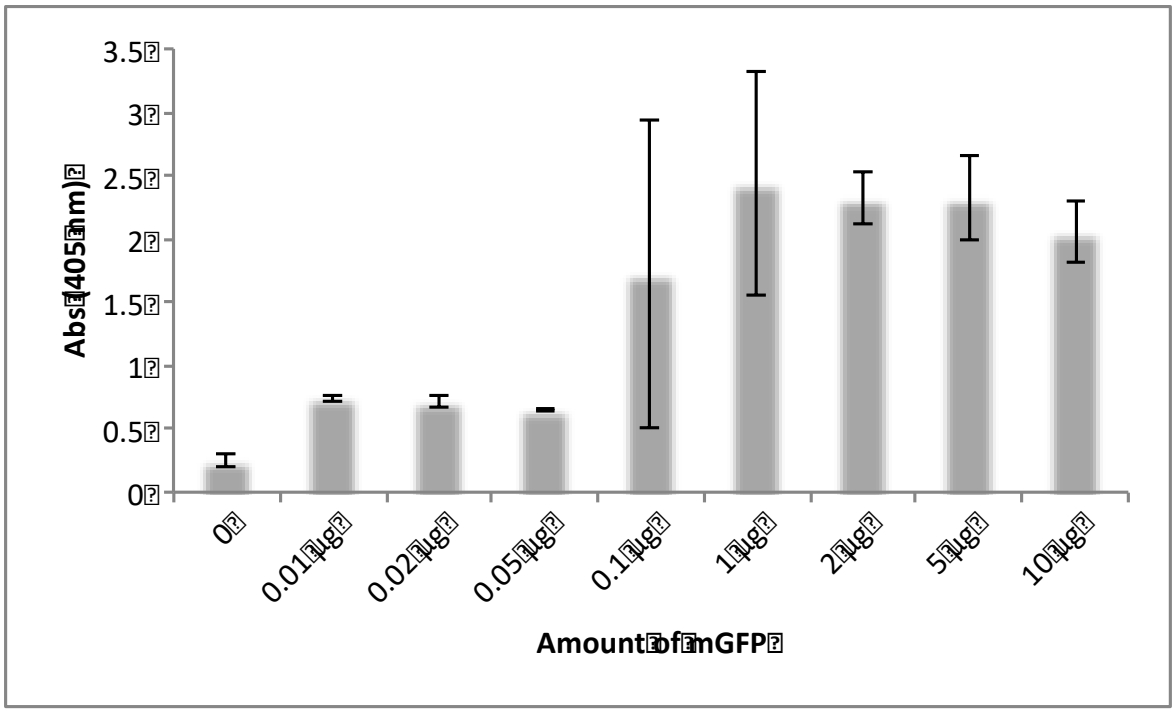

Figure 6.10 Sandwich enzyme-linked Affimer assay.

mGFP32 was used as a capture Affimer, and alkaline phosphatase linked mGFP21 was used for detection. 10 µg of mGFP32 were immobilised on streptavidin plates and three repeats of 0-10 µg of GFP were incubated with mGFP32, and detected with enzyme-linked mGFP21 Affimer. Concentrations above 2 µg/ ml of GFP were reliably detected

The background reading of 0.25 absorbance units is shown on the graph where the amount of mGFP added is zero. 0.01-0.05 μg shows a slight increase in signal above the background to 0.7-0.8 absorbance units. The data reading for 0.1 and 1 μg of GFP incubated on the plates shows an increase in absorbance to over 1.5 absorbance units on average, but there is a large error between the three repeats. 2, 5 and 10 μg of mGFP give a good signal of over 2 absorbance units. This experiment shows that 2 μg or more mGFP can be reliably detected by a sandwich enzyme-linked assay.

6.5 Split enzyme-linked Affimer assay

A split enzyme-linked Affimer assay was developed to establish a working example of the split alkaline phosphatase system. The split alkaline phosphatase (T59A-R62A) characterised in Chapter 5 was linked to mGFP32 and mGFP21 Affimers, as shown in the schematic in Figure 6.11

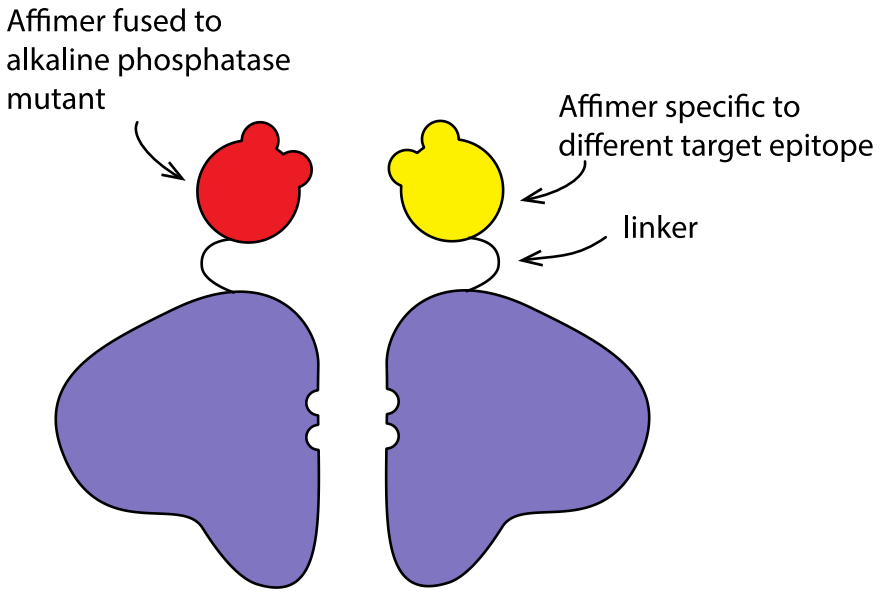

Figure 6.11 Schematic of split enzyme-linked Affimers.

There are two different Affimers fused to T59A-R62A alkaline phosphatase.

Two experiments were set up; one where the target was immobilised and one where the target was free in solution. For the immobilised target, dilutions of the mGFP between 10 and 0.1 µg/ml were prepared and added in duplicate to Maxisorp microtiter plates (Nunc), and were incubated overnight at 4 ^{o}C. After six washes with PBS, two split alkaline phosphatase linked Affimers were added and incubated for 2 h at room temperature, and then washed six times with PBS.

In parallel, dilutions of the target mGFP between 10 and 0.1 µg were added to 96 well plates (Nunc). Two split alkaline phosphatase linked Affimers were added and incubated for 2 h at room temperature. These plates were not washed because nothing has been immobilised, and the reaction should happen in solution.

Activity on both plates was measured by reading the absorbance at 405 nm after incubation with 100 µl of pNPP (2 mM final concentration) for 30 min, 60 min, 8 h, and 16 h at room temperature. Unfortunately, the readings were not above the background level, suggesting that functional dimers were not formed.

6.6 Discussion

Affimers for mGFP were explored to see if they could bind more than one epitope. mGFP21 was used to block its binding site on mGFP and, after being screened against a modest pool of other Affimers, mGFP32 was chosen as a binding partner. The Affimers were prone to precipitation, but after addition of 10 % glycerol, the amount of precipitate reduced. An analytical SEC was used to investigate if the Affimers were monomers or dimers. mGFP32 was a monomer, while mGFP21 was a mixture of monomer and dimer. The dimer and monomer were separated on a preparative SEC, but native gel data suggest the monomer – dimer formation was in equilibrium. As 80 % of the sample was in the monomer form, the two Affimer were chemically linked to wild-type alkaline phosphatase and T59A-R62A. These fusion proteins with wild-type alkaline phosphatase were used in enzyme-linked Affimer assays

and sandwich enzyme-linked Affimer assays. The fusion proteins with T59A-R62A were used in split enzyme-linked Affimer assays.

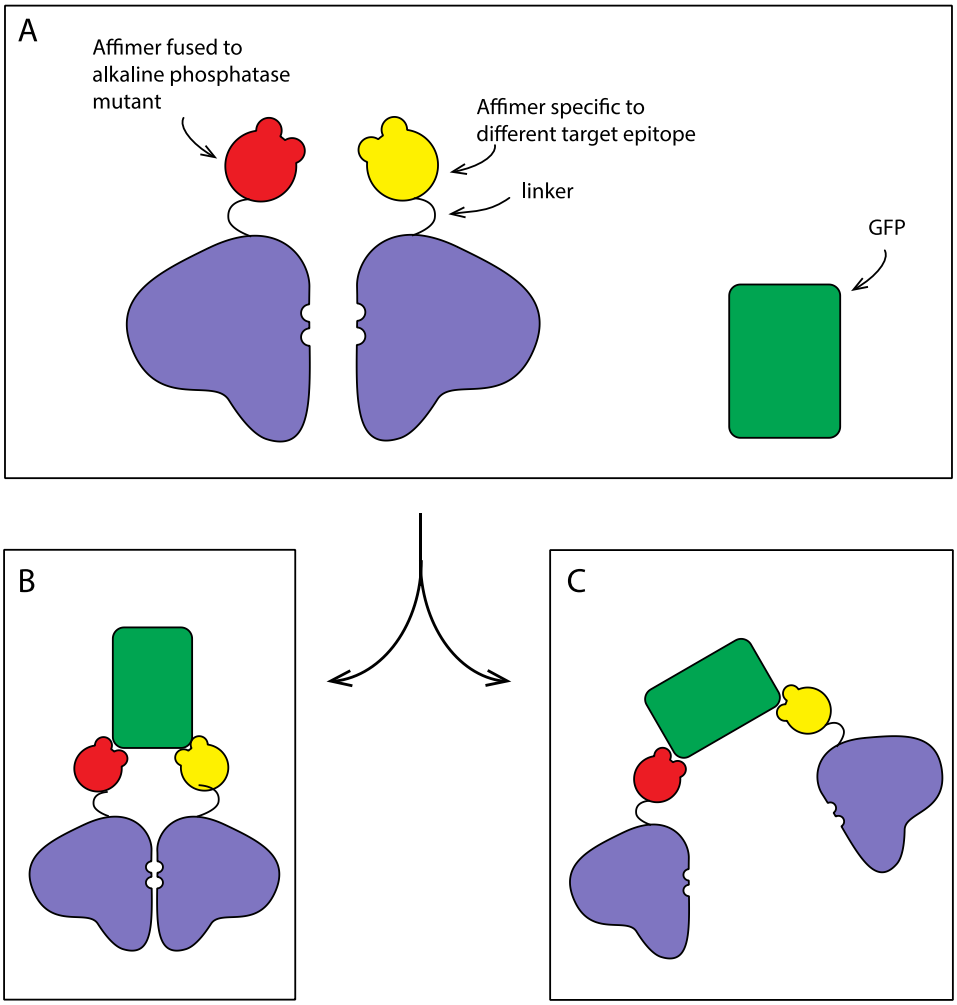

Figure 6.12 Split enzyme-linked Affimer assay.

A) Two different Affimers fused to T59A-R62A alkaline phosphatase. When GFP was introduced the experiment could progress one of two ways: B) successful signal produced upon the Affimer binding GFP, or C) Affimer binding at epitopes where the enzyme cannot establish the correct dimer form and turn over substrate.

The enzyme-linked Affimer assay establishes that AP linked mGFP21 can bind GFP and give a signal. The sandwich enzyme-linked assay determines that mGFP32 can hold GFP in place and AP linked mGFP21 can still give a signal. From these experiments, we know that mGFP21 and 32 bind and that the alkaline phosphatase remains active. We do not know, however, where the Affimers bind or the distance between the epitopes. The epitopes could be too far apart as demonstrated in Figure 6.12. Box A shows two Affimers fused to T59A-R62A alkaline phosphatase and the target, in this case GFP. Box B and C show how the experiment could proceed once the fusion proteins and GFP were mixed together: B) a successful signal produced upon the Affimer binding GFP, and C) the Affimers bind at epitopes where the enzyme cannot establish the correct dimer form and turn over substrate.

The data in Chapter 5 indicate that the distance dependence of the zif split alkaline phosphatase system is between 17 Å and 34 Å. A direct comparison cannot be made because the linker is different, as is the binding molecule. However, these measurements can be used as an approximation and can help determine what may have happened with the split enzyme-linked Affimer assay. The cylinder of GFP has a length of 42 Å, and a diameter of 24 Å (Hink, *et al*. 2000), therefore it is easy to imagine that the epitopes, where mGFP21 and 32 bind, are distant enough that they are not at a permissible distance.

mGFP21 was shown to be mixed species between a dimer and a monomer. It may improve the split AP assay if a pure monomer could be used. The sandwich phage ELISA revealed 13 Affimers that were negative and did not bind at the same time as MGFP21, but which probably bound at the same epitope. There were also 7 possible Affimers, including mGFP32, which could be further investigated.

The method of linking to Alkaline phosphatase was non-specific, and therefore the AP was not orientated in a particular way. This was fine for wild-type AP but split AP could need orientating. The linker between split AP was a chemical linker, $SM(PEG)_2$, which has a spacer arm of 17.6 Å. Optimisation of the linker type and length could help improve the split AP assay. SM(PEG)n can be bought with 2, 4, 6, 8, 12, and 24 PEG chain lengths, which would be an easy way to investigate linker length.

The ideal way forward would be to co-crystallise the different Affimers with mGFP and then rationally design linkers once the distance between the epitopes is known.

Chapter 7
Discussion

7.1 General discussion

The purpose of this study was to split an enzyme for use in biosensor technology. Initially as it was readily available and had been widely studied previously, β-lactamase was selected as a test system. In Chapter 3 N-terminal and C-terminal fragments of β-lactamase were cloned expressed and purified. Full-length and the C-terminal fragment were produced in the soluble fraction and were purified using a nickel column. The N-terminal fragment of β-lactamase was more difficult to produce, and was eventually purified from the insoluble fraction. It was solubilised in 8 M urea and purified using a nickel column. The chaotropic agent was removed once the protein fragment was bound to the nickel column. Purified N-terminal and C-terminal fragments of TEM-1 β-lactamase could be associated *in vitro* in a functional format by nickel ions that interacted with His tag regions on each monomer.

For use in a biosensor split enzyme system it is necessary to be able to produce the enzyme fragments in a simple and reproducible manner, to generate sufficient quantities of enzyme fragments that are capable of generating near-native levels of enzyme activity. Unfortunately, purified β-lactamase fragments proved difficult to produce and required refolding. The restored level of enzyme activity was only 5 % of that of the recombinant β-lactamase and only 0.3 % of native β-lactamase. There is such a vast difference here because the protein fragments are unstable, as they do not have their full structure to be able to fold correctly. Even when the fragments come together and the full sequence is available, the native chaperones in the cell are not available for efficient correct folding. There are disulphide bonds in β-lactamase, which required a non-reducing environment for correct folding, which is not available when folded in vitro or in the cytosol of *E. coli.* As the recombinant β-lactamase activity is already significantly reduced before the protein was even split, and was even lower afterwards, it was decided to investigate a different enzyme.

Alkaline phosphatase was a good candidate to begin using in a split enzyme system. Alkaline phosphatase, a homodimeric enzyme from *E. coli,* is simple to produce in at least 10 mg/L of recombinant protein, and it does not require

refolding. *E. coli* alkaline phosphatase is also a good model enzyme as it exhibits cooperativity, but only turns over substrate in a dimer form and not as a monomer (Garen and Levinthal 1960).

An inactive monomeric form of alkaline phosphatase was required for use in a split enzyme system such that when two monomers were associated they would give rise to enzyme activity. In order to disrupt the dimer interface to generate a monomeric form, amino acid residues at the dimer interface have been mutated. Previous reported studies provided a basis for this aspect of the work. The mutations R10A, R24A, T59A, T59R, and T81A (Boulanger and Kantrowitz 2003, Orhanovic, *et al*. 2006) were reported to reduce the stability of the dimer. Bioinformatics analysis of the dimer interface to identify residues that may affect interface stability was conducted during the present study, discussed in Chapter 4, and led to the identification of further residues that were subsequently mutated. These were D28A, R34A R62A and Y98A. A reduction in specific activity relative to wild type enzyme was used as an indicator of predominantly monomeric or dimeric state.

Eleven double mutants and nine R62X mutants were investigated in Chapter 5, initially by looking at the intramolecular re-complementation of the ability of the mutants to associate by inserting a coiled coil region. Several of the mutants showed an increase in activity by inserting a coiled coil region; three double mutants: D28A-Y98A, R34A-R62A, and T59A-R62A, and three R62X mutants: R62G, R62I, and R62N. Of these, T59A-R62A displayed the greatest gain in relative activity and was characterised further. T59A-R62A was shown by SEC and AUC to comprise a mixed population of monomer and dimer at pH 8.0, with the majority being in the monomer form. A zinc-binding assay indicated that T59A-R62A has a full complement of 2 zinc ions per monomer, as is required for full activity (Ma, *et al.* 1995).

In Chapter 5 Section 5.10, zinc finger motifs that bind to DNA were used to determine the permissible distance between two alkaline phosphatase monomers. Fusion proteins were designed to fuse a zinc finger motif to alkaline phosphatase. DNA oligos with the binding site for the zinc fingers were also designed. Several pairs of oligo were designed with the binding site being

moved along the DNA. Initial data showed that the permissible distance between two T59A-R62A monomers in a split system is between 17 and 34 Å.

The Affimer was chosen as a molecular recognition element in this study as it is a scaffold protein that behaves like an antibody molecule but it is only 12-14 KDa and can be produced in *E. coli.* Affimers that bind mGFP were used in a series of model experiments to see if a split enzyme system between Affimers and split alkaline phosphatase could be designed. Affimer mGFP21 and mGFP32 were selected as they bind at different epitopes on mGFP. Initially, wild-type alkaline phosphatase was cross-linked to Affimer mGFP21 and was used successfully in an enzyme-linked Affimer assay, much like an ELISA. The enzyme-linked Affimer assay indicated that levels of protein as low as 20 ng/ml of mGFP could be detected. Next, two Affimers were used in a sandwich enzyme-linked Affimer assay. mGFP32, a second mGFP binding protein, was used as a capture molecule, and enzyme-linked mGFP21 was used as a reporter molecule. The limits of detection for the sandwich assay were approximately 2 µg/ml of mGFP. The same Affimers were cross-linked to T59A-R62A, and used in a split enzyme-linked Affimer assay. Unfortunately, this assay was not successful, but further optimisation strategies are discussed in Section 7.3.1.

7.2 Comparison with other studies.

TEM-1 β-lactamase and fragments of TEM-1 β-lactamase were purified by de las Heras (2008) and the fragments were brought into a functional format with nickel ions in the same format as in this study. In the de las Heras (2008) study, full length β-lactamase was purified from the insoluble fraction, whereas in this study soluble expression was accomplished. In both studies the N-terminal fragment was purified from the insoluble fraction and had to be re-folded, while the C-terminal fragment was purified from the soluble fraction. Fry *et al.* (2008) took the purified split β-lactamase and used it in a cell free assay to investigate the interactions of the human cytomegalovirus (HCMV) as described in Chapter 1 Section 1.4.3.

A split linked β-lactamase has been used by Saunders *et al*. (2016) for screening a protein's inclination to aggregation and for the inhibition of aggregation. The systems involves placing a test protein the middle of the N and C-terminal domain of β-lactamase via two linkers, a schematic of the construct is shown in Figure 7.1.

Figure 7.1 Structure of test protein for protein aggregation.

The test protein is flanked by two G/S linkers, and the N and C-terminal of β-lactamase, adapted from Saunders (2016).

Each of the β-lactamase fragments are linked via a test protein, and if that test protein is correctly folded, the fragments would be accessible to each other and a functional β-lactamase could be formed. If the test protein was aggregated then the fragments would be held far apart from each other and would not be functional. This experimental investigation was done in the periplasm of *E. coli* and the system was able to measure the extent of protein aggregation via a simple readout of antibiotic resistance. Eight different proteins were investigated four that were prone to aggregation and four that were not inhibitors of aggregation were also tested (Saunders, *et al*. 2016).

The advantage to this approach is that it was done in cells, where β-lactamase is in its natural environment, along with the cells natural machinery to assist in folding. Each of the fragments are linked, via a test protein, so they will not diffuse away from each other, thus increasing the probability that the fragments will be able to form into a functional enzyme. In contrast, in this study the β-lactamase fragments were purified and experimental investigation was performed in an in vitro environment, and each fragment was free in solution.

As discussed in Chapter 1 Section 1.5.2.2 and Section 1.5.3, the kinetic properties of wild-type alkaline phosphatase and several mutants: R10A,

R10K, R24A, R24A, R24K, R10A-R24A, and T59A were assessed in a study by Martin *et al.* (1999). T81A was compared with wild-type in a study by Orhanovic *et al.* (2006). The T59R mutation also successfully produced a stable protein (Boulanger and Kantrowitz 2003). This mutant monomer was unlikely to be ever brought back into association as a homodimer as there is an obvious steric hindrance and positive charge repulsion (Boulanger and Kantrowitz 2003). No further work on the dimeric interface of *E. coli* alkaline phosphatase has been published to date. This is probably due to the difficult nature of producing stable variants, and difficulty in selecting mutations that would give the desired effect. The present study included the mutations from these previous studies and went further to include mutations at four additional amino acid residues D28, R34, R62, and Y98. The R62 mutation displayed properties of particular interest and the most effective mutant for monomer association as a dimer was T59A-R62A.

7.3 Future work

There are a number of areas that require more intensive investigation, such as the distance dependence of T59A-R62A dimerization interactions. This includes analysing different linker lengths and base pair gaps between the binding sites of the zinc finger. Furthermore, rational design of other mutants at the dimeric interface would be advantageous. However, pragmatically the most appropriate strategy would be the creation of a larger variant library to enable the screening of a much more substantial area of sequence space.

Whilst the concept underlying this research project was to develop a split enzyme system for use in a biosensor, such a system could be used in a system such as an assay or device that can simultaneously measure multiple analytes. A split enzyme system is designed to amplify the signal generated by a binding event between a binding protein and its analyte through catalytic turnover. However, despite the attraction of an intramolecular complementation system for the development of a high specificity biosensor that relies upon two binding events with the target molecule, the fundamental limitation is that full enzyme activity is highly unlikely to be achieved. The approach is essentially starting with a functional enzyme and dissecting it to

generate what ends up being a less efficient detection catalyst in the biosensor. Ultimately the point of a biosensor is to provide the most sensitive detection system for low concentrations of target analyte and thus one would want to achieve signal amplification at least equivalent to the parent enzyme. This leads to the suggestion that an alternative direction for consideration would be reversing an enzyme/inhibitor interaction upon binding or switchable enzymes. These various options will be discussed in the following section.

7.3.1 Distance dependence of T59A-R62A dimerization interactions

Initial data in Chapter 5 shows the permissible distance between two alkaline phosphatase monomer of the T59A-R62A variant is between 17 and 34 Å, which is promising. However, the experimental parameters, such as concentrations of the alkaline phosphatase variant and of the substrate, as well as the incubation time, need to be optimised with a duplex DNA oligo that is known to hold the T59A-R62A mutant alkaline phosphatase together. Next, the exact point where activity is lost needs to be investigated. The alkaline phosphatase variant was active when using oligos with a 5 bp (17 Å) gap and then inactive when using an oligo with a 10 bp (34 Å) gap. Using DNA oligonucleotides with 6, 7, 8, and 9 base pair gaps will give a more precise measurement of the permissible distance between two alkaline phosphatase monomers.

The protein linker length between the zinc finger and the T59A-R62A variant of alkaline phosphatase is 30 amino acids long. The linker length can be changed with a simple mutagenesis reaction providing a deletion of one or more amino acids, and the whole experiment could be repeated to investigate if this changes the permissible distance between the monomers. This information could then be translated into what length peptide linker could be used in an Alkaline phosphatase- linked Affimer experiment.

7.3.2 Rationally designed mutations

Given the position of R62, and the interaction it makes, as demonstrated in the simple graphic in Figure 7.2, it would be interesting to investigate the mutant Q416A as this would remove a fourth hydrogen bond, one more than T59A-R62A. The question to be investigated would then be whether Q416A would produce a fully monomeric alkaline phosphatase that can still be reactivated.

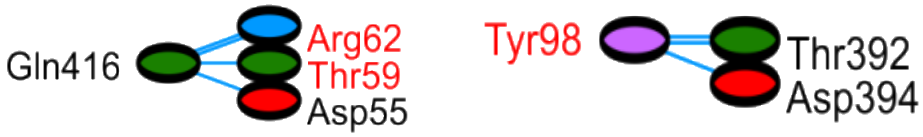

Figure 7.2 Graphic of the network of hydrogen bonds involving Gln 416 and Tyr 98.

There are two hydrogen bonds from Gln416 to Arg62, one from Gln416 to Thr59, and one from Gln416 to Asp55. Tyr98 has three hydrogen bonds, one to Thr392 and one to Asp394.

The data presented in Chapter 4 Section 4.9.1 suggest that Tyr98 is involved in creating a stable protein. When the Y98A mutation was introduced it did not have a notable detrimental effect on the activity of the enzyme. Y98A in combination with R10A and R24A again did not have much of an effect. When Y98A was in combination with D28A, R34A, T59A, R62A or T81A, the variant produced had very low activity. It would be interesting to look into a saturation mutagenesis experiment at the Y98 position. Further work in Chapter 5 Section 5.3.2 investigated the secondary structure using CD of some of the double mutants with low activity: D28A-Y98A, T59A-Y98A, R62A-Y98A and T81A-Y98A. This data indicated that two of these variants: T59A-Y98A and T81A-Y98A did not have secondary structure and were probably unfolded. Introducing T392A and D394A would reduce the amount of hydrogen bonds that were disrupted from 3 (Y98A) to 2 (T392A) or 1(D394A), using these addition mutations along with D28A, R34A, T59A, R62A or T81A could provide the right amount of instability to form a monomer, but with the ability to re-gain function.

7.3.3 Library generation

To investigate potential new mutations in alkaline phosphatase that may influence monomeric state and intramolecular complementation potential a library, or libraries, could be generated by directed evolution. In any mutagenesis reactions, the randomisation is at the DNA level (Nov 2012). In directed evolution experiments, random mutagenesis is a powerful tool for altering the properties of enzymes (Williams 2004). Mutations are often created by error-prone PCR, (Pritchard, *et al*. 2005) (Abou-Nader and Benedik 2010) or using mutator strains of *E. coli* (Miller 1998).

Error-prone PCR or mutator strains cannot change any single codon to every other codon. This is obvious from the codon table and the low rate of mutations which mean you would usually only generate 3-5 point mutations per coding region to ensure reasonable retention of enzyme activity and therefore you would never get 2 mutations in a single codon let alone three. However, error-prone PCR coupled with recombination, such as DNA shuffling will give rise to a diverse library. DNA shuffling is a method where copies of the same gene, each with different mutations, are randomly shuffled. This is done by digesting the library with DNAse I, then arbitrarily re-joining the fragments using self-priming PCR. DNA shuffling can be applied to any libraries including those using error prone PCR and/or mutator strains (Voet, *et al*. 2008). An advanatage to this approach is it allows the effects of different combinations of mutations to be tested, a disadvantage is that this technique is limited in searching sequence space. Stemmer (1994) used three cycles of DNA shuffling, in the directed evolution of β-lactamase. The variants were selected by increasing concentrations of the antibiotic. The variant reported had a 32,000-fold increase in its minimum inhibitory concentration from wild type (Stemmer 1994).

An alternative, more focussed approach would be to conduct more structure based combinatorial saturation mutagenesis experiments. As depicted in Figure 7.3, a saturation mutagenesis library uses a degenerate primer, or set of primers, in a mutagenesis reaction along with a parental plasmid containing the gene of interest. The parental plasmid is degraded using Dpn I and the

resulting mutant products can be directly transformed into *E. coli* (Parikh and Matsumura 2005).

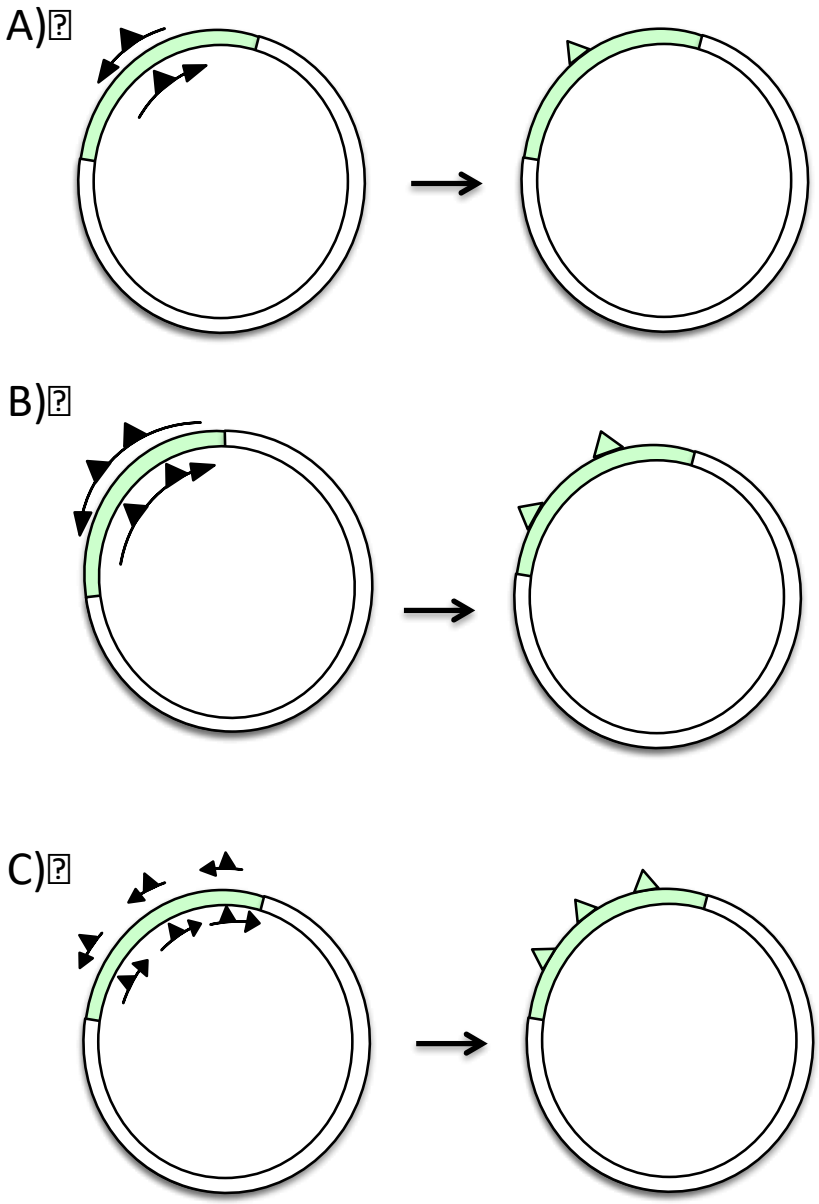

Figure 7.3 Methods for producing site directed mutagenesis libraries.

A parental plasmid can be used with a pair or more of complementary degenerate primers (small black arrows). The resulting PCR product can be directly transformed into *E. coli.* A) is an example of one set of degenerate primers and one mutation site. B) is an example of once set of degenerate primers but with two mutation sites. C) is an example of three sets of primers with three different mutation sites.

7.3.3.1 Bias when introducing the mutation.

Bias when making mutation libraries is introduced in three different ways. Initially, the genetic code exhibits bias as some amino acids have six codons, and some only have one. The chances of a mutation resulting in an arginine, leucine or a serine, which have six codons, are much higher than a tryptophan or methionine which only have one codon. Adding to the complexity, there are three stop codons, that if mutated in the middle of a gene, would result in a large change as the protein would be truncated. A second source of bias is due to the exponential nature of PCR which means that early mutations in the amplification process will be over-represented in the final library. Some polymerases used in mutagenesis reactions can display a preference for AT to GC substitutions or *vice versa* and the position of the mutation can also be affected by surrounding sequences, meaning randomisation to every amino acid is not equally likely at each position.

Primers can be fully degenerate using NNN, where N is any of the 4 bases: adenine (A), thymine (T), cytosine (C), or guanine (G), this uses 64 codons. The number of codons can be reduced using NNS, where S is either G or C reducing the number of codons to 32. NNK, where K is G or T, again reducing the number of codons to 32, or NNB where B is either C or G reducing the number of codon to 48 (Mena and Daugherty 2005). Moreover, using a more sophisticated randomisation scheme, such as that developed by Hughes *et al* (2003) called MAX; for maximally diverse libraries. A Max set of primers have just one codon per amino acid (Hughes, *et al*. 2003), removes the redundancy and gives each amino acid equal weighing.

7.3.3.2 Library size

An alkaline phosphatase monomer comprises 449 amino acids. If each of these residues was randomised to any of the 20 amino acids, this would give rise to 20^{449} number of mutants, which is too large to screen in any meaningful way. This number can be reduced by using saturation mutagenesis libraries. The number of mutants where all 8 positions; R10, R24, D28, R34, T59, R62, T81, and Y98 were randomised would be $20^8 = 2.6 \times 10^{10}$ mutants.

A library size of 2.6 $x10^{10}$ is still very large to be able to generate and screen effectively. Sub-libraries could be made; for example, as the alanine mutants at R10, R24, D28, and R34 appear to contribute less than T59, R62, T81 and Y98. Therefore a 4 positions library could be made which would have 20^4 = 1.6 $x10^5$ number of mutants. This would require a huge screening effort of over 3×10^6 clones for 95 % coverage (Hogrefe 2010), which is still a considerable challenge to screen.

7.3.3.3 Library screening

The method of screening in this study was low throughput, assaying each individual purified protein for activity. In this way, for a library of 4 mutations, sampling each just once would generate more than 1500, 96 well plates, which is not realistic. A higher throughput method, such as screening the colonies directly on an agar plate, would mean more mutants could be tested faster.

The first obstacle would be to make sure that the variants were translocated to the periplasm. A range of signal sequences used to direct the protein to the periplasmic space can be used. The native signal sequence on the PhoA gene is a starting point as it is the native signal sequence. The variants in this study had the PhoA leader sequence, but the protein was found to be produced in the cytoplasm. If, as in this study, PhoA does not produce alkaline phosphatase variants in the periplasm, then there are many other signal sequences that can be tried. There are other signal sequences that use the Sec pathway (Manting and Driessen 2000) similar to PhoA, and others that use the SRP (Luirink and Sinning 2004) pathway and the Tat pathway (Berks, *et al*. 2003, Berks, *et al.* 2005). Examples of signal sequencing that use the Sec pathway include: maltose-binding protein subunit, (MalE) (Lee and Bernstein 2001, Schierle, *et al.* 2003, Singh, *et al.* 2013); pectate lyase subunit, (PelB) (Singh, *et al.* 2013); alkaline phosphatase subunit, (PhoA) (Schierle, *et al*. 2003, Steiner, *et al.* 2006, Singh, *et al.* 2013); and outer membrane proteins, (OmpA) (Lee and Bernstein 2001, Steiner, *et al*. 2006). Examples of signal sequences that used the SRP pathway include: periplasmic sensory protein, (TorT) (Steiner, *et al.* 2006); subunit of the Tol-Pal cell envelope complex, (TolB) (Steiner, *et al*. 2006); and disulfide oxidoreductase, (DsbA) (Schierle, *et*

al. 2003, Steiner, *et al.* 2006). Finally, the Tat pathway can be used for translocation and signal sequences from penicillin acylase, (Pac) (Lee, *et al*. 2006); and subunit of trimethylamine N-oxide reductase I (TorA) (Blaudeck, Sprenger *et al.* 2001, Lee, *et al.* 2006) can be utilised to translocate a protein to the periplasmic space. A subset of these signal sequences should be tested with variants of alkaline phosphatase including at least one signal sequence from each pathway.

Once the secretion to the periplasm is confirmed, the colonies could be grown on a large, 24.5 cm square plate (Pierce) thereby increasing the area and number of colonies screened at once. A standard petri dish (Pierce) has an area of approximately 58 cm^2, the large 24.5 cm square plates have an area of 600 cm^2. Breed and Dotterer (1916) estimate the highest number of colonies allowable on a standard plate to be no more than 400. Therefore, 4000 colonies can be screened on the large plates, once plating the colonies was optimised. To screen a 4 position library, to 95% coverage as discussed earlier, would still require 750 plates.

For a direct colony assay, pNPP would not necessarily be the most appropriate substrate for a direct colony assay as it is yellow and would not stand out very well, but the colonies could be grown on a nictrocellulose or other filter on top of the pate and then this can be lifted off for assaying. The alkaline phosphatase substrate 5-bromo-4-chloro-3-indolyl phosphate (BCIP) (Sigma) is currently used in western blotting and immunohistological staining procedures, and produces a blue insoluble substance. The 4-Chloro-2-methylbenzenediazonium with 3-hydroxy-2-naphthoic acid 2,4-dimethylanilide phosphate (Sigma) substrate has been devised for use in western blotting and produces an insoluble intense red end product. These two substrates could be tested in a direct colony based assay. The colonies that change colour could then be picked and cultured, and then the plasmid DNA isolated and sequenced. Initially colonies expressing wild type alkaline phosphatase should be tested with increasing concentrations of BCIP, and/or 4-chloro-2-methylbenzenediazonium with 3-hydroxy-2-naphthoic acid 2,4-dimethylanilide to investigate the sensitivity of the experiment.

Another simple approach might be using the FKBP and FRB system discussed in Chapter 1 Section 1.4.1. Figure 1.11 shows that FKBP and FRB interact only in the presence of rapamycin. The alkaline phosphatase variant library could be designed with FKBP or FRB as fusion proteins. Cells that had low activity in the absence of rapamycin, but high activity in the presence of rapamycin would be considered a hit.

Luker *et al* (2004) packaged N- and C-terminal incremental truncation libraries of luciferase which were fused to FKBP and FRB in phage and *E. coli* was co-infected with the phage libraries. Selection was performed on agar plates, and colonies were blotted onto nitrocellulose filters which were soaked in the substrate luciferin. Positive clones were isolated and then tested with rapamycin. Plasmids were recovered from these clones to be further investigated (Luker, *et al.* 2004).

A high throughput system, investigating a library of variants of alkaline phosphatase fused to FKBP and FRB, could be performed in a similar fashion. Colonies with a colour change in the presence and no or less colour change in the absence of rapamycin could be isolated and then further characterised.

7.3.4 Using Affimers with split alkaline phosphatase in a system to measure multiple analytes.

Typical biosensors tend to use instruments capable of monitoring one interaction at a time (Chambers, *et al*. 2008, Bohunicky and Mousa 2010, Ataei, T *et al.* 2013, Sonuc and Sezginturk 2014, Azzouzi, *et al.* 2015). The first step towards measuring more than one different analyte at the same time is by using several different Affimer pairs in one system. The library of Affimers can be screened to bind many different targets (Paschke, *et al.* 2007, Tiede, *et al.* 2014, Raina, *et al.* 2015, Bedford, *et al.* 2017, Xie, *et al.* 2017), and can be linked to split alkaline phosphatase. These fusion proteins can be used as universal binding partners. One sample could be analysed for several binding partners in one test, which could be used to indicate contaminants in a food sample, for example. Moreover, this would also work for diagnostics in

healthcare. One blood sample to test several biomarkers would be a distinct advantage to streamline the diagnostic process, saving time and money.

The difficulty with a system where several analytes need to be measured is that the same sample preparation is required for all analytes, and the concentration or detection sensitivity for different analytes can vary over orders of magnitude. For example, B-type natriuretic peptide (BNP) is a biomarker for heart failure and the level in a healthy adult is 10 pg/ml, which rises to over 100 pg/ml when a patient is suffering from heart failure (Gaggin and Januzzi 2013). A second key biomarker for heart failure is Troponin T whose concentration is around 1 µg/ml, some 7 orders of magnitude greater than for BNP. Affimers could, in theory, be chosen to bind with different affinities to access a wide range of analyte concentrations.

Cross-reactivity could lead to false positive results and, therefore the Affimers would have to be very well characterised. However, having a system that uses two Affimers inherently increase selectivity for the specific analyte. Affimers have been raised against different Src Homology 2 (SH2) domains. Specificity was tested through binding to other SH2 family members, and the Affimers were shown to be selective to the specific SH2 domain that they were panned against in some cases (Tiede, *et al.* 2017).

A few instruments are now being developed as systems for measuring several analytes at the same time. They are powerful analytical tools and the commonly used ones include multiplex real-time PCR (Elnifro, *et al.* 2000), ELISA (Tighe, *et al.* 2015), microarrays (Moore, *et al.* 2016) and next-generation sequencing (Xuan, *et al.* 2013). These methods are good at accurate and precise diagnostic application, but they can require expensive equipment, can take several hours, and skilled users are needed to complete the test and analyse the results. With investment of time and money, and using Affimers as recognition elements and split alkaline phosphatase as an amplification tool, a biosensor that can measure several analytes simulatiously, that is inexpensive, specific, facile, fast and equipment-free could be made a reality.

Alkaline phosphatase as the amplification tool, in its current form would have limited use for many medical samples because human serum, for example, contains alkaline phosphatase at approximately 0.5 mg/ml (Bowers and McComb 1975). If a wash or separation step could be incorporated into the device then a split alkaline phosphatase could be used. A split alkaline phosphatase would however, be an excellent tool for environmental samples such as those mentioned in Chapter 1 Section 1.1.2.

7.3.5 Reversing an enzyme/inhibitor interaction upon binding

A different approach based upon a published patent (Balint and Her 2003), uses β-lactamase with β-lactamase inhibitor protein (BLIP). This system works by using an inhibitor to switch off the enzyme with inhibition being reversed upon binding of the analyte. This system could be used as a sensor for identifying the presence of a target molecule in a sample, much like the aims of this study. The sensor comprises β-lactamase and BLIP linked together by linkers that also include two epitope sequences for an antibody. Binding of the antibody displaces the BLIP from and prevents BLIP from rebinding to β-lactamase, thereby activating β-lactamase (Balint and Her 2003). It is proposed that this system could be adapted to identify a target analyte, as shown in Figure 7.4.

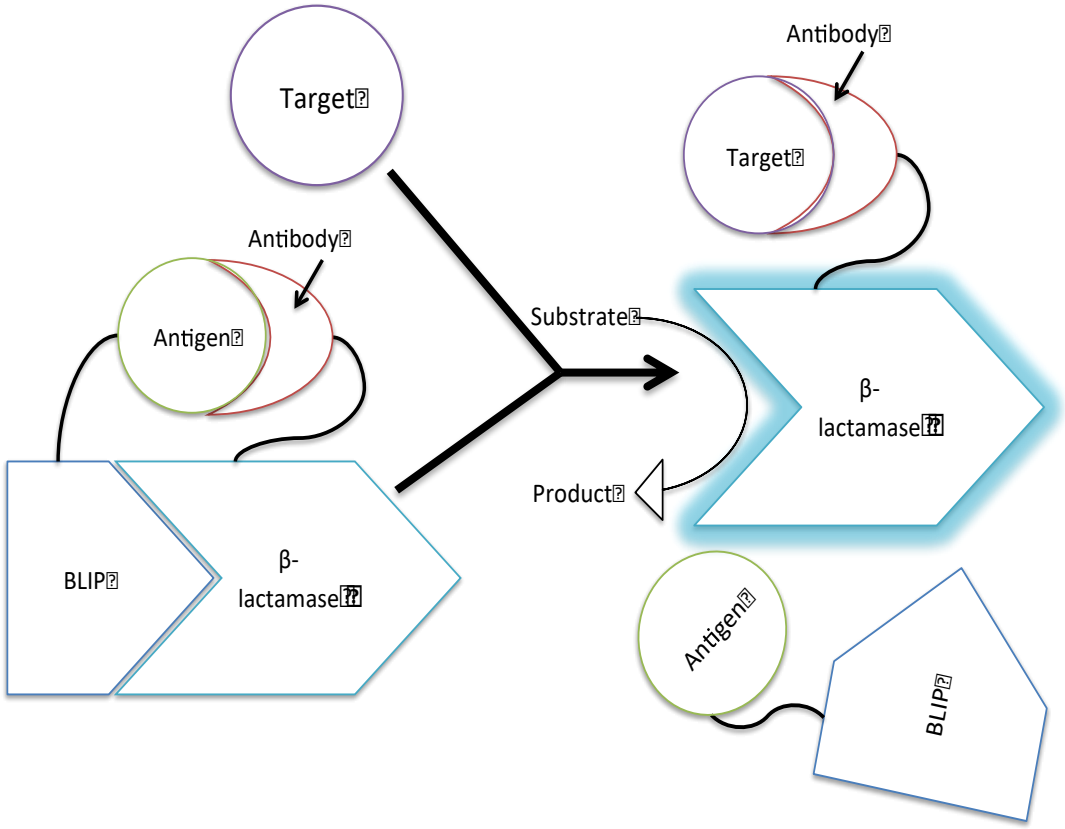

Figure 7.4 Schematic of dis-inhibition of β-lactamase.

β-lactamase is linked to an antibody, and BLIP is linked to a weak antigen for the antibody. Therefore, BLIP is held in place by the weak interaction and is inhibiting β-lactamase. When a target molecule is introduced, which binds strongly to the antibody, this displaces the weak antigen and β-lactamase can give a signal.

The biggest advantage of this approach is that β-lactamase is in its native format, meaning the turnover of the enzyme is optimal. A drawback is that this work is in the process of being patented, which, would restrict its use without permission. However, the principle could be applied to other enzyme inhibitor systems.

To use alkaline phosphatase instead of β-lactamase would overcome some IP issues, and the challenge is to find an appropriate inhibitor. There are many known inhibitors of *E. coli* alkaline phosphatase, but they are small molecules and not a protein like in the β-lactamase example shown in Figure 7.4 . Future work could therefore involve the cross-linking of a small inhibitor molecule to a weak antigen, and crosslinking an Affimer instead of an antibody with alkaline

phosphatase. If this proved successful and the presence of the small molecule linked antigen inhibited alkaline phosphatase, the next step would be to investigate if the antigen could be displaced, taking with it the linked small molecule and allowing alkaline phosphatase turnover.

The affinity of Affimer mGFP21 for eGFP and mGFP would need to be investigated, and if mGFP21 has low affinity for eGFP, and a high affinity for mGFP, this experiment could prove successful. An alkaline phosphatase linked Affimer has already been created with a mGFP21 Affimer in this study. Therefore the only other requirement for initial experiments is eGFP cross-linked to a small molecule inhibitor of alkaline phosphatase. Next, mGFP could displace the eGFP-linked inhibitor molecule, and the activity of alkaline phosphatase should be restored.

7.3.6 Using alkaline phosphatase as a switchable enzyme, in enzyme based logic gates.

A completely new direction for using split alkaline phosphatase is as a switchable enzyme in enzyme based logic gates. A wide array of applications in sensing and therapeutics could be enhanced by the ability to engineer synthetic enzymes that can be controlled by a signal such as pH (Ostermeier 2009). In particular there has been a lot of progress in biomolecular computing, which is a new field at the interface of biological science, engineering and computer science (Fu 2007). This has resulted in the emergence of various biological systems performing Boolean logic operations, simulating their electronic counterparts (Unger and Moult 2006).

Boolean algebra, first described by George Boole in 1848 can be used to describe logical expressions. The most common Boolean operators are gates called AND, OR and NOT. Each input and output of the gates must be one of two states: true / 1 or false / 0. An AND gate has two inputs and both have to be 1 in order for the output to be 1. The OR gate also has two inputs, either one or both inputs must be 1 for the output to be 1. A NOT gate has just one input, the output of the circuit will be the opposite of the input, so if 0 is input, then the output is 1. Each operator has a standard symbol shown in Figure 7.5

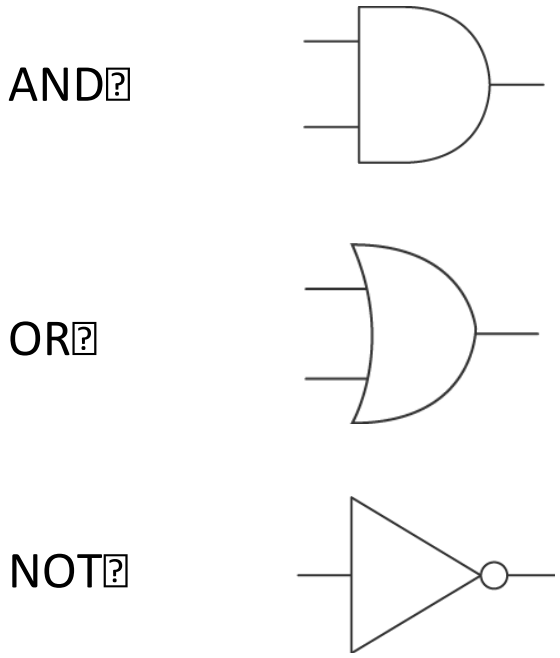

Figure 7.5 Boolean Logic Gates. The standard symbol for AND, OR and NOT operators are shown.

One method to engineer switchable enzymes is to create fusion proteins between an enzyme and a domain that responds to an input signal (Ostermeier 2009). In this study the K4 coiled coil fused to T59A-R62A alkaline phosphatase could be used as a biological system performing a Boolean logic operation. A change in enzyme activity is sought through the change from an input (Ostermeier 2009). In the case of a coiled coil fusion, the enzyme turns over at pH 11, but not at pH 8; thus, the input could be a pH change.

Electronic circuits look at two or more inputs and have to make decisions or an electrical output or process. This process uses electronic logic and is based on digital switches. Switchable enzymes can be used in Boolean operations where there usually needs to be two or more pairs of interacting domains. In this study a Boolean logic gate operation could be achieved by introducing 2 separate interacting coiled coils fused to the T59A-R62A variant of alkaline phosphatase. These two coils would replace the K4 homodimeric coiled-coil. Illustrated examples are given in Figure 7.6 and Figure 7.7

7.3.6.1 Composition of an AND gate

The final output signal is generated by turnover of alkaline phosphatase substrate, which could be electrochemical, see Chapter 1 Section 1.5.4.2. Figure 7.6 shows the modular design of an enzyme-based AND gate using the T59A-R62A variant of alkaline phosphatase with coiled-coils. In an AND gate, coiled coil fusion proteins use two different coiled coils which interact, and when coil 1 AND coil 2 are present then an output signal is generated. Preliminary data show this signal could be switched on or off by controlling pH and temperature.

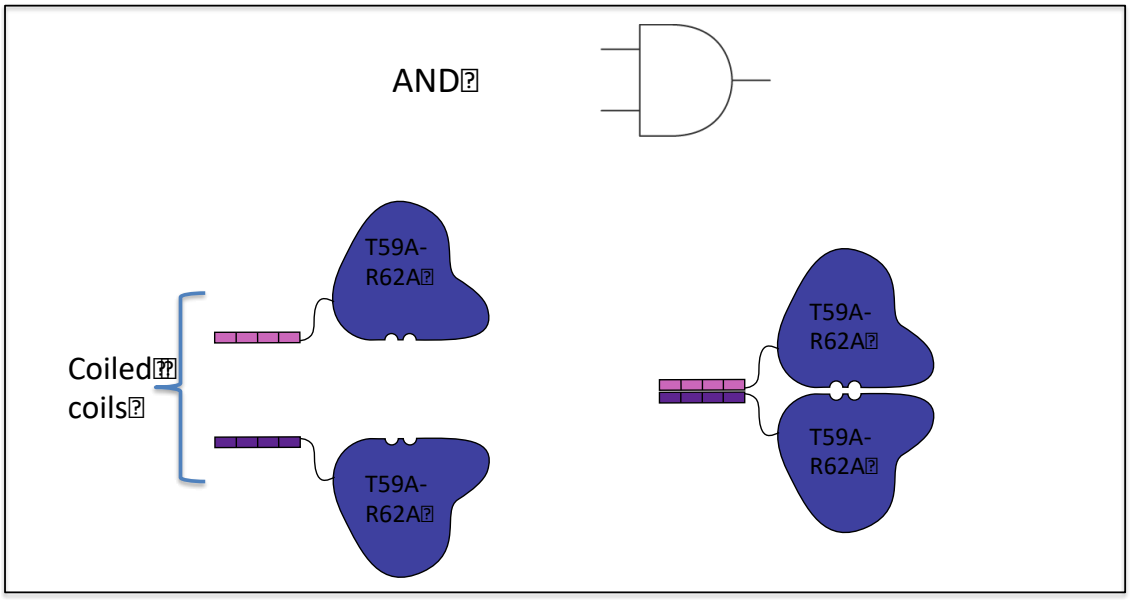

Figure 7.6 Modular design of an enzyme-based AND gate.

Two different coiled coils fused to the T69A-R62A variant of alkaline phosphatase are the inputs, and upon binding to each other the output from enzyme turnover would be observed.

7.3.6.2 Composition of an OR gate

Figure 7.7 shows the modular design of an enzyme-based OR gate using two coiled coils. In an OR gate, a coiled coil fusion protein with the T59A-R62A variant would be used, but the coiled coils need to be engineered, such that each coiled coil would be engineered to be homodimers as well as

hetrodimers. Therefore, when either 2 homodimeric coiled coils OR a hetrodimeric coiled coil are present an output signal is generated.

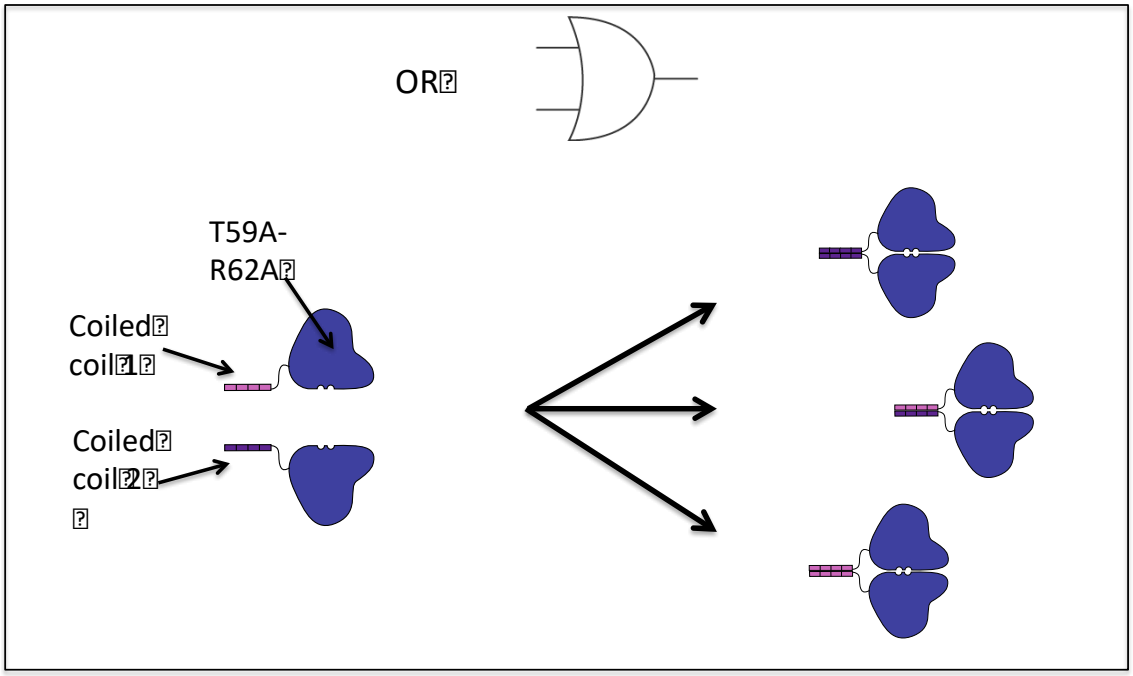

Figure 7.7 Modular design of an enzyme-based OR gate.

Two different coiled coils fused to T69A-R62A variants of alkaline phosphatase are the inputs, and upon binding each other, or themselves, the output from enzyme turnover would be observed.

7.3.6.3 NOT gate

The NOT gate is an inverter, thereby changing AND or OR to NAND and NOR respectively. The inverter for the coiled coil design could be simply the addition of free coiled coils in solution. However, a more sophisticated approach is to have another coiled coil peptide which binds with a higher affinity than the original coiled coils in the current system. The third coil would outcompete the bound coiled coil.

Different biological tools have been developed to assemble biochemical information processing systems for enzymes (Niazov, *et al*. 2006), DNA (Pei, *et al.* 2012), and RNA (Simpson, *et al.* 2001, Win and Smolke 2008). Here, coiled-coils can be used along with split alkaline phosphatase. Initially, each of the single logic gates should be proven as described, then future works

could involve integrated logic circuits, using a more complex design of several coiled coils.

7.4 Conclusions

The area of research into split proteins has been further extended with the development of a split alkaline phosphatase. Rationally designed mutations of alkaline phosphatase were identified by bioinformatics based on structures of *E. coli* alkaline phosphatase. The resulting variants were investigated to identify any that could regain activity after reactivation with a coiled-coil. The identification of the alkaline phosphatase variant T59A-R62A, that was reactivated to approximately 30% of wild-type activity, is a significant achievement and has potentially important applications in biosensor technology. The experiments described have provided a solid foundation for further studies. There are clear indications that a universal biosensor utilising a split alkaline phosphatase is a real possibility. Furthermore, the work presented here could be taken in new directions such as switchable enzymes and enzyme-based logic gates.

Chapter 8
References

Abe, K., H. Kondo, H. Watanabe, Y. Emori and S. Arai (1991). "Oryzacystatins as the first well-defined cystatins of plant origin and their target proteinases in rice seeds." Biomed Biochem Acta **50**(4-6): 637-641.
Abou-Nader, M. and M. J. Benedik (2010). "Rapid generation of random mutant libraries." Bioeng Bugs **1**(5): 337-340.
Allegra, C. J., J. M. Jessup, M. R. Somerfield, S. R. Hamilton, E. H. Hammond, D. F. Hayes, P. K. McAllister, R. F. Morton and R. L. Schilsky (2009). "American Society of Clinical Oncology provisional clinical opinion: testing for KRAS gene mutations in patients with metastatic colorectal carcinoma to predict response to anti-epidermal growth factor receptor monoclonal antibody therapy." J Clin Oncol **27**(12): 2091-2096.
Altschul, S. F., W. Gish, W. Miller, E. W. Myers and D. J. Lipman (1990). "Basic local alignment search tool." J Mol Biol **215**(3): 403-410.
Andrews, L. D., T. D. Fenn and D. Herschlag (2013). "Ground state destabilization by anionic nucleophiles contributes to the activity of phosphoryl transfer enzymes." PLoS Biol **11**(7): e1001599.
Applebury, M. L. and J. E. Coleman (1969). "Escherichia coli alkaline phosphatase. Metal binding, protein conformation, and quaternary structure." J Biol Chem **244**(2): 308-318.
Applebury, M. L., B. P. Johnson and J. E. Coleman (1970). "Phosphate binding to alkaline phosphatase. Metal ion dependence." J Biol Chem **245**(19): 4968-4976.
Ataei, F., M. Torkzadeh-Mahani and S. Hosseinkhani (2013). "A novel luminescent biosensor for rapid monitoring of IP(3) by split-luciferase complementary assay." Biosens Bioelectron **41**: 642-648.
Azzouzi, S., L. Rotariu, A. M. Benito, W. K. Maser, M. Ben Ali and C. Bala (2015). "A novel amperometric biosensor based on gold nanoparticles anchored on reduced graphene oxide for sensitive detection of l-lactate tumor biomarker." Biosens Bioelectron **69**: 280-286.
Balint, R. and J. H. Her (2003). Molecular sensors activated by disinhibition, Google Patents.
Baluka, S. A. and W. K. Rumbeiha (2016). "Bisphenol A and food safety: Lessons from developed to developing countries." Food Chem Toxicol **92**: 58-63.
Barhoumi, H., A. Maaref, M. Rammah, C. Martelet, N. Jaffrezic, C. Mousty, S. Vial and C. Forano (2006). "Urea biosensor based on Zn3Al–Urease layered double hydroxides nanohybrid coated on insulated silicon structures." Materials Sci.Eng: C **26**(2): 328-333.
Barnard E, M. N., Nelson J and Timson D (2007). "Detection of Protein-Protein Interactions Using Protein-Fragment Complementation Assays (PCA)." Curr. Proteomics **4**(4): 17-27.

Bedford, R., C. Tiede, R. Hughes, A. Curd, M. J. McPherson, M. Peckham and D. C. Tomlinson (2017). "Alternative reagents to antibodies in imaging applications." Biophys Rev.
Berks, B. C., T. Palmer and F. Sargent (2003). "The Tat protein translocation pathway and its role in microbial physiology." Adv Microb Physiol **47**: 187-254.
Berks, B. C., T. Palmer and F. Sargent (2005). "Protein targeting by the bacterial twin-arginine translocation (Tat) pathway." Curr Opin Microbiol **8**(2): 174-181.
Binkowski, B., F. Fan and K. Wood (2009). "Engineered luciferases for molecular sensing in living cells." Curr Opin Biotechnol **20**(1): 14-18.
Blaudeck, N., G. A. Sprenger, R. Freudl and T. Wiegert (2001). "Specificity of signal peptide recognition in tat-dependent bacterial protein translocation." J Bacteriol **183**(2): 604-610.
Bobyr, E., J. K. Lassila, H. I. Wiersma-Koch, T. D. Fenn, J. J. Lee, I. Nikolic-Hughes, K. O. Hodgson, D. C. Rees, B. Hedman and D. Herschlag (2012). "High-resolution analysis of Zn(2+) coordination in the alkaline phosphatase superfamily by EXAFS and x-ray crystallography." J Mol Biol **415**(1): 102-117.
Bohunicky, B. and S. A. Mousa (2010). "Biosensors: the new wave in cancer diagnosis." Nanotechnol Sci Appl **4**: 1-10.
Boulanger, R. R., Jr. and E. R. Kantrowitz (2003). "Characterization of a monomeric Escherichia coli alkaline phosphatase formed upon a single amino acid substitution." J Biol Chem **278**(26): 23497-23501.
Bowers, G. N., Jr. and R. B. McComb (1975). "Measurement of total alkaline phosphatase activity in human serum." Clin Chem **21**(13): 1988-1995.
Breed, R. S. and W. D. Dotterrer (1916). "The Number of Colonies Allowable on Satisfactory Agar Plates." J Bacteriol **1**(3): 321-331.
Brook, I. and A. E. Gober (1984). "Rapid method for detecting beta-lactamase producing bacteria in clinical specimens." J Clin Pathol **37**(12): 1392-1394.
Butler-Ransohoff, J. E., D. A. Kendall, S. Freeman, J. R. Knowles and E. T. Kaiser (1988). "Stereochemistry of phospho group transfer catalyzed by a mutant alkaline phosphatase." Biochemistry **27**(13): 4777-4780.
Chaidaroglou, A., D. J. Brezinski, S. A. Middleton and E. R. Kantrowitz (1988). "Function of arginine-166 in the active site of Escherichia coli alkaline phosphatase." Biochemistry **27**(22): 8338-8343.
Chaidaroglou, A. and E. R. Kantrowitz (1989). "Alteration of aspartate 101 in the active site of Escherichia coli alkaline phosphatase enhances the catalytic activity." Protein Eng **3**(2): 127-132.
Chambers, J. P., B. P. Arulanandam, L. L. Matta, A. Weis and J. J. Valdes (2008). "Biosensor recognition elements." Curr Issues Mol Biol **10**(1-2): 1-12.
Chang, C. N., W. J. Kuang and E. Y. Chen (1986). "Nucleotide sequence of the alkaline phosphatase gene of Escherichia coli." Gene **44**(1): 121-125.
Chen, L., D. Neidhart, W. M. Kohlbrenner, W. Mandecki, S. Bell, J. Sowadski and C. Abad-Zapatero (1992). "3-D structure of a mutant (Asp101-->Ser) of

E.coli alkaline phosphatase with higher catalytic activity." Protein Eng **5**(7): 605-610.
Chen, X., J. L. Zaro and W. C. Shen (2013). "Fusion protein linkers: property, design and functionality." Adv Drug Deliv Rev **65**(10): 1357-1369.
Coleman, J. E. (1992). "Structure and mechanism of alkaline phosphatase." Annu Rev Biophys Biomol Struct **21**: 441-483.
Cornett, J. K. and T. J. Kirn (2013). "Laboratory Diagnosis of HIV in Adults: A Review of Current Methods." Clin. Infect. Dis. **57**(5): 712-718.
Daemen, F. J. and J. F. Riordan (1974). "Essential arginyl residues in Escherichia coli alkaline phosphatase." Biochemistry **13**(14): 2865-2871.
Daniels, J. S. and N. Pourmand (2007). "Label-Free Impedance Biosensors: Opportunities and Challenges." Electroanalysis **19**(12): 1239-1257.
De Crescenzo, G., J. R. Litowski, R. S. Hodges and M. D. O'Connor-McCourt (2003). "Real-time monitoring of the interactions of two-stranded de novo designed coiled-coils: effect of chain length on the kinetic and thermodynamic constants of binding." Biochemistry **42**(6): 1754-1763.
de las Heras, R., S. R. Fry, J. Li, E. Arel, E. H. Kachab, S. L. Hazell and C. Y. Huang (2008). "Development of homogeneous immunoassays based on protein fragment complementation." Biochem Biophys Res Commun **370**(1): 164-168.
Dealwis, C. G., C. Brennan, K. Christianson, W. Mandecki and C. Abad-Zapatero (1995). "Crystallographic analysis of reversible metal binding observed in a mutant (Asp153-->Gly) of Escherichia coli alkaline phosphatase." Biochemistry **34**(43): 13967-13973.
Dealwis, C. G., L. Chen, C. Brennan, W. Mandecki and C. Abad-Zapatero (1995). "3-D structure of the D153G mutant of Escherichia coli alkaline phosphatase: an enzyme with weaker magnesium binding and increased catalytic activity." Protein Eng **8**(9): 865-871.
Degani, Y. and A. Heller (1987). "Direct electrical communication between chemically modified enzymes and metal electrodes. I. Electron transfer from glucose oxidase to metal electrodes via electron relays, bound covalently to the enzyme." J. Phys. Chem **91**(6): 1285-1289.
Delaney, K. P., B. M. Branson, A. Uniyal, S. Phillips, D. Candal, S. M. Owen and P. R. Kerndt (2011). "Evaluation of the performance characteristics of 6 rapid HIV antibody tests." Clin Infect Dis **52**(2): 257-263.
Deng, Q., D. Wang, X. Xiang, X. Gao, P. R. Hardwidge, R. S. Kaushik, T. Wolff, S. Chakravarty and F. Li (2011). "Application of a split luciferase complementation assay for the detection of viral protein-protein interactions." J Virol Methods **176**(1-2): 108-111.
Easton, D. F., D. Ford and D. T. Bishop (1995). "Breast and ovarian cancer incidence in BRCA1-mutation carriers. Breast Cancer Linkage Consortium." Am J Hum Genet **56**(1): 265-271.
Eaton, D. R. and K. Zaw (1972). "Geometry of nickel(II) complexes." J. Am.Chem. Soc.**94**(12): 4394-4395.

Elnifro, E. M., A. M. Ashshi, R. J. Cooper and P. E. Klapper (2000). "Multiplex PCR: optimization and application in diagnostic virology." Clin Microbiol Rev **13**(4): 559-570.
Freire, R. S., C. A. Pessoa, L. D. Mello and L. T. Kubota (2003). "Direct electron transfer: an approach for electrochemical biosensors with higher selectivity and sensitivity." Journal of the Brazilian Chemical Society **14**: 230-243.
Fry, S. R., J. Li, R. de las Heras, J. A. McCourt, E. Arel, E. H. Kachab, S. L. Hazell and C. Y. Huang (2008). "Detection of HSV type-1 and type-2 IgG using an in vitro PCA based homogeneous immunoassay." Biochem Biophys Res Commun **372**(4): 542-546.
Fu, P. (2007). "Biomolecular computing: is it ready to take off?" Biotechnol J **2**(1): 91-101.
Gaggin, H. K. and J. L. Januzzi, Jr. (2013). "Biomarkers and diagnostics in heart failure." Biochim Biophys Acta **1832**(12): 2442-2450.
Galarneau, A., M. Primeau, L. E. Trudeau and S. W. Michnick (2002). "Beta-lactamase protein fragment complementation assays as in vivo and in vitro sensors of protein protein interactions." Nat Biotechnol **20**(6): 619-622.
Gamella, M., S. Campuzano, J. Manso, G. Gonzalez de Rivera, F. Lopez-Colino, A. J. Reviejo and J. M. Pingarron (2014). "A novel non-invasive electrochemical biosensing device for in situ determination of the alcohol content in blood by monitoring ethanol in sweat." Anal Chim Acta **806**: 1-7.
Garen, A. and S. Garen (1963). "Complementation in vivo between structural mutants of alkaline phosphatase from E. coli." J Mol Biol **7**: 13-22.
Garen, A. and C. Levinthal (1960). "A fine-structure genetic and chemical study of the enzyme alkaline phosphatase of E. coli. I. Purification and characterization of alkaline phosphatase." Biochim Biophys Acta **38**: 470-483.
Gilligan, T. D., J. Seidenfeld, E. M. Basch, L. H. Einhorn, T. Fancher, D. C. Smith, A. J. Stephenson, D. J. Vaughn, R. Cosby, D. F. Hayes and O. American Society of Clinical (2010). "American Society of Clinical Oncology Clinical Practice Guideline on uses of serum tumor markers in adult males with germ cell tumors." J Clin Oncol **28**(20): 3388-3404.
Gomez-Anquela, C., T. Garcia-Mendiola, J. M. Abad, M. Pita, F. Pariente and E. Lorenzo (2015). "Scaffold electrodes based on thioctic acid-capped gold nanoparticles coordinated Alcohol Dehydrogenase and Azure A films for high performance biosensor." Bioelectrochemistry **106**(Pt B): 335-342.
Gorton, L., A. Lindgren, T. Larsson, F. D. Munteanu, T. Ruzgas and I. Gazaryan (1999). "Direct electron transfer between heme-containing enzymes and electrodes as basis for third generation biosensors." Anal Chim Acta **400**(1): 91-108.
Guo, Z., W. A. Johnston, V. Stein, P. Kalimuthu, S. Perez-Alcala, P. V. Bernhardt and K. Alexandrov (2016). "Engineering PQQ-glucose dehydrogenase into an allosteric electrochemical Ca(2+) sensor." Chem Commun (Camb) **52**(3): 485-488.

Guo, Z., L. Murphy, V. Stein, W. A. Johnston, S. Alcala-Perez and K. Alexandrov (2016). "Engineered PQQ-Glucose Dehydrogenase as a Universal Biosensor Platform." J Am Chem Soc **138**(32): 10108-10111.
Harman, C., K. E. Tollefsen, O. Bøyum, K. Thomas and M. Grung (2008). "Uptake rates of alkylphenols, PAHs and carbazoles in semipermeable membrane devices (SPMDs) and polar organic chemical integrative samplers (POCIS)." Chemosphere **72**(10): 1510-1516.
Heller, A. and B. Feldman (2008). "Electrochemical glucose sensors and their applications in diabetes management." Chem. Rev. **108**(7): 2482-2505.
Henry, N. L. and D. F. Hayes (2012). "Cancer biomarkers." Mol Oncol **6**(2): 140-146.
Heppel, L. A., D. R. Harkness and R. J. Hilmoe (1962). "A study of the substrate specificity and other properties of the alkaline phosphatase of Escherichia coli." J Biol Chem **237**: 841-846.
Hernández, C. N., M. B. G. García, D. H. Santos, M. A. Heras, A. Colina and P. Fanjul-Bolado (2016). "Aqueous UV–VIS spectroelectrochemical study of the voltammetric reduction of graphene oxide on screen-printed carbon electrodes." Electrochem. Commun. **64**: 65-68.
Hey, T., E. Fiedler, R. Rudolph and M. Fiedler (2005). "Artificial, non-antibody binding proteins for pharmaceutical and industrial applications." Trends Biotechnol **23**(10): 514-522.
Hink, M. A., R. A. Griep, J. W. Borst, A. van Hoek, M. H. Eppink, A. Schots and A. J. Visser (2000). "Structural dynamics of green fluorescent protein alone and fused with a single chain Fv protein." J Biol Chem **275**(23): 17556-17560.
Hogrefe, H. H. (2010). Fine-Tuning Enzyme Activity Through Saturation Mutagenesis. In Vitro Mutagenesis Protocols: Third Edition. J. Braman. Totowa, NJ, Humana Press**:** 271-283.
Holtz, K. M., B. Stec and E. R. Kantrowitz (1999). "A model of the transition state in the alkaline phosphatase reaction." J Biol Chem **274**(13): 8351-8354.
Holtz, K. M., B. Stec, J. K. Myers, S. M. Antonelli, T. S. Widlanski and E. R. Kantrowitz (2000). "Alternate modes of binding in two crystal structures of alkaline phosphatase-inhibitor complexes." Protein Sci **9**(5): 907-915.
Hughes, M. D., D. A. Nagel, A. F. Santos, A. J. Sutherland and A. V. Hine (2003). "Removing the redundancy from randomised gene libraries." J Mol Biol **331**(5): 973-979.
Hull, W. E., S. E. Halford, H. Gutfreund and B. D. Sykes (1976). "31P nuclear magnetic resonance study of alkaline phosphatase: the role of inorganic phosphate in limiting the enzyme turnover rate at alkaline pH." Biochemistry **15**(7): 1547-1561.
Janeway, C. A., K. P. Murphy, P. Travers and M. Walport (2008). Janeway's immunobiology. New York, NY ; London, Garland Science.
Johnsson, N. and A. Varshavsky (1994). "Split ubiquitin as a sensor of protein interactions in vivo." Proc Natl Acad Sci U S A **91**(22): 10340-10344.

Justino, C. I., A. C. Duarte and T. A. Rocha-Santos (2016). "Immunosensors in Clinical Laboratory Diagnostics." Adv Clin Chem **73**: 65-108.
Justino, C. I., K. Duarte, S. Lucas, P. Chaves, P. Bettencourt, A. C. Freitas, R. Pereira, S. Cardoso, A. C. Duarte and T. A. Rocha-Santos (2014). "Assessment of cardiovascular disease risk using immunosensors for determination of C-reactive protein levels in serum and saliva: a pilot study." Bioanalysis **6**(11): 1459-1470.
Justino, C. I., A. C. Freitas, J. P. Amaral, T. A. Rocha-Santos, S. Cardoso and A. C. Duarte (2013). "Disposable immunosensors for C-reactive protein based on carbon nanotubes field effect transistors." Talanta **108**: 165-170.
Kelly, S. M., T. J. Jess and N. C. Price (2005). "How to study proteins by circular dichroism." Biochimica et Biophysica Acta (BBA) - Proteins and Proteomics **1751**(2): 119-139.
Kerppola, T. K. (2006). "Complementary methods for studies of protein interactions in living cells." Nat Methods **3**(12): 969-971.
Kerppola, T. K. (2006). "Design and implementation of bimolecular fluorescence complementation (BiFC) assays for the visualization of protein interactions in living cells." Nat Protoc **1**(3): 1278-1286.
Kerppola, T. K. (2006). "Visualization of molecular interactions by fluorescence complementation." Nat Rev Mol Cell Biol **7**(6): 449-456.
Kerppola, T. K. (2008). "BIMOLECULAR FLUORESCENCE COMPLEMENTATION (BiFC) ANALYSIS AS A PROBE OF PROTEIN INTERACTIONS IN LIVING CELLS." Annual review of biophysics **37**: 465-487.
Kim, E. E. and H. W. Wyckoff (1991). "Reaction mechanism of alkaline phosphatase based on crystal structures. Two-metal ion catalysis." J Mol Biol **218**(2): 449-464.
Lan, T., J. Zhang and Y. Lu (2016). "Transforming the blood glucose meter into a general healthcare meter for in vitro diagnostics in mobile health." Biotechnology Advances **34**(3): 331-341.
Larkin, M. A., G. Blackshields, N. P. Brown, R. Chenna, P. A. McGettigan, H. McWilliam, F. Valentin, I. M. Wallace, A. Wilm, R. Lopez, J. D. Thompson, T. J. Gibson and D. G. Higgins (2007). "Clustal W and Clustal X version 2.0." Bioinformatics **23**(21): 2947-2948.
Laskowski, R. A. (2001). "PDBsum: summaries and analyses of PDB structures." Nucleic Acids Res **29**(1): 221-222.
Laskowski, R. A., E. G. Hutchinson, A. D. Michie, A. C. Wallace, M. L. Jones and J. M. Thornton (1997). "PDBsum: a Web-based database of summaries and analyses of all PDB structures." Trends Biochem Sci **22**(12): 488-490.
Lata, K., V. Dhull and V. Hooda (2016). "Fabrication and Optimization of ChE/ChO/HRP-AuNPs/c-MWCNTs Based Silver Electrode for Determining Total Cholesterol in Serum." Biochem Res Int **2016**: 1545206.
Le Du, M. H., C. Lamoure, B. H. Muller, O. V. Bulgakov, E. Lajeunesse, A. Menez and J. C. Boulain (2002). "Artificial evolution of an enzyme active site:

structural studies of three highly active mutants of Escherichia coli alkaline phosphatase." J Mol Biol **316**(4): 941-953.
Lee, H. C. and H. D. Bernstein (2001). "The targeting pathway of Escherichia coli presecretory and integral membrane proteins is specified by the hydrophobicity of the targeting signal." Proc Natl Acad Sci U S A **98**(6): 3471-3476.
Lee, P. A., D. Tullman-Ercek and G. Georgiou (2006). "The bacterial twin-arginine translocation pathway." Annu Rev Microbiol **60**: 373-395.
Li, H., X. Liu, L. Li, X. Mu, R. Genov and A. J. Mason (2016). "CMOS Electrochemical Instrumentation for Biosensor Microsystems: A Review." Sensors (Basel) **17**(1).
Lin, K., R. Lipsitz, T. Miller, S. Janakiraman and U. S. P. S. T. Force (2008). "Benefits and harms of prostate-specific antigen screening for prostate cancer: an evidence update for the U.S. Preventive Services Task Force." Ann Intern Med **149**(3): 192-199.
Liu, M., Y. Wen, J. Xu, H. He, D. Li, R. Yue and G. Liu (2011). "An amperometric biosensor based on ascorbate oxidase immobilized in poly(3,4-ethylenedioxythiophene)/multi-walled carbon nanotubes composite films for the determination of L-ascorbic acid." Anal Sci **27**(5): 477.
Luirink, J. and I. Sinning (2004). "SRP-mediated protein targeting: structure and function revisited." Biochim Biophys Acta **1694**(1-3): 17-35.
Luker, K. E., M. C. Smith, G. D. Luker, S. T. Gammon, H. Piwnica-Worms and D. Piwnica-Worms (2004). "Kinetics of regulated protein-protein interactions revealed with firefly luciferase complementation imaging in cells and living animals." Proc Natl Acad Sci U S A **101**(33): 12288-12293.
Ma, L. and E. R. Kantrowitz (1996). "Kinetic and X-ray structural studies of a mutant Escherichia coli alkaline phosphatase (His-412-->Gln) at one of the zinc binding sites." Biochemistry **35**(7): 2394-2402.
Ma, L., T. T. Tibbitts and E. R. Kantrowitz (1995). "Escherichia coli alkaline phosphatase: X-ray structural studies of a mutant enzyme (His-412-->Asn) at one of the catalytically important zinc binding sites." Protein Sci **4**(8): 1498-1506.
Mandecki, W., M. A. Shallcross, J. Sowadski and S. Tomazic-Allen (1991). "Mutagenesis of conserved residues within the active site of Escherichia coli alkaline phosphatase yields enzymes with increased kcat." Prot. Eng. Des. Sel. **4**(7): 801-804.
Manting, E. H. and A. J. Driessen (2000). "Escherichia coli translocase: the unravelling of a molecular machine." Mol Microbiol **37**(2): 226-238.
Martell, J. D., M. Yamagata, T. J. Deerinck, S. Phan, C. G. Kwa, M. H. Ellisman, J. R. Sanes and A. Y. Ting (2016). "A split horseradish peroxidase for the detection of intercellular protein-protein interactions and sensitive visualization of synapses." Nat Biotechnol **34**(7): 774-780.

Martin, D. C., S. C. Pastra-Landis and E. R. Kantrowitz (1999). "Amino acid substitutions at the subunit interface of dimeric Escherichia coli alkaline phosphatase cause reduced structural stability." Protein Sci **8**(5): 1152-1159.
Masson, M., O. V. Runarsson, F. Johannson and M. Aizawa (2004). "4-Amino-1-naphthylphosphate as a substrate for the amperometric detection of alkaline phosphatase activity and its application for immunoassay." Talanta **64**(1): 174-180.
Mena, M. A. and P. S. Daugherty (2005). "Automated design of degenerate codon libraries." Protein Eng Des Sel **18**(12): 559-561.
Michnick, S. W. (2003). "Protein fragment complementation strategies for biochemical network mapping." Curr Opin Biotechnol **14**(6): 610-617.
Michnick, S. W., P. H. Ear, C. Landry, M. K. Malleshaiah and V. Messier (2010). "A toolkit of protein-fragment complementation assays for studying and dissecting large-scale and dynamic protein-protein interactions in living cells." Methods Enzymol **470**: 335-368.
Millan, J. L. (2006). "Alkaline Phosphatases : Structure, substrate specificity and functional relatedness to other members of a large superfamily of enzymes." Purinergic Signal **2**(2): 335-341.
Miller, J. H. (1998). "Mutators in Escherichia coli." Mutat Res **409**(3): 99-106.
Moore, C. D., O. Z. Ajala and H. Zhu (2016). "Applications in high-content functional protein microarrays." Curr Opin Chem Biol **30**: 21-27.
Morell, M., S. Ventura and F. X. Aviles (2009). "Protein complementation assays: approaches for the in vivo analysis of protein interactions." FEBS Lett **583**(11): 1684-1691.
Moulton, S. E., J. N. Barisci, A. Bath, R. Stella and G. G. Wallace (2003). "Investigation of protein adsorption and electrochemical behavior at a gold electrode." J Colloid Interface Sci **261**(2): 312-319.
Murphy, J. E., B. Stec, L. Ma and E. R. Kantrowitz (1997). "Trapping and visualization of a covalent enzyme-phosphate intermediate." Nat Struct Biol **4**(8): 618-622.
Murphy, J. E., T. T. Tibbitts and E. R. Kantrowitz (1995). "Mutations at positions 153 and 328 in Escherichia coli alkaline phosphatase provide insight towards the structure and function of mammalian and yeast alkaline phosphatases." J Mol Biol **253**(4): 604-617.
Newman, J. D. and A. P. Turner (2005). "Home blood glucose biosensors: a commercial perspective." Biosens Bioelectron **20**(12): 2435-2453.
Niazov, T., R. Baron, E. Katz, O. Lioubashevski and I. Willner (2006). "Concatenated logic gates using four coupled biocatalysts operating in series." Proc Natl Acad Sci U S A **103**(46): 17160-17163.
Nov, Y. (2012). "When second best is good enough: another probabilistic look at saturation mutagenesis." Appl Environ Microbiol **78**(1): 258-262.
O'Brien, P. J., J. K. Lassila, T. D. Fenn, J. G. Zalatan and D. Herschlag (2008). "Arginine coordination in enzymatic phosphoryl transfer: evaluation of the

effect of Arg166 mutations in Escherichia coli alkaline phosphatase." Biochemistry **47**(29): 7663-7672.
Oakley, M. G. and P. S. Kim (1998). "A buried polar interaction can direct the relative orientation of helices in a coiled coil." Biochemistry **37**(36): 12603-12610.
Ohmuro-Matsuyama, Y., C. I. Chung and H. Ueda (2013). "Demonstration of protein-fragment complementation assay using purified firefly luciferase fragments." BMC Biotechnol **13**: 31.
Okuda, J. and K. Sode (2004). "PQQ glucose dehydrogenase with novel electron transfer ability." Biochem Biophys Res Commun **314**(3): 793-797.
Orhanovic, S., V. Bucevic-Popovic, M. Pavela-Vrancic, D. Vujaklija and V. Gamulin (2006). "Effect of a T81A mutation at the subunit interface on catalytic properties of alkaline phosphatase from Escherichia coli." Int J Biol Macromol **40**(1): 54-58.
Ostermeier, M. (2009). "Designing switchable enzymes." Curr Opin Struct Biol **19**(4): 442-448.
Page, M. I. and P. Proctor (1984). "Mechanism of .beta.-lactam ring opening in cephalosporins." J. Am. Chem. Soc. **106**(13): 3820-3825.
Parikh, M. R. and I. Matsumura (2005). "Site-saturation Mutagenesis is more Efficient than DNA Shuffling for the Directed Evolution of β-Fucosidase from β-Galactosidase." J. Mol. Biol. **352**(3): 621-628.
Parr, T. R., Jr., C. H. Pai and L. E. Bryan (1984). "Simple screening method for beta-lactamase-positive and -negative ampicillin-resistant Haemophilus influenzae isolates." J Clin Microbiol **20**(1): 131-132.
Paschke, M., C. Tiede and W. Hohne (2007). "Engineering a circularly permuted GFP scaffold for peptide presentation." J Mol Recognit **20**(5): 367-378.
Paschon, D. E., Z. S. Patel and M. Ostermeier (2005). "Enhanced Catalytic Efficiency of Aminoglycoside Phosphotransferase (3′)-IIa Achieved Through Protein Fragmentation and Reassembly." J. Mol. Biol. **353**(1): 26-37.
Paulmurugan, R. and S. S. Gambhir (2003). "Monitoring protein-protein interactions using split synthetic renilla luciferase protein-fragment-assisted complementation." Anal Chem **75**(7): 1584-1589.
Paulmurugan, R. and S. S. Gambhir (2005). "Firefly luciferase enzyme fragment complementation for imaging in cells and living animals." Anal Chem **77**(5): 1295-1302.
Paulmurugan, R., P. Ray, A. De, C. T. Chan and S. S. Gambhir (2005). "Imaging protein–protein interactions in living subjects." TrAC Trends in Analytical Chemistry **24**(5): 446-458.
Paulmurugan, R., P. Ray, A. De, C. T. Chan and S. S. Gambhir (2006). "Split luciferase complementation assay for studying interaction of proteins x and y in cells." CSH Protoc **2006**(6).

Paulmurugan, R., P. Ray, A. De, C. T. Chan and S. S. Gambhir (2006). "Split luciferase complementation assay for studying interaction of proteins x and y in living mice." CSH Protoc **2006**(6).
Peck, A., F. Sunden, L. D. Andrews, V. S. Pande and D. Herschlag (2016). "Tungstate as a Transition State Analog for Catalysis by Alkaline Phosphatase." J Mol Biol **428**(13): 2758-2768.
Pedotti, M., E. V. Ferrero, T. Lettieri, P. Colpo, S. Follonier, L. Calzolai and L. Varani (2015). "Rationally Modified Estrogen Receptor Protein as a Bio-Recognition Element for the Detection of EDC Pollutants: Strategies and Opportunities." International Journal of Environmental Research and Public Health **12**(3).
Pei, H., L. Liang, G. Yao, J. Li, Q. Huang and C. Fan (2012). "Reconfigurable three-dimensional DNA nanostructures for the construction of intracellular logic sensors." Angew Chem Int Ed Engl **51**(36): 9020-9024.
Pelletier, J. N., F. X. Campbell-Valois and S. W. Michnick (1998). "Oligomerization domain-directed reassembly of active dihydrofolate reductase from rationally designed fragments." Proc Natl Acad Sci U S A **95**(21): 12141-12146.
Peng, B., J. Lu, A. S. Balijepalli, T. C. Major, B. E. Cohan and M. E. Meyerhoff (2013). "Evaluation of enzyme-based tear glucose electrochemical sensors over a wide range of blood glucose concentrations." Biosens Bioelectron **49**: 204-209.
Piggot, P. J., M. D. Sklar and L. Gorini (1972). "Ribosomal alterations controlling alkaline phosphatase isozymes in Escherichia coli." J Bacteriol **110**(1): 291-299.
Pritchard, L., D. Corne, D. Kell, J. Rowland and M. Winson (2005). "A general model of error-prone PCR." J Theor Biol **234**(4): 497-509.
Qureshi, S. A. (2007). "Beta-lactamase: an ideal reporter system for monitoring gene expression in live eukaryotic cells." Biotechniques **42**(1): 91.
Raina, M., R. Sharma, S. E. Deacon, C. Tiede, D. Tomlinson, A. G. Davies, M. J. McPherson and C. Walti (2015). "Antibody mimetic receptor proteins for label-free biosensors." Analyst **140**(3): 803-810.
Regidor, E. (2006). "Social determinants of health: a veil that hides socioeconomic position and its relation with health." J Epidemiol Community Health **60**(10): 896-901.
Remy, I., F. X. Campbell-Valois and S. W. Michnick (2007). "Detection of protein-protein interactions using a simple survival protein-fragment complementation assay based on the enzyme dihydrofolate reductase." Nat Protoc **2**(9): 2120-2125.
Remy, I., G. Ghaddar and S. W. Michnick (2007). "Using the beta-lactamase protein-fragment complementation assay to probe dynamic protein-protein interactions." Nat Protoc **2**(9): 2302-2306.
Remy, I. and S. W. Michnick (2003). "Dynamic visualization of expressed gene networks." J Cell Physiol **196**(3): 419-429.

Remy, I. and S. W. Michnick (2006). "A highly sensitive protein-protein interaction assay based on Gaussia luciferase." Nat Methods **3**(12): 977-979.
Robida, A. M. and T. K. Kerppola (2009). "Bimolecular fluorescence complementation analysis of inducible protein interactions: effects of factors affecting protein folding on fluorescent protein fragment association." J Mol Biol **394**(3): 391-409.
Saglam, O., B. Kizilkaya, H. Uysal and Y. Dilgin (2016). "Biosensing of glucose in flow injection analysis system based on glucose oxidase-quantum dot modified pencil graphite electrode." Talanta **147**: 315-321.
Sambrook, J., E. F. Fritsch and T. Maniatis (1989). Molecular cloning: a laboratory manual. Cold Spring Harbor, NY, Cold Spring Harbor Laboratory Press.
Sanni, S., E. Lyng and D. M. Pampanin "III: Use of biomarkers as Risk Indicators in Environmental Risk Assessment of oil based discharges offshore." Marine Environ. Res.
Saunders, J. C., L. M. Young, R. A. Mahood, M. P. Jackson, C. H. Revill, R. J. Foster, D. A. Smith, A. E. Ashcroft, D. J. Brockwell and S. E. Radford (2016). "An in vivo platform for identifying inhibitors of protein aggregation." Nat Chem Biol **12**(2): 94-101.
Schierle, C. F., M. Berkmen, D. Huber, C. Kumamoto, D. Boyd and J. Beckwith (2003). "The DsbA signal sequence directs efficient, cotranslational export of passenger proteins to the Escherichia coli periplasm via the signal recognition particle pathway." J Bacteriol **185**(19): 5706-5713.
Schlesinger, M. J. (1965). "The reversible dissociation of the alkaline phosphatase of Escherichia coli. II. Properties of the subunit." J Biol Chem **240**(11): 4293-4298.
Schlesinger, M. J. (1966). "Activation of a mutationally altered form of the Escherichia coli alkaline phosphatase by zinc." J Biol Chem **241**(13): 3181-3188.
Schlesinger, M. J. and L. Andersen (1968). "MULTIPLE MOLECULAR FORMS OF THE ALKALINE PHOSPHATASE OF ESCHERICHIA COLI*." Ann. N.Y. Acad. Sc. **151**(1): 159-170.
Schlesinger, M. J. and K. Barrett (1965). "The reversible dissociation of the alkaline phosphatase of Escherichia coli. I. Formation and reactivation of subunits." J Biol Chem **240**(11): 4284-4292.
Schnee, M., F. M. Wagner, U. H. Koszinowski and Z. Ruzsics (2012). "A cell free protein fragment complementation assay for monitoring the core interaction of the human cytomegalovirus nuclear egress complex." Antiviral Res **95**(1): 12-18.
Schuck, P. (2000). "Size-distribution analysis of macromolecules by sedimentation velocity ultracentrifugation and lamm equation modeling." Biophys J **78**(3): 1606-1619.
Sharma, R., S. E. Deacon, D. Nowak, S. E. George, M. P. Szymonik, A. A. Tang, D. C. Tomlinson, A. G. Davies, M. J. McPherson and C. Walti (2016).

"Label-free electrochemical impedance biosensor to detect human interleukin-8 in serum with sub-pg/ml sensitivity." Biosens Bioelectron **80**: 607-613.
Sharma, U., D. Pal and R. Prasad (2014). "Alkaline Phosphatase: An Overview." Indian Journal of Clinical Biochemistry **29**(3): 269-278.
Shekhawat, S. S. and I. Ghosh (2011). "Split-protein systems: beyond binary protein-protein interactions." Curr Opin Chem Biol **15**(6): 789-797.
Shekhawat, S. S., J. R. Porter, A. Sriprasad and I. Ghosh (2009). "An autoinhibited coiled-coil design strategy for split-protein protease sensors." J Am Chem Soc **131**(42): 15284-15290.
Sideraki, V., W. Huang, T. Palzkill and H. F. Gilbert (2001). "A secondary drug resistance mutation of TEM-1 β-lactamase that suppresses misfolding and aggregation." Proc. Natl. Acad. Sci. U.S.A. **98**(1): 283-288.
Simpson, M. L., G. S. Sayler, J. T. Fleming and B. Applegate (2001). "Whole-cell biocomputing." Trends Biotechnol **19**(8): 317-323.
Singh, P., L. Sharma, S. R. Kulothungan, B. V. Adkar, R. S. Prajapati, P. S. Ali, B. Krishnan and R. Varadarajan (2013). "Effect of signal peptide on stability and folding of Escherichia coli thioredoxin." PLoS One **8**(5): e63442.
Siontis, K. C., G. C. M. Siontis, D. G. Contopoulos-Ioannidis and J. P. A. Ioannidis (2014). "Diagnostic tests often fail to lead to changes in patient outcomes." J. Clin. Epidemiol. **67**(6): 612-621.
Skerra, A. (2003). "Imitating the humoral immune response." Curr Opin Chem Biol **7**(6): 683-693.
Skerra, A. (2007). "Alternative non-antibody scaffolds for molecular recognition." Curr Opin Biotechnol **18**(4): 295-304.
Sone, M., S. Kishigami, T. Yoshihisa and K. Ito (1997). "Roles of disulfide bonds in bacterial alkaline phosphatase." J Biol Chem **272**(10): 6174-6178.
Sonuc, M. N. and M. K. Sezginturk (2014). "Ultrasensitive electrochemical detection of cancer associated biomarker HER3 based on anti-HER3 biosensor." Talanta **120**: 355-361.
Stec, B., M. J. Hehir, C. Brennan, M. Nolte and E. R. Kantrowitz (1998). "Kinetic and X-ray structural studies of three mutant E. coli alkaline phosphatases: insights into the catalytic mechanism without the nucleophile Ser102." J Mol Biol **277**(3): 647-662.
Stec, B., K. M. Holtz and E. R. Kantrowitz (2000). "A revised mechanism for the alkaline phosphatase reaction involving three metal ions." J Mol Biol **299**(5): 1303-1311.
Steiner, D., P. Forrer, M. T. Stumpp and A. Pluckthun (2006). "Signal sequences directing cotranslational translocation expand the range of proteins amenable to phage display." Nat Biotechnol **24**(7): 823-831.
Stemmer, W. P. (1994). "Rapid evolution of a protein in vitro by DNA shuffling." Nature **370**(6488): 389-391.
Strimbu, K. and J. A. Tavel (2010). "What are biomarkers?" Curr Opin HIV AIDS **5**(6): 463-466.

Sun, K., N. Xia, L. Zhao, K. Liu, W. Hou and L. Liu (2017). "Aptasensors for the selective detection of alpha-synuclein oligomer by colorimetry, surface plasmon resonance and electrochemical impedance spectroscopy." Sensors and Actuators B: Chemical **245**(Supplement C): 87-94.
Sunden, F., A. Peck, J. Salzman, S. Ressl and D. Herschlag (2015). "Extensive site-directed mutagenesis reveals interconnected functional units in the alkaline phosphatase active site." Elife **4**.
Tannous, B. A., D. E. Kim, J. L. Fernandez, R. Weissleder and X. O. Breakefield (2005). "Codon-optimized Gaussia luciferase cDNA for mammalian gene expression in culture and in vivo." Mol Ther **11**(3): 435-443.
Tibbitts, T. T., J. E. Murphy and E. R. Kantrowitz (1996). "Kinetic and structural consequences of replacing the aspartate bridge by asparagine in the catalytic metal triad of Escherichia coli alkaline phosphatase." J Mol Biol **257**(3): 700-715.
Tibbitts, T. T., X. Xu and E. R. Kantrowitz (1994). "Kinetics and crystal structure of a mutant Escherichia coli alkaline phosphatase (Asp-369-->Asn): a mechanism involving one zinc per active site." Protein Sci **3**(11): 2005-2014.
Tiede, C., R. Bedford, S. J. Heseltine, G. Smith, I. Wijetunga, R. Ross, D. AlQallaf, A. P. Roberts, A. Balls, A. Curd, R. E. Hughes, H. Martin, S. R. Needham, L. C. Zanetti-Domingues, Y. Sadigh, T. P. Peacock, A. A. Tang, N. Gibson, H. Kyle, G. W. Platt, N. Ingram, T. Taylor, L. P. Coletta, I. Manfield, M. Knowles, S. Bell, F. Esteves, A. Maqbool, R. K. Prasad, M. Drinkhill, R. S. Bon, V. Patel, S. A. Goodchild, M. Martin-Fernandez, R. J. Owens, J. E. Nettleship, M. E. Webb, M. Harrison, J. D. Lippiat, S. Ponnambalam, M. Peckham, A. Smith, P. K. Ferrigno, M. Johnson, M. J. McPherson and D. C. Tomlinson (2017). "Affimer proteins are versatile and renewable affinity reagents." Elife **6**.
Tiede, C., A. A. Tang, S. E. Deacon, U. Mandal, J. E. Nettleship, R. L. Owen, S. E. George, D. J. Harrison, R. J. Owens, D. C. Tomlinson and M. J. McPherson (2014). "Adhiron: a stable and versatile peptide display scaffold for molecular recognition applications." Protein Eng Des Sel **27**(5): 145-155.
Tighe, P. J., R. R. Ryder, I. Todd and L. C. Fairclough (2015). "ELISA in the multiplex era: potentials and pitfalls." Proteomics Clin Appl **9**(3-4): 406-422.
Tomassetti, M., M. Serone, R. Angeloni, L. Campanella and E. Mazzone (2015). "Amperometric enzyme sensor to check the total antioxidant capacity of several mixed berries. Comparison with two other spectrophotometric and fluorimetric methods." Sensors (Basel) **15**(2): 3435-3452.
Torriani, A. (1960). "Influence of inorganic phosphate in the formation of phosphatases by Escherichia coli." Biochim Biophys Acta **38**: 460-469.
Trivedi, U. B., D. Lakshminarayana, I. L. Kothari, N. G. Patel, H. N. Kapse, K. K. Makhija, P. B. Patel and C. J. Panchal (2009). "Potentiometric biosensor for urea determination in milk." Sensors and Actuators B: Chemical **140**(1): 260-266.

Tsien, R. Y. (1998). "The green fluorescent protein." Annu Rev Biochem **67**: 509-544.
Tuerk, C. and L. Gold (1990). "Systematic evolution of ligands by exponential enrichment: RNA ligands to bacteriophage T4 DNA polymerase." Science **249**(4968): 505-510.
Tyler-Cross, R., C. H. Roberts and J. F. Chlebowski (1989). "Proteolytic modification of Escherichia coli alkaline phosphatase." J Biol Chem **264**(8): 4523-4528.
Unger, R. and J. Moult (2006). "Towards computing with proteins." Proteins **63**(1): 53-64.
Vasquez, G., A. Rey, C. Rivera, C. Iregui and J. Orozco (2017). "Amperometric biosensor based on a single antibody of dual function for rapid detection of Streptococcus agalactiae." Biosens Bioelectron **87**: 453-458.
Villalobos, V., S. Naik, M. Bruinsma, R. S. Dothager, M. H. Pan, M. Samrakandi, B. Moss, A. Elhammali and D. Piwnica-Worms (2010). "Dual-color click beetle luciferase heteroprotein fragment complementation assays." Chem Biol **17**(9): 1018-1029.
Villalobos, V., S. Naik and D. Piwnica-Worms (2008). "Detection of protein-protein interactions in live cells and animals with split firefly luciferase protein fragment complementation." Methods Mol Biol **439**: 339-352.
Voet, D., J. G. Voet and C. W. Pratt (2008). Principles of biochemistry. Hoboken, N.J., Wiley.
Walcarius, A., S. D. Minteer, J. Wang, Y. Lin and A. Merkoci (2013). "Nanomaterials for bio-functionalized electrodes: recent trends." Journal of Materials Chemistry B **1**(38): 4878-4908.
Wang, J. and E. R. Kantrowitz (2006). "Trapping the tetrahedral intermediate in the alkaline phosphatase reaction by substitution of the active site serine with threonine." Protein Sci **15**(10): 2395-2401.
Wang, J., K. A. Stieglitz and E. R. Kantrowitz (2005). "Metal specificity is correlated with two crucial active site residues in Escherichia coli alkaline phosphatase." Biochemistry **44**(23): 8378-8386.
Wehr, M. C. and M. J. Rossner (2016). "Split protein biosensor assays in molecular pharmacological studies." Drug Discovery Today **21**(3): 415-429.
Wehrman, T., B. Kleaveland, J. H. Her, R. F. Balint and H. M. Blau (2002). "Protein-protein interactions monitored in mammalian cells via complementation of beta -lactamase enzyme fragments." Proc Natl Acad Sci U S A **99**(6): 3469-3474.
Wen, Y., J. Xu, M. Liu, D. Li and H. He (2012). "Amperometric vitamin C biosensor based on the immobilization of ascorbate oxidase into the biocompatible sandwich-type composite film." Appl Biochem Biotechnol **167**(7): 2023-2038.
Wende, A., P. Johansson, R. Vollrath, M. Dyall-Smith, D. Oesterhelt and M. Grininger (2010). "Structural and biochemical characterization of a halophilic archaeal alkaline phosphatase." J Mol Biol **400**(1): 52-62.

Williams, C. (2004). "cAMP detection methods in HTS: selecting the best from the rest." Nat Rev Drug Discov **3**(2): 125-135.
Win, M. N. and C. D. Smolke (2008). "Higher-order cellular information processing with synthetic RNA devices." Science **322**(5900): 456-460.
Wohlfahrt, G., S. Witt, J. Hendle, D. Schomburg, H. M. Kalisz and H. J. Hecht (1999). "1.8 and 1.9 A resolution structures of the Penicillium amagasakiense and Aspergillus niger glucose oxidases as a basis for modelling substrate complexes." Acta Crystallogr D Biol Crystallogr **55**(Pt 5): 969-977.
Wu, Y., F. Wang, K. Lu, M. Lv and Y. Zhao (2017). "Self-assembled dipeptide-graphene nanostructures onto an electrode surface for highly sensitive amperometric hydrogen peroxide biosensors." Sensors and Actuators B: Chemical **244**: 1022-1030.
Wurch, T., P. Lowe, V. Caussanel, C. Bes, A. Beck and N. Corvaia (2008). "Development of novel protein scaffolds as alternatives to whole antibodies for imaging and therapy: status on discovery research and clinical validation." Curr Pharm Biotechnol **9**(6): 502-509.
Wurch, T., A. Pierre and S. Depil (2012). "Novel protein scaffolds as emerging therapeutic proteins: from discovery to clinical proof-of-concept." Trends Biotechnol **30**(11): 575-582.
Xie, C., C. Tiede, X. Zhang, C. Wang, Z. Li, X. Xu, M. J. McPherson, D. C. Tomlinson and W. Xu (2017). "Development of an Affimer-antibody combined immunological diagnosis kit for glypican-3." Sci Rep **7**(1): 9608.
Xuan, J., Y. Yu, T. Qing, L. Guo and L. Shi (2013). "Next-generation sequencing in the clinic: promises and challenges." Cancer Lett **340**(2): 284-295.
Zalatan, J. G., T. D. Fenn and D. Herschlag (2008). "Comparative enzymology in the alkaline phosphatase superfamily to determine the catalytic role of an active-site metal ion." J Mol Biol **384**(5): 1174-1189.
Zheng, L., Y. Wan, L. Yu and D. Zhang (2016). "Lysozyme as a recognition element for monitoring of bacterial population." Talanta **146**: 299-302.